



**Kazi Mohammed  
Saidul Huq**

**Eficiência Energética Avançada Para Sistema  
OFDMA CoMP Coordenação Multiponto**

**Advanced Energy Efficient Coordinated Multi-Point  
Transmission for OFDMA**





**Kazi Mohammed  
Saidul Huq**

**Eficiência Energética Avançada Para Sistema  
OFDMA CoMP Coordenação Multiponto**

**Advanced Energy Efficient Coordinated Multi-Point  
Transmission for OFDMA**

Tese apresentada à Universidade de Aveiro para cumprimento dos requisitos necessários à obtenção do grau de Doutor em Engenharia Electrotécnica, realizada sob a orientação científica do Doutor Jonathan Rodriguez Gonzalez, Professor Auxiliar Convidado e Doutor Rui Luís Andrade Aguiar, Professor Associado com Agregação do Departamento de Electrónica, Telecomunicações e Informática da Universidade de Aveiro.

Apoio financeiro da FCT com a  
referência SFRH/BD/62165/2009.



**o júri / the jury**

presidente / president

**Fernando Manuel Bico Marques**

Professor Catedrático da Universidade de Aveiro (por delegação da Reitora da Universidade de Aveiro)

vogais / examiners committee

**Fernando José da Silva Velez**

Professor Auxiliar  
Departamento de Engenharia Electromecânica  
Universidade da Beira Interior

**Carlos Miguel Nogueira Gaspar Ribeiro**

Professor Adjunto  
Departamento de Engenharia Electrotécnica  
Escola Superior de Tecnologia e Gestão  
Instituto Politécnico de Leiria

**Adão Paulo Soares da Silva**

Professor Auxiliar  
Departamento de Electrónica Telecomunicações e Informàtica  
Universidade de Aveiro

**Jonathan Rodriguez (Orientador)**

Professor Auxiliar Convidado  
Departamento de Electrónica Telecomunicações e Informàtica  
Universidade de Aveiro

**Shahid Mumtaz**

Investigador Pós-Doc  
Instituto de Telecomunicações - Aveiro



## **agradecimentos**

Queria usar este pequeno espaço para deixar os meus mais sinceros agradecimentos aqueles que foram essenciais neste percurso.

Desde já agradeço ao meu orientador Professor Dr. Jonathan Rodriguez e co-orientador Professor Dr. Rui Luís Andrade Aguiar pela orientação, ajuda e confiança demonstradas ao longo destes anos.

À Fundação para a Ciência e Tecnologia (FCT) pelo apoio financeiro.

Aos projectos GREEN-T, GREENET e ROMEO, no âmbito dos quais foi desenvolvido parte deste trabalho.

Ao Instituto de Telecomunicações pelos excelentes meios e recursos disponibilizados.

Aos colegas do grupo 4TELL pela ajuda e partilha de ideias.

Aos meus amigos pelos momentos de descontração passados juntos.

Aos meus pais pela inspiração que sempre foram para mim.



**Palavras-chave**

Sistemas Multi-Utilizador, Systema OFDMA, Canal, Energia, Coordenação Multiponto, Eficiencia Energética

**Resumo**

O aumento do consumo de energia nas TICs e em particular nas redes de comunicação móveis, estimulado por um crescimento esperado do tráfego de dados, tem servido de impulso aos operadores móveis para reorientarem os seus projectos de rede, planeamento e implementação no sentido de reduzir o custo por bit, o que ao mesmo tempo possibilita um passo significativo no sentido de reduzir as despesas operacionais. Como um passo no sentido de uma incorporação eficaz em termos destes custos, o sistema móvel 3GPP LTE-Advanced adoptou a técnica de transmissão Coordenação Multi-Ponto (identificada na literatura com a sigla CoMP) devido à sua capacidade de mitigar e gerir Interferência entre Células (sigla ICI na literatura). No entanto a ICI pode ainda ser mais proeminente quando vários nós no interior da célula utilizam recursos comuns com diferentes níveis de energia, como acontece nos chamados ambientes de redes heterogéneas (sigla HetNet na literatura). As HetNets são constituídas por duas ou mais camadas de células. A primeira, ou camada superiora, constitui uma implantação tradicional de sítios de célula, muitas vezes referidas neste contexto como macrocells. Os níveis mais baixos são designados por células pequenas, e podem aparecer como microcells, picocells ou femtocells. A HetNet tem atraído grande interesse por parte dos principais fabricantes como sendo facilitador para transmissões de dados de alta velocidade a baixo custo. A investigação tem revelado até à data, vários dos principais obstáculos que devem ser superados para que as HetNets possam atingir todo o seu potencial: (i) os estrangulamentos no backhaul devem ser aliviados; (ii) bem como sua perfeita interoperabilidade com CoMP. Nesta tese exploramos este último constrangimento e apresentamos ideias inovadoras em como a técnica CoMP poderá ser aperfeiçoada por forma a trabalhar em sinergia com a implementação da HetNet, complementado ainda com uma nova perspectiva na alocação de recursos rádio para um controlo e gestão mais apertado de interferência nas HetNets. Com recurso a simulação a nível de sistema para analisar o desempenho dos algoritmos e protocolos propostos, os resultados obtidos concluíram que ganhos até à ordem dos 20% poderão ser atingidos em termos de eficiência energética.



**Keywords**

4G, CoMP, Energy-Efficiency, Green, HetNet, OFDMA

**Abstract**

The ever-growing energy consumption in mobile networks stimulated by the expected growth in data traffic has provided the impetus for mobile operators to refocus network design, planning and deployment towards reducing the cost per bit, whilst at the same time providing a significant step towards reducing their operational expenditure. As a step towards incorporating cost-effective mobile system, 3GPP LTE-Advanced has adopted the coordinated multi-point (CoMP) transmission technique due to its ability to mitigate and manage inter-cell interference (ICI). Using CoMP the cell average and cell edge throughput are boosted. However, there is room for reducing energy consumption further by exploiting the inherent flexibility of dynamic resource allocation protocols. To this end packet scheduler plays the central role in determining the overall performance of the 3GPP long-term evolution (LTE) based on packet-switching operation and provide a potential research playground for optimizing energy consumption in future networks. In this thesis we investigate the baseline performance for down link CoMP using traditional scheduling approaches, and subsequently go beyond and propose novel energy efficient scheduling (EES) strategies that can achieve power-efficient transmission to the UEs whilst enabling both system energy efficiency gain and fairness improvement. However, ICI can still be prominent when multiple nodes use common resources with different power levels inside the cell, as in the so called heterogeneous networks (HetNet) environment. HetNets are comprised of two or more tiers of cells. The first, or higher tier, is a traditional deployment of cell sites, often referred to in this context as macrocells. The lower tiers are termed small cells, and can appear as microcell, picocells or femtocells. The HetNet has attracted significant interest by key manufacturers as one of the enablers for high speed data at low cost. Research until now has revealed several key hurdles that must be overcome before HetNets can achieve their full potential: bottlenecks in the backhaul must be alleviated, as well as their seamless interworking with CoMP. In this thesis we explore exactly the latter hurdle, and present innovative ideas on advancing CoMP to work in synergy with HetNet deployment, complemented by a novel resource allocation policy for HetNet tighter interference management. As system level simulator has been used to analyze the proposed algorithm/protocols, and results have concluded that up to 20% energy gain can be observed.



# Table of contents

<b>Table of contents</b>	<b>i</b>
<b>List of Acronyms</b>	<b>v</b>
<b>List of Symbols</b>	<b>xi</b>
<b>List of Figures</b>	<b>xiii</b>
<b>List of Tables</b>	<b>xvii</b>
<b>List of Algorithms</b>	<b>xix</b>
<b>1 Introduction</b>	<b>1</b>
1.1 Introduction . . . . .	1
1.2 Overview of CoMP transmission techniques . . . . .	2
1.2.1 Joint Processing (JP) . . . . .	3
1.2.2 Coordinated Scheduling / Beamforming (CS/CB) . . . . .	5
1.3 Motivation and Objectives . . . . .	5
1.4 Scientific Methodology Applied . . . . .	7
1.5 Thesis Contribution . . . . .	7
1.6 Organization of the Dissertation . . . . .	9
<b>2 4G System Level Energy Efficiency Performance</b>	<b>13</b>
2.1 Energy Efficient Radio Resource Management . . . . .	13
2.1.1 Fundamental Trade-Offs in RRM Protocol Design . . . . .	14
2.1.2 Cross-Layer Framework for Energy-Efficient Resource Allocation . . . . .	15
2.1.3 Load Adaptive Resource Management . . . . .	16
2.1.4 Service Differentiation . . . . .	17
2.2 Exploitation of Multi-User Diversity . . . . .	18
2.3 Relay Scheduling . . . . .	18
2.4 Energy Analysis SISO vs. MIMO with Packet Scheduling . . . . .	20
2.4.1 Energy Efficiency in classical Packet Scheduling Techniques . . . . .	20
2.4.2 Energy Efficiency based Coordinated RRM for Multi-cell Systems . . . . .	24
2.5 Interference Management for Heterogeneous networks . . . . .	25
2.6 Conclusions . . . . .	26

<b>3</b>	<b>SE-EE Trade-Off</b>	<b>27</b>
3.1	Background . . . . .	27
3.1.1	Point-to-Point AWGN Channel . . . . .	28
3.1.2	Wireless OFDMA System . . . . .	30
3.2	Single Cell Spectral Efficiency-Energy Efficiency . . . . .	31
3.2.1	System Model Description . . . . .	31
3.2.2	SE-EE Trade-off Relation . . . . .	33
3.2.3	Bounds on The SE-EE curve . . . . .	35
3.3	Significance Of Circuit Power In SE-EE Trade-Off . . . . .	35
3.4	Multi cell Spectral Efficiency-Energy Efficiency . . . . .	38
3.4.1	System Model . . . . .	38
3.4.2	Bounds on the SE-EE Curve . . . . .	40
3.5	Trade-off between SE-EE in MU-MIMO CoMP . . . . .	41
3.5.1	System Model . . . . .	41
3.5.2	Novel Algorithm for Achieving Maximum EE . . . . .	44
3.5.3	Simulation Results . . . . .	46
3.6	Conclusions . . . . .	50
<b>4</b>	<b>CoMP Energy Efficiency Performance Evaluation</b>	<b>51</b>
4.1	Energy Efficiency . . . . .	52
4.2	CoMP Frame Architecture . . . . .	52
4.2.1	LTE Frame Architecture . . . . .	52
4.2.2	JT-Frame . . . . .	53
4.2.3	DPS-Frame . . . . .	54
4.2.4	CS/CB Frame . . . . .	55
4.3	Deployment of CoMP . . . . .	55
4.4	System Level Simulator . . . . .	56
4.4.1	Energy Module . . . . .	58
4.4.2	Performance Metrics . . . . .	60
4.5	Simulation Results and Discussion . . . . .	60
4.6	Conclusion . . . . .	64
<b>5</b>	<b>Advanced Energy Efficient Scheduling for CoMP Transmission</b>	<b>65</b>
5.1	Architecture of Mixed Traffic Packet Scheduler . . . . .	65
5.2	Novel Energy Efficient Packet Scheduling Algorithm . . . . .	66
5.2.1	Simulation and Discussions . . . . .	69
5.3	Traffic state based Novel Energy Efficient Transmission Algorithm . . . . .	73
5.3.1	Problem Formulation . . . . .	73
5.3.2	Proposed Algorithm . . . . .	74
5.3.3	Simulation Results ad Discussion . . . . .	75
5.4	Conclusions . . . . .	77
<b>6</b>	<b>Advanced HetNet CoMP Architectures for OFDMA</b>	<b>79</b>
6.1	Novel Energy Efficient Design for HetNet CoMP Architecture . . . . .	80
6.1.1	System Model . . . . .	81
6.1.2	Proposed Novel Energy Efficient Design (NEED) Architecture . . . . .	84
6.1.3	Additional performance Metrics . . . . .	87

6.1.4	Simulation Results and Discussion . . . . .	88
6.2	Frequency Allocation for HetNet CoMP:	
	Energy Efficiency Analysis . . . . .	93
6.2.1	System Model and Characteristics . . . . .	93
6.2.2	Simulations and Discussions . . . . .	95
6.3	Optimization of Energy Efficiency considering Backhaul Power . . . . .	100
6.3.1	HetNet CoMP Backhaul Architecture for Power Consumption Model .	100
6.3.2	Power Consumption Model Including Backhaul . . . . .	102
6.3.3	Novel Iterative Algorithm for EE Maximization . . . . .	105
6.3.4	Numerical Results . . . . .	107
6.4	Conclusions . . . . .	112
<b>7</b>	<b>Concluding Remarks</b>	<b>113</b>
7.1	Summary of the Thesis . . . . .	113
7.2	Future Research Directions . . . . .	115
7.2.1	Spectral Efficiency and Energy Efficiency Trade-off . . . . .	115
7.2.2	Interference Modeling and Management in Heterogeneous Networks .	116
7.2.3	Signaling Overhead . . . . .	116
7.2.4	CoMP with Carrier Aggregation . . . . .	116
7.2.5	D2D Application in CoMP System . . . . .	117
	<b>References</b>	<b>119</b>
	<b>Appendix</b>	<b>130</b>
<b>A</b>	<b>System Level Simulator for 4G Networks</b>	<b>131</b>
A.1	Introduction . . . . .	131
A.2	Link to System Interface mapping . . . . .	131
A.3	Deployment Scenario . . . . .	132
A.4	Channel Modeling . . . . .	133
A.5	Link Adaptation . . . . .	134
A.6	Resource allocation . . . . .	134
A.6.1	LTE-A Frame Architecture . . . . .	135
A.7	Hybrid Automatic Repeat Request (HARQ) . . . . .	136
A.8	Packet Scheduler . . . . .	137
A.9	Traffic Modeling . . . . .	137
A.9.1	User Level Traffic Model . . . . .	137
A.9.2	IP packet level traffic model . . . . .	137
A.10	Energy Module Modeling . . . . .	138
A.11	Performance metrics . . . . .	139
A.11.1	Average Service Throughput per-Cell . . . . .	139
A.11.2	Per-User Average Service Throughput . . . . .	140
A.11.3	Throughput Outage . . . . .	140
A.11.4	Cell Edge User Throughput . . . . .	140
A.11.5	Spectral Efficiency (bps/Hz) . . . . .	140
A.11.6	System Outage . . . . .	140
A.11.7	System Capacity . . . . .	140

A.11.8 Energy Efficiency (EE) . . . . .	141
A.11.9 Fairness Index (GINI) . . . . .	141
A.12 System level Simulation Process . . . . .	142
A.13 Enhanced System Level Simulator . . . . .	143
A.14 Conclusions . . . . .	146
<b>B Calculation of precoding vector <math>\mathbf{W}</math> and power vector <math>\mathbf{P}</math></b>	<b>147</b>
<b>Index</b>	<b>149</b>

# List of Acronyms

<b>3GPP</b>	3rd Generation Partnership Project.
<b>4G</b>	Fourth Generation.
<b>AMC</b>	Adaptive Modulation & Coding.
<b>AWGN</b>	Additive White Gaussian Noise.
<b>BE</b>	Best Effort.
<b>BER</b>	Bit Error Rate.
<b>BLER</b>	Block Error Rate.
<b>BS</b>	Base Station.
<b>CA</b>	Carrier Aggregation.
<b>CAPEX</b>	Capital Expenditures.
<b>CB</b>	Coordinated Beamforming.
<b>CCN</b>	Conventional Cellular Network.
<b>CDF</b>	Cumulative Distribution Function.
<b>CDMA</b>	Code Division Multiple Access.
<b>CL</b>	Cross-Layer.
<b>CoMP</b>	Coordinated MultiPoint.
<b>CQI</b>	Channel Quality Indicator.
<b>CS/CB</b>	Coordinated Scheduling / Beamforming.
<b>CSI</b>	Channel State Information.
<b>CSIT</b>	Channel State Information at the Transmitter.
<b>CU</b>	Central Unit.
<b>D2D</b>	Device-to-Device.

<b>DAS</b>	Distributed Antenna System.
<b>DCA</b>	Dynamic Channel Adaptation.
<b>DCI</b>	Dynamic Channel Indicator.
<b>DCS</b>	Dynamic Cell Selection.
<b>DE</b>	Deployment Efficiency.
<b>DPS</b>	Dynamic Point Selection.
<b>DRA</b>	Dynamic Resource Allocation.
<b>DRX</b>	Discontinuous Reception.
<b>ECR</b>	Energy Consumption Ratio.
<b>EE</b>	Energy Efficiency.
<b>EES</b>	Energy-Efficient Scheduling.
<b>eNB</b>	evolved NodeB.
<b>FFR</b>	Fractional Frequency Reuse.
<b>FTP</b>	File Transfer Protocol.
<b>GHG</b>	GreenHouse Gas.
<b>GRC</b>	Green Radio Communications.
<b>GSM</b>	Global System for Mobile Communications.
<b>HARQ</b>	Hybrid Automatic Repeat Request.
<b>HetNet</b>	Heterogeneous Network.
<b>ICI</b>	Inter-Cell Interference.
<b>ICIC</b>	Inter-Cell Interference Coordination.
<b>ICT</b>	Information an Communication Technology.
<b>ISI</b>	Inter-Symbol Interference.
<b>JP</b>	Joint Processing.
<b>JT</b>	Joint Transmission.
<b>LA</b>	Link Adaptation.
<b>LPN</b>	Low Power Node.
<b>LTE</b>	Long Term Evolution.
<b>LTE-A</b>	Long Term Evolution-Advanced.

<b>LUT</b>	Look Up Table.
<b>MA</b>	Margin Adaptation.
<b>MAC</b>	Multiple Access Channel.
<b>MCI</b>	Maximum Carrier-to-Interference Ratio.
<b>MCS</b>	Modulation Coding & Scheme.
<b>MHC</b>	MU-MIMO HetNet CoMP.
<b>MIMO</b>	Multiple Input Multiple Output.
<b>MMSE</b>	Minimum Mean Square Error.
<b>MPDU</b>	MAC Protocol Data Unit.
<b>MU-MIMO</b>	Multi-User MIMO.
<b>MUD</b>	Multi-User Diversity.
<b>MUI</b>	Multi-User Interference.
<b>NLOS</b>	Non-Line-of-Sight.
<b>NRT</b>	Non-Real Time.
<b>NRTV</b>	Near Real Time Video.
<b>OFDM</b>	Orthogonal Frequency Division Multiplexing.
<b>OFDMA</b>	Orthogonal Frequency Division Multiple Access.
<b>OPEX</b>	Operational Expenditures.
<b>P-SCH</b>	Primary Synchronization Channel.
<b>PBCH</b>	Physical Broadcast Channel.
<b>PDCCH</b>	Physical Downlink Control Channel.
<b>PDSCH</b>	Physical Downlink Shared Channel.
<b>PER</b>	Packet Error Rate.
<b>PF</b>	Proportional Fairness.
<b>PHY</b>	Physical Layer.
<b>PMI</b>	Precoding Matrix Indicator.
<b>PRB</b>	Physical Resource Block.
<b>PSS</b>	Primary Synchronization Channel.
<b>QoS</b>	Quality of Service.

<b>QoS</b>	Quality of Experience.
<b>RA</b>	Rate Adaptation.
<b>RBG</b>	Resource Block Group.
<b>RI</b>	Rank Indicator.
<b>RR</b>	Round Robin.
<b>RRH</b>	Remote Radio Head.
<b>RRM</b>	Radio Resource Management.
<b>RT</b>	Real Time.
<b>S-SCH</b>	Secondary Synchronization Channel.
<b>SBS</b>	Small base Station.
<b>SCF</b>	Store Carry and Forward.
<b>SE</b>	Spectral Efficiency.
<b>SFBC</b>	Space-Frequency Block Coding.
<b>SFP</b>	small-form factor pluggable.
<b>SINR</b>	Signal to Interference plus Noise Ratio.
<b>SIR</b>	Signal to Interference Ratio.
<b>SISO</b>	Single Input Single Output.
<b>SLS</b>	System Level Simulation.
<b>SM</b>	Spatial Multiplexing.
<b>SNR</b>	Signal to Noise Ratio.
<b>SoA</b>	State-of-The-Art.
<b>SON</b>	Self Optimizing Networks.
<b>SSS</b>	Secondary Synchronization Channel.
<b>SU-MIMO</b>	Single-User MIMO.
<b>TB</b>	Transport Block.
<b>TDMA</b>	Time Division Multiple Access.
<b>TTI</b>	Transmission Time Interval (TTI).
<b>UE</b>	User-Equipment.
<b>UMTS</b>	Universal Mobile Telecommunications System.

<b>VoIP</b>	Voice over Internet Protocol.
<b>WCDMA</b>	Wideband Code Division Multiple Access.
<b>WiMAX</b>	Worldwide Interoperability for Microwave Access.
<b>WLAN</b>	Wireless Local Area Network.
<b>WWW</b>	World Wide Web.
<b>ZF</b>	Zero-Forcing.



# List of Symbols

$(.)^H$	Hermitian transpose operator
$(.)^T$	Transpose operator
$\mathcal{J}$	Denotes a set of entity indicated by calligraphic letters
$ \mathcal{J} $	denotes the cardinality of the set $\mathcal{J}$ .
$\ \cdot\ _F$	Frobenius Norm
$ \mathbf{a} $	Denotes the L2 norm of a vector $\mathbf{a}$
$ a $	Denotes the absolute value of a scalar $a$
$\mathbb{E}\{\cdot\}$	Denotes mathematical Expectation
$\mathbb{C}$	Complex number
$\mathbb{R}$	Real number
$\sigma^2$	Noise variance
<b>A</b>	Upper case bold letter is used for matrices
<b>a</b>	Lower case bold letter for column vectors
<b>H</b>	Channel matrix
<b>W</b>	Precoding matrix
$C$	Number of CoMP clusters
$E$	Number of eNBs
$M$	Number of PRBs
$N_{RX}$	Number of receive antenna
$N_{TX}$	Number of transmit antenna
$P$	Transmit power
$P_c$	Circuit power
$P_{BH}$	Backhaul power

$tr(.)$	Trace operator
$U$	Number of UEs

# List of Figures

1.1	Wireless capacity interpretation . . . . .	1
1.2	Joint Transmission . . . . .	3
1.3	Dynamic point selection . . . . .	4
1.4	Coordinated Scheduling / Beamforming . . . . .	5
1.5	Thesis Organization . . . . .	11
2.1	Framework of EE based Cross-Layer Resource Allocation . . . . .	16
2.2	Relay Cellular Network . . . . .	19
2.3	MCI Packet Scheduling technique . . . . .	21
2.4	RR Packet scheduling technique . . . . .	22
2.5	PF Packet Scheduling Technique . . . . .	22
2.6	Energy efficiency packet scheduling in LTE-Advanced . . . . .	23
2.7	EE vs. Users . . . . .	24
3.1	SE-EE Trade-off in Ideal AWGN channel Scenario . . . . .	28
3.2	SE-EE Trade-off in Practical Scenario . . . . .	29
3.3	Energy-Aware Resource Management in OFDMA . . . . .	30
3.4	Single Cell OFDMA Network . . . . .	32
3.5	SE-EE in downlink OFDMA, scenario 1 . . . . .	33
3.6	SE-EE in downlink OFDMA, scenario 2 . . . . .	34
3.7	SE-EE in downlink OFDMA, scenario 3 . . . . .	34
3.8	Impact of Circuit Power in SE-EE Trade-off . . . . .	36
3.9	Impact of Circuit Power in SE-EE Trade-off . . . . .	37
3.10	Impact of Circuit Power in SE-EE Trade-off . . . . .	38
3.11	Multi Cell OFDMA Network . . . . .	39
3.12	SE-EE Trade-off relation between Multi-cell and Single-cell . . . . .	40
3.13	Hexagonal layout of the reference CoMP cluster . . . . .	42
3.14	Convergence performance of the optimization method . . . . .	47
3.15	Comparison of convergence of EE of different PRBs . . . . .	48
3.16	Convergence of different dynamic circuit power . . . . .	49
3.17	EE vs. SE Trade-off relation . . . . .	49
3.18	EE vs. SE with various power amplifier efficiency . . . . .	50
4.1	LTE-Frame Structure . . . . .	53
4.2	User Scheduling for one JT frame . . . . .	54
4.3	User scheduling for one DPS frame . . . . .	54
4.4	User Scheduling for one CS/CB frame . . . . .	55

4.5	Logical Simulation Component of CoMP . . . . .	56
4.6	Energy Module . . . . .	58
4.7	CDF of the signal quality of different coordination . . . . .	60
4.8	Energy Efficiency vs. number of user . . . . .	61
4.9	Relative gain with respect to RR packet scheduling . . . . .	62
4.10	Relative EE gain respect to CS/CB transmission . . . . .	62
4.11	EE vs. SE . . . . .	63
5.1	Mixed Traffic Packet Scheduler . . . . .	66
5.2	Energy-efficient packet Scheduling Algorithm . . . . .	67
5.3	CDF of the capacity for mixed traffic users . . . . .	69
5.4	Average cell energy efficiency for different number of users . . . . .	70
5.5	Average cell-edge energy efficiency for different number of users . . . . .	71
5.6	Average cell EE with different transmit power . . . . .	71
5.7	Normalized EE distribution per user . . . . .	72
5.8	EE fairness of different Packet Scheduling algorithm . . . . .	73
5.9	Traffic based energy-efficient Algorithm . . . . .	75
5.10	Throughput comparison in different frame . . . . .	76
5.11	ECR vs. Cell radius . . . . .	77
6.1	MU-MIMO HetNet CoMP (MHC) system model . . . . .	82
6.2	Proposed NEED architecture . . . . .	84
6.3	ICI coordination for proposed MU-MIMO HetNet-CoMP (MHC) architecture . . . . .	86
6.4	LTE-A downlink signaling elements . . . . .	87
6.5	Deployment of the MHC system . . . . .	88
6.6	Capacity CDF of different CoMP schemes . . . . .	89
6.7	Energy Efficiency of different CoMP schemes . . . . .	90
6.8	Radio signaling overhead comparison of different HetNet CoMP . . . . .	91
6.9	Backhaul overhead comparison for different MU-MIMO HetNet CoMP . . . . .	92
6.10	Energy consumption ratio of the different techniques. . . . .	92
6.11	CoMP HetNet . . . . .	94
6.12	CoMP HetNet with FFR . . . . .	94
6.13	Deployment of one reference CoMP HetNet cell . . . . .	95
6.14	Average cell capacity comparison . . . . .	97
6.15	Comparison of Energy Efficiency for different HetNet . . . . .	97
6.16	CDF of CoMP HetNet between different frequency planning . . . . .	98
6.17	Cell-edge EE per user . . . . .	98
6.18	Cell average EE vs. Number of user . . . . .	99
6.19	System Model with backhaul layout . . . . .	101
6.20	Area power consumption for the different types of intra-HetNet-CoMP backhaul. . . . .	108
6.21	Different types of backhaul comparison. . . . .	109
6.22	Convergence behavior using integer static step size . . . . .	109
6.23	Convergence behavior using fractional static step size . . . . .	110
6.24	Impact of the dynamic step size . . . . .	111
6.25	Spectral efficiency vs. Energy efficiency. . . . .	111
7.1	Coordinated paradigm for D2D Communication . . . . .	117

A.1	Omnidirectional-hexagonal Layout . . . . .	132
A.2	Sectorized hexagonal Layout . . . . .	132
A.3	System model of LTE networks . . . . .	133
A.4	MIMO Modeling . . . . .	134
A.5	LTE Frame Architecture with PRB allocation . . . . .	136
A.6	Traffic Models . . . . .	139
A.7	Packet decoding process . . . . .	142
A.8	Simulation Steps . . . . .	144
A.9	Logical Simulation Component of CoMP . . . . .	145



# List of Tables

3.1	Key simulation parameters . . . . .	47
4.1	Key simulation parameters . . . . .	59
4.2	EE gain according Figure 4.10 . . . . .	63
4.3	Optimal EE according to Figure 4.11 . . . . .	64
5.1	Key simulation settings . . . . .	76
6.1	Simulation parameters . . . . .	96
6.2	Simulation parameters for power consumption model . . . . .	107
A.1	Modulation and coding schemes-20 MHz . . . . .	135
A.2	Traffic parameter used for mixed class traffic in the simulator . . . . .	138
A.3	Modulation and Coding schemes-CoMP (20 MHz) . . . . .	146



# List of Algorithms

3.1	Algorithm for achieving maximum EE . . . . .	46
5.1	Traffic Threshold based EE Algorithm . . . . .	75
6.1	ICI Coordination Algorithm . . . . .	86
6.2	The novel optimizing rate allocation algorithm to maximize EE . . . . .	107



# Chapter 1

## Introduction

*We begin the chapter by overviewing the LTE-Advanced approach highlighting the key challenges to be solved in terms of enabling energy and spectral efficiency. Next, we discuss the motivation and objectives of the thesis, with an overview of the research contributions. The chapter ends with a presentation of the organization of this thesis to guide the reader along the research roadmap adopted in order accomplish the objectives of this thesis.*

### 1.1 Introduction

With the emergence of fourth generation (4G) and beyond, the demand for mobile traffic applications will continue to rise which is exemplified by Martin Cooper of Arraycom [1], that observed how network capacity has augmented since inception in response to continued rise in user demand. He quoted, “The wireless capacity has doubled every 30 months over the last 104 years.” This translates into an approximately million-fold capacity increase since 1957.

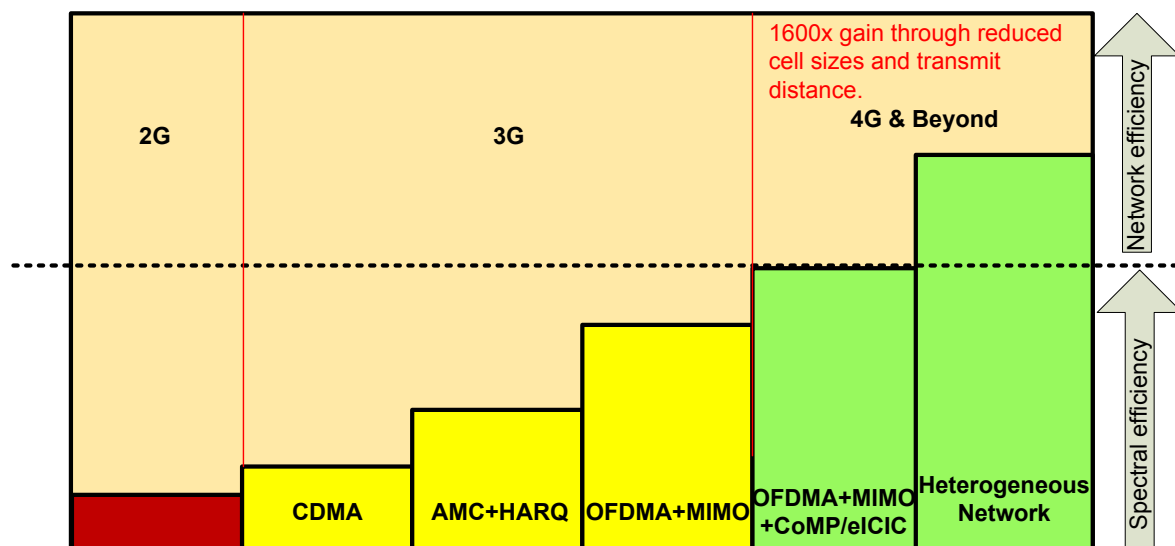


Figure 1.1: Wireless capacity interpretation [2]

Breaking down these gains identifies a 25x (times) improvement from wider spectrum,

5x improvement by dividing the spectrum into smaller slices, 5x improvement by designing better modulation schemes, and a whopping 1600x gain due to reduced cell sizes and transmit distance. The enormous gains reaped from smaller cell sizes arise from efficient spatial reuse of spectrum, or alternatively, a higher area spectral efficiency (SE) [3] as shown by Figure 1.1. According to the above observation, the smaller the distance, the higher the data transfer rate and the lower the delay and energy consumption.

Increased data rate and now energy efficiency (EE) are the key design requirements driving the evolution of wireless communication systems. Conventionally, these requirements have been fulfilled by increasing both the transmit power and increasing the available bandwidth. However, nowadays the radio spectrum available for wireless services is staggeringly scarce, and power consumption in cellular networks is not only a monetary load for operators, but a main source of greenhouse gas emission (GHG). As a consequence, a better system design for utilizing the limited resources is needed. Orthogonal Frequency Division Multiple Access (OFDMA), Multiple-Input Multiple-Output (MIMO), and base station (BS) cooperation such as Coordinated Multi-Point (CoMP) are considered viable solutions to achieve the aforementioned objectives [4], and are key enabling technologies forming part of 4G Mobile Systems. Moreover, 4G goes beyond this by unifying the communication core, and exploiting the complementary attributes of the different technologies and paradigms of wireless networks. In order to appropriately position the key motivators and objectives for this thesis, we provide an overview of Long Term Evolution-Advanced (LTE-A) that provides the benchmark for future enhancements, as well as providing the reader with an insight towards the current limitations.

## 1.2 Overview of CoMP transmission techniques

CoMP, as defined in LTE-Advanced, is a multi-point cooperative transmission and reception technology, which can be easily deployed in a semi-distributed communication system with distributed antennas but centralized control functionality [5]. CoMP is considered as a topology to improve coverage, cell-edge throughput, and/or system efficiency. The basic idea on the CoMP is to increase the data transmission rates and to ensure consistent service quality and throughput on wireless broadband networks. By coordinating and combining signals from multiple transmission points, CoMP will make possible for mobile users to have consistent performance and quality when they access high-bandwidth services, regardless of their cell location. In CoMP, the transmission points [6] are termed as eNB [7] (base Station of LTE System). CoMP allows a signal from another cell to be used as the desired signal, and thus become a prime candidate for improving not only the throughput at the cell edge, but also the average cell throughput [8].

Several eNBs are linked to one central unit (CU), whereas each eNB may contain one or multiple antenna elements. Multiple UEs can be served simultaneously by one or multiple transmission points of the same or different eNB's. The coordinated central controllers retrieve information from distributed transmission points and allocate resources to satisfy the QoS requirements of the UE's while maximizing the network performance. Downlink CoMP implies dynamic coordination between downlink transmissions from multiple geographically separated eNBs [5]. In CoMP, UE could be jointly served by multiple eNBs over the same radio resource and is a basis for increasing spectrum efficiency while maintaining the macro diversity and/or spatial multiplexing gain [9].

CoMP scheme is categorized mainly into two types [6, 7, 10]. These are 1) Joint Processing (JP), 2) Coordinated Scheduling / Beamforming (CS/CB). Brief descriptions of these transmission techniques are given in the following.

### 1.2.1 Joint Processing (JP)

Data for a UE is available at more than one point in the CoMP cooperating set for a time-frequency resource [6]. With the increase in the numbers of users, there is a proportional increase in the feedback of CSI to the BSs. This poses very high backhauling requirements for the BSs to cooperate. Thus, suitable JP algorithms are needed to reduce this burden on the backhaul. The user needs to feedback the CSI from all the BSs in the cluster to the serving BS. This information is passed onto a central unit for interference avoidance. The central unit is an additional component in the network or it can reside in one of the BSs of the cluster. The central unit uses this global CSI for power allocation and beamforming. In this approach, given that the beamformer is well conditioned and the central unit has the complete CSI, the intra-CoMP cluster interference is completely removed. This algorithm poses tremendous requirements on backhauling, since the CSI from all the cooperating BSs needs to be available at the central unit for precoding. JP is also further divided into two types:– joint transmission (JT), and dynamic point selection (DPS).

#### 1.2.1.1 Joint transmission (JT)

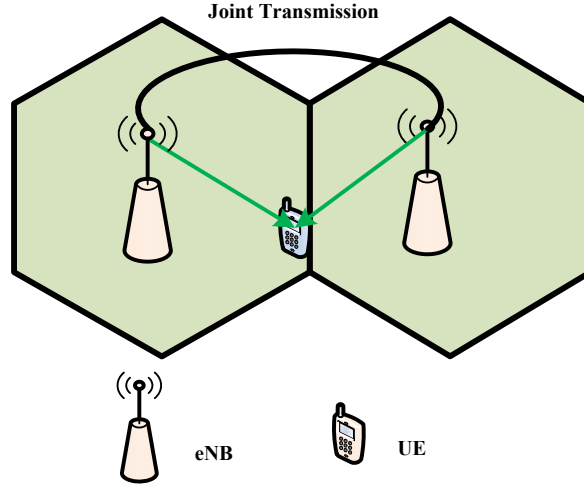


Figure 1.2: Joint Transmission

Simultaneous data transmission from multiple points (part of or entire CoMP cooperating set) to a single UE or multiple UEs in a time-frequency resource. Figure 1.2 illustrates the JT-CoMP scenario [11]. In the category of JT, data to a single UE is simultaneously transmitted from multiple eNBs to improve the received signal quality and/or cancel actively interference for other UEs. In this case, data intended for a particular UE is shared among different cells and is jointly processed at these cells. As a result of this joint processing, the received signals at the intended UE will be coherently or non-coherently added up together [5]. Data is available simultaneously at multiple eNBs.

For the joint transmission downlink technique the signal is received on the basis of the transmission weight, such as the precoding matrix. Note that as the activity factor increases, individual user data rates decrease because of increased interference and thereby decreases the SINR. The served traffic however increases as the number of active users increase. It is seen that the CoMP system yields significant performance gains, and the gains are larger for the system with more coordinated cells [7].

### 1.2.1.2 Dynamic Point Selection (DPS)

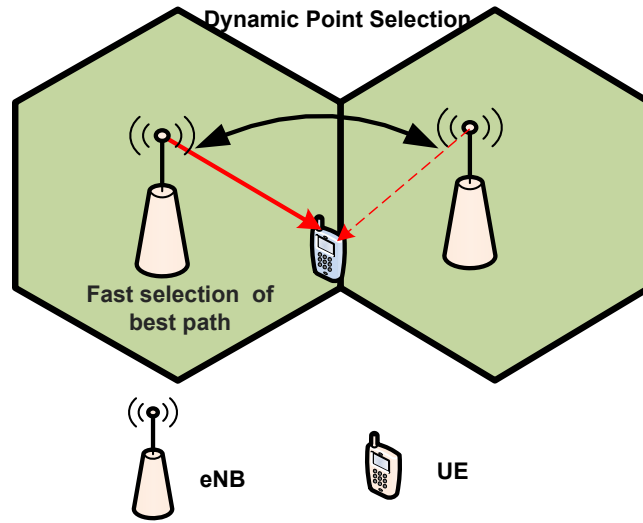


Figure 1.3: Dynamic point selection

The CoMP DPS is a modified version of the basic CoMP JP as illustrated in Figure 1.3. Data is transmitted from one point (within the CoMP cooperating set) in a time-frequency resource in this system. The transmitting/muting point may change from one subframe to another including varying over the PRB pairs within a subframe [6, 10, 7]. This technique is also called dynamic cell selection (DCS) due to its fast selection of cell which exploits path-loss or channel condition [6, 12, 7]. In a given timeslot, only one cell will be selected to perform transmission. The DCS method is limited to one chosen transmission cell which may not get the better performance of the cell edge users [6, 12]. DPS may be combined with JT in which case multiple eNBs can be selected for data transmission in the time-frequency resource. When one eNB is selected for transmitting data, the other eNBs are muted.

In the DPS transmission method, like JT, eNBs jointly transmit signals to a single UE, but transmission of coordinated data for a given UE terminal is performed at a single eNB at each time instance, while the data is available at multiple coordinated eNBs. The other cells among the coordinated cells are muted (i.e., they do not transmit the PRB), so the cell edge UE does not receive other-cell interference [7]. Therefore, the maximum received signal power is obtained, and the interference from neighboring cells is significantly mitigated. eNB enables UE to be dynamically scheduled by the most appropriate eNB by exploiting changes in the channel fading conditions.

### 1.2.2 Coordinated Scheduling / Beamforming (CS/CB)

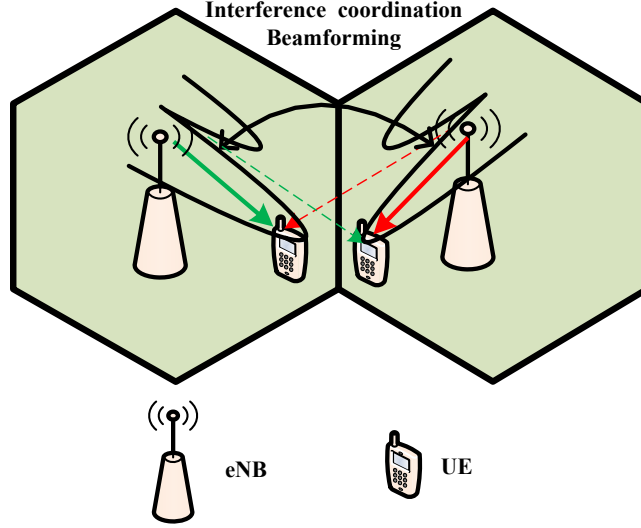


Figure 1.4: Coordinated Scheduling / Beamforming

Data for an UE is only available at and transmitted from one point in the CoMP cooperating set (downlink data transmission is done from that point) for a time-frequency resource, but user scheduling/ beamforming decisions are made with coordination among points corresponding to the CoMP cooperating set. The transmitting points are chosen semi-statically [12, 11, 7]. Figure 1.4 illustrates the CS/CB-CoMP scenario.

In other words, the data intended for a particular UE is not shared while some information related to the channels are shared among different cells [7]. For example, dynamic coordination in the scheduling or fast switching of the transmission to a UE between the transmission points can be used to perform CS/CB. In this approach, data to the mobile terminal is instantaneously transmitted from one of the eNBs while the scheduling decisions are coordinated to control the interference generated in a set of coordinated cells.

In conventional single cell systems these weighting factors cause large interference to the UEs on each other. On the other hand, in CS/CB, the precoding vectors are jointly optimized in such a way [13] that the SINRs at the UEs are improved; i.e. the CoMP cluster jointly chooses the precoding vectors and scheduling decisions taking into account the inter-cell interference. This means that the transmit beamforming weights for each UE set are generated to reduce the unnecessary interference to other UE scheduled within the coordinated cells.

## 1.3 Motivation and Objectives

The network operators need to maximize the utilization of spectral resources in order to meet the ambitious data rate targets defined for next generation communication systems (4G and beyond), whilst taking a step further to reduce the overall energy consumption in the network to minimize the transmission cost per bit leading to competitive tariffs. Hence, there is a need to develop solutions in terms of new networking topologies and technologies that are more energy compliant, and provide a vehicle for enhancing the transmission quality of

the link. In fact, the operator would like to operate between these two boundaries (energy and spectral), since these two states can be dependent (mutually coupled), which requires a delicate engineering trade-off to obtain the desired operating point in the network. What these boundaries are, how to achieve this trade-off and their relationship are all open challenges that need to be addressed, and provide the motivation for this thesis.

The energy efficiency of a system, defined as the amount of information bits per unit energy (b/J) is often used as a figure of merit. The energy efficiency determines the required amount of energy to meet the service requirements such as spectral efficiency, fairness, etc. Energy efficiency is not only a topic that is driving future research trends, but has been given significant attention in the design of LTE-A, which is expected to provide 1 Gbps in downlink. The question arises on how to transmit more data whilst the power remains constant. Ideally, we need to find an approach that will try to adapt a dirty channel that constitutes multipath interference, fast fading, multi-user interference, and other sources of noise pollution into an Additive White Gaussian Noise (AWGN) channel, whilst maintaining the power consumption. The ideal way to increase capacity along with energy efficiency is by minimizing the transmission distance between the transmitter and receiver antenna, which create the dual benefits of higher quality link and more spatial reuse. This is the idea behind the small cell paradigm, that is now seen as a way forward for enhancing capacity in LTE-A and beyond. An alternative way to reduce energy deals with interference management that controls which users are scheduled for transmission. An approach used in LTE-A is known as coordinated multipoint transmission, that increases the energy efficiency by centralizing and coordinating the transmission between a cluster of cells to mitigate interference [6]. Furthermore, current research trends point towards the concept of low power nodes coupled with high power macro base stations to construct so called Heterogeneous Network (HetNets) [14] to obtain further gains in coverage and capacity. Due to their short transmit-receive distance, home base stations can greatly lower transmit power and achieve a higher SINR. This translates into improved reception and higher capacity, leading to an enhanced spectrum and energy efficiency.

Another aspect of optimizing service and system performance, relates to Radio Resource Management (RRM) and scheduling. The notion of RRM is concerned with overseeing the distribution of radio resources to different users, or different classes of users, and attempts to strike a balance by catering for user requirements while achieving profitability for the network operator. Given the scarcity of radio resources, RRM frameworks are designed to maximize the number of services in a cost-effective manner, but new challenges lie in how these can be extended to provide better interference management and energy efficiency. Different functionalities take part in RRM frameworks: for instance, admission control judges whether or not a call can be admitted into the network; scheduling addresses the priority assigned to each user based on satisfying some objective functions; and provisioning attempts to recognize demand patterns in the network such as long-term resource distribution satisfying the operator's objectives. All of these can be further extended towards energy efficiency.

It can be seen that all these approaches are driven by common engineering design traits: **“Optimizing next generation mobile systems towards reducing the energy and cost per bit or increasing bit per energy.”** This design challenge is adopted herein, and provides the drivers for the following research objectives:

- **Investigate energy and spectral efficiency trade-off for OFDMA Systems**
  - Introduces the concept of energy efficiency and spectral efficiency trade-off in

OFDMA networks which is the radio access technique for the 4G LTE/LTE-A system. The SE-EE trade-off is overviewed along with theoretical bounds to delineate the operating region for the single cell and multi cell scenario.

- Finally, an optimization algorithm is presented which maximizes EE given the SE constraints for an LTE-A system such as CoMP.

- **Investigate energy efficient CoMP Transmission and architectures.**

- Provides an attempt to analyze the energy efficiency (EE) of different downlink packet scheduling in CoMP for LTE networks using classical packet scheduling algorithm approaches such as Maximum Carrier to Interference ratio (MCI), Proportional Fairness (PF) and the Round Robin (RR) scheduling for benchmarking the baseline performance.
- Extend the benchmark performance to develop new energy aware scheduling (in terms of packet-scheduling and traffic-aware) for CoMP.

- **Investigate energy-efficiency and optimization for HetNet CoMP taking into account the power consumption of the backhaul.**

- Investigate different frequency planning and different transmission architecture.
- Investigate EE taking into account backhaul power consumption and maximize EE applying convex optimization theory.

## 1.4 Scientific Methodology Applied

The main objective of this PhD study is to provide a system level performance evaluation on the key approaches proposed in this thesis. Indeed, the system level performance can be analyzed by various means such as analytical approach based on system model, computer aided simulation and field trial in operational network. Analytical approach may render a feasible approach when the system model is simplistic in nature, but becomes impracticable for modern wireless cellular systems which are complex and involve very large number of assumptions and constraints. The system level performance of modern cellular systems depends on a large number of parameters whose behavior cannot be forecasted in advance, making it impractical to formulate a theoretical framework. On the other hand field trial requires the availability of the network, which may not always be feasible. In such condition the computer aided simulation approach delivers a suitable option. If the metrics are meaningful and the methodology reflects realistic networks, computer aided simulation is an effective way to compare different concepts and predict the network performance [15]. For this reason a computer aided system level simulation (SLS) has been used in this PhD study as the main performance assessment methodology, sometimes supported by the theoretical analysis to understand the simulation results more accurately. A short-description of the simulator which was used to analyze performance is given by Appendix A.

## 1.5 Thesis Contribution

This PhD study mainly contributes towards providing analytical and system level understanding of various 4G scenarios for enhancing both energy and spectrum utilization. The

LTE-Advanced system is mainly considered for this study.

The main contributions and novelty of this PhD study lies in the following:

- Until now, there was no analytical framework that provides the spectral and energy efficient trade-off dilemma for multi cell OFDMA wireless system. This thesis provides the SE-EE bound for multi cell scenario in OFDMA systems.
- No such performance study was available in the open literature for energy efficiency in CoMP for packet scheduling; this work not only provides a baseline for traditional scheduling policies, but goes beyond to propose advanced scheduling based on minimizing the energy per bit.
- No such performance study was available in the open literature investigating energy efficiency for HetNet CoMP scenario with backhaul power consumption. This thesis analyzes this aspect leading to specific design guidelines for future emerging green wireless networks.

The results of this study have resulted in fifteen scientific works, four of which have been accepted in international peer-reviewed journals with impact factor greater than one, these include:

- **Book Chapters**

1. Kazi Mohammed Saidul Huq, Shahid Mumtaz, Jonathan Rodriguez, and Rui L. Aguiar, “**Overview of Spectral- and Energy-Efficiency Trade-off in OFDMA Wireless System**” in *Green Communication in 4G Wireless Systems*, ISBN: 978-879-298-2056, River Publishers, Denmark, March, 2013.

- **Scientific Journal Papers**

2. Kazi Mohammed Saidul Huq, Shahid Mumtaz, Jonathan Rodriguez, and Rui L. Aguiar, “**A Novel Energy Efficient Packet-Scheduling Algorithm for CoMP**” in *Elsevier Journal on Computer Communications*, 2014.
3. Shahid Mumtaz, Kazi Mohammed Saidul Huq, Ayman Radwan, and Jonathan Rodriguez, “**Energy Efficient Scheduling in LTE-A D2D Communication,**” *IEEE Comsoc MMTC E-letter (Multimedia Communications Technical committee)*, in January, 2014.
4. Kazi Mohammed Saidul Huq, Shahid Mumtaz, Firooz B. Saghezchi, Jonathan Rodriguez, and Rui L. Aguiar, “**Energy Efficiency of Downlink Packet Scheduling in CoMP,**” in *Wiley Transactions on Emerging Telecommunication Technologies (ETT)*, 2013.
5. Shahid Mumtaz, Henrik Lundqvist, Kazi Mohammed Saidul Huq, Jonathan Rodriguez, and Ayman Radwan, “**Smart Direct-LTE Communication: An Energy Saving Perspective,**” in *Elsevier Journal on Ad Hoc Networks*, 2013.
6. Kazi Mohammed Saidul Huq, Shahid Mumtaz, Joanna Bachmatiuk, Jonathan Rodriguez, and Rui L. Aguiar, “**Green HetNet CoMP: Energy Efficiency Analysis and Optimization**” in *IEEE Transactions on Vehicular Technology*, 2013. (under revision)

7. Shahid Mumtaz, Kazi Mohammed Saidul Huq, and Jonathan Rodriguez, “**Direct Mobile to Mobile Communication: Paradigm for 5G**”, in *IEEE Wireless Communications Magazine*, 2013. (Submitted).
8. Shahid Mumtaz, Henrik Lindquist, Kazi Mohammed Saidul Huq, Ayman Radwan, and Jonathan Rodriguez, “**Odyssey of LTE-A D2D Communication: Tutorial Approach**”, in *IEEE Survey and Tutorial*, 2013. (Submitted).

- **Scientific Conference Papers**

9. Kazi Mohammed Saidul Huq, Shahid Mumtaz, Jonathan Rodriguez, and Christos Verikoukis, “**Investigation on Energy Efficiency in HetNet CoMP Architecture**,” in *IEEE International Conference on Communications (ICC)*, Sydney, Australia, 2014.
10. Shahid Mumtaz, Kazi Mohammed Saiul Huq, Jonathan Rodriguez, and Rui L. Aguiar, “**Energy Efficient Interference Aware Resource Allocation in LTE D2D Communication**,” in *IEEE International Conference on Communications (ICC)*, Sydney, Australia, 2014.
11. Shahid Mumtaz, Kazi Mohammed Saiul Huq, and Jonathan Rodriguez, “**Coordinated Paradigm for D2D Communications**,” in *1<sup>st</sup> International Workshop on Green Cognitive Communication and Computer Networking (GCCCN), IEEE International Conference on Computer Communications (INFOCOM)*, Toronto, Canada, 2014.
12. Kazi Mohammed Saidul Huq, Shahid Mumtaz, Muhammad Alam, Jonathan Rodriguez, and Rui L. Aguiar, “**Frequency Allocation for HetNet CoMP: Energy Efficiency Analysis**,” in *IEEE International Symposium on Wireless Communication Systems (ISWCS)*, Ilmenau, Germany, 2013.
13. Kazi Mohammed Saidul Huq, Shahid Mumtaz, Muhammad Alam, Ayman Radwan and J. Rodriguez, “**Energy Efficient CoMP Transmission in LTE-Advanced**,” in *IEEE Global Communications Conference (GlobeCom)*, pp. 401-404, Anaheim, California, USA, 2012.
14. Kazi Mohammed Saidul Huq, Shahid Mumtaz, Jonathan Rodriguez, and Rui L. Aguiar, “**Comparison of Energy Efficiency in Bits per Joule on Different Downlink CoMP Techniques**,” in *IEEE International Conference on Communications (ICC)*, pp. 5716-5720, Ottawa, Canada, 2012.
15. Kazi Mohammed Saidul Huq, Shahid Mumtaz, Jonathan Rodriguez, and Rui L. Aguiar, “**Energy Efficiency Optimization in MU-MIMO System with Spectral Efficiency Constraint**,” in *IEEE Symposium on Computers and Communications (ISCC)*, Madeira, Portugal, 2014.

## 1.6 Organization of the Dissertation

The PhD dissertation is organized as follows:

### **Chapter 2: 4G System Level Energy Efficiency Performance.**

This chapter provides the state-of-the-art analysis on the current energy efficient approaches for 4G/OFDMA systems. These results will act as benchmark for comparison against the

energy efficient approaches to be developed in subsequent chapters. In order to position our work, we review briefly the key components, and decision metrics that can influence the system level performance from a spectral and energy efficiency perspective.

**Chapter 3: Spectral and Energy Efficiency Trade-off in OFDMA Wireless System.**

This chapter introduces briefly the concept of Energy efficiency and Spectral efficiency trade-off in OFDMA networks, which is the radio access technique for 4G LTE-Advanced system. This study presents an overview of SE-EE trade-offs from an OFDMA wireless system perspective. Theoretical bounds on SE-EE trade-off are also discussed, followed by a single cell and multi cell study. Finally, an optimization algorithm is presented which maximizes EE given SE constraints for any given LTE-Advanced system such as Multi-User MIMO (MU-MIMO), and CoMP.

**Chapter 4: CoMP Energy Efficiency Performance Evaluation.**

This chapter analyzes the energy efficiency (EE) of different downlink packet scheduling in CoMP for LTE networks using classical state-of-the-art (SoA) packet scheduling algorithm approaches such as Maximum Carrier-to-Interference ratio (MCI), Proportional Fairness (PF) and the Round Robin (RR) scheduling applying different kinds of CoMP techniques.

**Chapter 5: Advanced Energy Efficient Scheduling in CoMP.**

This chapter proposes a novel energy efficient scheduling (EES) technique that can deliver energy efficient transmission to the UEs whilst providing fairness. The proposed algorithm is based on a novel scheduling metric that targets the ratio of the transmit energy per bit, and allocates the physical resource block (PRB) to the UE that requires the least amount of energy. Through computer simulation, the performance of the proposed EES packet-scheduling algorithm using mixed traffic is compared with the SoA packet scheduling algorithms such as MCI, PF and RR, which eventually shows a significant improvement. Moreover, a heuristic framework for CoMP scenario which minimizes the energy consumption of the network using the sleep and active mode of the transmission points on the basis of the traffic threshold is proposed.

**Chapter 6: Advanced HetNet CoMP architectures for OFDMA.**

This chapter extends the homogeneous CoMP architecture to a heterogeneous architecture where coordination between macro eNB and low power remote radio heads (RRH) is investigated. To this end, intra-CoMP and inter-CoMP architectures are studied to check the outcome of the coordination. Finally, a novel Energy-Efficient Design (NEED) incorporating a CoMP architecture base on MU-MIMO which was demonstrated to improve the spectral and energy efficiency, whilst reducing the interference. Moreover, applying the single frequency CoMP approach towards HetNet scenarios as a baseline, different frequency planning approaches such as FFR are investigated. The simulation results suggest that HetNet CoMP transmission can achieve enhanced overall cell energy efficiency for single frequency whereas using FFR increases cell-edge energy efficiency per user which evolves as a trade-off for the operator. Furthermore, this chapter investigates the energy efficiency (EE) maximization using convex maximization theory where the primary optimization criterion is the data rate in a downlink multiuser CoMP HetNet. Given QoS requirements, a constrained optimization problem is formulated, and we apply a novel resource allocation algorithm to promote EE further. Analytical insights and simulation results demonstrate the effectiveness of the proposed scheme for the targeted complex wireless systems.

**Chapter 7: Concluding Remarks.**

The contributions of the thesis are summarized here. We present conclusive remarks as general

design guidelines for promoting energy efficiency in OFDMA systems, along with suggestions for future research.

The organization of dissertation is shown in Figure 1.5.

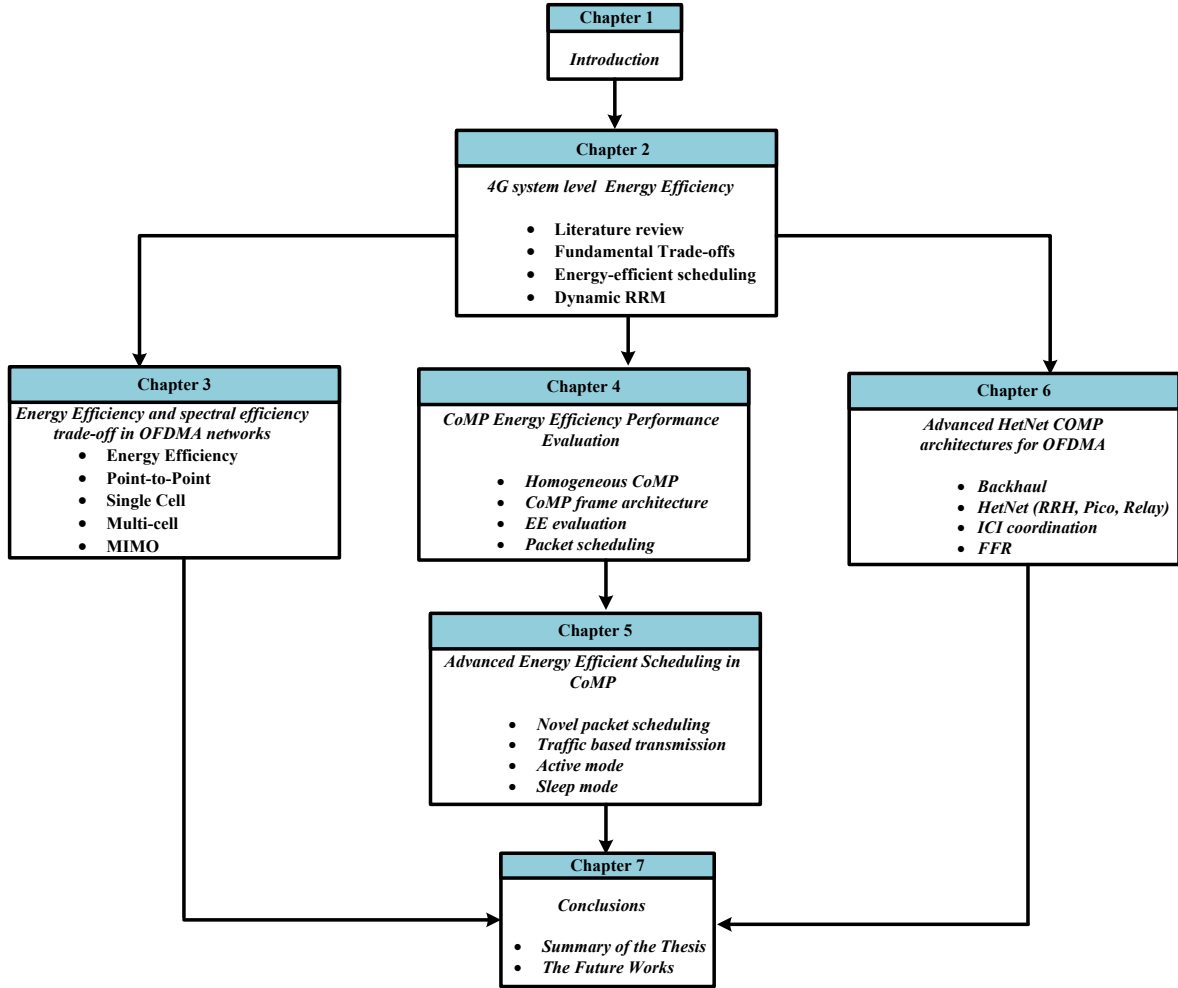


Figure 1.5: Thesis Organization



## Chapter 2

# 4G System Level Energy Efficiency Performance

*Wireless networking play a key role to reduce the energy and carbon footprint associated with information and communication technologies (ICT). In fact, the ICT industry constitutes 3% of the global energy consumption and contributes towards 2% of the worldwide CO<sub>2</sub> emissions [16]. This is comparable to the worldwide CO<sub>2</sub> emissions by airplanes or one quarter of the worldwide CO<sub>2</sub> emissions by cars [17]. According to [18], [11], the 57% of the energy consumption of the ICT infrastructure is attributed to users and network devices in cellular and wireless networks, the scale of which is still growing rapidly [19]. Given the dramatic expansion of wireless networks worldwide, the development of energy-efficient solutions for wireless networks can significantly reduce the energy consumption in the ICT sector. From the viewpoint of telecommunication operators, minimizing the energy consumption is not only a matter of being environmentally responsible, but can substantially reduce their operational expenditure. Furthermore, developing energy efficient products will open up new business models, since end-users will enjoy enhanced mobile services with longer battery lifetime [20]. This chapter provides the state-of-the-art (SoA) analysis on the current energy efficient approaches for 4G/OFDMA systems. These results will act as benchmark for comparison against the energy efficient approaches to be developed in subsequent chapters. In order to position our work, we review briefly the key components, and decision metrics that can influence the system level performance from a spectral and energy efficient perspective.*

### 2.1 Energy Efficient Radio Resource Management

Here, we provide state-of-the-art on energy efficient radio resource management (RRM) in wireless networks. Wireless communications are dynamic in nature. This dynamic nature arises from multiple dimensions: propagation conditions, cell load level, interference, etc. Thus, proper radio management of the available radio resources are needed.

Radio management is performed by an RRM entity with an associated number of parameters that need to be chosen, measured, analyzed and optimized. Efficient utilization of the radio resources leads to higher capacity, Quality of Service (QoS) guarantees, and better user experience. RRM functions should take into account the constraints imposed by the radio interface in order to make decisions regarding the configuration of the different elements and parameters (e.g., the cell size, antenna numbers, the number of users transmitting at the same

time). It is pretty evident that the number of parameters to be considered as well as their nature identifies a set of RRM functions whose joint behavior should lead to an overall radio access network optimization [21]. In order to perform properly in a real network environment, RRM schemes should be low in complexity, and require low signaling overhead whilst delivering high performance. Furthermore, they must provide stability and overload protection to the network, in addition to allowing the network to autonomously adapt to dynamic traffic and environment changes. The following subsections cover the above mentioned aspects related to “energy efficient” RRM, where we first describe the design requirement/trade-offs.

### 2.1.1 Fundamental Trade-Offs in RRM Protocol Design

RRM protocol design implies several trade-offs involving energy efficiency. In [22] the authors present four fundamental trade-offs for energy efficiency to drive the design of RRM in next generation cellular networks, which are briefly described herein.

- **Deployment Efficiency versus Energy Efficiency Trade-off**

Deployment efficiency (DE) is a performance indicator of a wireless networks which quantifies system throughput in terms of per unit of deployment cost. Deployment cost includes Capital expenditures (CAPEX) and operational expenditures (OPEX). Wireless engineers estimate the network CAPEX and OPEX are addressed during network planning and EE is mostly considered during network operation.

As an example (see [23]) cell radius has a relevant impact on EE: the greater the radius means a reduction in the EE. As a consequence, to maximize EE we need to deploy additional transmission points, which in turn could increase the deployment cost. This implies the need to identify the proper balance between the DE and EE requirements. LTE-Advanced adopted a heterogeneous networks paradigm, which could provide enhanced deployment functionalities (femto/small cells, coordinated multi-point (CoMP), etc.) to enable proper DE-EE trade-offs.

- **Spectral Efficiency versus Energy Efficiency Trade-off**

Traditional research on wireless networks mainly focuses on system capacity and spectral efficiency (SE), defined as the system throughput per unit of bandwidth. The spectral efficiency is a key performance indicator of wireless cellular networks and the peak value of SE is always among the key performance indicators of 3GPP evolution. On the other hand, energy efficiency (EE) accounts for energy consumption: i.e. using less energy to provide the same level of service or using same energy to accomplish improved services.

For point-to-point transmission in an additive white Gaussian noise (AWGN) channel, the relationship between EE and SE is shown to be in general monotonically decreasing[22]. However, for next generation wireless networks (3GPP LTE, WiMAX), reference OFDM/OFDMA technology [12, 24] and non-Gaussian channel models make such relationship more complex. Rate adaptation (RA, which maximizes throughput and thus increases SE) and margin adaptation (MA, which minimizes total transmit power, and thus increased EE) [25] are the two main resource allocation schemes to control the SE-EE trade-off in such framework. Improving the SE-EE trade-off curves as a whole and tuning the operation point on the curve to balance the specific system requirements are expected to guide practical system designs toward energy compliant solutions. Moreover, an accurate closedform approximation of the SE-EE trade-off has

not been discussed for multi-cell scenario, which is a contribution to be addressed by this thesis. Nevertheless, the concepts demonstrated in this section can be used for evaluating the impact of MIMO, coordinated multi point transmission/reception and relay on the SE-EE trade-off.

- **Bandwidth-Power Trade-off**

Bandwidth (BW) and power (PW) are the most important yet limited resources in wireless communications. From Shannon's capacity formula, the relationship between transmit power and signal bandwidth demonstrate a monotonic trend [22]. For future wireless system such as UMTS and LTE, the trend remains similar.

Future wireless systems such as LTE-Advanced demonstrate more flexibility in spectrum usage compared to GSM and UMTS, since spectrum re-farming is built-in LTE-Advanced. The deployment of different heterogeneous networks in LTE, such as coordinated multiple point (CoMP) and distributed antenna system DAS, introduces additional infrastructure nodes into the network, which increases control on the BW-PW trade-off.

- **Delay-Power Trade-off**

Delay (DL) is defined as service latency, i.e. a measure of quality of service (QoS) and quality of experience (QoE) [22]. Design of wireless networks should cope with both channel and traffic uncertainties, which makes the characterization of DL-PW trade-off more complex.

Few published works deal with DL-PW trade-off in wireless cellular networks, even though wireless systems need to deal with service latency in order to support users' expectations. As a consequence, it is necessary to analyze when and how to trade service delay with power consumption.

### 2.1.2 Cross-Layer Framework for Energy-Efficient Resource Allocation

A key component in RRM is the scheduling approach that identifies how to map the available resources to the user queues according to a priority assignment. This assignment is based on a given scheduling policy that can exploits specific network parameters (or context information) to feed a predetermined cost function. This function is intellectual property and governed by the network operator, and we can immediately observe that the type of function will have a large bearing on the operating performance of the network, and therefore energy efficient operation can be directly linked to the way we design this function

An energy-efficient design can benefit from a cross-layer (CL) approach as several layers of system design have impact on power consumption ranging from silicon to applications. The authors in [26] particularly focused on a system-based approach towards optimal energy transmission and resource management across time, frequency, and spatial domains. A framework for EE is developed in [27] and depicted in Figure 2.1. The mentioned paper focuses on improving device energy-efficiency. Cross-layer approaches exploit interactions between different layers and can significantly improve energy-efficiency as well as adaptability to service, traffic, and environment dynamics. Since wireless network is a shared medium, layering is not the best approach to create impact on device energy consumption comprising a point-to-point

communication link, because it impacts the entire network due to the interaction between links. Therefore a system approach better suits energy-efficient wireless communications.

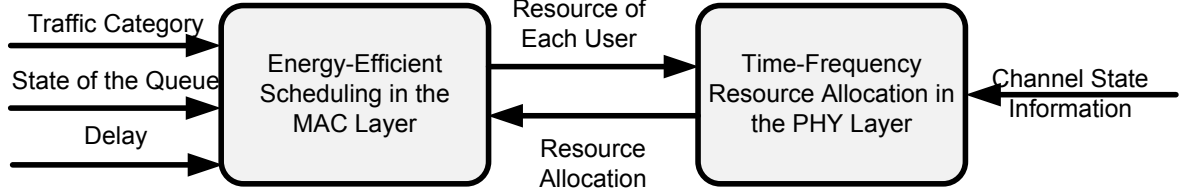


Figure 2.1: Framework of EE based Cross-Layer Resource Allocation

The medium access control (MAC) layer deals with wireless resources for PHY layer and directly affects overall network performance. Traditional wireless systems have no power adaptation. System-level energy-efficiency is determined by a set of PHY parameters. The performance of the system ought to be adjusted to adapt the real user requirements (e.g. throughput and power consumption) and environments (such as propagation and multipath channel model) to trade off energy-efficiency and spectral efficiency. The MAC layer ensures that wireless resources are efficiently allocated to maximize network-wide performance metrics while maintaining user quality-of-service (QoS) requirements. According to [26] two types of access are discussed. In distributed access schemes, the MAC should be enhanced to reduce the number of wasted transmissions that are corrupted by other user interference or antenna elements, while in centralized access schemes, efficient scheduling algorithms should exploit the variations across users to maximize overall energy efficiency of users in the network. From the Shannon capacity, energy-efficiency can only be obtained at the cost of infinite or huge bandwidth and results in zero or very low spectral efficiency.

The MAC layer can enhance energy efficiency using the following three methodologies [26].

- ⇒ Energy can be saved in mobile devices by shutting down system components when inactive. The MAC can enable inactive periods by scheduling shutdown intervals according to buffer states, traffic requirements, and channel states.
- ⇒ The MAC layer controls medium access to assure both individual QoS and network fairness. In distributed access schemes, the MAC should be improved to reduce the number of retransmissions; while in centralized access schemes, efficient scheduling algorithms should exploit the channel and traffic variations across users to maximize overall energy efficiency in the network.
- ⇒ Power management at the MAC layer reduces the standby power by developing tight coordination between users such that they can wake up precisely when they need to transmit or receive data.

### 2.1.3 Load Adaptive Resource Management

To satisfy the users' QoS requirements most current network dimensioning is peak load oriented. As a matter of fact, the majority of the existing literature [28, 29, 30] demonstrated that everyday traffic loads at base stations change widely over time and space. Therefore, a great deal of energy is wasted when the traffic load is low. Vendors and operators realized this

problem and acted upon this. For example, Alcatel-Lucent proclaimed a new feature in their software upgrades called dynamic power save, which is quoted to save 27% power consumption for BSs deployed by China Mobile [31]. Energy-saving solutions through cell-size breathing and sleep modes, based on traffic loads, were proposed by the OPERA-Net project [32].

In [33], [27], a measured traffic pattern was analyzed enabling optimal power-saving schemes using cell switch-off under a trapezoidal traffic pattern, where it is shown that a 25-30% energy saving is feasible by merely switching off the active cells during the periods of low traffic activity. Nevertheless, the impact of switch-off on coverage was not investigated. In [29], the authors investigated the notion of blocking probability requirement enabling a traffic-aware BS mode (active or sleeping) switching algorithm. One minimum mode holding time was also recommended to avoid frequent BS mode switching. It was demonstrated that changing the holding time over a specified range will cause trivial performance change on either energy saving or blocking probability [29]. The effect of the traffic mean and variance as well as the BS density on the energy saving strategy with BS switching was extensively studied in [30], which proved that energy savings will increase with the BS density and the statistical ratio of the traffic load. In [34], they presented some possible approaches to establish energy consumption of the BS's scale with the traffic load across space, frequency and time domains. According to [35], joint reconfiguration of the bandwidth and the number of antennas and carriers according to the traffic load gained maximum energy saving. Similar energy-saving solutions based on user load variations on the terminal side were described in [36].

#### 2.1.4 Service Differentiation

Service differentiation mainly deals with the trade-off between energy consumption and delay [37]. The trade-off between energy consumption and delay was extensively studied in the literature for wired non-cellular network. For cellular wireless networks, only few works had been done in the early systems (1G, 2G systems), because only limited service types (mainly voice communications) were available. However, the evolution cellular systems provided the vehicle for more sophisticated services and devices (smart phones, iPhone, and the blackberry among others). To be precise, some applications, such as video conferencing, web-based seminars, and video games, require real-time service; and other applications, such as email, and downloading files for offline processing are delay tolerant services. Therefore, it is useful to separate the types of wireless traffic and build the energy consumption mechanism protocol with the traffic type.

Several researchers have targeted the efforts on the service latency of applications to reduce the energy consumption in cellular networks. In [38], energy-efficient power and rate control with delay QoS constraints using a game-theoretic approach was presented. The demonstration was based on CDMA system. They translated the delay constraint of a user into a lower bound on the user's output SIR (signal-to-interference ratio) requirement; afterwards the Pareto-dominant equilibrium solution is derived. The delay performance of users at the Nash equilibrium was also analyzed. Inspired by mobility-prediction-based transmission strategies, which are usually used in delay tolerant networks, a store-carry-and forward (SCF), relay-aided cellular architecture was proposed in [39, 40]. According to [35], in the SCF scheme, when the application data is not delay prone, a user can first transmit the data to a mobile relay (for instance, a vehicle) which conveys the message close to the BS, and then the mobile relay retransmits the data to the BS. Numerical results in [40] depicted that,

for delay insensitive services, a factor of more than 30 in energy savings can be obtained by SCF compared to direct transmission.

## 2.2 Exploitation of Multi-User Diversity

The process of multiple users experiencing independent fading channels is known as multi-user diversity (MUD). In an energy efficient context, it turns out that the sum capacity (sum of the simultaneous user capacities) is maximized if, for each time instant, the user with the best energy efficient channel gain is scheduled. The gain achieved with such strategy can be defined as energy efficient MUD gain. According to [41, 42], the most feasible solution takes into account a power control law which uses more transmit power for strong channels than weak channels. This solution is the opposite to conventional power control which uses transmit power to compensate weak channels.

A major problem for energy consumption multi-user diversity adaptation is how to design heuristic algorithms that achieve the multi user diversity gain while ensuring minimum energy consumption or increasing the QoS requirements using same amount of power under realistic conditions.

## 2.3 Relay Scheduling

Relaying is widely acknowledged as a means to improve capacity and coverage in Wireless Broadband Networks [43]. The properties of the relay concept and the benefits that can be expected are as follows:

- Radio coverage can be improved in scenarios with high shadowing (e.g. bad urban or indoor scenarios). This allows to significantly increase the QoS of users in areas that are heavily shadowed. The extension of the radio range of BS by means of relay allows operating much larger cells with broadband radio coverage than with a conventional one-hop system.
- Using relaying can reduce the overall system level energy consumption and pave the way to public acceptance, while in the case of mobile terminals it has the potential to increase battery lifetime.
- The fixed relay concept provides the possibility of installing temporary coverage in areas where permanent coverage is not needed (e.g. construction sites, conference-/meeting-rooms) or where a fast initial network roll-out has to be performed.
- The wireless connection of the relay to the fixed network substantially reduces infrastructure costs, which in most cases are the dominant part of the roll-out and operational costs; relay only requires a main supply. In cases where no main supply is available, relays could rely on solar power supply. A relay cellular network is illustrated in Figure 2.2.

A standard-conformant integration of the relays into any MAC frame based system would allow for a stepwise enhancement of the coverage region of an already installed system. Investments in new BS can be saved, and any hardware product complying with a wireless MAC frame based standard can be used without modifications.

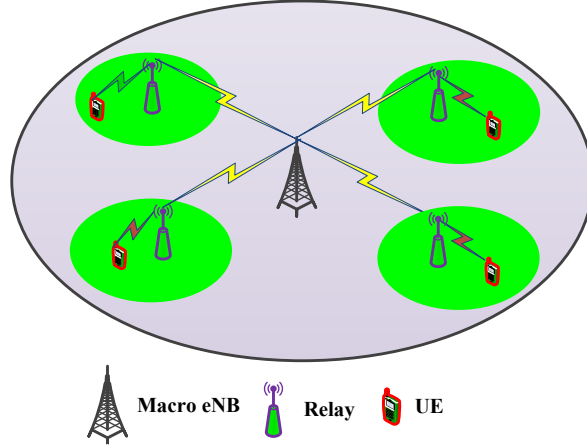


Figure 2.2: Relay Cellular Network

An application of relay technology is the LTE-A system. LTE-A promises to provide improved performance with the aim of achieving high speed, high-capacity communication, and service capabilities beyond LTE. LTE Release-10 includes all the features of Rel-8/9 and several new ones, the most important of which are: carrier aggregation enhanced multi-antenna support, improved support for heterogeneous deployments, and relaying [21]. In LTE-Advanced an important issue in addition to achieving high-speed and capacity is to provide greater throughput for cell-edge users which could be accomplished by employing relay technology. Few of the main reasons for choosing relay technology for the LTE-A system are given as follows.

- **Lack of Fairness:** In a conventional cellular network (CCN), a base station (BS) controls a number of mobile stations (MS) within its own coverage area and all the terminals communicate directly with the BS. The current conventional deployment of cellular systems exhibit certain inherent problems such as low signal-to-noise-ratio (SNR) at the cell edge, lack of fairness, coverage holes that exist due to shadowing and non-line-of-sight (NLOS) connections.
- **Energy consumption:** The CCN has been primarily designed to meet the challenges of service quality. More recently, there is a growing focus on the importance of energy consumption, both from an operational expenditure (OPEX) point of view and from a climate change perspective. Over the past few years, the communication industry has pledged to reduce carbon emissions of wireless networks by up to 50% by 2020 [44]. Minimizing energy consumption in LTE-A network has been at the forefront of system design, and architectural approaches which recently have been proposed include femto-cells, advanced spectrum management, efficient power amplifier, antenna technologies, etc.

however, using relay technology can amplify the energy gain further. It can be considered as an extension of the specific base station/eNB, and it uses the base-station air interface resources; therefore it does not require a separate backhaul connection while the femtocell and picocell act as separated base station using specific resources and hence require a separate backhaul connection. Picocell and Femtocell differ from each other in power range and capacity level [45].

Most existing work concentrates on single-point-to-single-point transmission; how to allocate resources in multi-point-to-single-point or multi-point-to-multi-point transmission, as in the multi-cell case needs further attention. Incremental time and power may be used for resource allocation during relay transmission. How to minimize the total energy consumption to ensure greater energy efficiency taking the additional overhead into account is not known succinctly.

## 2.4 Energy Analysis SISO vs. MIMO with Packet Scheduling

Han et al. analyzed and demonstrated energy efficiency of SISO and MIMO [46] and use LTE standpoint as a case study. LTE already specified the Alamouti-based [47] space-frequency block coding (SFBC) technique for MIMO. They also considered spatial multiplexing (SM) as another MIMO approach. In SM, independent symbols are transmitted over different antennas as well as over different symbol times. They described for specific data rates, the energy efficiency of SISO and MIMO schemes employing different levels of modulation order and coding rates. In [46], the authors described two types of energy analysis in the LTE system. These include:

1. Energy efficiency performance evaluation without considering overhead.
2. Energy efficiency performance evaluation with overhead.

The power level of the overhead shows a significant impact on the energy consumption ratio (ECR) of all schemes at low spectral efficiency range as the power required by transmitting user data is relatively low. As a result, the ECR of all schemes for low spectral efficiency transmission is significantly increased. These are the stepping stone of the energy efficiency analysis of SISO and MIMO.

Some of the open issues for multi-user and multi cell environments in MIMO still require attention, such as how to utilize the spatial resource to maximize EE while suppressing interference, since the existence of inter user and inter cell interference complicates the design of energy-efficient MIMO systems. Effective but simple algorithms need to be developed to obtain a trade-off between complexity and performance for MIMO-OFDMA system.

### 2.4.1 Energy Efficiency in classical Packet Scheduling Techniques

The three major SoA resource scheduling algorithms which deal with downlink packet transmission are here discussed herein, these include maximum carrier-to-interference ratio (MCI) [48], round robin (RR) [49] and proportional fairness (PF) [50].

In the MCI method the users are scheduled to use radio resources based on maximum channel gain. This scheme is straight forward, in the sense that users are ranked according to their experienced channel gain. In other words, the user with the best channel quality indicator (CQI) has the highest ranking and is scheduled to utilize the physical resource blocks (PRB) for the specific time. The user with the next best CQI condition is then scheduled to utilize PRBs and so forth. The ranking ' $U$ ' can be found using the following equation:

$$U = \arg \max_u (\beta_{u,m}(t)) \quad \text{for PRB } m \quad (2.1)$$

where  $\beta$  is the vector of experienced channel gain of UE,  $u$ , for one PRB,  $m$ , in time  $t$ . The flowchart of the MCI scheduling is depicted in Figure 2.3.

In order to perform scheduling, terminals send (in uplink) CQI to the BS. Basically in the downlink, the BS transmits the reference signal (downlink pilot) to the terminals. These reference signals are used by the UE for measuring the CQI; a high value for CQI means high quality channel condition. We should keep in mind that CQI is reported per PRB. MCI scheduling [51] can increase the cell capacity at the expense of fairness. For conventional cellular networks exploiting this scheduling strategy, terminals located far from the base station (i.e. cell-edge users) are unlikely to be scheduled.

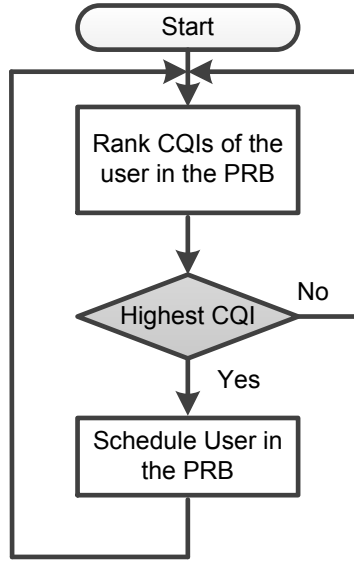


Figure 2.3: MCI Packet Scheduling technique

In RR, the radio resources i.e., PRBs, are allocated to UEs in a round robin fashion irrespective of channel condition. The first opted UE is served for a specific time period and then these resources are revoked back and assigned to the next user for another time period. The previously served user is placed at the end of the waiting queue so that it can be served with radio resources in the next round. Newly arriving requests are also placed at the tail of the waiting queue. This scheduling continues in the same manner [49]. Thus every user is equally scheduled without taking the CQI into account as illustrated in Figure 2.4. The principal advantage of Round Robin scheduling is the guaranty of fairness for all users, and it is easily implemented. Since Round Robin does not take the channel quality information into account, it results in low user throughput.

In the PF algorithm, for PRB  $m$ , the highest ranked user  $u'$  is scheduled to transmit according to the following:

$$u' = \arg \max_u \left( \frac{R_{u,m}(t)}{T_u(t)} \right) \quad (2.2)$$

Where,  $R_{u,m}(t)$  denotes the instantaneous achievable rate at PRB  $m$  and  $T_u(t)$  is the user's average throughput. The average throughput,  $T_u(t)$ , is updated for each new time interval (after all PRBs are allocated).

This scheduler aims to combine throughput efficiency with long term resource-fairness. Practically, this scheduling policy provides the same fraction of resources for all the users in the long-term perspective. However, in each time-instance users are prioritized based on their normalized channel condition. The normalization factor is the past profile of each user, i.e. the exponential averaged data rate. As in equation (2.2), the numerator of this scheduling metric is in favor of the best-channel users, while the denominator tries to balance resource-fairness by penalizing the users with good past profile [49]. PF is throughput efficient and provides long term fairness through equalizing the resources allocated to different users in the system. Figure 2.5 depicts the flowchart of the PF algorithm. This policy does not provide any explicit bound on the QoS requirement of different users in the system [49].

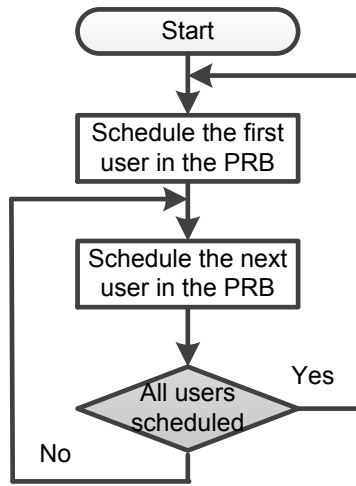


Figure 2.4: RR Packet scheduling technique

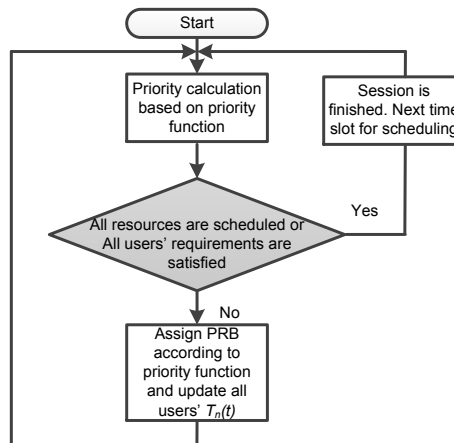


Figure 2.5: PF Packet Scheduling Technique

In [52], the performance of an LTE system with various packet scheduling algorithms was studied from an energy efficiency point of view. In this work, the performance of various classical scheduling algorithms such as RR, PF and MCI was used as a basis for the assessment of further innovative energy aware algorithms. They also analyze gains in terms of the energy consumption index (with respect to Round Robin scheduler). Figure 2.6 presents a benchmark of different packet scheduling in terms of EE in LTE system.

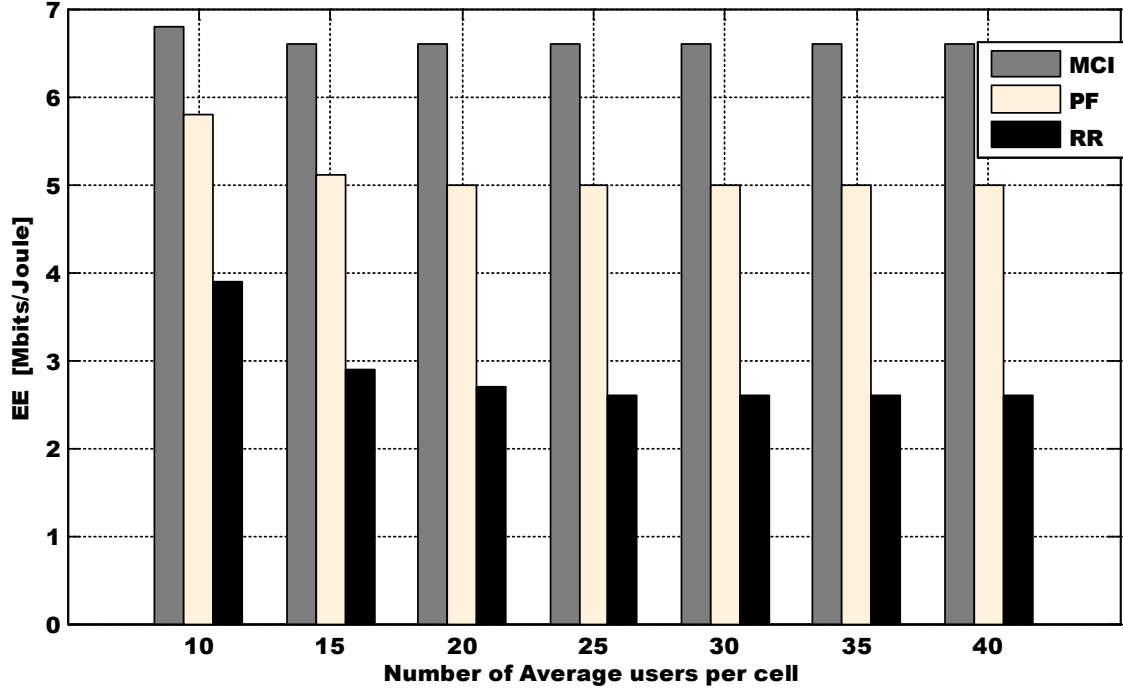


Figure 2.6: Energy efficiency packet scheduling in LTE-Advanced

The paper [53] presents a link level analysis of the rate and energy efficiency performance of the LTE downlink considering the unitary codebook based precoding scheme. The authors consider a multi-user environment to improve the performance gain by exploiting multi-user diversity in the time, frequency and space domains, and translating the gains to an energy reduction at the base station. Several existing and novel dynamic resource allocation algorithms were studied, such as PF, FCA (Fair Cluster Algorithm), RSSA (Received Strength Scheduling Algorithm) and EG-DA (Equal Gain Dynamic Allocation) among others, for the LTE system. The authors mainly focus on the rate and power consumption performance of the 3GPP LTE-OFDMA downlink system employing SU-MIMO. Both of the above mentioned works employ standard transmission scheme using no coordination or cooperation between cells.

On the other hand, some works have already analyzed CoMP concepts. According to [54], a gain in the downlink cell-edge throughput as well as cell average throughput can be achieved in LTE-Advanced network with the CoMP transmission architecture. It refers to the possibility to coordinate the downlink transmission towards the same user adopting multiple base stations.

Similarly, our work in [55] shows important benchmark EE analysis of different CoMP

techniques. As presented in Figure 2.7, the EE increases with the number of users, which is due to multi user diversity, and is more improved in techniques that exploit a larger number of users with more antenna diversity. To clarify this, Joint Transmission (JT) and Dynamic Point Selection (DPS) are more EE when compared to Coordinated Scheduling / Beamforming (CS/CB) due to greater antenna diversity of coherent transmission of multi antenna and base stations, that is muted in the case of DPS. Both these techniques outperform CS/CB thanks to their capability to transmit more reliable bits per unit of energy consumed. From our own simulations, we observed that until a certain number of users are reached, EE is virtually similar for both CB and DPS. Increasing the number of users beyond, widens the EE gap between CB and DPS.

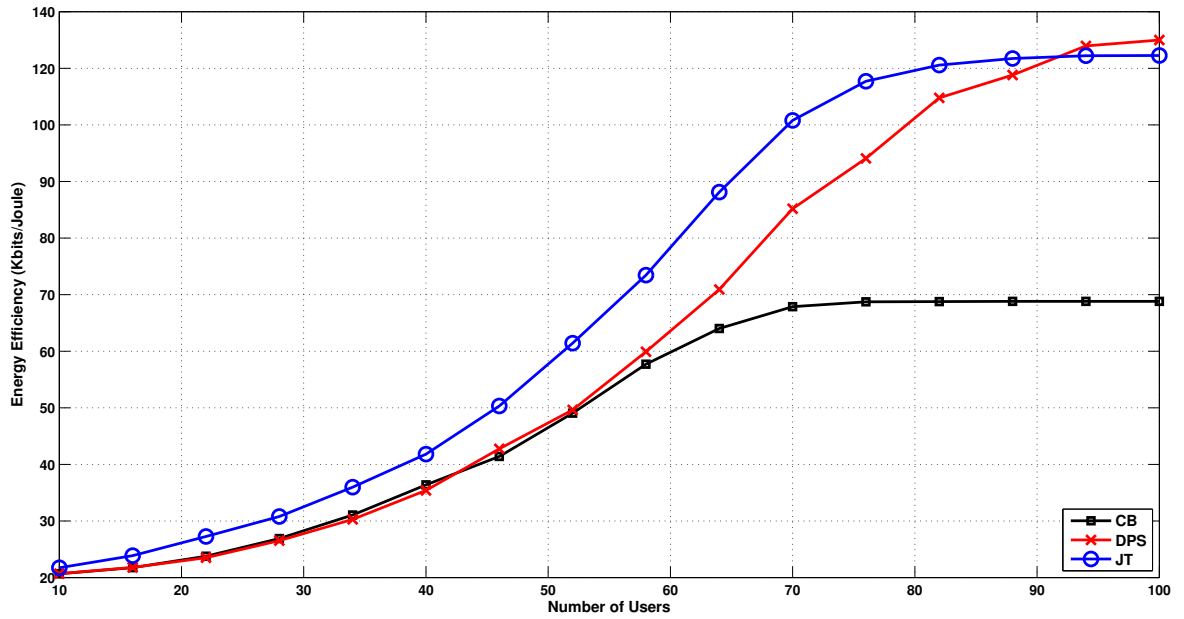


Figure 2.7: EE vs. Users

No work has been done to analyze EE of different CoMP techniques for classical SoA packet scheduling algorithms in LTE-Advanced. The benchmark results above provides us the impetus to analyze three packet scheduling methods in terms of EE for different CoMP techniques that include JT, DPS, and CS/CB which will be discussed later on.

## 2.4.2 Energy Efficiency based Coordinated RRM for Multi-cell Systems

Here we deal with coordinated RRM based on multi-cell scheduling. Wireless communication networks are generally deployed and adapted according to the average expected traffic load, by carefully designing the cell radius and the reuse factor. However, this static approach under performs and fails to reach the accepted limits in the context of spectral efficiency, in particular at low reuse rates. Since there is no mechanism in place for coordinating the sector bandwidth allocation to match the instantaneous spatial distribution of the users, their QoS requirements, and link quality.

In general, mobile user distribution within a cell and their channel condition are responsible for the reuse factor selection. Thus, using a single reuse factor within a cell is not particu-

larly efficient. For instance, users that are close to their serving BS can reuse resources since interference is low, whereas cell-edge users, which are close to other sectors, should rely on an exclusive allocation of spectrum policy. The scheduling policy, which determines the users to be served, impacts on the suitability of the reuse factor and, therefore, the reuse factor determination should be included in the scheduling process. The study in [56] demonstrated a large potential for improvement in terms of spectral efficiency, but at the cost of increased information overhead for coordinating sectors of adjacent antennas. However, it remains low in comparison with the CoMP approach where full cooperation is utilized and, thus, it can be seen as a practical approach. In EARTH [56], one coordinated RRM was proposed for uplink scenario from the point of view of energy efficiency. However, nothing was done for downlink multi-cell scenario which is still an open issue.

## 2.5 Interference Management for Heterogeneous networks

Heterogeneous networks phenomenon was proposed in LTE-Advanced framework as a means to increase the spectral efficiency [57], and provide seamless coverage. According to [58], a multi-tier network topology appears to increase system performance due to the achievable radio link performance, providing a system level gain close to the theoretical limit of 3G. In this strategy, macro base stations are used to provide blanket coverage, on the other hand, small low power base stations are introduced to eliminate the coverage holes and at the same time increase the system capacity in hotspots [57]. Recently these heterogeneous networks are investigated to increase the energy efficiency of the network, however this new scenarios requires more stringent interference management.

The Interference problem can arise in difference forms. One type of interference is defined as intra-cell interference, which is defined as the interference from users within the same cell, whereas interference emanating from other cells refers to inter-cell interference; both of which lead to reduced system coverage and degrade the delivered QoS. Sometimes we misinterpret fading and interference. Fading is a phenomenon that is created by the natural random process from different copies of the signal after traveling through a time-variant multipath environment. In comparison, interference is mainly caused by artificially created signals that coexist with the desired signal along the same physical dimensions: code, frequency, space and time.

The term interference cancellation is commonly used in the literature for signal processing applications that exploit algorithms in which the “interference signals” can be estimated and emulated in a reliable way, and canceled from the desired signal [59]. Various kinds of interference are present depending on the type of communication systems, the source of interference, and who is being subject to such interference. For instance, in WLAN [60], the interference occurs when neighboring systems that work in adjacent, or in the same frequency bands. This type of interference is called inter-system interference; and, as expected, its reduction or complete mitigation implies using complex and expensive devices.

One of the best known types of interference in wireless channels arises from transmitting a finite alphabet symbol through a multipath or band-limited channel, which is called inter-symbol interference [59]. Intersymbol interference had been the subject of substantial research efforts during the last decades or so. As another example, OFDM systems, experience inter-carrier interference that is caused by carrier frequency offset and phase noise due to the imperfect nature of the transmitter and receiver ends, thus causing the signal at a particular

subcarrier to being affected by the superposition of several other subcarriers. A cyclic prefix is designed to combat this [61], different users might be assigned different subcarriers when OFDM technology is used as the multiple access technique, (i.e. OFDMA), hence, intercarrier interference is also known as inter-user or multiple access interference.

One of the main objectives of energy efficient BS cooperation is to ensure that all the energy that is spent by the base stations is fully used to transport data [56]. In EARTH they demonstrated that interference can be seen as a waste of energy if it is uncontrolled. Several methods were proposed for BS cooperation using the backhaul links [56]. Depending on the capacity of these links, the cooperation can be implemented in the data plane by using joint or distributed processing algorithms, or in the control plane by coordinating the allocated resources for the users that are impacted by the inter-BS interference. They denoted a mechanism based on fractional frequency reuse (FFR) that exploits the reuse planning strategy. It consists in adjusting dynamically the parameters of the FFR strategy depending on the density of the served users. Still this system needs more research from an energy efficiency perspective.

Reference [1] describes the femto cellular networks from both the technical and business aspects. They also emphasized the challenges of implementing these types of networks and focused on some potential research opportunities. It is indicated in [1] that femto cellular networks must deal with additional timing and synchronization, as well as interference management issues, which result in additional signaling overhead and potentially greater energy consumption. Thus, how to design and manage energy-efficient femto cellular networks is still an open research issue. Reference [62] emphasized one major problem for future research regarding the interference of heterogeneous networks. How to manage interference and design algorithms with respect to EE for heterogeneous networks. Since there will be more transmitter sources and access points with heterogeneous deployment, there is the potential greater interference and more frequent handoffs.

## 2.6 Conclusions

In this chapter, we provided the state-of-the-art (SoA) analysis on the current energy efficient approaches for 4G/OFDMA systems. We provided a brief overview of the main concepts used in the energy efficient radio resource management (RRM) and then summarized existing fundamental works and advanced techniques for energy efficiency for OFDMA based cellular networks. The discussions and the results in this chapter will act as benchmark for comparison against the energy efficient approaches to be developed in subsequent chapters.

## Chapter 3

# Spectral Efficiency and Energy Efficiency Trade-off in OFDMA Wireless System

*Spectral efficiency (SE), defined as the system throughput per unit of bandwidth, is a widely adopted indicator for wireless network performance evaluation. The peak value of SE is always among the key performance indicators of 3GPP evolution. For example, the downlink SE target of 3GPP is a factor of 10 on the GSM standard [22]. Energy saving and environmental conservation are becoming global trends, shifting wireless communications researchers and engineers are shifting their efforts towards EE oriented design, that is, green radio communications (GRC) [22]. There have been several research efforts aimed at energy savings in wireless networks, such as designing ultra-efficient power amplifiers, reducing feeder losses, and introducing passive cooling [63]. However, striving to achieve a balanced trade-off between EE and SE can be challenging and is even a contentious paradox [26, 64]. Studying how to dimension future emerging cellular networks from these two perspectives in particular for OFDMA systems, is an open issue. Orthogonal frequency division multiplexing (OFDM) is the accepted technology for delivering this performance in LTE [65] or also referred to 4G. OFDM has the ability to combat frequency-selective fading as well as a vehicle for high data rate connectivity. While OFDMA can provide high throughput and SE, its EE performance has not been comprehensively investigated. To comply with the green radio communication paradigms, it is necessary for OFDMA to ensure a certain level of EE. This chapter introduces the concept of energy efficiency and spectral efficiency trade-off in OFDMA networks. The SE-EE trade-off is investigated along with theoretical bounds to delineate the operating region for the single cell and multi cell scenario. Finally, an optimization algorithm is presented which maximizes EE given the SE constraints for any given LTE-Advanced system such as CoMP.*

### 3.1 Background

Given an available bandwidth, the act of balancing the achievable rate and associated energy consumption of the system is defined as the SE-EE trade-off. Firstly, we discuss the SE-EE relation in the case of a point-to-point connection. Later we provide an overview of SE-EE in an OFDMA system for a single cell.

### 3.1.1 Point-to-Point AWGN Channel

For a point-to-point transmission, the relation between SE and EE is clearly discussed in [22], assuming additive white Gaussian noise (AWGN) channels. Using their work as a reference, we describe in more detail the SE-EE curve and trade-off.

To characterize the SE-EE trade-off for point-to-point transmission in AWGN channels, Shannon's capacity formula obviously plays a key role. From Shannon's formula [66], the achievable transmission rate,  $R$ , under a given transmit power,  $P$ , and system bandwidth,  $B$ , is

$$R = B \log_2 \left( 1 + \frac{P}{BN_0} \right) \quad (3.1)$$

where  $N_0$  is the noise spectral density.

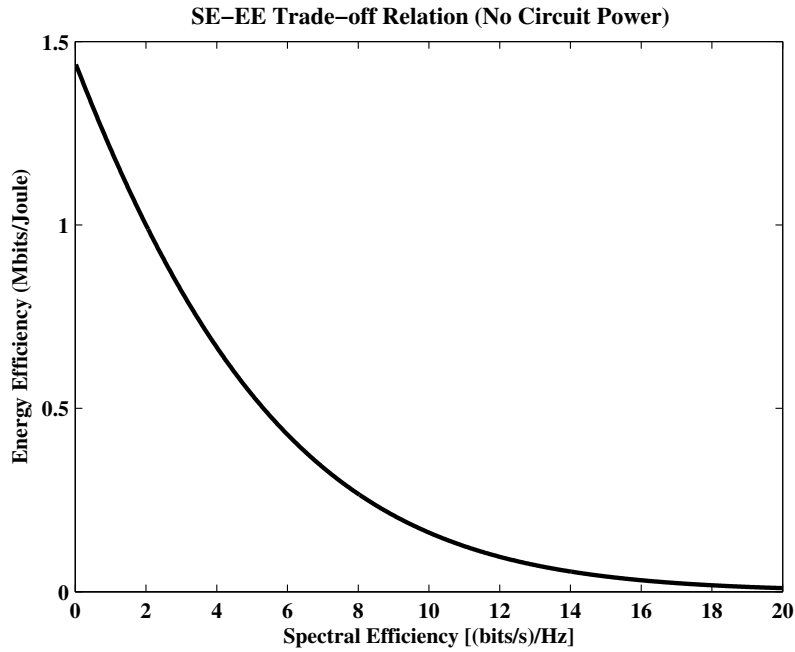


Figure 3.1: SE-EE Trade-off in Ideal AWGN channel Scenario

The maximum achievable transmission rate is the channel capacity of a system which is measured in spectral efficiency. The SE has originally been defined as the ratio of the transmission rate (bits per second) to the spectrum bandwidth (Hertz) [67, 68]. According to the definition of SE, that is, how efficiently a limited frequency spectrum is utilized and is usually expressed in terms of bits/s/Hz. So, Mathematically we can express SE as,

$$SE = \log_2 \left( 1 + \frac{P}{BN_0} \right) \quad (3.2)$$

EE has first been introduced in [69] and is simply defined as the ratio of the capacity to the rate of signal power i.e. the number of bits that can be transmitted per unit energy of energy consumed. For example, in a channel with power  $P$  watts and achievable transmission rate  $R$ , the EE can be expressed in the following,

$$EE = \frac{R}{P} = B \log_2 \left( 1 + \frac{P}{BN_0} \right) / P \quad (3.3)$$

EE is expressed as bits-per-Joule capacity (bits/Joule) \*. For a high capacity system, when a large number of bits are transmitted, for the sake of convenience EE can be expressed as kilobits-per-Joule (Kbits/Joule), megabits-per-Joule (Mbits/Joule) and so on. Using equation (3.2) and (3.3) we can derive the SE-EE relation as follows–

$$EE = \frac{B \log_2 \left( 1 + \frac{P}{BN_0} \right)}{P} = \frac{BSE}{P} = \frac{BSE}{(2^{SE} - 1)BN_0} = \frac{SE}{(2^{SE} - 1)N_0} \quad (3.4)$$

The relation is depicted in Figure 3.1.

The SE-EE relation is monotonically decreasing [22]. The EE tends to converge to a constant when the SE tends to zero [22]; that is

$$\lim_{SE \rightarrow 0} EE = \lim_{SE \rightarrow 0} \frac{SE}{(2^{SE} - 1)N_0} = \frac{1}{N_0 \ln 2} \quad (3.5)$$

On the other hand, the EE tends to zero when the SE tends to infinity; that is

$$\lim_{SE \rightarrow \infty} EE = \lim_{SE \rightarrow \infty} \frac{SE}{(2^{SE} - 1)N_0} = 0 \quad (3.6)$$

Therefore, we have the closed-form expression of the SE-EE trade-off for point-to-point transmission under ideal AWGN channel case scenario.

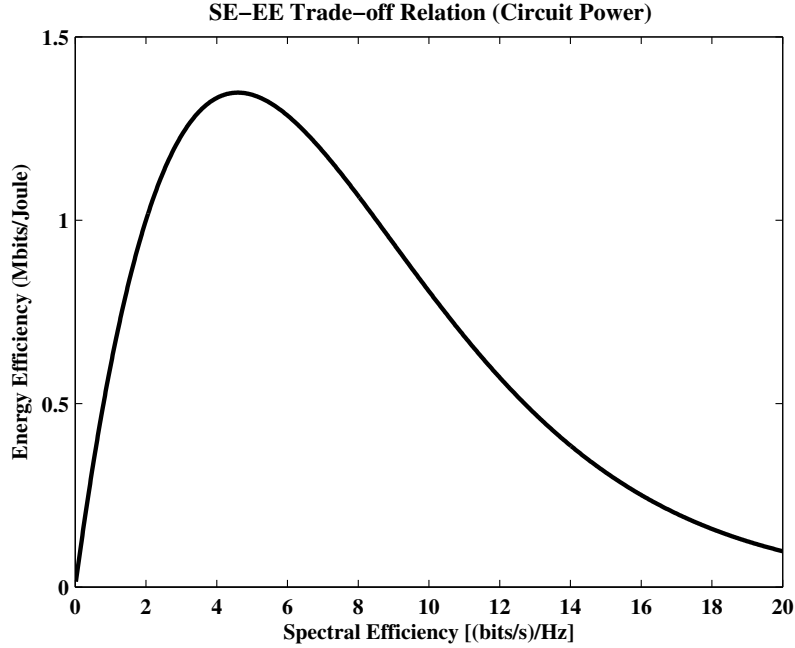


Figure 3.2: SE-EE Trade-off in Practical Scenario

However, in reality, the SE-EE trade-off relation is not as simple as the above mentioned scenario. In particular, under practical concerns apart from the transmission power, circuit power is also a component in the energy consumption. Therefore, and including circuit power

---

\*  $EE = \frac{\text{bits/Second}}{\text{Watt}} = \frac{\text{bits}}{\text{Second} \times \text{Watt}} = \frac{\text{bits}}{\text{Joule}}$

as well, EE is defined as the transmitted bits per unit energy consumption at the transmitter side, where the energy consumption includes transmission energy consumption and circuit energy consumption. More precisely, if circuit power is considered, the SE-EE curve is a bell shape curve which cannot be expressed in closed-form [70] as depicted in Figure 3.2.

### 3.1.2 Wireless OFDMA System

The above mentioned SE-EE trade-off relation is only adequate for modeling a point-to-point transmission, and not a multi-user network. OFDM is the accepted technology for supporting high data rate transmission with low inter-symbol-interference (ISI) in future generation networks. Moreover, the access scheme, OFDMA, offers a quite flexible framework for RRM as it allows allocation of different portions of radio resources to different users in both the frequency and time domains. In this section we overview the SE-EE trade-off for OFDMA networks.

In next-generation wireless communication systems, such as WiMAX and the 3GPP-LTE, OFDMA has been widely investigated from a SE viewpoint. In OFDMA, system resource, such as subcarriers and transmit power, needs to be properly allocated to different users to achieve high performance. Allocation of system resources to trade-off SE and EE efficiently for OFDMA network is not in itself a simple task. Figure 3.3 illustrates the resource allocation of a downlink OFDMA network, where subcarriers and power are allocated based on users' channel state information (CSI) and QoS requirements by the base station (BS).

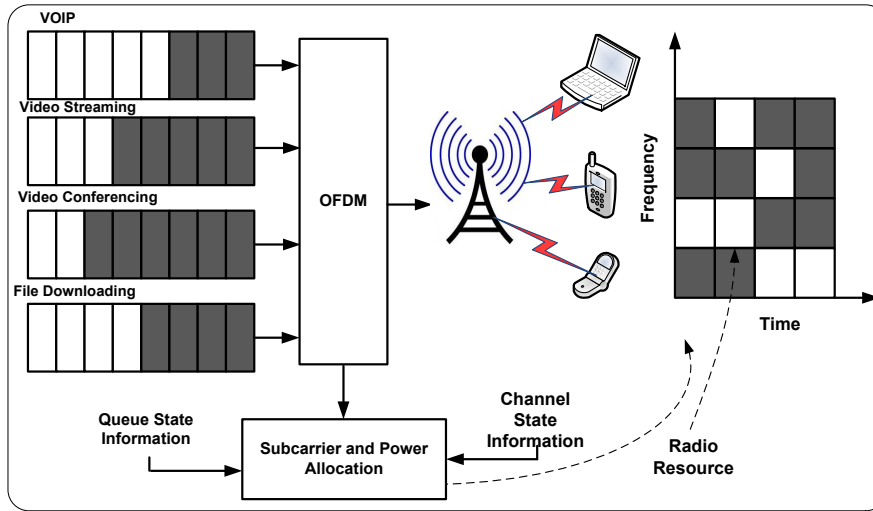


Figure 3.3: Energy-Aware Resource Management in OFDMA [26]

The SE-EE relation for downlink OFDMA networks is quite complex. According to [25], rate adaptation (RA), which maximizes throughput, and margin adaptation (MA), which minimizes total transmit power, are the two main resource allocation schemes which are commonly used. Therefore, RA aims at SE while MA targets transmit power efficiency. However, neither of them is necessarily energy-efficient. While OFDMA can provide high throughput and spectral efficiency, its energy consumption is sometimes large. EE and SE do not inevitably agree and a trade-off is required. EE and throughput efficiency can be

balanced, e.g. in the uplink, according to user QoS demands and availability of battery power [26].

While SE can always be improved by increasing transmit power in an interference free environment, Miao et. al. [26] shows that this does not hold in interference limited communication scenarios since increased transmit power also brings higher interference to the network. On the other hand, conservative energy-efficient communications reduce interference to other users and thus improve overall network spectral-efficiency. In [71] an energy-efficient design in multi cell scenarios with inter-cell interference for uplink is studied. As shown there, energy-efficient power distribution not only boosts system EE but also refines the SE-EE trade-off due to the conservative nature of power allocation, which sufficiently restricts interference from other cells and improves network throughput. According to [62] there is at least a 15% reduction in energy consumption when frequency diversity is exploited. For uplink transmission with flat fading channels [71], e.g., it is demonstrated that, by applying adaptive modulation, the EE increases as the user moves in the direction of the BS; and the nearer the user is to the BS, the higher the modulation order in the link adaptation.

## 3.2 Single Cell Spectral Efficiency-Energy Efficiency

A single cell network is the first step to understand a system, whether it is OFDMA or CDMA or TDMA. From a single cell evaluation we get an idea about the trend of the link level which is used as a benchmark for the system perspective. In this section, the fundamental trade-off between SE and EE in downlink OFDMA networks is addressed. To get a clear idea about the SE-EE trade-off relation a general framework is needed. Cong et al. [70] provide a generic framework for that trade-off relation. We discuss the trend of the SE-EE curve in single cell scenario and discuss the impact of channel power gain and circuit power on the SE-EE relation. Finally, we discuss the bounds of the SE-EE curve, which is challenging to achieve in a closed form expression [70].

### 3.2.1 System Model Description

We assume that the base station (BS) is placed in the center on a regular hexagonal grid, as shown in Figure 3.4. Here we consider a standard downlink OFDMA system where a single BS is transmitting data towards a number of users utilizing a number of orthogonal subcarriers. The number of users and the subcarriers are denoted by  $\mathcal{U} = 1, \dots, U (u \in \mathcal{U})$  and  $\mathcal{S} = 1, \dots, S (s \in \mathcal{S})$  respectively. We assume that: one subcarrier is exclusively assigned to at most one user to avoid interference among different users, the subcarrier frequency spacing is wide enough and inter-subcarrier interference can be ignored, subcarrier allocation which is aligned with the 3GPP LTE standard and related literature [12, 70].

The BS, as well as all users, is assumed to be equipped with a single antenna. It has been assumed that each subcarrier which belongs to a particular user is under frequency-selective fading, for example using ITU Pedestrian-B model. The channel information, i.e., CSI, is sent to the BS over a feedback channel from each user. Furthermore, the BS has perfect channel knowledge for each user instantly. Based on this information, the BS allocates a set of subcarrier to each user and decides on the number of bits in each subcarrier. It is assumed that each subcarrier is exclusively allocated to one user, i.e., sharing a subcarrier by two or more users is not allowed at any given time.

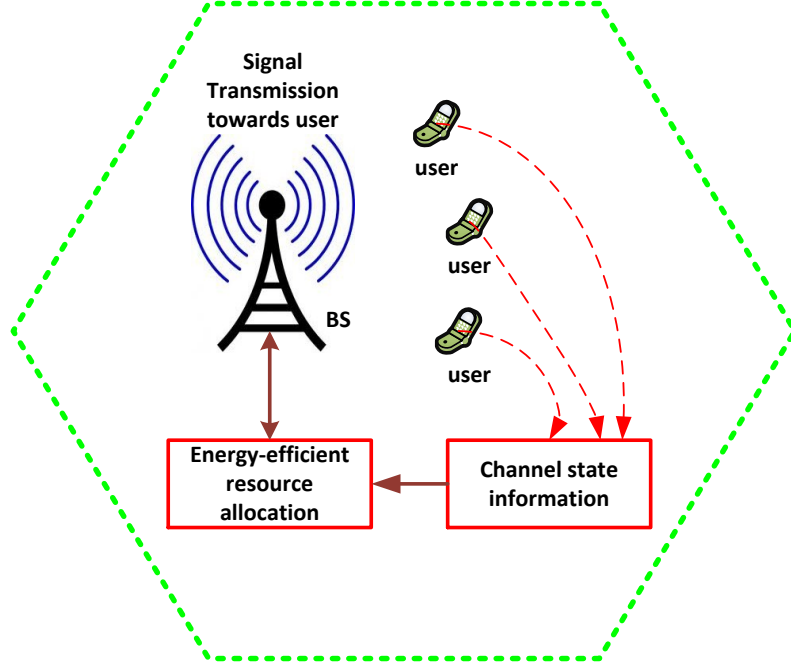


Figure 3.4: Single Cell OFDMA Network [72]

To elaborate, we consider total bandwidth  $B$  is equally divided into  $S$  subcarrier, each with a bandwidth of  $b = B/S$ . Using Shannon formula, we define the maximum achievable data rate for a OFDMA system of user  $u$  on subcarrier  $s$  as [70]

$$r_{u,s} = b \log_2 \left( 1 + \frac{p_{u,s} g_{u,s}}{N_0 b} \right) \quad (3.7)$$

where  $p_{u,s}$ ,  $g_{u,s}$  and  $N_0$  defines the transmit power, the channel power gain of user  $u$  on subcarrier  $s$  and the noise spectral density respectively. Therefore, the total system throughput ( $R$ ) and the total transmit power ( $P_T$ ) for a single cell downlink OFDMA system is –

$$R = \sum_{u=1}^U \sum_{s=1}^S r_{u,s} \text{ and } P_T = P = \sum_{u=1}^U \sum_{s=1}^S p_{u,s} \quad (3.8)$$

Eventually, we define the EE as transmitted bits per unit energy consumption at the transmitter side, where the total energy consumption includes total transmit power and circuit power, measured in bits/Joule, and SE as the total transmitted bits per unit spectrum, measured in bits/Hertz. For a downlink OFDMA network, EE and SE are –

$$EE = \frac{R}{P_{Total}} = \frac{R}{P_T + P_c} \text{ and } SE = \frac{R}{B} \quad (3.9)$$

where  $P_T$  and  $P_c$  is the transmit power and circuit power respectively. The EE is thus

expressed as:–

$$EE = \frac{\sum_{u=1}^U \sum_{s=1}^S r_{u,s}}{\sum_{u=1}^U \sum_{s=1}^S p_{u,s} + P_c} \quad (3.10)$$

### 3.2.2 SE-EE Trade-off Relation

To understand the SE-EE trade-off it is important to understand the shape of the SE-EE curve. If we plot equation (3.10) for any given SE the shape of the curve would be like quasiconcave, which means EE is quasiconcave in SE. Cong et al. [70] provide a list of theorems to illustrate this idea. [70] provides a theorem for the relation between SE-EE. For any given SE, EE is strictly quasiconcave in SE if there are a sufficiently large number of subcarriers and a solution for the traffic allocation. Moreover, in the SE region (from minimum SE to maximum SE), the EE provides three types of scenarios in quasiconcavity, as explained hereafter. The theorem demonstrates the quasiconcavity of EE on SE and reconfirms the existence and the uniqueness of the globally optimal EE as illustrated in Figure 3.5, 3.6 and 3.7. This approach gives us a uniform SE (or total rate) perspective rather than that of a vector of split user rates, which makes it easier to track the SE-EE relation.

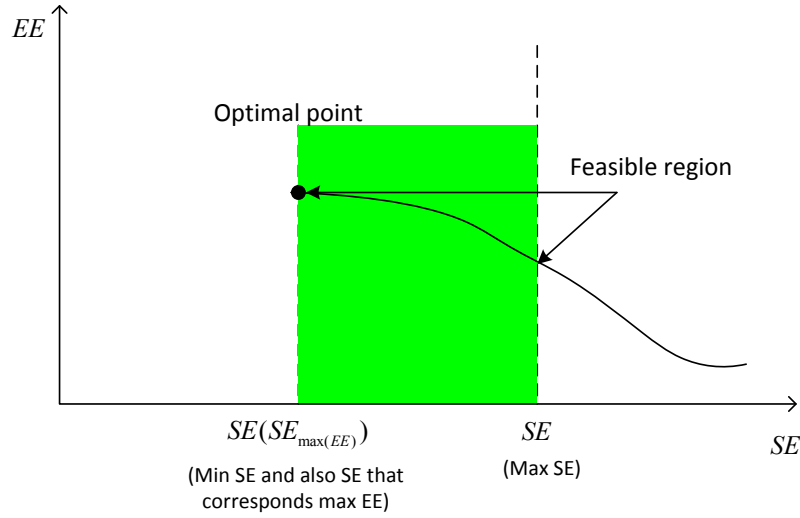


Figure 3.5: SE-EE in downlink OFDMA, scenario 1

Three possible scenarios for the SE-EE curve are discussed in [70] as depicted in Figure 3.5, 3.6 and 3.7. In scenario 1, the optimal point of SE-EE trade-off i.e. the point of the optimal EE is reached when the point of the optimal SE equals the point of minimum SE, as illustrated in Figure 3.5. In scenario 2, the optimal EE point is reached when the point of the optimal SE equals the point of maximum SE i.e. the trade-off point (optimal point of EE) is found on the point where the point of maximum SE is reached as illustrated in Figure

3.6. In scenario 3, the point of optimal EE is reached when optimal SE equals  $SE_{\max(EE)}$  ( $SE_{\max(EE)} \rightarrow$  the SE that corresponds the maximum EE ) as sketched in Figure 3.7. We should keep in mind that the point of optimal SE is the optimal SE of equation (3.9).

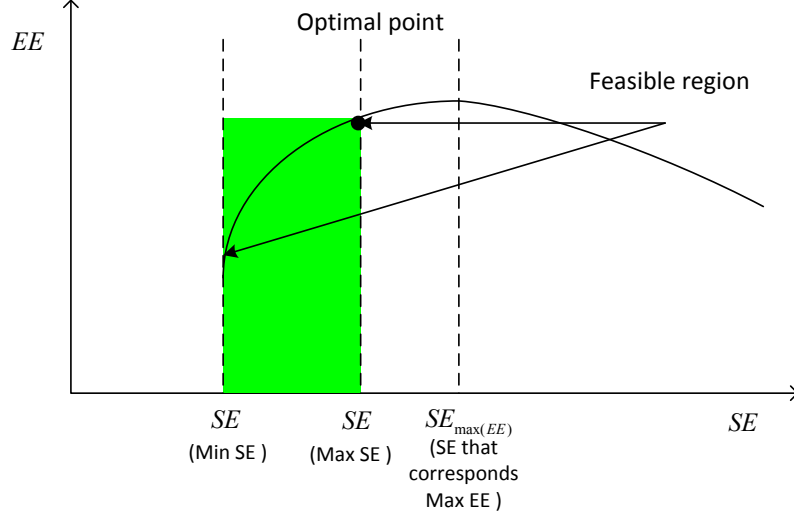


Figure 3.6: SE-EE in downlink OFDMA, scenario 2

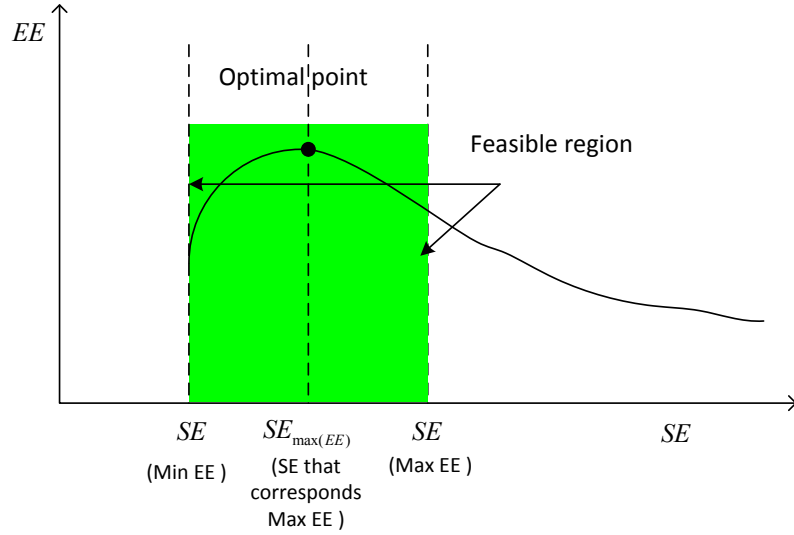


Figure 3.7: SE-EE in downlink OFDMA, scenario 3

Note that the SE-EE trade-off points such as the optimal EE point equals maximum EE point in scenarios 1 and 3 while it is smaller than the latter in scenario 2. In addition,

this SE-EE trend offers a simple and adaptive way to determine a desirable and feasible data transmission rate, in practical situations [70]. For simplicity, we should assume data transmission is appropriately predetermined.

To have more insight into the SE-EE trade-off relation and to understand the impact of the channel power gain and circuit power on the SE-EE relation some of the properties based on the above mentioned work are given verbatim in the following [70]:

**Property 1.** *For any fixed SE, the EE is non-decreasing with channel power gain. Consequently, both the optimal EE and the global maximum EE are non-decreasing with channel power gain [70].*

**Property 2.** *For any fixed SE, the EE is strictly decreases with circuit power. Consequently both the optimal EE and the global maximum EE strictly decrease with the circuit power,  $P_c$ . Besides, the optimal SE is non-decreasing with the static power [70].*

**Property 3.** *The optimal EE is not necessarily achieved at minimum SE even if circuit power is zero [70].*

### 3.2.3 Bounds on The SE-EE curve

In spite of the known trends of the SE-EE curve, it is very difficult to find the exact solution of the upper bounds and lower bounds of the curve. As it is extensively studied in [70], Lagrange Dual Decomposition (LDD) [73] is used to find the bounds of the SE-EE curve, an approach that has been used in [74, 75] for similar OFDMA allocation problems. Since our goal is to give an overview to the reader, this allocation process is out of scope.

The water-filling algorithm [76] is used to allocate subcarriers for each user so that we have an idea about the bounds of the SE-EE trade-off. Using the water-filling algorithm, the achievable upper bound of SE-EE curve on the minimum transmit power is found. This method is completely described in [70]. On the other hand, a lower bound on the minimum transmit power can be obtained by relaxing the channel allocation.

Interestingly, although it is hardly possible to derive a closed-form expression for the upper and lower bound of the curve, the differentiation of the equation (3.10) with respect to SE can give us some idea, because the differentiation of that function can easily and accurately determine its sign to solve bounds on the transmit power minimization. This coincides with and relates to theorem 4 of [70].

In this section, we have presented the SE-EE relation in a single cell downlink OFDMA network, which is important for designing Green Wireless Communications that require a better balance between SE and EE. The SE-EE relation is shown to be a quasiconcave function with the help of the ground breaking research article [70], and the impact of channel power gain and circuit power is also discussed. Methods for finding a lower and upper bound on the SE-EE curve are summarized in a comprehensive way avoiding complex mathematical analysis. Similar theoretical approaches will be used in the next section for multi cell OFDMA networks.

## 3.3 Significance Of Circuit Power In SE-EE Trade-Off

In this section, we focus on some of the results we achieved through our investigation. As already mentioned in the previous section, EE is defined as the transmitted bits per

unit energy consumption at the transmitter side, where the energy consumption includes transmission energy and circuit energy consumption of transmitter in the active mode.

$$EE = \frac{R}{P} = \frac{R}{P_{Total}} = \frac{R}{P_{Transmit} + P_{Circuit}} \quad (3.11)$$

In the transmit/active mode of transmitter, and besides transmit power, the energy consumption also includes circuit energy consumption that is incurred by signal processing and active circuit blocks, such as analog-to-digital converter, digital-to-analog converter, synthesizer, and mixer [77].

From [78, 79], circuit power can be divided into two parts. One is static circuit power which is also a fixed entity; whilst the other is a dynamic circuit power consumption which is a dynamic circuit power factor in terms of per unit data rate. Hence the circuit power is modeled as follows [79].

$$P_{Circuit} = P_{Static} + P_{Dynamic} = P_{Static} + \rho R \quad (3.12)$$

where  $\rho$  [79] is a constant denoting dynamic power consumption per unit data rate ( $R$ ).

Figure 3.8 demonstrates SE-EE curve of an LTE-Advanced downlink system. From the Figure 3.8 we can attain SE-EE trade-off relation while using different power consumption models. As we already know, in a ideal scenario EE always decreases in terms of SE, while in practical scenario EE is quasiconcave in SE. The showing of this result is given by Figure 3.8.

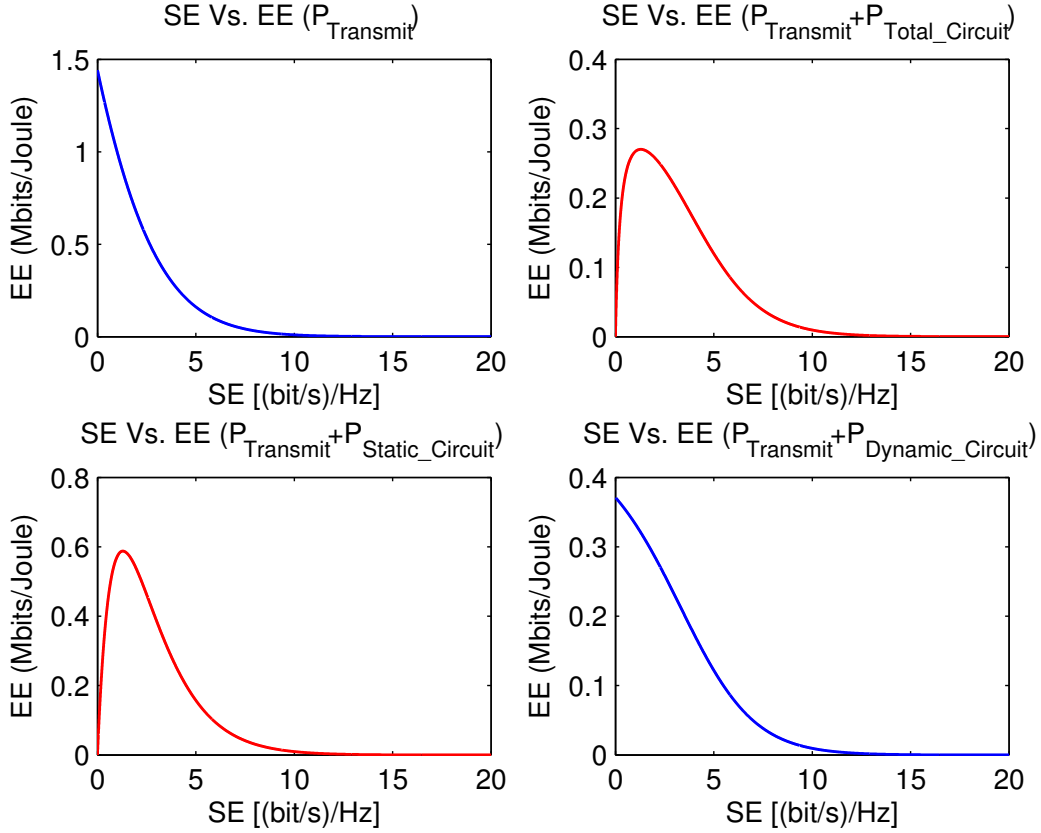


Figure 3.8: Impact of Circuit Power in SE-EE Trade-off

The SE-EE curve in transmit power and transmit-plus-dynamic-circuit power shows the similar trend. The reasoning behind this trend is that the dynamic circuit power factor actually scales the data transmission rate which has no relation to any static circuit power factor. Therefore, the trend remains the same as in the ideal SE-EE scenario. On the other hand, the SE-EE curve trend is quasiconcave in terms of both the total circuitry power consumption and the static circuitry power consumption. From Figure 3.8, it is evident that the static circuit power plays a pivotal role the quasiconcave nature of the curve. The reason being is that the static circuit power has no coupling with the transmission rate (as well as spectral-efficiency or bandwidth). This type of circuit power is responsible for the quasi-concave trend of the curve; not the dynamic circuit power. So if we use only static circuit power without considering dynamic circuitry consumption, the SE-EE curve trend remains quasiconcave like the SE-EE curve trend using the total circuit power (both static and dynamic circuitry consumption).

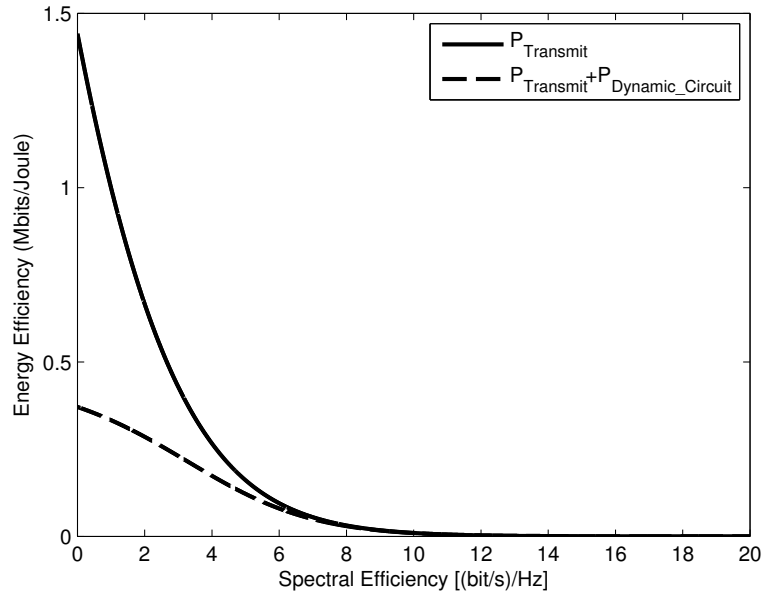


Figure 3.9: Impact of Circuit Power in SE-EE Trade-off

In Figure 3.9 and 3.10 we compare EE amongst the different types of energy consumption such as using only transmission power, transmission power-plus-only dynamic circuit power, transmission power-plus-total circuit power and transmission power-plus-only static circuit power.

The energy-efficiency decreases when consumed power includes transmit power and dynamic circuit power factor as illustrated in Figure 3.9. That means dynamic circuit power reduces the EE. In the case of comparing EE between total power (which includes both transmit power and total circuit power) and the power considering transmit-plus-static circuit power we find that EE decreases in the latter much more aggressively, as demonstrated in Figure 3.10. It is fairly evident that to have a SE-EE balance, circuit power plays a major role towards shaping this trade-off.

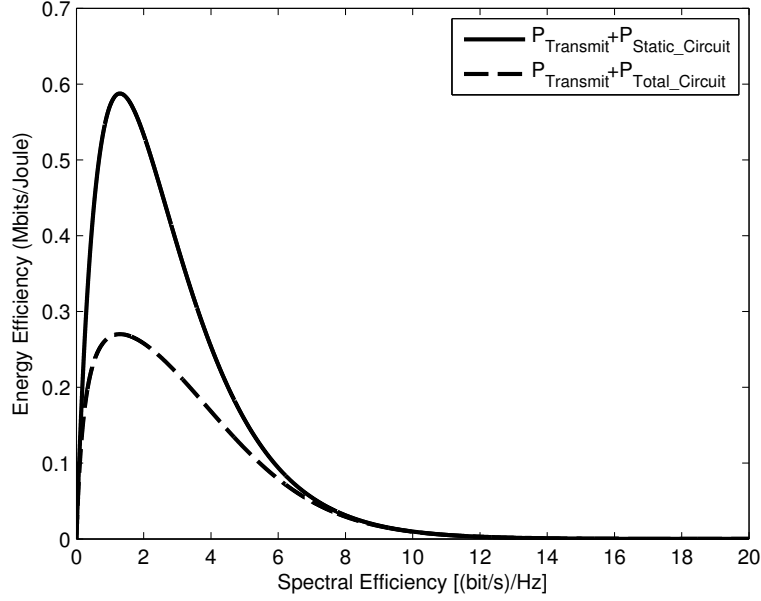


Figure 3.10: Impact of Circuit Power in SE-EE Trade-off

### 3.4 Multi cell Spectral Efficiency-Energy Efficiency

Miao et al. [80] have extensively studied energy-efficient design in multi cell scenarios with inter-cell interference for uplink OFDMA system. They reported that due to the conservative nature of the power allocation, SE-EE trade-off is reduced using energy-efficient power distribution which also increases the system EE. That means the SE-EE trade-off relation is able to restrict interference from other cells and improves network throughput. Since the above mentioned research activity is based on the uplink, there is still very few works on the downlink for multi cell OFDMA.

For the multi cell OFDMA system the EE is a function which includes interference from other cells and co-channel interference. The trade-off between SE and EE in this system mainly depends on accurate channel state information at the transmitter (CSIT) and feedback power consumption. Analyzing the EE under more practical conditions the CSIT model provides more practical significance, and can lead to insights in the SE-EE trade-off relation. Existing work on the above topic is relatively limited, since even the SE of the multi cell multi user systems is still under investigation.

#### 3.4.1 System Model

In this section, we describe the system model of a generic multi cell OFDMA downlink system. For example, we consider a multi cell OFDMA system: the overall frequency bandwidth  $B$  is divided into  $S$  subcarriers/subchannels each with a bandwidth of  $b = B/S$  and all the subchannels are reused among  $C$  distinct cells. In each cell, the unique BS is located at the center of the cell, and the served user terminals are randomly spread throughout the service area. From now on we use the terms BS and cell interchangeably.

The propagation channel is frequency selective and slowly time-varying, such that each BS is able to exchange CSI with the served user terminals via a dedicated feedback channel. If we consider a system consisting of one tier of 6 cells with a central cell as a starting point, then, as a result, all the transmitted signals are collected from the central cell, with the other 6 cells serving as interferers. A system with 19 cells has then six cells in tier two, whereas the other 12 cells constitute tier three, with the central cell treated as tier one. With this approach the increase in the cell number leads to more tiers in the system. Figure 3.11 illustrates a multi cell scenario of a downlink OFDMA system.

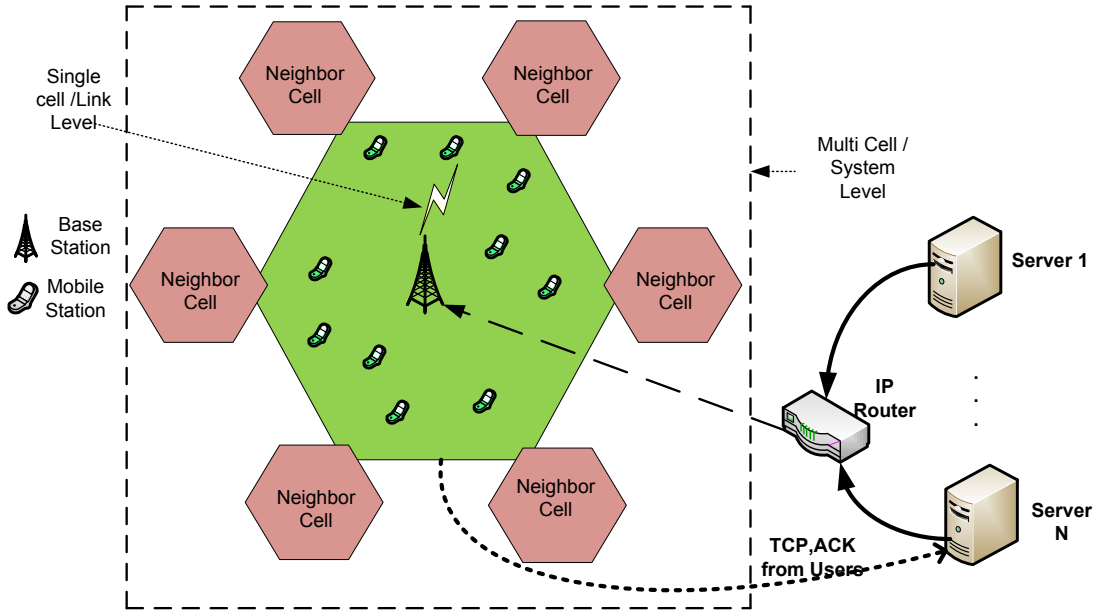


Figure 3.11: Multi Cell OFDMA Network

The major difference between a single cell and multi cell system is the inter-cell interference which occurs in a multi-cellular system. Generally, interference acts as a flat fading signal from the interfering base stations. Interference from BS to BS also termed as a co-channel interference. Thus we shall apply equation (3.7) with signal-to-noise-ratio ( $SNR = \frac{p_{u,s}g_{u,s}}{N_0b}$ ) replaced by the signal-to-interference-plus-noise-power-ratio ( $SINR = \frac{p_{u,s}g_{u,s}}{I + N_0b}$ ).

For example, we define  $\mathcal{C} = \{1, \dots, C\}$  (for any  $c, c \in \mathcal{C}$ ) as the set of cells/BSs in the system, and also the set of the number of users and the subcarriers are denoted by  $\mathcal{U} = \{1, \dots, U\}$  (for any  $u, u \in \mathcal{U}$ ) and  $\mathcal{S} = \{1, \dots, S\}$  (for any  $s, s \in \mathcal{S}$ ) respectively. For the downlink cases, due to the co-channel interference from other cells, the output SINR at the receiver for the user  $u$  user on subcarrier  $s$  from the BS  $c$  is defined in the following –

$$SINR = \frac{p_{u,s}^c g_{u,s}^c}{I + N_0b} \quad (3.13)$$

where  $p_{u,s}^c$ ,  $g_{u,s}^c$  and  $N_0$  defines the transmit power and the channel power gain of user  $u$  on subcarrier  $s$  from the BS  $c$  and the noise spectral density respectively.  $I$  denotes the interfering

signal power from the neighboring BSs. We can elaborate the value of  $I$  as  $I = \sum_{i=1, i \neq c}^C p_{u,s}^i$ . After substituting the value of  $I$  in equation (3.13) we get,

$$SINR = \frac{p_{u,s}^c g_{u,s}^c}{\sum_{i=1, i \neq c}^C p_{u,s}^i + N_0 b} \quad (3.14)$$

### 3.4.2 Bounds on the SE-EE Curve

Using Shannon formula [66], the maximum achievable data rate for a multi-cell OFDMA system of user  $u$  on subcarrier  $s$  from the BS  $c$  is

$$r_{u,s} = b \log_2 \left( 1 + \frac{p_{u,s}^c g_{u,s}^c}{I + N_0 b} \right) \quad (3.15)$$

$$r_{u,s} = b \log_2 \left( 1 + \frac{p_{u,s}^c g_{u,s}^c}{\sum_{i=1, i \neq c}^C p_{u,s}^i + N_0 b} \right)$$

According to the definition of  $EE$  from the previous section, we define the  $EE$  for a multi-cell scenario in the following

$$EE = \frac{\sum_{u=1}^U \sum_{s=1}^S r_{u,s}^c}{\sum_{u=1}^U \sum_{s=1}^S p_{u,s}^c + P_c} \quad (\text{for any } c; c \in \mathcal{C}) \quad (3.16)$$

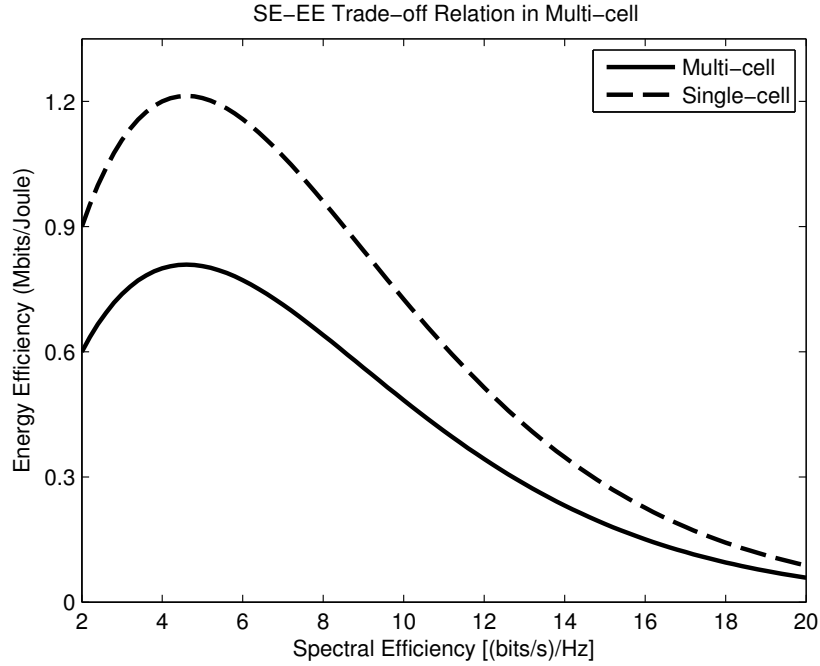


Figure 3.12: SE-EE Trade-off relation between Multi-cell and Single-cell

Due to interference-limited scenario in multi-cell system, the EE decreases in the multi-cell compared to the single-cell case as illustrated in Figure 3.12. From the Figure we can get the same quasiconcave trend of SE-EE relation i.e.,  $EE$  is quasiconcave in  $SE$ .

Very few works have been done for SE-EE trade-off in multi-cell OFDMA system. [77] provides some insight of the SE-EE bound although it does not consider complete practical channel propagation model such as frequency-selective fading channel. [77] concludes with a proposition which demonstrates that the EE tends to zero when the transmitted power tends either to zero or infinity. Eventually, they clarify EE admits a maximum for some non-null and a finite value of the transmitted power in terms of SE; the value of the optimal power depends on the configuration of the network. More interested readers can refer to [77] to understand the proof. However, the SE-EE relation for general multi cell networks, including downlink OFDMA network, is a subject that still needs extensive research.

### 3.5 Trade-off between SE-EE in MU-MIMO CoMP

This section investigates the trade-off between EE and SE in downlink multi-antenna multi-user Coordinated Multi-Point (CoMP) system which is adopted by 3GPP LTE-A due to its ability to mitigate and/or coordinate inter-cell interference (ICI). Given the SE requirement, a constrained optimization problem is formulated to maximize EE. Moreover, a novel resource allocation algorithm is proposed to achieve maximum EE. Simulations results demonstrate the effectiveness of the proposed scheme and illustrate the fundamental trade-offs between energy and spectral efficient transmission. Our analytical results are of great help for future “green” network planning in downlink multi-user CoMP systems.

Several EE methods have been proposed for different layers of wireless communication networks. Energy efficient orthogonal frequency-division multiplexing (OFDM) systems have been first addressed as considering circuit consumption in [71]. The authors have demonstrated that there is at least a 20% reduction in energy consumption by performing EE optimization. For single cell orthogonal frequency-division multiple accesses (OFDMA) networks, EE is analyzed in [70]. In [26], cross-layer design for energy efficient wireless communications has been discussed in details. It has been shown that using both power and modulation order adaptation, the EE-oriented design always consumes less energy than the traditional fixed power schemes. In [81], EE in distributed antenna systems (DAS) is also analyzed. However, to the best of the authors’ knowledge, there is no literature discussed about EE in the downlink multi-antenna multi-user CoMP systems.

In this section, the trade-off between EE and SE in downlink multi-antenna multi-user CoMP is addressed. We account for both circuit and transmit power when designing optimal EE systems. The optimization objective is to maximize EE while satisfying SE requirements. This objective function, which is measured as the transmitted bits per unit energy consumption, is particularly suitable for designing green communication systems. Hence, we first formulate the optimization problem and then we propose a novel resource allocation algorithm to achieve maximum EE in a given SE.

#### 3.5.1 System Model

We consider CoMP OFDMA networks with interference coordination between different CoMP cells. A CoMP system composed of several conventional cells. Each CoMP system

consists of one central unit CU and several eNBs as shown in the Figure 3.13 based on LTE technology. For example, our CoMP system is composed of  $C$  CoMP clusters, indicated by set of all CoMP clusters  $\mathcal{C}$ , where  $\mathcal{C} = \{1, 2, \dots, c, \dots, C\}$ , where a CoMP cluster comprises one centralized point CU with  $E$  (indicated by set of eNBs  $\mathcal{E} = \{1, 2, \dots, e, \dots, E\}$ ) number of eNBs, in our scenario  $E = 3$ , serving  $U$  user equipments (UEs) which are uniformly distributed over its coverage area. A set of  $E$  such eNBs which intend to cooperate form a cluster. Furthermore, each eNB in a cluster is assumed to have  $N_{TX}$  transmit antennas and  $N_{RX}$  receive antennas per UE.

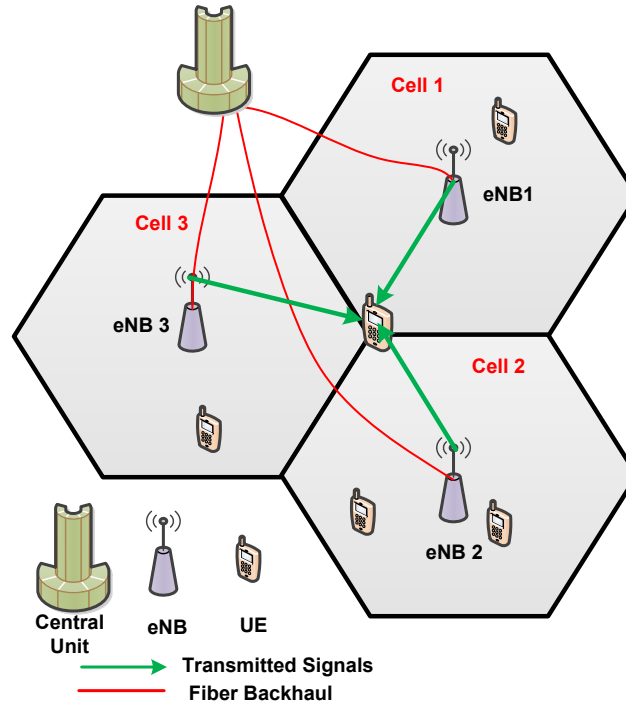


Figure 3.13: Hexagonal layout of the reference CoMP cluster

The CoMP system can be seen as a distributed multi-user MIMO (MU-MIMO) system using eNBs as a distributed antenna array [82]. For the CoMP system, interference is classified as intra-CoMP and inter-CoMP interference. The inter-CoMP interference is defined when the interference originates from eNBs of other CoMP-cells. This interference is assumed to be coordinated. Indeed, using the backhaul, CoMP systems become able to exchange data, control information with the all eNBs under the command of the CU, and consequently, coordinate inter-CoMP interference. The intra-CoMP interferences are originated from eNBs of the same CoMP cluster. To mitigate this interference, linear precoding techniques are often considered by future wireless systems due to its simplicity and good performance. To this end, zero-forcing (ZF) precoding is considered, which transmits the signals towards the intended user's direction and nulls in the direction of other users, thus eliminating intra-CoMP cluster interference [83].

Usually, subcarriers are not allocated individually, because of signaling constraints, but

in blocks of adjacent subcarriers, which represent the Physical Resource Blocks (PRBs) [84]. There exists  $M$  PRBs in the system and each of them might be assigned to one or more UEs in each CoMP-cell. In our work, adaptive power allocation (according to the 3GPP LTE adaptive modulation and coding (AMC) scheme) using the channel condition among PRBs is considered and the total transmit power  $P$   $\left(P = \sum_{u=1}^U p^u = \sum_{u=1}^U \sum_{m=1}^M p^{u,m}\right)$  available on each  $C$  is divided among the PRBs based on the channel condition of the UE. In a nutshell, in the LTE-based system [85], all PRB's allocated to the same user must use the same modulation and coding scheme (MCS). Compared to resource allocation in conventional systems [86, 87], LTE specification requires that all RB's corresponding to the same user in any given transmission time interval (TTI) must use the same MCS. Transmit power for a UE is equally divided among the PRBs which are allocated to that UE. That means if a channel condition is better for a UE it receives high power and if the channel condition of a UE is poorer it receives less power. Whatever transmit power a UE receives due to its channel condition, the power is equally divided among the PRBs it is allocated. In this way we can improve the system throughput by power allocation among UEs. The power allocated to each PRB is

$$p^{u,m} = \frac{p^u}{|\mathcal{M}^u|}, \quad \left[ p^u = \sum_{m \in \mathcal{M}^u} p^{u,m} \text{ and } \sum_{u=1}^U |\mathcal{M}^u| = M \right]. \quad (3.17)$$

Where,

$p^u$  is the total transmitted power for the user allocated to the total PRB,

$\mathcal{M}$  is the set of all PRBs, defined as  $\{1, 2, \dots, m, \dots, M\}$ ,

$\mathcal{M}^u$  is the set of all PRBs allocated to UE  $u$ , obviously  $\mathcal{M}^u \in \mathcal{M}$ ,

$|\mathcal{M}^u|$  is the cardinality of the set  $\mathcal{M}^u$  (the total number of PRBs allocated to the UE  $u$ ),

and  $\sum_{u=1}^U |\mathcal{M}^u| \leq M$ .

In order to determine whether a transmission has been successful, the SINR measured for a given path is employed to determine the packet error rate (PER) for the block of data sent on each PRB. The SINR,  $\Gamma_{c,u}^m$  perceived by a UE  $u$  on PRB  $m$  of the CoMP cluster  $c$  can be expressed as

$$\Gamma_{c,u}^m = \frac{p_{c,u}^m |\mathbf{H}_{c,u}^m \mathbf{W}_{c,u}^m|^2}{\sum_{u' \neq u}^U p_{c,u'}^m |\mathbf{H}_{c,u}^m \mathbf{W}_{c,u'}^m|^2 + \sum_{c' \neq c}^C \sum_{u'}^U p_{c',u'}^m |\mathbf{H}_{c',u}^m \mathbf{W}_{c',u'}^m|^2 + \sigma^2} \quad (3.18)$$

where  $u \in \{1, 2, \dots, U\}$ ;  $\mathbf{H}_{c,u}^m \in \mathbb{C}^{\{N_{RX} \times (E \times N_{TX})\}}$  is the complex channel matrix whose elements combine path loss, shadowing and fast fading and which models the link between the  $u^{th}$  UE and all  $E$  eNBs of the CoMP cluster  $c$ ;  $\mathbf{W}_{c,u}^m \in \mathbb{C}^{\{(E \times N_{TX}) \times N_{RX}\}}$  is the precoding matrix for the link between the eNBs of CoMP cluster  $c$  and the UE  $u$ ; and  $\sigma^2$  is the noise power as perceived by the UE.

Since the inter-CoMP-cluster interference is coordinated and assumed to be removed, hence, generalization in the above equation (3.18) simplifies to (See Appendix B for detailed explanation)

$$\Gamma_{c,u}^m = \frac{p_{c,u}^m |\mathbf{H}_{c,u}^m \mathbf{W}_{c,u}^m|^2}{\sum_{u' \neq u}^U p_{c,u'}^m |\mathbf{H}_{c,u}^m \mathbf{W}_{c,u'}^m|^2 + \sigma^2} \quad (3.19)$$

And the intra-CoMP-cluster interference is mitigated using zero-forcing precoding design, taking into account the pseudo-inverse of the channel matrix.

The total bandwidth  $B$  is equally divided into PRB, each with a bandwidth of  $b = B/M$ . Then, the spectral efficiency,  $SE$  obtained by Shannon theorem, for user  $u$  on PRB  $m$  is

$$SE_u^m = \log_2 (1 + \Gamma_{c,u}^m) \quad (3.20)$$

Then, the maximum achievable data rate,  $\bar{s}_u^m$ , of user  $u$  on PRB  $m$  is

$$\bar{s}_u^m = b \cdot SE_u^m \quad (3.21)$$

We can also introduce,  $s_u^m$ , the data rate for user  $u$  on PRB  $m$ . Then, the overall system throughput ( $S$ ) and total transmit power ( $P$ ) are  $S = \sum_{u=1}^U \sum_{m=1}^M s_u^m$ ;  $P = \sum_{u=1}^U \sum_{m=1}^M p_u^m$ , where  $p_u^m$  is the transmit power for user  $u$  on PRB  $m$ . Transmission power also counts on the reciprocal of the drain efficiency of the power amplifier, which is denoted as  $\alpha$ . The power consumption is represented as  $\alpha \cdot p_u^m$ . Apart from the transmission power we consider circuit power as well. From [70], circuit energy consumption,  $P_c$  can be divided into a static (fixed) part and a dynamic part that depend on the parameters of active links.  $P_c = P_{st} + \delta \cdot S$ , where  $P_{st}$  is the static circuit power in the transmit mode and  $\delta$  is a constant denoting dynamic power consumption per unit data rate.

### 3.5.2 Novel Algorithm for Achieving Maximum EE

#### 3.5.2.1 Problem Formulation in terms of Energy Efficiency

For a downlink CoMP OFDMA network, EE is defined as

$$EE = \frac{S}{\alpha \cdot P + P_c} \quad (3.22)$$

Throughout this paper, EE is defined as transmitted bits per unit energy consumption at the transmitter side, where the energy consumption includes transmission energy consumption ( $\alpha \cdot P$  times transmission time) and circuit energy consumption ( $P_c$  times transmission time) of transmitter. Accordingly, the optimization problem can be formulated as

$$\begin{aligned} \max_{\mathbf{s}} \quad & EE \left( = \frac{\sum_{u=1}^U \sum_{m=1}^M s_u^m}{\alpha \cdot \sum_{e=1}^E P_{Tx_e} + P_{st} + \delta \cdot \sum_{u=1}^U \sum_{m=1}^M s_u^m} \right) \\ \text{subject to:} \quad & 1) \hat{s}_u^m \leq s_u^m \leq \bar{s}_u^m \text{ or } s_u^m = 0 \\ & 2) s_u^m \geq 0 \end{aligned} \quad (3.23)$$

where  $\hat{s}_u^m$  denotes the minimum rate requirement and is the maximum achievable rate for user  $u$  on PRB  $m$ .  $P_{Tx}$  represents the transmit power from eNB respectively, whereas the coefficients denote power consumption that scales with average radiated power due to amplifier and feeder losses. Our optimization variable is the rate vector  $\mathbf{s}$ . To ensure the convexity of the proposed optimization problem, we redefined our constraint using a similar approach as in [88]. We reformulated our constraint based on non-negativity, as given in the following

$$(s_u^m) \cdot (s_u^m - \hat{s}_u^m) \cdot (\bar{s}_u^m - s_u^m) \geq 0 \quad (3.24)$$

From here, we then derive four conditions and find the 1<sup>st</sup> and 3<sup>rd</sup> conditions which satisfy our constraint's non-negativity and convexity. The four conditions are:

$$\begin{aligned}
& 1) s_u^m = 0; \\
& 2) s_u^m \in (0, \hat{s}_u^m); \\
& 3) s_u^m \in [\hat{s}_u^m, \bar{s}_u^m]; \\
& 4) s_u^m \in (\bar{s}_u^m, +\infty)
\end{aligned} \tag{3.25}$$

### 3.5.2.2 Optimization

Our problem has an optimal solution since its objective function is concave and the solution space defined by the constraints is convex [89]. In other words, this is a convex optimization problem. Using standard optimization techniques in [89], we obtain the Lagrangian of (3.23)

$$L(\mathbf{s}, \lambda) = EE + \sum_{u=1}^U \sum_{m=1}^M \lambda_u^m [(s_u^m) (s_u^m - \hat{s}_u^m) (\bar{s}_u^m - s_u^m)] \tag{3.26}$$

where  $\lambda$  is the introduced Lagrange multiplier. After differentiating with respect to  $s_u^m$ , we have

$$\begin{aligned}
\frac{\partial L(\mathbf{s}, \lambda)}{\partial s_u^m} &= \frac{\alpha \cdot \sum_{e=1}^E P_{Tx_e} + P_{st}}{\left( \alpha \cdot \sum_{e=1}^E P_{Tx_e} + P_{st} + \delta \sum_{u=1}^U \sum_{m=1}^M s_u^m \right)^2} \\
&\quad + \lambda_u^m ((s_u^m - \hat{s}_u^m) (\bar{s}_u^m - s_u^m) + s_u^m (\bar{s}_u^m - s_u^m) - s_u^m (s_u^m - \hat{s}_u^m))
\end{aligned} \tag{3.27}$$

We obtain the necessary conditions for the optimal solution

$$\frac{\partial L(\mathbf{s}, \lambda)}{\partial s_u^m} \begin{cases} > 0, \\ = 0, \\ < 0, \end{cases} \quad \begin{cases} s_u^m = \bar{s}_u^m \\ \hat{s}_u^m < s_u^m < \bar{s}_u^m \\ s_u^m = 0 \end{cases} \tag{3.28}$$

Then the optimal solution can be expressed as

$$s_u^m(OPT) = \max(D, \bar{s}_u^m) \tag{3.29}$$

where

$$\begin{aligned}
D &= \left[ \begin{aligned} & \sum_{e=1}^E P_{Tx_e} + P_{st} + \\ & \left( \alpha \cdot \sum_{e=1}^E P_{Tx_e} + P_{st} + \delta \sum_{u=1}^U \sum_{m=1}^M s_u^m \right)^2 \\ & \cdot \left[ \lambda_u^m \left\{ (s_u^m - \hat{s}_u^m) (\bar{s}_u^m - s_u^m) + \right. \right. \\ & \quad \left. \left. s_u^m (\bar{s}_u^m - s_u^m) - s_u^m (s_u^m - \hat{s}_u^m) \right\} \right] \end{aligned} \right]^+ \\
&= \left[ \begin{aligned} & \sum_{e=1}^E P_{Tx_e} + P_{st} + \\ & \left( \alpha \cdot \sum_{e=1}^E P_{Tx_e} + P_{st} + \delta \sum_{u=1}^U \sum_{m=1}^M s_u^m \right)^2 \\ & \cdot \left[ -\lambda_u^m \left\{ 3(s_u^m)^2 - 2s_u^m (\hat{s}_u^m + \bar{s}_u^m) + \hat{s}_u^m \cdot \bar{s}_u^m \right\} \right] \end{aligned} \right]^+
\end{aligned} \tag{3.30}$$

where  $[x]^+ = \max(x, 0)$ . We get the estimated  $s_u^m$  values through numerical search [81]. Let  $\Omega_u^m = \lambda_u^m$ . From Eq. (3.27), the upper bound of the numerical search can be expressed as in the following, when  $s_u^m = \bar{s}_u^m$

$$\Omega_{UB} = \frac{\sum_{e=1}^E P_{Tx_e} + P_{st}}{\left( \alpha \cdot \sum_{e=1}^E P_{Tx_e} + P_{st} + \delta \sum_{u=1}^U \sum_{m=1}^M s_u^m \right)^2 \cdot \left\{ 3(s_u^m)^2 - 2s_u^m (\hat{s}_u^m + \bar{s}_u^m) + \hat{s}_u^m \cdot \bar{s}_u^m \right\}} \quad (3.31)$$

When  $s_u^m = 0$ , the lower bound of the numerical search  $\Omega_u^m$  can be expressed as

$$\Omega_{LB} = \frac{\sum_{e=1}^E P_{Tx_e} + P_{st}}{\left( \alpha \cdot \sum_{e=1}^E P_{Tx_e} + P_{st} \right)^2 \cdot \left\{ \hat{s}_u^m \cdot \bar{s}_u^m \right\}} \quad (3.32)$$

### 3.5.2.3 Sub-Optimal Resource Allocation Algorithm

According to the analysis of the above subsection, the following proposes the optimal resource allocation algorithm for achieving maximum EE in the downlink CoMP in Algorithm 3.1.

---

#### Algorithm 3.1 Algorithm for achieving maximum EE

---

- 1: **Step 1:** Initialization  
Set  $s_u^m(0)$  and  $\lambda_u^m(0)$  to some non-negative value for all users and resource blocks
  - 2: **Step 2:** Apply Optimizing method  
Apply optimization technique using equations (3.26)-(3.29)
  - 3: **Step 3:** Numerical search Bounds Calculation  
Calculate the numerical search upper bound ( $\Omega_{UB}$ ) and the lower bound ( $\Omega_{LB}$ ) according to equations (3.31) and (3.32)
  - 4: **Step 4:**  $s_u^m$  calculation  
take  $\Omega_u^m = \frac{(\Omega_{UB} + \Omega_{LB})}{2}$  and calculate  $s_u^m$  according to equation (3.29)
  - 5: **Step 5:**  
If  $s_u^m > \bar{s}_u^m$ , then  $\Omega_{UB} = \Omega_u^m$ ; otherwise  $\Omega_{LB} = \Omega_u^m$ ;
  - 6: **Step 6:** Iterate until the implementation converges to the optimality (or the number of iteration is reached)
- 

### 3.5.3 Simulation Results

In this section, simulation results are presented to demonstrate the performance of the proposed algorithm. We conduct a numerical experiment to implement the above mentioned optimization algorithm. The optimization model is numerically solved to evaluate the convergence behavior of the proposed algorithm and demonstrate that it is able to achieve the maximum throughput and the corresponding maximum EE as well. We consider a LTE network for our simulation. The system parameters used in our simulations are given in Table 3.1.

Figure 3.14 presents the convergence behavior of the optimization algorithm. It can be seen that all allocated data rates, using the Lagrangian technique, approach the optimal

value after 50 iterations. Therefore our algorithm converges quickly enough (roughly  $\sim 50$  milliseconds) to have a realistic implementation in a system level basis. Using these results, we can design optimal energy consumption (maximize EE) network based on rate-oriented method for MU-MIMO if the power is fixed.

Table 3.1: Key simulation parameters

Parameter Name	Value
Simulation mode	Combined snapshot-Dynamic
Carrier Frequency, $f_c$	2.6 GHz
Bandwidth	20 MHz
TTI	1 millisecond (1 sub-frame)
Number of PRB	100
Noise Density	-174 dBm/Hz
Multipath Model 3GPP	Spatial Channel Model [90]
Antenna Configurations	Downlink: (eNB,UE) $\rightarrow$ (2,2)
Antenna Separation (eNB, UE)	$(10, 0.5) \times \text{wavelength}$
Transmitter Processing	Zero-Forcing
Number of Users	5
User Speed	3 km/h
Power of each eNB	46 dBm
Circuit power	20 dBm
Power amplifier efficiency, $\alpha$	0.38
Dynamic circuit power per unit data rate, $\delta$	2 W/Mbps
Minimum SE	2 bps/Hz
AMC PER $_{Target}$	1%

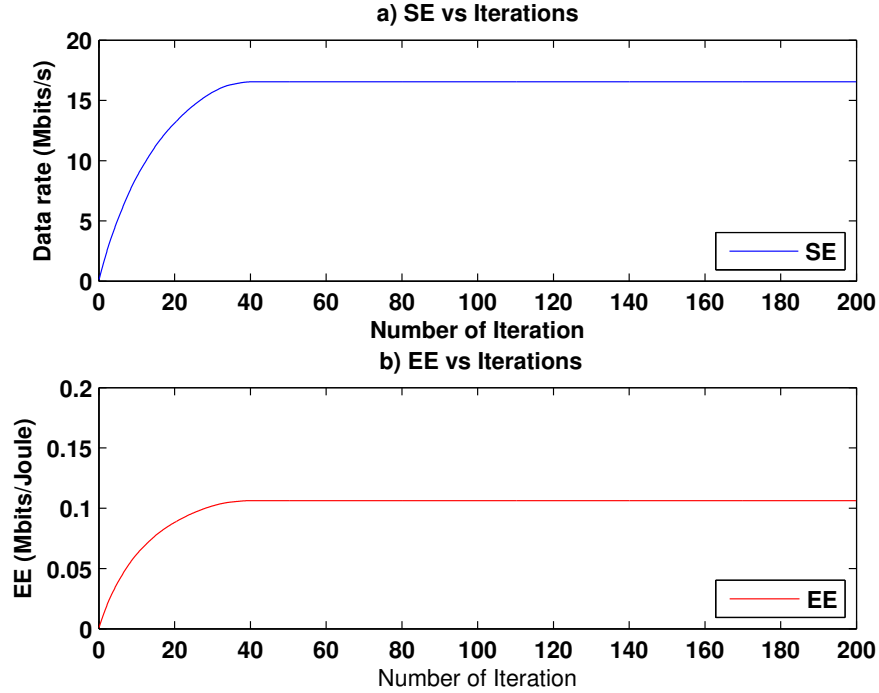


Figure 3.14: Convergence performance of the optimization method

Figure 3.15 presents the effect of different PRB demands using the proposed algorithm. Increasing the number of PRB enhance the EE of the system since it increases the data rate. From the figure we notice that the smaller the number of the PRBs the faster the algorithm converges, since more PRB takes more iterations to converge. Furthermore, faster convergence occurs if we need to adhere to lower SE requirement, whilst convergence becomes slower when considering higher SE requirement.

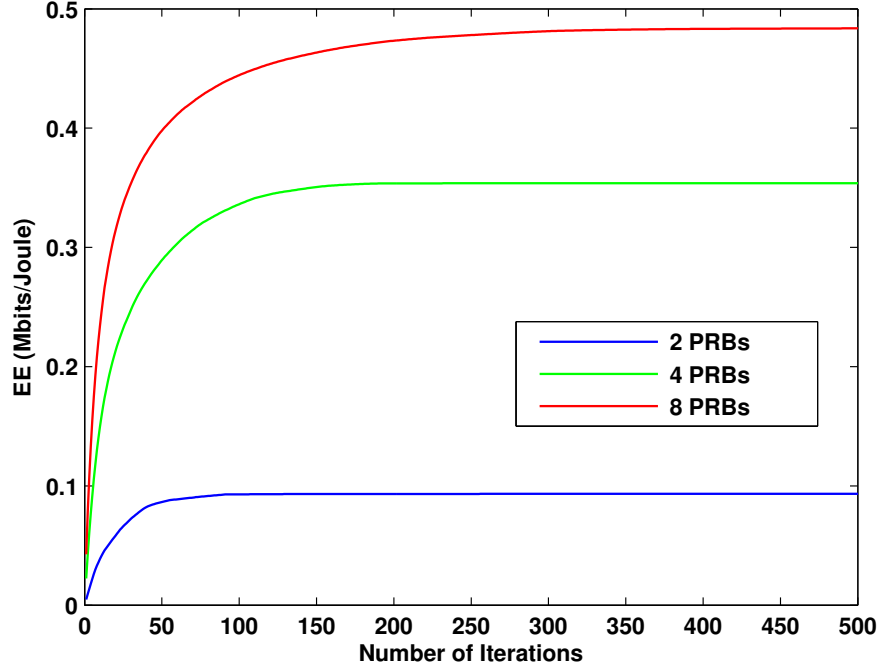


Figure 3.15: Comparison of convergence of EE of different PRBs

Figure 3.16 demonstrates the impact of the dynamic power factor  $\delta$  in our optimization algorithm. The EE is improved if we do not consider the dynamic power factor ( $\delta = 0$ ) and also converges very quickly compared to the scenario when  $\delta$  is considered. The value of  $\delta$  makes a impact on the EE; the greater the value of  $\delta$ , the smaller the EE of the system. Increasing  $\delta$ , needs more iterations to converge but makes the smaller optimization smoother so that abrupt change would make less impact on the system.

Figure 3.17 represents the average cell energy efficiency as function of the spectral efficiency (see Eq.(3.23)) as well as the bounds deduced from the above section 3.5.2.2. We observe that EE increases with SE until some point and then decreases. In order to interpret this result, we need to recall that the energy efficiency is a monotonic increasing function until circuit power is considered. The curve tends to be quasiconcave on SE which justifies the basic criterion of SE-EE curve depicted in [70]. According to [91], a function  $f : Q \rightarrow \mathbb{R}$  is quasiconcave on  $Q$  if and only if for all  $x, y \in Q$  and for all  $\lambda \in (0, 1)$  it is the case that

$$f[\lambda x + (1 - \lambda)y] \geq \min \{f(x), f(y)\} \quad (3.33)$$

which justifies the quasiconcavity shows in the figure. Figure 3.17 also shows the optimal envelop of the entire SE-EE region, which offers a global perspective on the SE-EE trade-off.

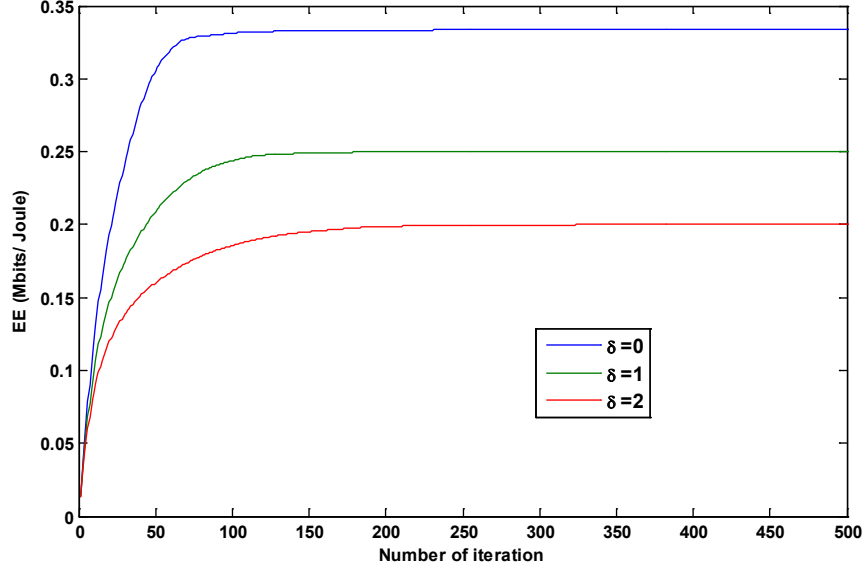


Figure 3.16: Convergence of different dynamic circuit power

The optimal EE emphasizes the existence of a saturation point, beyond which the EE can no longer be further increased, regardless of how many additional resources are used. Using this result, on the one hand, allow us to design the optimal energy consumption networks based on EE-oriented methods for MU-MIMO, if the system SE is not limited. On the other hand, we can maximize the energy efficiency while satisfying a given SE (rate) requirement. It is better for operators to set up the system operational SE around the point of peak EE.

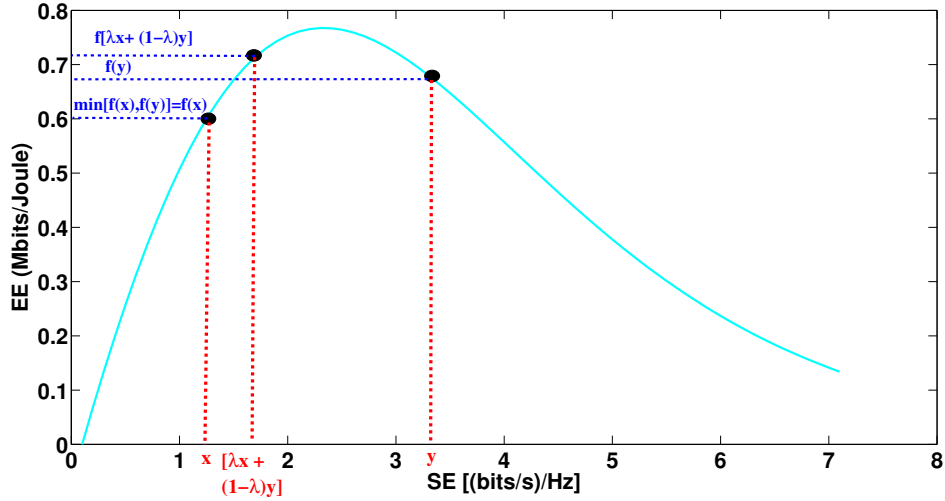


Figure 3.17: EE vs. SE Trade-off relation

We have also investigated what effect the power amplifier efficiency had on energy efficiency as seen in Fig. 3.18. It is clear that the higher power amplifier efficiency leads to higher energy efficiency. All simulation results indicated that the algorithm of achieving maximum

EE for MU-MIMO antenna configurations not only dramatically increases energy efficiency, but provides a low complexity solution to implement as a pragmatic solution.

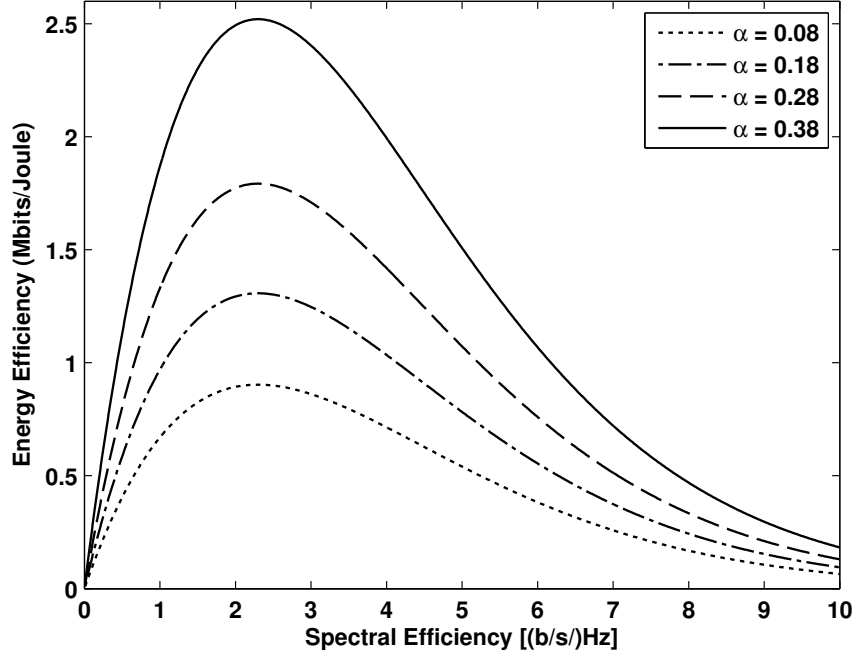


Figure 3.18: EE vs. SE with various power amplifier efficiency

### 3.6 Conclusions

In this chapter, we have discussed a framework for SE-EE trade-off in OFDMA wireless cellular networks, which should be at the forefront of system design for more energy compliant networks. We have overviewed that, in practical systems, the trade-off relations usually deviate from the simple monotonic curves derived from the Shannon's formula as summarized in the state-of-the-art section. Moreover, most of the existing literature mainly focuses on the point-to-point single cell case. Therefore, the SE-EE trade-off relations under more realistic and complex network scenarios deserve further investigation. The insights, such as how to improve the SE-EE trade-off curves from a holistic view and how to tune the operating point on the curve to balance the specific system requirements, are expected to guide practical system designs toward more energy conscious networks, and define the next step in Green Communication research.

In this chapter, we also investigated the EE-SE relation in downlink multi-antenna multi-user CoMP system. Simulation and analysis of results show that there is a trade-off between EE and SE, and thereafter proposed a novel resource allocation algorithm to maximize EE. We establish an analytical method to optimize energy efficiency of CoMP system with respect to target SE constraints. We use this method to analyze the sensitivity of the efficiency to the network parameters. The results will place wireless system engineers in good stead to design optimal energy efficient networks based on EE-method, for multi cell MIMO system such as MU-MIMO CoMP.

## Chapter 4

# CoMP Energy Efficiency Performance Evaluation

*In the framework of 3GPP, several solutions are proposed for LTE to mitigate ICI and to enhance cell edge throughput, Relaying and Coordinated Multipoint (CoMP) are examples of such. CoMP transmission and reception techniques utilize multiple transmit and receive antennas from multiple antenna site locations, which may or may not belong to the same physical cell, to enhance the received signal quality as well as decrease the received spatial interference [6]. Using CoMP the cell average and cell edge throughput are boosted, unlike Relay technology, which only increases the cell edge throughput [92]. CoMP has been an active area of research, and a study item in 3GPP targets has included CoMP in the latest releases (LTE release 11 [11]). Until recently, the spectral efficiency (SE) of the cell, cell-edge throughput and the users' fairness are used as performance indicators for CoMP technology. As green communication plays a more prominent role, energy efficiency (EE) now carries equal weighting in terms of performance. Packet scheduling operation in LTE-Advanced networks plays a major role in QoS delivery, that also influences the spectral and energy efficiency of the system. The aim of packet scheduling is to allocate the resources and transmission power to the different users in each subframe to optimize a set of metrics (like spectral efficiency, throughput, fairness, delay, and outage probability). So far packet scheduling algorithms have been extensively studied from a capacity and QoS perspective, but in a green communication context, it is required to go beyond this and consider EE as an optimization parameter. The focus of this chapter is to study the SE-EE performance for downlink CoMP using traditional scheduling policies. To achieve this baseline, in particular, we investigate scheduling approaches that include Round Robin (RR), Proportional Fairness (PF) and Maximum Carrier to Interference ratio (MCI). To analyze the performance, a dynamic system level simulator is used that models in detail all the features of the downlink LTE system in a multi-cell environment (covering aspects such as Hybrid Automatic Repeat request (HARQ), link adaptation (LA) and multi-antenna techniques). In particular the first step involves describing the different transmission techniques for CoMP in LTE based on using the aforementioned resource allocation policies. These are evaluated from an EE perspective, as well as showing the relative gains of the different CoMP transmission scenarios; this methodology is valid for SoA schedulers [93], but also serves as a benchmark for evaluating innovative energy aware algorithms where few works exist.*

## 4.1 Energy Efficiency

Energy channel capacity is usually defined in bits per joule, as in [69]. We adopt that definition as metric for energy efficiency. For this article, we refer to this as the average EE i.e., the successfully delivered bits over the total power, denoted as  $P_{Total}$ , consumed by the wireless network. It means how many bits per unit power can be transported per second, in other words, the bits per joule. Hence, this definition is useful for measuring whether a wireless system is efficient in terms of consuming energy. The network EE,  $\eta_{EE}$ , is defined [94] as the ratio of the total network throughput per unit bandwidth over the network power consumption within a given period (unit: bits/Joule):

$$\eta_{EE} = \frac{TP_{net}}{P_{Total}} = \frac{TP_{net}}{P_{Tx}} \quad (4.1)$$

where  $TP_{net}$  is the average throughput of the network per unit time (unit: bps or bits/s) and  $P_{Tx}$  is the transmission power of the network (unit: Watt). Therefore, the energy consumption is the multiple of power (Watt) and time (second) whose unit is Joule. Typically, in energy efficient communications, the aim is to maximize the amount of meaningful data transmitted for a given amount of energy. In addition to the transmit power, some power is consumed in the circuitry or dissipated in the form of heat. This kind of power is counted as circuit power, denoted as  $P_{Circuit}$ , which is mostly independent of the transmission state. Then EE can be defined as:

$$\eta_{EE} = \frac{TP_{net}}{P_{Total}} = \frac{TP_{net}}{P_{Tx} + P_{Circuit}} \quad (4.2)$$

It should be kept in mind that the above mentioned metric was not directly related to the throughput performance of the system such as GSM and WCDMA since their main service is voice (and here, performance is not measured by the data rate). Nevertheless, in 4G cellular systems like LTE, all services are data. Therefore, this opens the door to measure the performance of the system in terms of throughput by exploring the data rate. Hence bits/Joule is the basic EE metric for fourth generation cellular systems and beyond [95], for any type of service.

## 4.2 CoMP Frame Architecture

Our architecture is based on the reference LTE architecture.

### 4.2.1 LTE Frame Architecture

The general frame structure for LTE-FDD [24] is shown in Figure 4.1. The time duration of one LTE FDD frame is 10 ms which subdivide into 10 subframes with each 1 ms of duration. In LTE simulation Transmission Time Interval (TTI) is equal to 1 subframe. These subframes are further divided into slots of each 0.5 ms. So, each subframe contains 2 slots. The slot is the smallest time-frequency unit for downlink transmission and is called a Physical Resource Block (PRB). Data is allocated to each user in units of PRB. PRB spans 12 consecutive sub-carriers at a sub-carrier spacing of 15 kHz, and 7 consecutive symbols over a slot duration of 0.5ms. Thus, a PRB has 84 resource elements (12 sub-carriers  $\times$  7 symbols) corresponding to one slot in the time domain and 180 kHz (12 sub-carriers  $\times$  15 kHz spacing) in the frequency

domain. Each user assigns one or more slot according to their traffic demand in time and frequency domain. The size of a PRB is the same for all bandwidths; therefore, the number of available PRBs depends on the transmission bandwidth. In the frequency domain, the number of available PRBs can range from 6 (when transmission bandwidth is 1.4 MHz) to 100 (when transmission bandwidth is 20 MHz). It should be kept in mind that we consider 20%-40% of signaling overhead in each TTI (i.e., first 3 symbols [96, 97]).

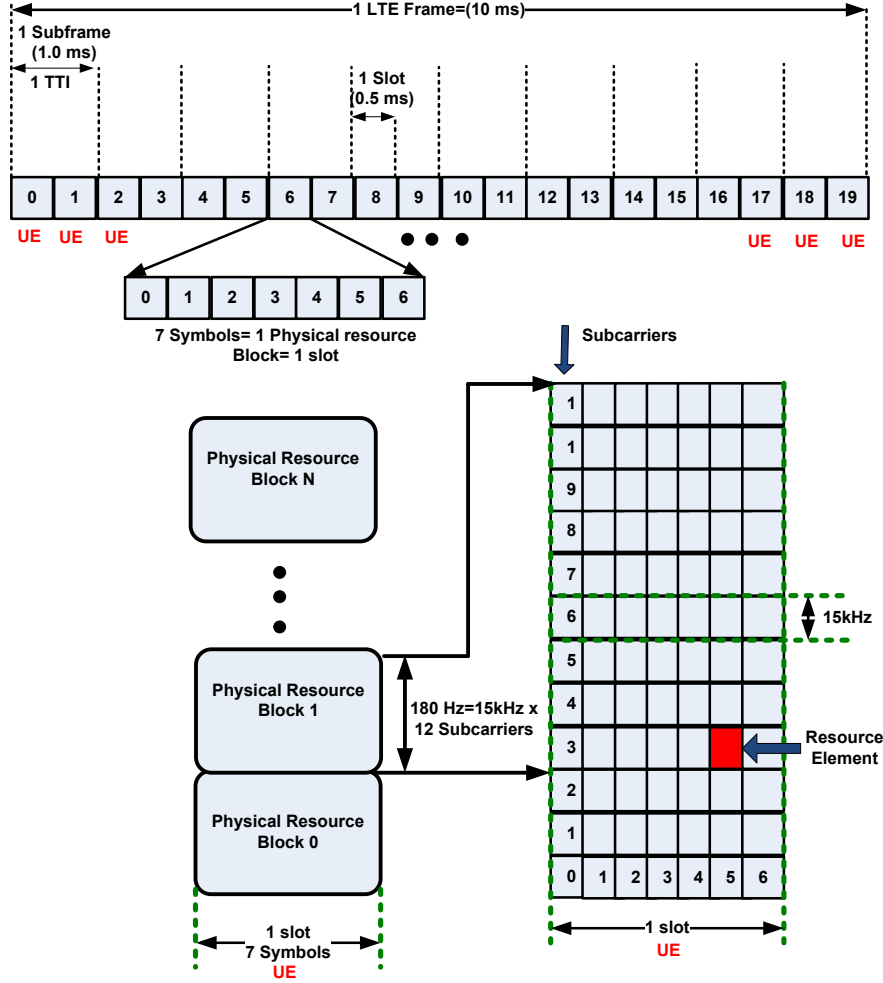


Figure 4.1: LTE-Frame Structure

We adopted a basic LTE FDD frame structure for three CoMP transmission techniques. For the sake of simplicity, we explain the frame of each of the three CoMP techniques on the basis of 1.4 MHz transmission bandwidth which consist 6 PRBs.

#### 4.2.2 JT-Frame

In Figure 4.2, we illustrate JT-CoMP frame. Data is transmitted from all eNB using the same resources (for example, in one PRB). The same PRB of the PDSCH (Physical Downlink Shared Channel) is transmitted from multiple eNBs associated with a UE specific demodulation reference signal (US-RS) among coordinated cells (i.e., from non-serving cell(s)

as well as the serving cell). For instance, JT is achieved by codebook-based precoding to reduce feedback signal overhead [7].

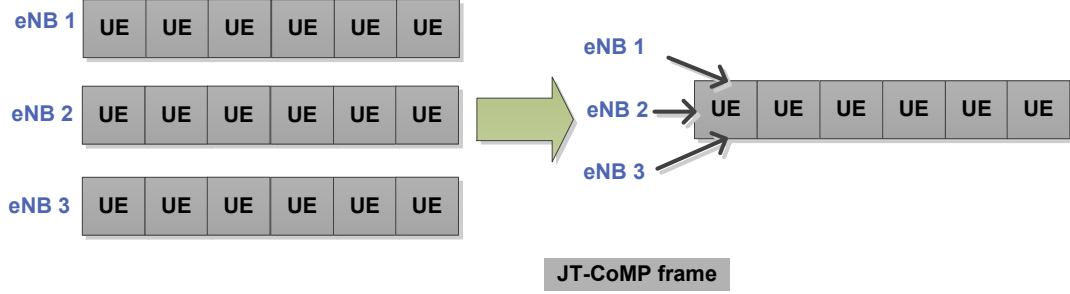


Figure 4.2: User Scheduling for one JT frame

#### 4.2.3 DPS-Frame

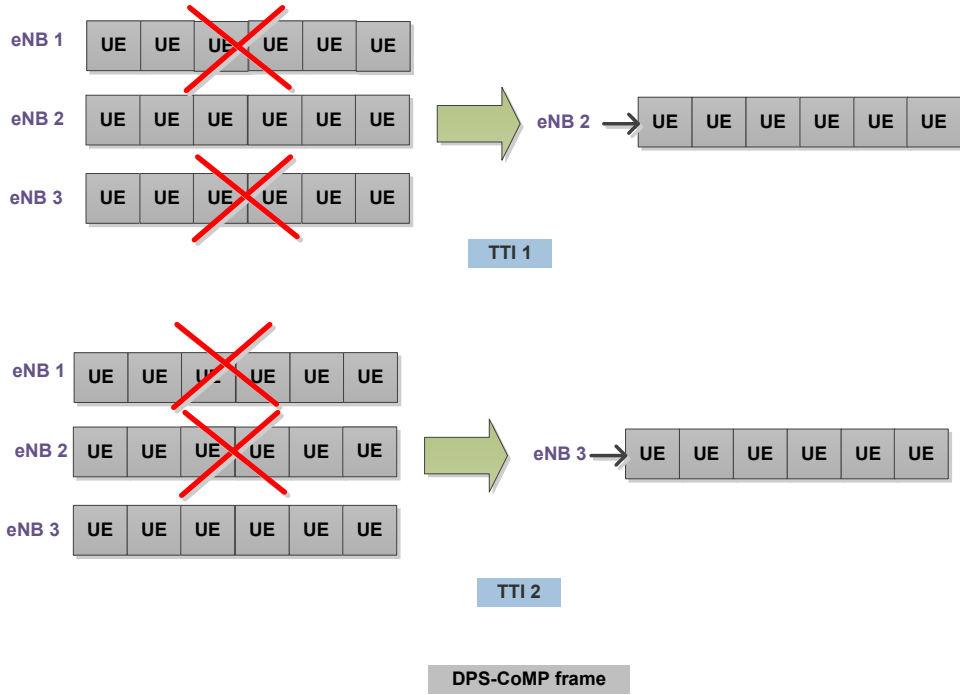


Figure 4.3: User scheduling for one DPS frame

In the DPS-CoMP frame, as illustrated in Figure 4.3, we can see that in TTI 1, let's say, a UE is configured to receive a signal from 3 eNBs. From eNB2, the UE got the best channel condition, so eNB2 is fast/ dynamically selected for TTI 1 and the other 2 eNBs (eNB1, eNB3) are muted. In the next TTI 2, UE is selected by eNB3 due to better channel condition. Since all the eNBs are coordinated, the other 2 eNBs (eNB1, eNB2) are muted.

#### 4.2.4 CS/CB Frame

Figure 4.4 shows the operating principle of CS/CB-CoMP frame coordinating 3 eNBs. Unlike the aforementioned DCS, a PRB (data) is transmitted only from the serving eNB while 'scheduling' or 'beamforming' is coordinated within 3 eNBs together with the PDCCH (Physical Downlink Control Channel). Hence, a PRB is assigned to the UE with CS/CB by scheduling in the serving cell. Therefore, in particular, the cell edge user throughput can be improved due to the increase in received SINR. CS/CB frame can be characterized by multiple coordinated eNBs sharing only CSI for multiple UE terminals, while frames (data packets) that need to be conveyed to a UE terminal are available only at one eNB.

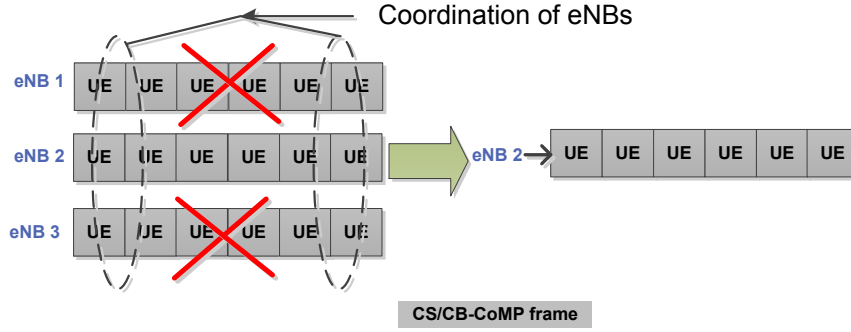


Figure 4.4: User Scheduling for one CS/CB frame

### 4.3 Deployment of CoMP

There are two ways to deploy CoMP technology—autonomous distributed control based on an independent eNB configuration which processes every signal of its own, or centralized control based on centrally controlled eNB configuration connected via fiber through CU [7]. The obvious question is whether coordination between cells can be distributed or centralized [5]. There is no impact on any radio-interface for independent eNB coordination. In autonomous eNB configuration, coordination is used between eNB. This method is more complex than the others since signaling delay and overhead between eNB is still an open challenge. Therefore in our analysis, we deploy CoMP with the centralized control where coordination of eNBs is done on CU as shown in Figure 3.13.

We consider a centrally controlled CoMP for our EE evaluation. In this approach, a processing unit located centrally uses a diverse set of information—channel state information (CSI) which includes CQI, precoding matrix index (PMI) and rank indicator (RI) informed by the UE—to decide which sets of eNB are best suited for serving the user. Since the processing is centrally controlled, the central processor, in this case the CU, will handle all the digital signal processing. The phase components of the waveforms for transmission are precomputed at the central processing units and extracted into the set of eNBs that are best suited to serve the UE. The data to and from the eNB is sent via a common backhaul interface typically carried over an optical network, and the bandwidth requirement to handle waveforms in either direction can be in gigabits per second depending on the capacity the eNB is dimensioned to provide. The Centrally controlled CoMP concept is illustrated in Figure 3.13.

## 4.4 System Level Simulator

The implementation, analysis and comparison of these scheduling algorithms were done through simulations executed on a C++-based downlink system level simulator [98, 99].

Typically, network simulations are divided into two parts: link level and system level simulations (SLS). Although a single simulator approach would be preferred, the complexity of such a simulator (including everything from transmitted waveforms to multi-cell network) is far too high with the required simulation resolution and time. Also, the time granularity of both domains are dramatically different: at link level bit transmissions are in the order of milliseconds (ms), while at the system level traffic and mobility models require time intervals of some tens of seconds to minutes. Therefore, separating link-level and system-level simulations is a necessity.

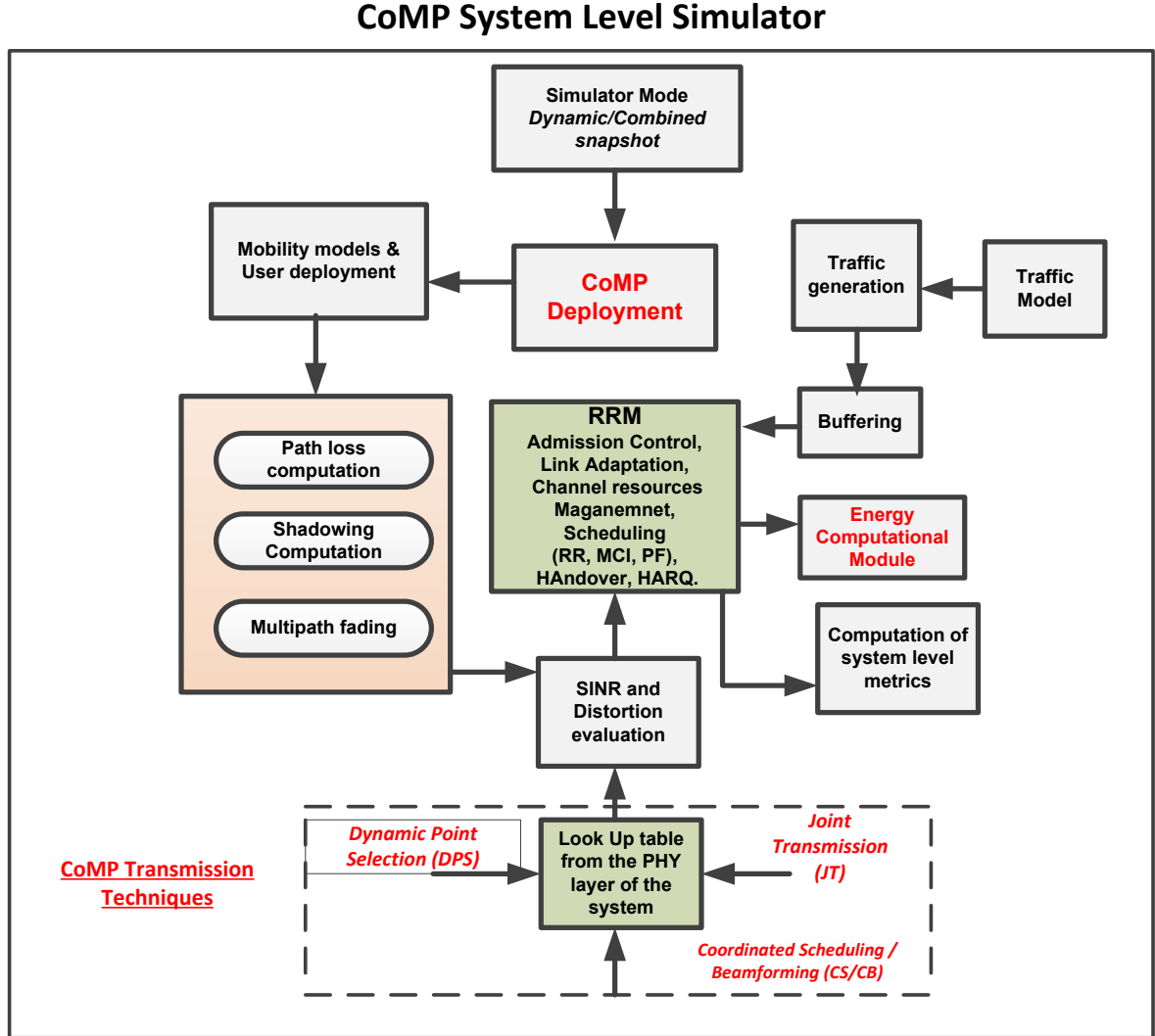


Figure 4.5: Logical Simulation Component of CoMP

For SLS purposes, we consider a LTE-A cellular system consisting of 19 CoMP cell sites,

with six CoMP cell sites in the first tier and twelve CoMP cell sites in the second tier, surrounding the central CoMP cell. Each CoMP cell site includes three 120-degree hexagonal sectors, i.e., 57 sectors in total are simulated. All the simulation results are collected from the three central hexagonal sectors in the central CoMP cell site, with the other 54 sectors serving as interferers. A wrap-around model is used to avoid border effects [54].

Figure 4.5 demonstrates the logical SLS component of the CoMP. The SLS interfaces with the link level simulator (done through simulations executed on a MATLAB-based downlink link level simulator from the Vienna University [100]) through Look up tables (LUTs) as an input to the simulator. Link level simulation is done by assuming single cell and multiple users. In the link level simulator we deploy different transmission schemes for CoMP i.e. DPS, JT, and CS/CB. These transmission schemes are then simulated using frequency selective channel and different coding and modulation schemes. The output of the link level simulator is in the form of LUTs which reflect the function of SNR vs. BLER (block error rate) performance curves. In practice, we have 3 different LUTs used [101] for three different CoMP transmissions which are then fed to the system level simulation platform. The system level simulator then computes the successfully transmitted packets given the mobility, traffic and channel profiles employed. Specifically, the outputs are the parameters that usually characterize packet transmissions: Throughput, BLER, Packet Delay etc.

The traffic generation block contains real (i.e., VoIP, WWW) time service traffic models with full queue. The Handover block includes the handover algorithm. The radio resource management block comprises a call admission control algorithm to regulate the operation of the network; a link adaptation (LA) algorithm to select the appropriate parameters in function of the current radio conditions and a scheduler that decides how to allocate the appropriate resources based on the service type, the amount of data, the current load in the cell, etc. The Power control block contains mechanisms to provide similar service quality to all communication links despite the variations in the channel conditions. The interference block determines the average interference power received by central base station, i.e., inter-cell interference.

Finally, the computations of the system level metrics block returns the network results such as Service Throughput (average spectral efficiency), BLER and Packet Delay. The mobility block models the mobile movements in the indoor, urban, and rural environments. Parameters associated with mobility include speed, probability to change speed at position update, probability to change direction, and the de-correlation length. The propagation block models path loss, shadow fading and Multipath fading. Channel models for indoor environments, outdoor urban and rural environments are available. The scheduler mechanism will generate the arrival process of the users, according to a Poisson arrival process.

The objective of Call Admission Control is to regulate the operation of a network in such a way that ensures the uninterrupted service provision to the already existing connections and at the same time accommodates the new connection request in an optimum manner. The scheduler decides how to allocate the appropriate resources based on the service type, the amount of data, the load on the common and shared channels, the current loading in the cell and the radio performance of each type of transport channel. LA can be considered as a component of Dynamic Channel Allocation (DCA). With the power control mechanism, similar service quality is provided to all communication links despite the variations in the channel conditions, which means larger proportion of the total available power is consumed for the bad channel conditions. Handover is common to all dynamic system level simulators, and required to maintain link quality at the cell boundaries. Simulation Map describes the

cellular layout, which includes the cell descriptions, base station locations, and the manner in which it will model mobile movement at the system boundaries. HARQ is employed for non-real time services. DCA algorithm provides extra performance, but it is not a crucial element in the simulator.

In SLS, two different types of simulations can be performed: Combined Snapshot-Dynamic mode or a Fully Dynamic mode. In the fully dynamic mode, mobility and handover are enabled and path loss, fast and slow fading are re-computed at every Transmission Time Interval (TTI). In combined Snapshot dynamic mode, mobility and handover are not enabled. Mobiles are randomly deployed in every TTI, path loss and slow fading are computed once at the beginning of each TTI. It is worth to mention that we use combined snapshot-dynamic mode

#### 4.4.1 Energy Module

The energy computation model metrics have been introduced in the simulator [98, 99] to compare the different schedulers from an energy point of view. Its' operation is as follows:

- ⇒ In each TTI number of resource block are simulated according to given channel bandwidth.
- ⇒ Data rate of each resource block is calculated which is a function of the selected MCS scheme, i.e.  $f(R_u^m, MCS_u^m)$  where  $R_u^m \rightarrow$  data rate on each  $m^{th}$  PRB for  $u^{th}$  UE.
- ⇒ SINR of selected MCS scheme are found from the LUTs (which feed from link level simulator [102]) for CoMP transmission schemes according to [103].
- ⇒ Then the data rate achieved according to selected SINR for each PRB.
- ⇒ Data rate of each PRB is aggregated and divided by total power (aggregated transmit power of all PRBs and the circuit power) provides us the EE in bit per joule (see equation (4.3))
- ⇒ An average measurement will be taken over all TTI.

A pictorial depiction of the energy module is demonstrated by Figure 4.6

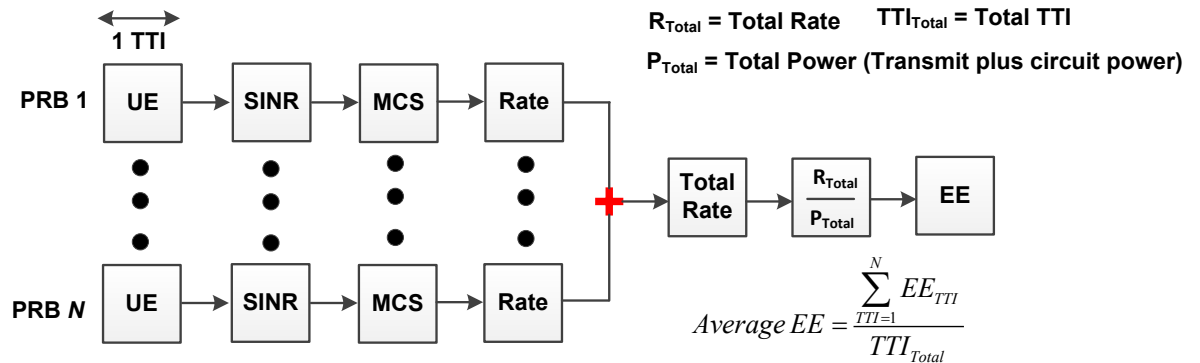


Figure 4.6: Energy Module

Simulation parameters are illustrated in Table 4.1

Table 4.1: Key simulation parameters

Parameter Name	Value	
Simulation mode	Combined snapshot-dynamic	
Carrier Frequency, $f_c$	2.6 GHz	
Bandwidth	20 MHz	
Duplex Mode	FDD	
Noise Density	-174 dBm/Hz	
Multipath Model	3GPP Spatial Channel Model [90]	
Path-Loss Model	LOS	PL(dB)= $22\log_{10}(d)+34.02$ ; where $10\text{m}<d<320\text{m}$ [10] PL(dB)= $40\log_{10}(d)-11.02$ ; where $320\text{m}<d<5000\text{m}$
	NLOS	PL(dB)= $39\log_{10}(d/1000)+136.8245$
Log-normal Shadowing Variance $\sigma$ (dB)	LOS	$\sigma = 4(\text{dB})$
	NLOS	$\sigma = 8(\text{dB})$
Cellular Layout	19 CoMP cell sites / 57 hexagonal cell sectors, 3 hexagonal cells per CoMP cell site with 70 degree sector beam width	
Antenna Configurations	Downlink: 2-by-2	
Number of Users	2.....16 per cell site	
User Speed	3 km/h	
User Power	23 dBm	
eNB Power	46 dBm	
Circuit power	20 dBm	
Inter-site distance	500 meters	
Minimum distance between UE and cell	35 meters	
TTI	1 ms (sub-frame)	
Number of Resource Block	100 RB in each slot, 7 symbol, number of subcarriers per RB=12, total subcarrier=1200	
Reference symbol overhead	DM-RS: 12 RE PRB for 1-2 orthogonal DM-RS ports CSI-RS: 2 RE/PRB per 10 ms [11] CRS: 2 CRS Release-8 legacy overhead [65]	
Link to system interfacing	EESM (Effective Exponential SNR Mapping)	
MCS types	QPSK, 16-QAM, 64-QAM	
Link Adatation	MCSs according to [101]	
Traffic model	Full Queue (Continuous Data) 10 user/cell/Sec	
Scheduling Algorithm	RR, PF, MCI	
Channel estimation	Ideal	
Turbo decoder	Max Log Map (8 iterations)	
HARQ	Number of process=6, Retransmission interval= 6ms, Chase combining, Max. No. of retransmission=3	
AMC $PER_{Target}$	10%	
CQI delay	Each TTI, with 2ms delay	
Link Level Simulator (LUTs)	JT, DPS, CS/CB	

#### 4.4.2 Performance Metrics

In this work we use the metrics EE, EE gain and SE for our performance analysis with respect to different downlink packet scheduling algorithm for various CoMP transmissions. In this section we provide the metrics in details. Energy metrics, for maximizing energy efficiency EE, is defined in our simulation purpose, as the ratio of the total transmitted bits per unit energy consumption [94] (unit: bits/Joule).

$$EE = \frac{\text{Data rate}}{\text{Power}} \left[ \frac{\text{bits/Second}}{\text{Watt}} = \frac{\text{bits}}{\text{Second} \times \text{Watt}} = \text{bits/Joule} \right] \quad (4.3)$$

To demonstrate the EE gain compared to different scheduling and transmission techniques, the following performance metric are employed, called Relative EE gain (unit: percentage):

$$EE_{\text{gain}}(\%) = \frac{EE_{CS} - EE_{BM}}{EE_{BM}} \times 100$$

$$EE_{\text{gain}}(\%) = \left( \frac{EE_{CS}}{EE_{BM}} - 1 \right) \times 100 \quad (4.4)$$

where  $EE_{CS}$  is the energy efficiency of the compared scheduling technique and  $EE_{BM}$  is the energy efficiency of the scheduling which is used as a benchmark to find out the relative gain.

We also use existing spectrum efficiency metrics for wireless networks, SE, the data rate of each user per unit bandwidth per cell, in bps/Hz ([bits/s]/Hz).

#### 4.5 Simulation Results and Discussion

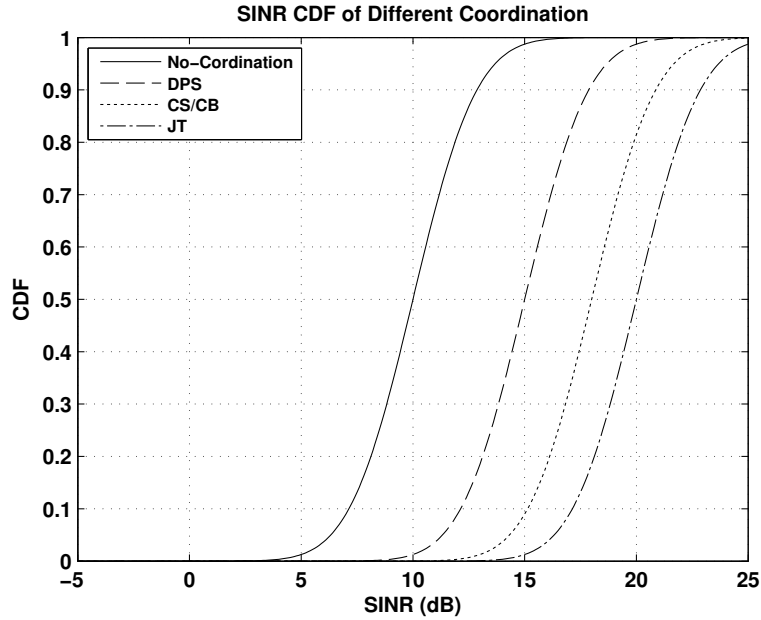


Figure 4.7: CDF of the signal quality of different coordination

Figure 4.7 shows the SINR CDF of different coordination techniques. As expected, JT provides the best performance due to their multi-antenna diversity using same resources in

a different space dimension. 50% of the JT UEs get 20 dB SINR whereas Non-coordinated, DPS and CS/CB user received 10 dB, 15 dB and 18 dB respectively. The higher the SINR the better chance to achieve higher MCS which will eventually result in higher system gain in terms of throughput. Although in terms of the UE signal quality, JT CoMP is superior to the DPS as shown in Figure 4.7; the JT CoMP SINR gain comes at the cost of using the resources from two different points. Therefore, in terms of system complexity, the DPS CoMP can be a more efficient scheme than the JT CoMP.

Figure 4.8 shows the EE of the different CoMP system with a variable number of users in terms of the SoA packet scheduling algorithms. It can be clearly seen, that the EE increases with the number of users which is due to multi user diversity. This EE is also enhanced by adding more antennas which gives us more diversity in terms of coherent transmission and beamforming. In reality, DPS provides less throughput than the other two techniques (CS/CB and JT), due to their signal quality; however, their EE is higher than other one due to the muting of eNB. Since, for each TTI in DPS, only the transmitted eNB is transmitting power so the consumption of the transmitted power is one-third compared to the other two CoMP techniques. The EE eventually saturates due to reaching the cell capacity.

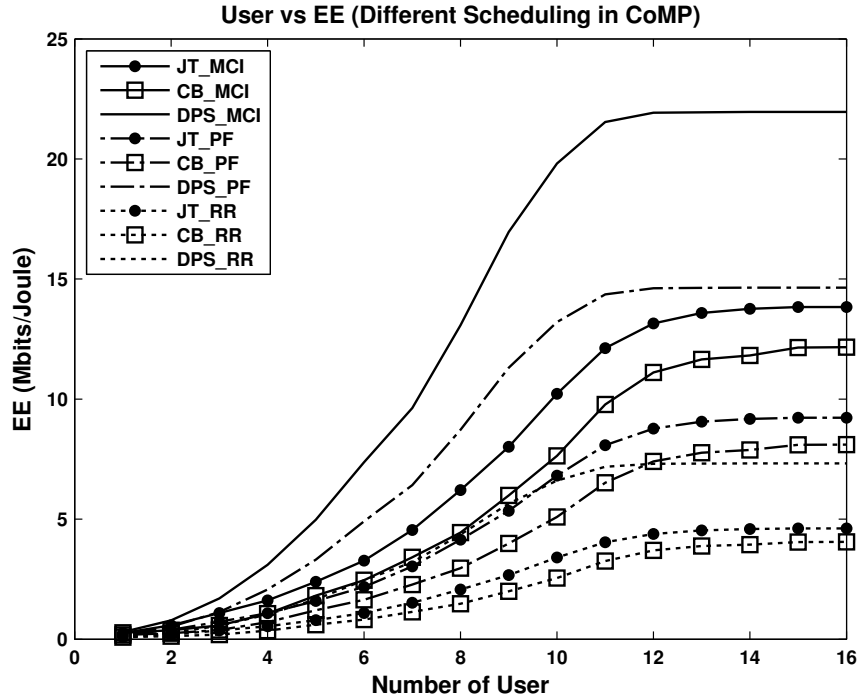


Figure 4.8: Energy Efficiency vs. number of user

Since RR is a non-channel aware scheduling technique provides the least energy efficient outcome, compared to other scheduling approaches. So we consider RR as our benchmark for comparison against energy-aware scheduling approaches in terms of relative gain. Figure 4.9 shows a comparison in terms of the relative gain with respect to RR scheduler for different CoMP techniques. In this case, the EE of the RR is  $EE_{BM}$ , where the EE of the PF and MCI works as  $EE_{CS}$ . Figure 4.9(a), 4.9(b) and 4.9(c) demonstrates EE gain of PF and MCI scheduling over RR for JT, CS/CB, and DPS transmission respectively for the same number

of users. As we can see, the obtained gains (especially for the MCI scheduler) depend on the number of users in the cell, even if the network is fully loaded: this scenario is due to the packet scheduling algorithms being dependent on the exploitation of multi-user diversity.

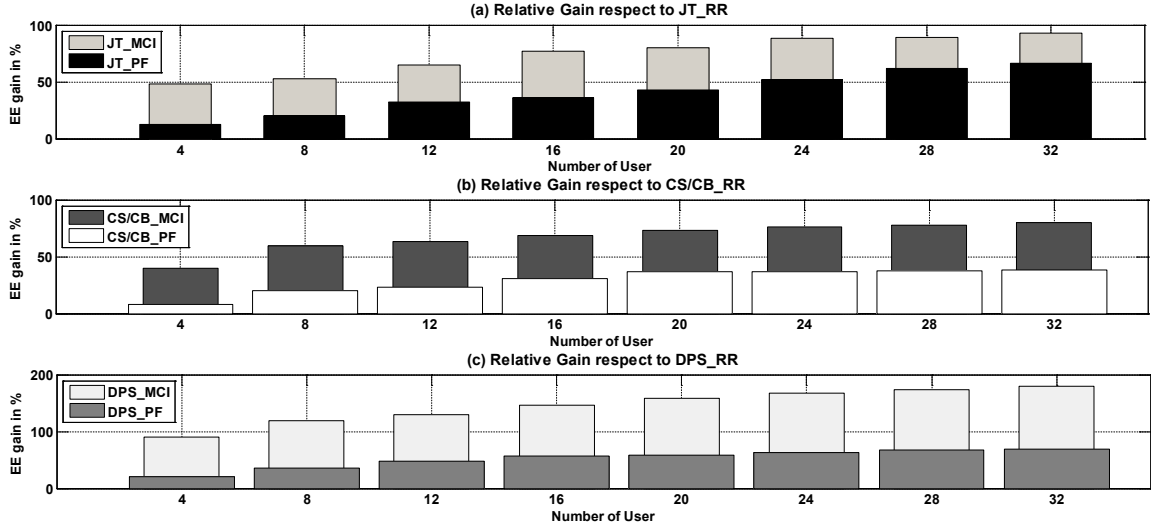


Figure 4.9: Relative gain with respect to RR packet scheduling

Among the three CoMP transmission techniques, CS/CB shows the worst performance in terms of EE due to their transmission nature, which resulted with less data rate per unit power compared to the other two techniques (In reality CS/CB provides more throughput than DPS but they consume more transmit power since all the RRH is simultaneously transmitted in every TTI).

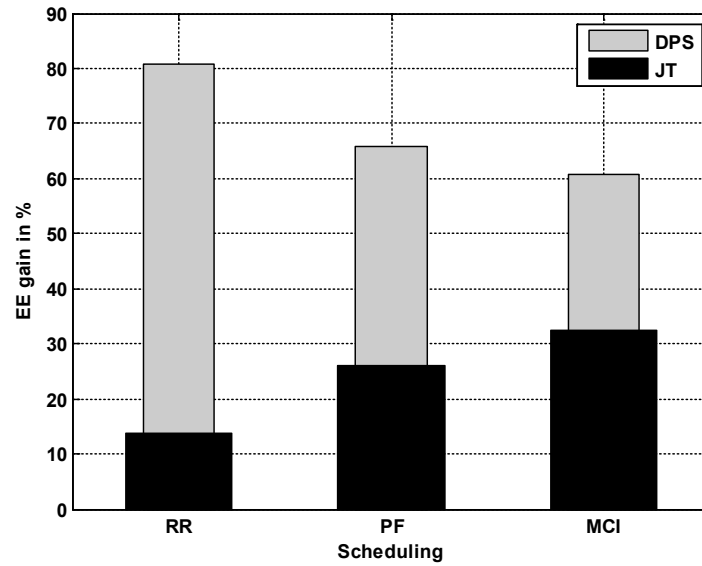


Figure 4.10: Relative EE gain respect to CS/CB transmission

We consider CS/CB as our baseline CoMP technique for comparing the relative gain against the other two approaches (DPS, JT), the numerical value of the performance gain (user number=20) is shown by Figure 4.10. Since in JT, data is transmitted from 3 eNBs simultaneously, and in CS/CB data is beamformed from 1 eNB whilst the other 2 eNBs are used for signaling, which increases the transmitted power and eventually decreases the energy efficiency. The numerical value of the performance gain (User number=20) is given in Table 4.2

Table 4.2: EE gain according Figure 4.10

Scheduling Technique	EE (Mbits/Joule) of CoMP Transmission			EE gain in (%) respect to CS/CB	
	DPS	CS/CB	JT	JT	DPS
RR	7.3320	4.0541	4.6125	13.7734	80.8540
PF	9.2940	5.6008	7.0552	25.9677	65.9406
MCI	11.7339	7.2988	9.6756	32.5643	60.7648

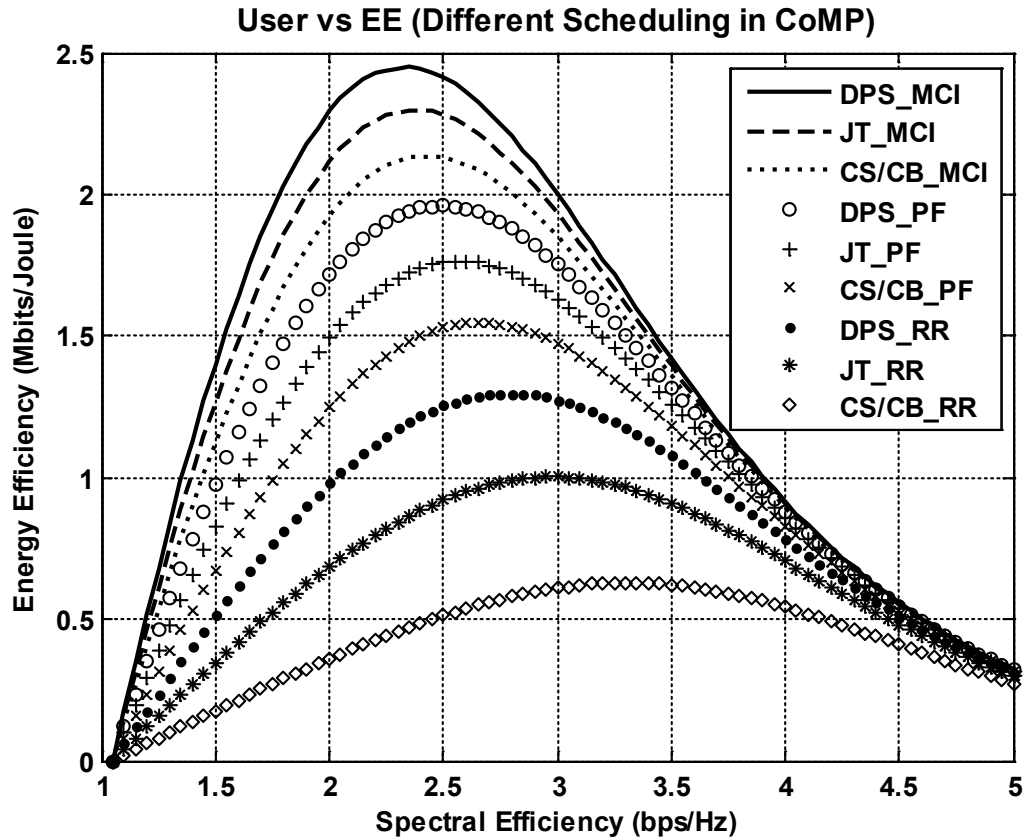


Figure 4.11: EE vs. SE

Figure 4.11 shows the energy-efficiency versus Spectral-efficiency for different scheduling policies in CoMP modes, where the number of users is 20. It is shown that CS/CB\_RR has the least optimal EE. We also observe that the optimal EE value increases with CS/CB, JT

and DPS respectively, irrespective of the scheduling. Transmitting only one RRH in each TTI improves the energy-efficiency of the DPS. Typically EE decreases when SE increases, but considering circuit power makes this trend quasi-concave [70, 104]. This quasi-concavity property of the EE in Figure 4.11 with respect to the SE is of particular importance for the multiuser scenario. The numerical value of the optimal EE in terms of SE for different CoMP scheduling is given by Table 4.3.

Table 4.3: Optimal EE according to Figure 4.11

Scheduling	CoMP Techniques	Energy Efficiency (Mbits/Joule)
RR	JT	1.002
	DPS	1.297
	CB/CS	0.6283
PF	JT	1.765
	DPS	1.96
	CB/CS	1.547
MCI	JT	2.298
	DPS	2.449
	CB/CS	2.136

## 4.6 Conclusion

Typically packet schedulers have been compared from a more traditional perspective (spectral efficiency), with disregard to energy efficiency. In this chapter, the performances of various classical scheduling algorithms are considered for benchmarking within a CoMP scenario for LTE-A. In CoMP operation, multiple points coordinate with each other in such a way that the transmission signals from/to other points do not incur serious interference, or can even be exploited for improving received signal performance. The goal of the study is to evaluate the potential performance benefits of CoMP techniques in terms of EE while considering downlink packet scheduling. Gains in terms of the energy efficiency index (with respect to the reference Round Robin scheduler) are analyzed for different CoMP techniques in Figure 4.9. It can be shown that the DPS can deliver greater EE (80%, 65% and 60% EE gain for RR, PF and MCI respectively) whereas JT provides higher system throughput. CS/CB provides neither optimum energy efficient nor system throughput, but offers a lower complexity solution in terms of LTE scheduling. As shown in this chapter, a good compromise between maximum energy efficiency and SE among the considered schedulers are given by the MCI algorithm in Figure 4.11. This technique can be an effective trade-off between energy efficiency and system throughput as far as the operator point-of-view is concerned.

## Chapter 5

# Advanced Energy Efficient Scheduling for CoMP Transmission

*As a step towards incorporating energy compliant mobile systems, platforms in future networks, 3GPP LTE-Advanced has adopted Coordinated Multi-Point (CoMP) transmission / reception due to its ability to mitigate and/or coordinate inter-cell interference (ICI). However, there is room for reducing energy consumption further by exploiting the inherent flexibility of dynamic resource allocation protocols. To this end packet scheduler plays the central role in determining the overall performance of the 3GPP long-term evolution (LTE) based on packet-switching operation and provide a potential research playground for optimizing energy consumption in future networks. In chapter 4 we investigated the baseline performance for down link CoMP using traditional scheduling approaches, in this chapter we go beyond and propose novel energy efficient scheduling (EES) strategies that can achieve power-efficient transmission to the UEs whilst enabling both system energy efficiency gain and fairness improvement. The proposed algorithm is based on a novel scheduling metric focusing exploiting the ratio of the transmit energy per bit. Through system level simulation, the performance of the proposed EES packet-scheduling algorithm using mixed traffic is compared with the state-of-the-Art (SoA) packet-scheduling algorithms such as maximum carrier-to-interference ratio (MCI), proportional fairness (PF), and round robin (RR) that results in significant gain. Moreover, a heuristic framework for CoMP scenario which minimizes the energy consumption of the network using the sleep and active mode of the transmission points on the basis of the traffic threshold is proposed.*

### 5.1 Architecture of Mixed Traffic Packet Scheduler

In a mixed traffic system, a classifier is necessary for the efficiency of packet scheduling [105]. The QoS manager checks UEs' QoS requirements and the packet scheduler calculates packet scheduling metrics. Figure 5.1 demonstrates a mixed packet scheduler architecture.

Four types of traffic models are considered in the simulations and in the validation of the proposed scheduler: VoIP and Near Real Time Video (NRTV) with 64 kbps, which are of type real time (RT) traffic, WWW with 32Kbps, which is of type non-real time (NRT), and File Transfer Protocol (FTP) with 64 kbps, which is of type Best Effort (BE).

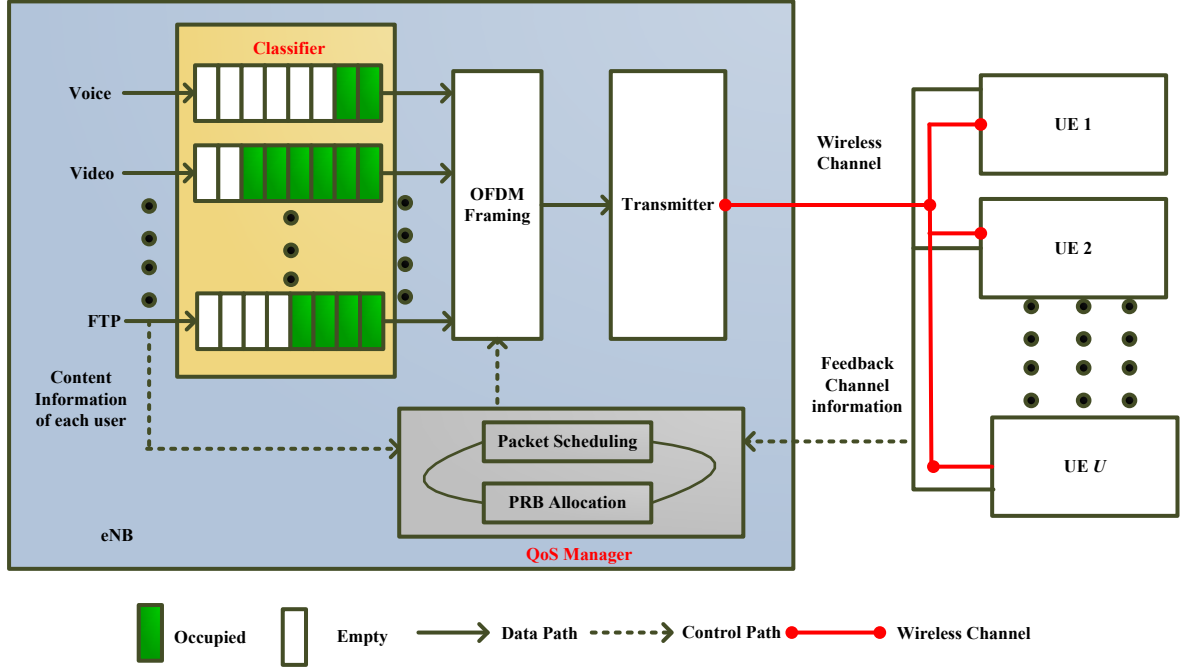


Figure 5.1: Mixed Traffic Packet Scheduler

## 5.2 Novel Energy Efficient Packet Scheduling Algorithm

In this section, a novel energy efficient Scheduling (EES) approach is proposed that considers the minimum transmitted energy per transmitted bits for measuring system performance [105]. The basic flow chart of the proposed EES scheduling algorithm for MU-MIMO CoMP is shown by Figure 5.2.

In the proposed scheduling scheme, the scheduling metric selects the UEs to be allocated in ascending order of the ratio of the to transmit energy,  $E_u^m$ , to the number of transmission bits  $B_u^m$ , of the PRB  $m$  of the UE  $u$  as follows [105]:

$$\Psi(u, m) = \arg \min_{u, m} \frac{E_u^m}{B_u^m} = \arg \min_{u, m} \frac{P_u^m \cdot T}{B_u^m} \quad (5.1)$$

where  $\Psi(u, m)$  is the scheduling metric which denotes the index of selected UE  $u$  and PRB  $m$  respectively; energy is the multiple of power and time (1ms). i.e.  $P_u^m \cdot T$ . Since  $P_u^m = \frac{\xi(B_u^m)}{h_u^m}$  [86], we can redefine the metrics given below

$$\arg \min_{u, m} \frac{P_u^m T}{B_u^m} = \arg \min_{u, m} \frac{\xi(B_u^m) \cdot T}{h_u^m \cdot B_u^m} \quad (5.2)$$

where  $h_u^m$  is the channel power gain and  $\xi(B_u^m)$  is the minimum transmit power required for  $B_u^m$  transmitted bits on the PRB  $m$  of the UE  $u$ . The  $\xi(B_u^m)$  required for transmission of  $B_u^m$  bits with the target bite error rate (BER) of Probability of Error (POE) is given by [86]

$$\xi(B_u^m) = \frac{(\sigma_u^m)^2}{3} \left[ Q^{-1} \left( \frac{POE}{4} \right) \right]^2 (2^{B_u^m} - 1) \quad (5.3)$$

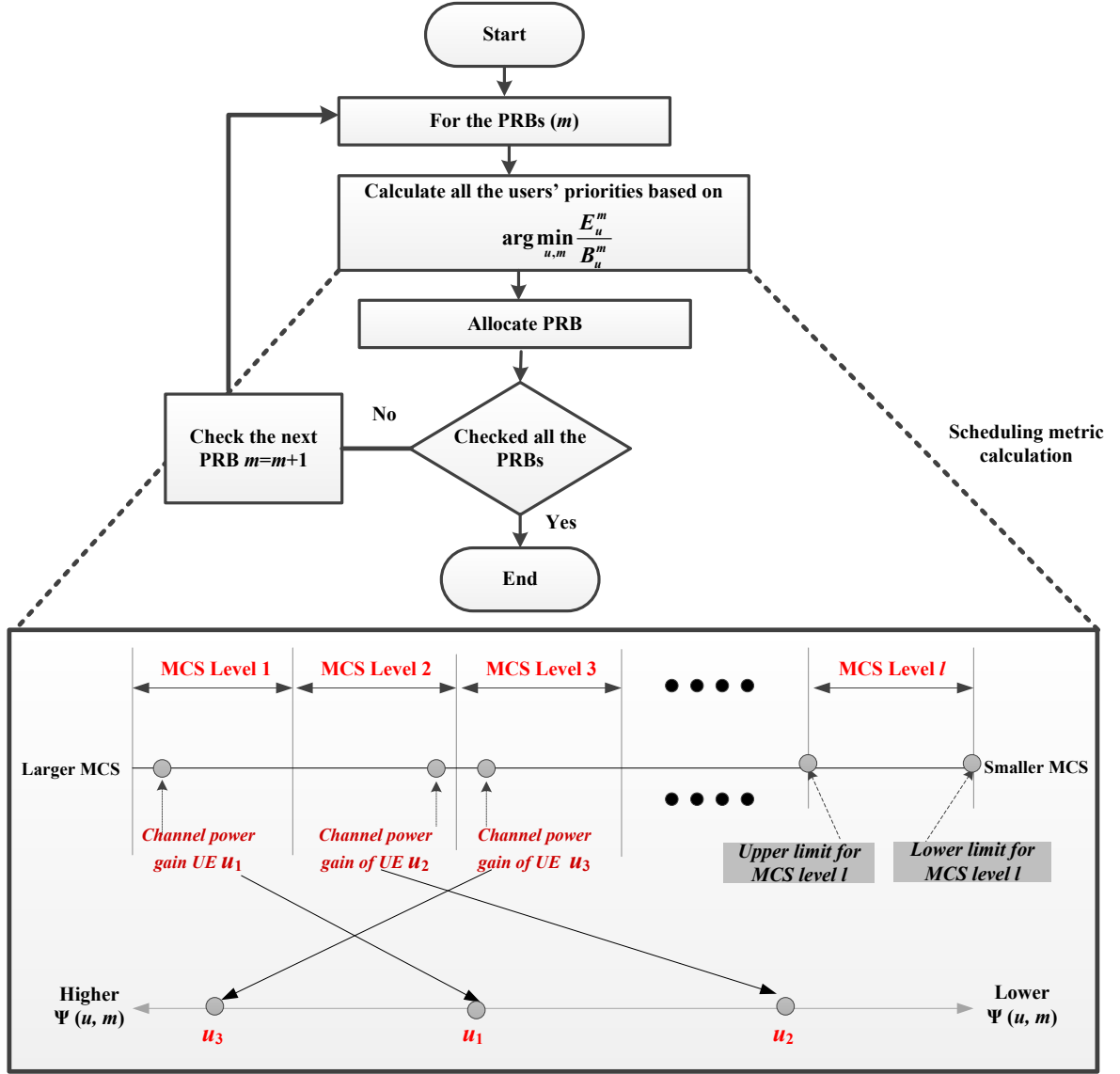


Figure 5.2: Energy-efficient packet Scheduling Algorithm

where  $\sigma_{u,m}^2$  is the noise variance for the subcarriers in the PRB  $m$  at the UE  $u$ , and  $Q(x) = 1/\sqrt{2\pi} \cdot \int_x^\infty e^{-t^2/2} dt$ . Let  $\hat{P}_u^m$  denote the maximum transmit power at the transmitter that can be assigned for the UE  $u$  and the PRB  $m$ . Then, the minimum channel gain required for successful transmission of  $B_u^m$  bits through the PRB  $m$  is given by  $h_{\min}(B_u^m) = \xi(B_u^m)/\hat{P}_u^m$ , where  $\xi(B_u^m)$  is expressed in equation (5.3). Since we have  $h_u^m(B_u^m) = \xi(B_u^m)/P_u^m$ , the excess channel gain,  $\Omega_u^m$  ( $B_u^m$  is the maximum positive integer that satisfies  $\Omega_u^m \geq 0$ ) is written as

$$\Omega_u^m = h_u^m - h_{\min}(B_u^m) = \xi(B_u^m) \left( \frac{1}{P_u^m} - \frac{1}{\hat{P}_u^m} \right) \quad (5.4)$$

From equation (5.4), we get

$$\frac{1}{P_u^m} = \frac{\Omega_u^m}{\xi(B_u^m)} + \frac{1}{\hat{P}_u^m} \Rightarrow P_u^m = \frac{1}{\frac{\Omega_u^m}{\xi(B_u^m)} + \frac{1}{\hat{P}_u^m}} \quad (5.5)$$

Using equation (5.5) in (5.2), we get

$$\Psi(u, m) = \arg \min_{u, m} \left( \frac{T}{\left( \frac{\Omega_u^m}{\xi(B_u^m)} + \frac{1}{\hat{P}_u^m} \right) \cdot B_u^m} \right) \quad (5.6)$$

When the  $\hat{P}_u^m$  of the transmitter is too large, equation (5.6) can be rewritten as

$$\begin{aligned} \Psi(u, m) &= \arg \min_{u, m} \left( \frac{T}{\left( \frac{\Omega_u^m}{\xi(B_u^m)} + 0 \right) \cdot B_u^m} \right) \\ &= \arg \min_{u, m} \left( \frac{T}{\frac{\Omega_u^m}{\xi(B_u^m)} \cdot B_u^m} \right) \end{aligned} \quad (5.7)$$

Afterwards,

$$\begin{aligned} \Psi(u, m) &= \arg \min_{u, m} \left( \frac{T}{\frac{\Omega_u^m}{\xi(B_u^m)} \cdot B_u^m} \right) = \arg \min_{u, m} \left( \frac{T}{\frac{\Omega_u^m}{(\xi(B_u^m)/B_u^m)}} \right) \\ &= \arg \min_{u, m} \left( \frac{(\xi(B_u^m)/B_u^m) \cdot T}{\Omega_u^m} \right) = \arg \min_{u, m} \left( \frac{(\bar{E}(B_u^m)/B_u^m)}{\Omega_u^m} \right) \end{aligned} \quad (5.8)$$

where,  $\bar{E}(B_u^m) = \xi(B_u^m)T \rightarrow$  is minimum received energy. Equation (5.8) can be rewritten as

$$\arg \min_{u, m} \left( \frac{(\bar{E}(B_u^m)/B_u^m)}{\Omega_u^m} \right) = \arg \max_{u, m} \left( \frac{\Omega_u^m}{(\bar{E}(B_u^m)/B_u^m)} \right) \quad (5.9)$$

Because,  $\arg \min(x) = \arg \max(\frac{1}{x})$ . Eventually, the scheduling metric can be expressed as  $\Psi(u, m)$

$$\Psi(u, m) = \arg \max_{u, m} \left( \frac{\Omega_u^m}{(\bar{E}(B_u^m)/B_u^m)} \right) \quad (5.10)$$

The proposed EES scheduler allocates the PRB  $m$  to the UE with largest excess channel gain in contrast to the required received energy per bit as in equation (5.10). In the case of the UEs who have similar value of excess channel gain, the envisaged scheduling mechanism allocates the PRB to the UE with the lowest received energy per bit. For instance, we order UE  $u_1$ ,  $u_2$ , and  $u_3$  in Figure 5.2 in terms of MCS 1, 2, and 3, respectively. According to the MCS levels, the MCS level 1 sends the highest data rate while the MCS level  $l$  transmits the lowest data rate. Thanks to the 3GPP LTE, adaptive modulation coding (AMC) scheme [85], UE  $u_1$  is capable to transmit more bits than UE  $u_2$ , but UE  $u_1$  needs lower transmit energy per bit than UE  $u_2$ . The reason behind is that, the channel power gain of UE  $u_1$  is much higher than the minimum required channel power gain for the MCS level 1 which needs small transmit energy, while the channel power gain for UE  $u_2$  is roughly the minimum value for the MCS level 2 which needs higher transmit energy than the other instances. In the meantime, UE  $u_3$  poses roughly similar excess channel gain as UE  $u_1$ , but it needs less received energy per bit,  $(\bar{E}(B_u^m)/B_u^m)$  than UE  $u_1$  because  $(\bar{E}(B_u^m)/B_u^m)$ , in Equ. (5.10) increases in an exponential manner with  $B_u^m$ ; therefore, the value of  $(\bar{E}(B_u^m)/B_u^m)$  for UE  $u_3$  is lower than UE  $u_1$  in spite of having higher MCS level than UE  $u_3$ . Consequently, the EES scheduler in the system chooses the UEs to be assigned UE  $u_3$ , UE  $u_1$ , and UE  $u_2$  respectively.

### 5.2.1 Simulation and Discussions

In this section we discuss the performance analysis of the proposed algorithm along with the other SoA algorithm. The simulation parameters are given by Table 4.1. One additional metric we define here is the fairness index.

#### 5.2.1.1 Additional Performance Metric

##### GINI fairness Index

The fairness index (FI) termed as the GINI co-efficient [106], is used to measure the equality/inequality of the resources. The generic GINI co-efficient formula is [107] given by the following –.

$$FI_{GINI} = \frac{\sum_{i=1}^n \sum_{j=1}^n |x_i - x_j|}{2n^2 \bar{x}} \quad (5.11)$$

- where  $x$  is an observed value,  $n$  is the total number of values observed and  $\bar{x}$  is the mean value.

The value of FI lies between 0 and 1. If the value is 0 complete fairness is achieved, and 1 otherwise. For our simulation we observed the energy efficiency of different users to measure fairness using the GINI formula.

#### 5.2.1.2 Results Analysis

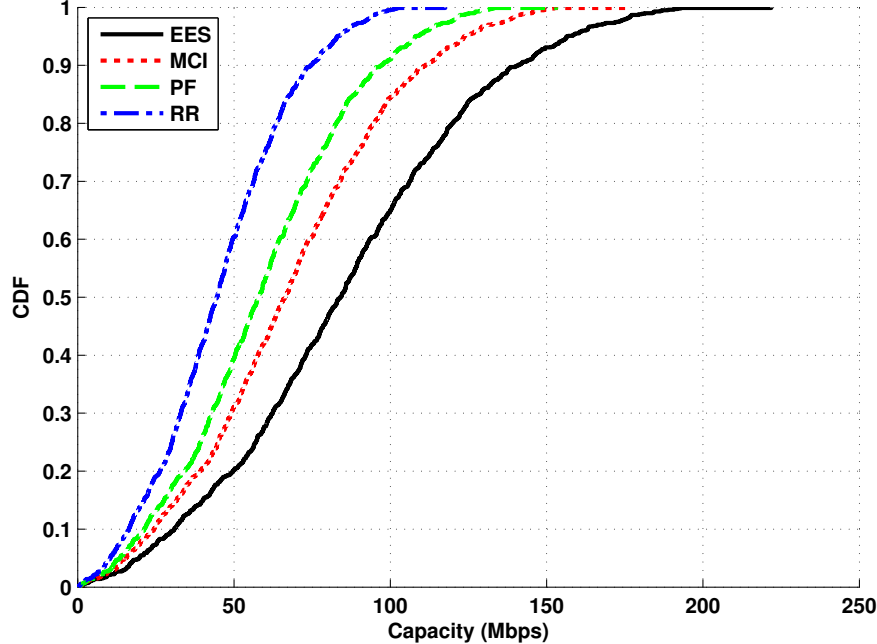


Figure 5.3: CDF of the capacity for mixed traffic users

Figure 5.3 shows the cumulative distribution function (CDF) concerning the cell capacity of different packet scheduling for MU-MIMO CoMP. The figure shows that the EES scheme is capable of outperforming all counterparts; in particular compared with MCI, the EES

algorithm outperforms by up to 28%. The proposed technique allows more users at the cell-edge to be allocated PRB due to proper utilization of all transmitted power in a certain time period which eventually increases the overall cell capacity.

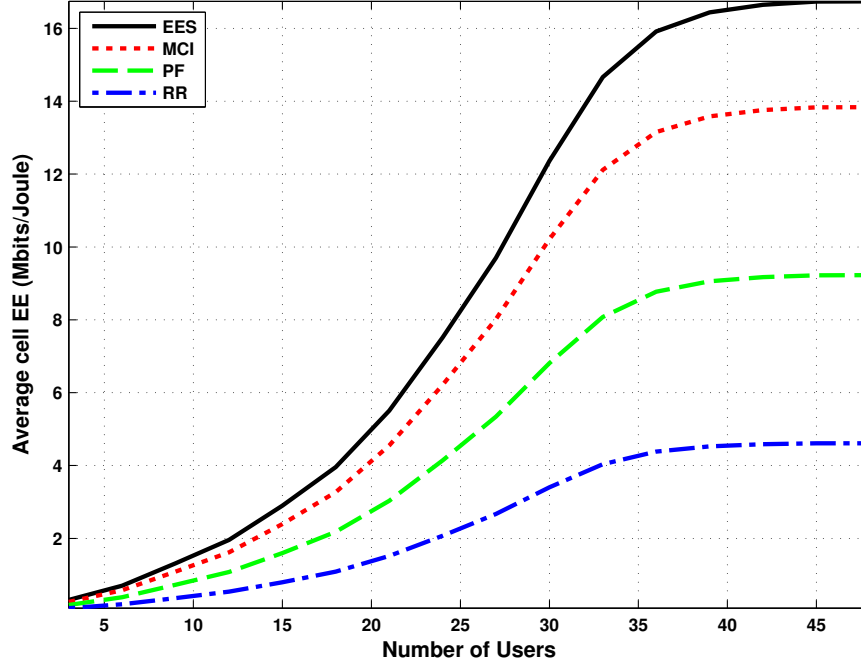


Figure 5.4: Average cell energy efficiency for different number of users

Figure 5.4 shows the average cell EE (i.e., the average of the 19 cell EEs) against the number of users, assuming a maximum of 48 UEs in each cell. It shows that the EES algorithm achieves the best average cell energy efficiency. As the user number increases, the EES algorithm shows more prominent performance. For example, when number of the users are 45, the algorithm shows 16% gain in the average cell EE compared to the MCI algorithm. This result indicates that better average cell EE occurs with increasing UEs. This is mainly due to the efficiency of the received transmit energy consumption. When the cell becomes overloaded, the transmit energy consumption becomes a more critical issue since energy is a limited resource. Hence, we deduce from the results that the packet scheduling algorithm that exploits the ratio of the transit energy to the number of transmission bits provides a greater increase in the average cell EE.

Figure 5.5 shows the average EE at the cell edge with increasing users. In the simulation, 20% of the UEs were located at the cell boundary in which the energy efficiency is particularly important. Compared to the MCI algorithm, 25% gain in the EES algorithm at the cell edge is obtained for 48 users. The improved EE occurs because the proposed EES scheduling algorithm considers the ratio of the transmit energy to the number of transmission bits.

Figure 5.6 shows the average cell throughput against the total transmit power, where the maximum allowable transmit power is 40 Watt as given in the 3GPP LTE downlink specification [10]. From this figure, the EES algorithm can sustain more than 1 Mbits/Joule average cell EE with 1 Watt. In addition, we can deduce that the EES algorithm can save the transmit power by up to 10 Watt when compared to the than the MCI algorithm while

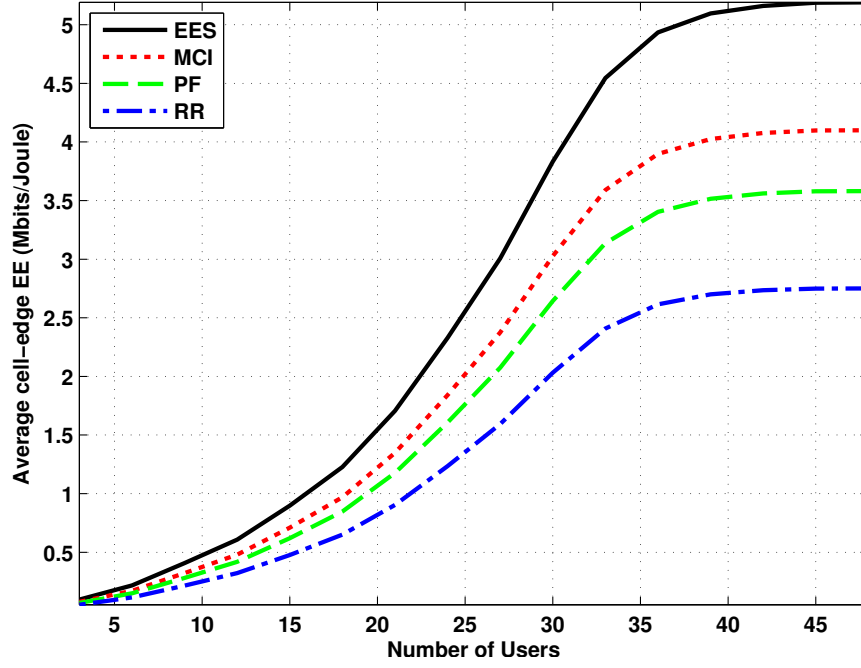


Figure 5.5: Average cell-edge energy efficiency for different number of users

sustaining the same cell EE.

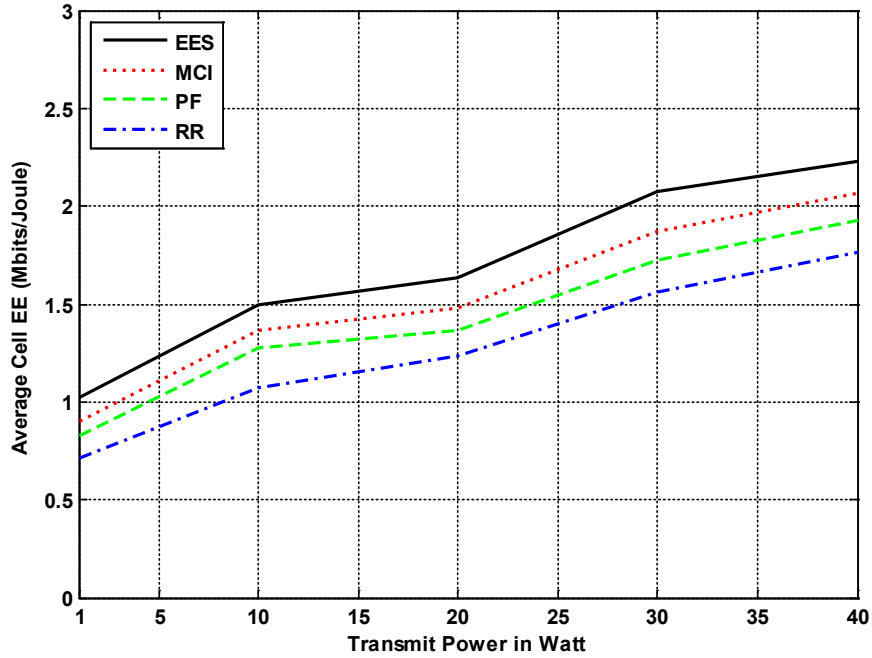


Figure 5.6: Average cell EE with different transmit power

Figure 5.7 shows the distribution of normalized EE with respect to the UE indication (i.e. index of each user). Here, the normalized EE is defined as the ratio of the EE per UE to the

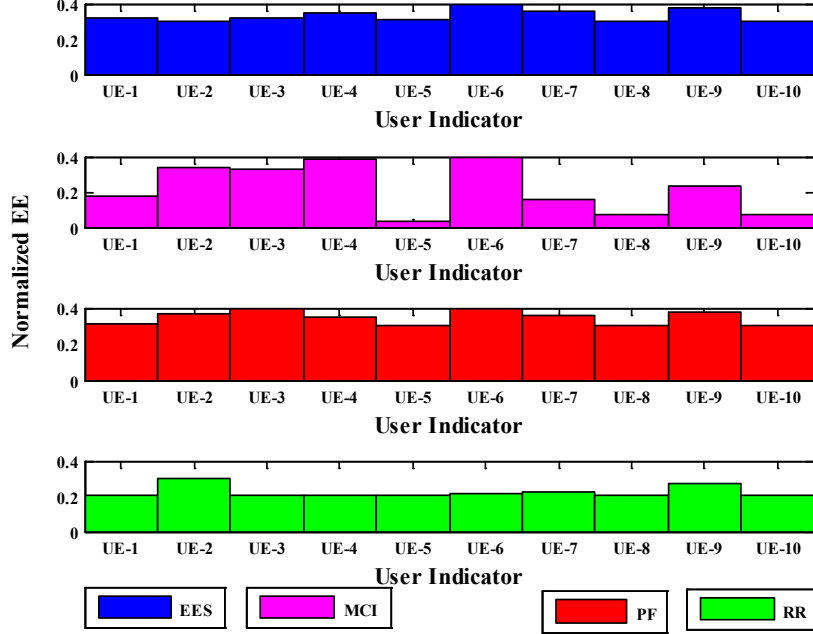


Figure 5.7: Normalized EE distribution per user

total EE in a cell. From this figure, it can be found in the case of MCI, that a large portion of the normalized EE is centralized in only a few UEs with good channel conditions. However, the normalized EE for the RR, PF, and EES algorithms are fairly distributed. The normalized EE in the case of the EES algorithm shows relatively equal transmission probabilities for all UEs, similar to RR. Although each user's normalized EE in RR ( $\sim 0.2$  Mbits/Joule) is lower compared to the EES ( $\sim 0.38$  Mbits/Joule).

In Figure 5.8, the EE-based fairness comparison between conventional scheduling methods and the proposed scheme are shown.

$$FI_{Gini} = \frac{\sum_{u=1}^U \sum_{q=1}^U |EE_u - EE_q|}{2U^2 \overline{EE}} \quad (5.12)$$

where  $EE_u$  is the observed energy efficiency value of user  $u$  and  $EE_q$  is the observed energy efficiency value of user  $q$ ,  $U$  is the total number of users, and  $\overline{EE}$  is the average energy efficiency of all users in the cell.

It can be observed that in our proposed scheme, the fairness index gradually improves as the number of users increase. As anticipated, MCI shows less fairness since it tries to allocate the resources to users with best channel condition. In fact this channel-aware policy monopolizes all the resources for good-channel users that are usually located close to the base station, while cell edge users starve with low data rates. This starvation is significantly reduced by granting more equal access to users using the proposed packet scheduling algorithm. The greater the number of users, the greater the tendency towards fairness in terms of throughput. EES demonstrates more fairness compared to MCI and PF, but not more than RR; since RR does not comply with channel awareness.

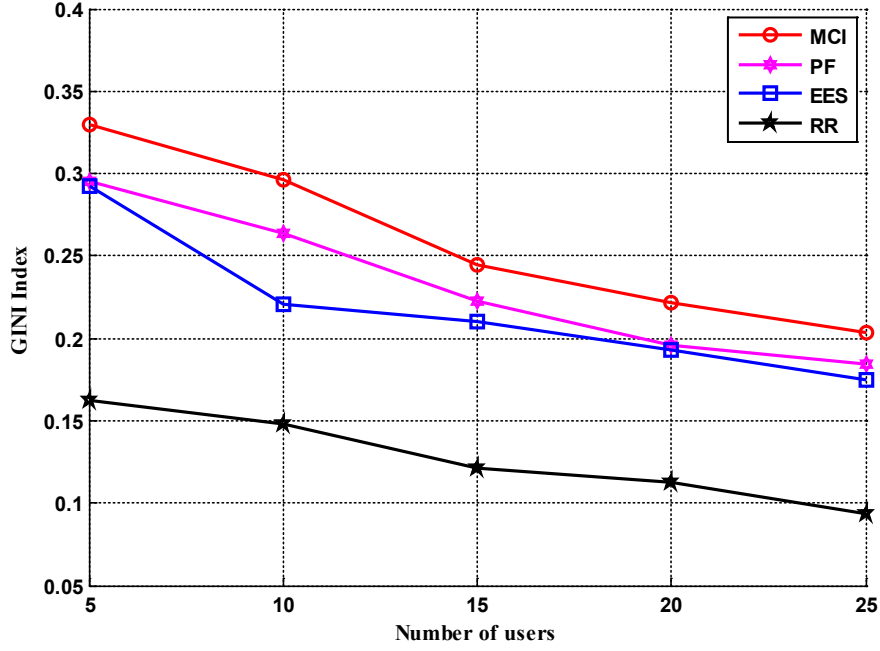


Figure 5.8: EE fairness of different Packet Scheduling algorithm

### 5.3 Traffic state based Novel Energy Efficient Transmission Algorithm

The green radio evolution has provided the impetus for energy efficient mechanism, and power management strategies. This approach adjusts the transmission power according to the traffic load. Currently, power-management is usually implemented by timer-based approaches. For example, in 3GPP LTE, user equipments (UEs) in discontinuous reception (DRX) mode [108] start a timer when there is no data to receive and turn off its circuit when the counts exceed a threshold. It has been found out that a large percentage of the energy inefficiency is attributed to the static overhead consumption of eNB, as well as attempting to achieve a quality of service for the cell-edge users [33]. The energy consumption depends on the operating mode of the eNB. A BS is able to function in an operational or in a non-operational state. Furthermore, in an operational state different conditions can be distinguished, e.g., low traffic and peak traffic modes are available. Amongst all states a transition time is required to reach the new state, e.g., the power-on of a eNB demands a dedicated amount of time and energy [78]. Switching off the eNB when traffic is low reduces the number of active cells in low traffic periods, given that the remaining active cells are able to cope with their own traffic as well as the switched-off cells' traffic. Following the idea behind [33], we propose a CoMP based energy efficient algorithm that determines how many transmission points should be in sleep mode.

#### 5.3.1 Problem Formulation

The energy saving problem in this CoMP scenario is to minimize the average energy consumption of the each eNB, while satisfying the traffic requirement for each user.

Herein, we discuss the energy consumption related to eNB, as each eNB is centrally controlled by the CU. Consider that each eNB can work in two states: active (with power  $P_{\max}^e$ ) and sleeping (with power  $P_{\min}^e$ ) assuming that in sleeping mode each eNB consume negligible energy. Irregular distribution of the traffic intensity among the cells is applied using Poisson process. Therefore, the energy consumption of eNB can be modeled by two values:  $\{0, P^e\}$ . The optimization problem is formalized as follows:

$$\begin{aligned} \min \text{ Energy } & \left\{ = \sum_{e=1}^E P^e \text{ sign} \left( \sum_{u=1}^U y_{eu}(t) \right) \right\} \\ \text{such that} & \\ 1) \sum_{e=1}^E y_{eu}(t) &= 1, \forall u = 1, \dots, u(t), \\ 2) \sum_{u=1}^U y_{eu}(t) &\leq 4, \forall e = 1, \dots, e(t), \\ y_{eu}(t) &\in \{0, 1\}, \forall e = 1, \dots, E, \forall u = 1, \dots, U \end{aligned} \tag{5.13}$$

where  $\text{sign}(y)$  is the sign function, which equals 1 when  $y > 0$ , otherwise 0.  $u(t)$  is the number of users at time  $t$ , and binary variable  $y_{eu}(t)$  represents the association relation between user  $u$  and eNB  $e$ . The first constraint limits that each user has to select at least one eNB. The second constraint limit that every eNB is capable of serving a maximum of four users at a time.

In problem (5.13), the computation is based on the time average. Due to the randomness of users, it is not possible to solve (5.13) directly. Therefore, in our design, the eNB on-off decision is made in certain time slots, separated by a fixed length period,  $T_0$ . Also, one must take the traffic variation between the consecutive decision times based on the optimization problem.

### 5.3.2 Proposed Algorithm

The idea of the proposed algorithm is influenced by the work in [29], which is based on blocking probability using a conventional single cell. We proposed and simplified the algorithm on the basis of the traffic threshold according to our scenario based on JT CoMP technique which consists of cluster of coordinated eNBs. We consider a frequent eNB state transition prevention approach to save energy consumption. To enable this we must consider a process called state holding time which is defined in [29]. State holding time is defined as the time interval in which eNB keeps its current state.

The algorithm works according to the traffic intensity in a timely manner. When the procedure is finished, the system delivers services on the basis of the updated set of active eNBs. A flowchart of the algorithm is demonstrated by Figure 5.9.

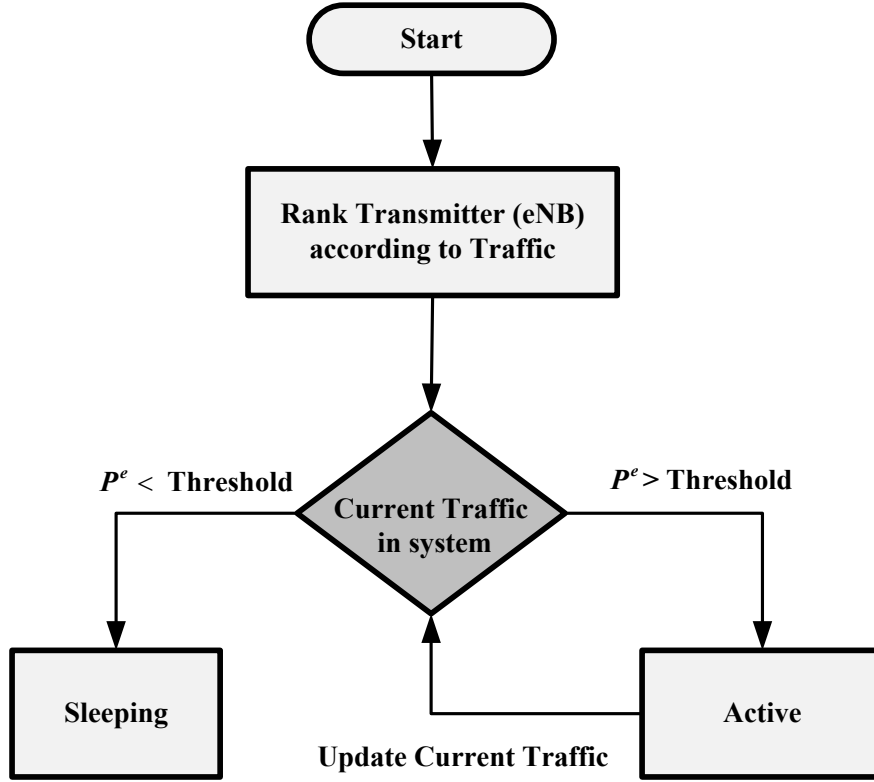


Figure 5.9: Traffic based energy-efficient Algorithm

The strategy is presented as follows in Algorithm 5.1:

---

**Algorithm 5.1** Traffic Threshold based EE Algorithm

---

1: State – **S**→**A** (Sleeping to **Active**):

In this state eNB is promoted from sleeping to active state.  $P^e$  of the sleeping eNB  $e$  that comply with the minimum state holding time requirement is calculated according to the traffic load of its other eNB inside the same CoMP cluster. The eNB will be activated if  $P^e$  exceeds the pre-defined threshold.

2: State – **A**→**S** (**Active** to **Sleeping**):

In this state, eNB steps from active state to sleeping state. At first, the  $P^e$  of the active eNB  $e$  is calculated in a similar fashion by comprising the traffic of itself. If  $P^e$  is less than the predefined threshold, handover effect should be considered. The handover effect can be solved by using the method described in [109]. The eNB will go to sleeping mode only when the active users of this eNB are handed over to neighboring active eNB.

---

### 5.3.3 Simulation Results ad Discussion

This section represents simulation results of the proposed algorithm. Geographically, the simulated radio network consists of one centrally controlled CU (or one coordinated cluster of eNBs), which consists of three hexagonal sectors or cell laid out around, each resulting in a total of 3 eNBs. In order to avoid border effects and to obtain the same interference load in all cells, wraparound mapping is applied. The model used for such radio

phenomena, as fading and dispersion, is the 3GPP Typical Urban model [55]. Monte Carlo simulation is used where the users are randomly distributed over the geographical area. Full-queue traffic model is used for all the users, which means they always have information ready to be transmitted [55]. The key parameters of the simulated system are set according to the LTE standard which is summarized in Table 5.1

Table 5.1: Key simulation settings

Parameter Name	Value
Carrier frequency, $f_c$	2.6 GHz
Bandwidth	20MHz
Channel model	3GPP Spatial channel Urban
Cellular Layout	19 CoMP cluster / 57 hexagonal cell , 3 hexagonal cells per CoMP cluster with 70 degree sector beam width
Number of Users	100 per cell
User speed	3 km/h
eNB transmit power	46dBm
Inter-cell distance	500m
Time transmission interval (TTI)	1 ms (sub-frame)
Number of Resource Block	100 RB in each slot, 7 symbol, number of subcarriers per RB=12, total subcarrier=1200
Link to system interfacing	EESM (Exponential Effective SNR Mapping)
Traffic model	Full Queue
Arrival Rate	10 user/cell/Sec
Scheduling	PF
Link Adaptation	MCSs according to [101]

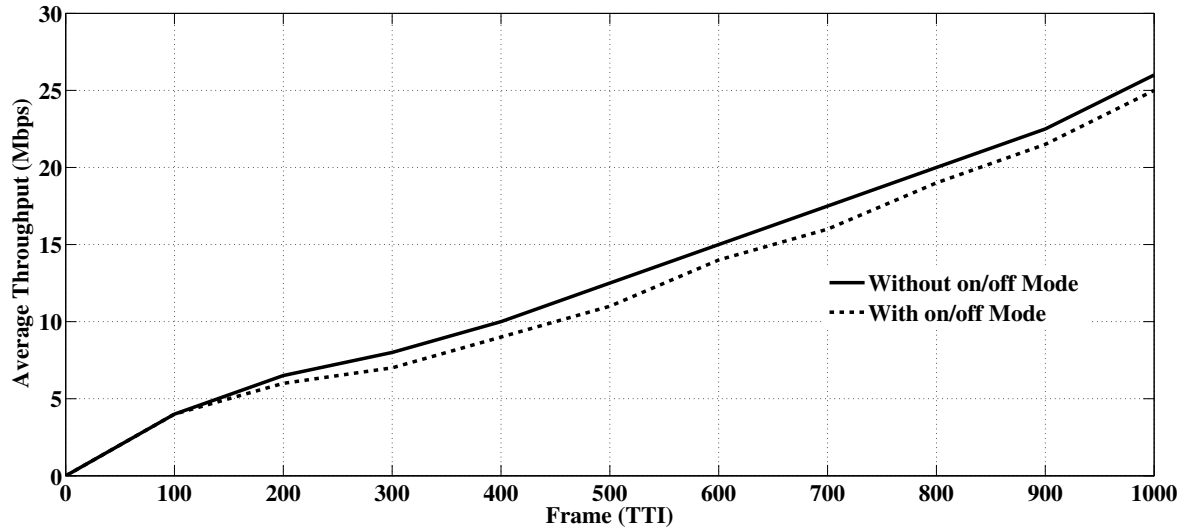


Figure 5.10: Throughput comparison in different frame

Figure 5.10 shows the average throughput versus frame comparison. It shows that us-

ing conventional transmission system the throughput increases gradually compared to our algorithm, where not all the transmission points (eNBs) are on. Using our method, all the resources are allocated to the transmission points which are selected for data transmission. It compares the throughput for networks in terms of energy per frame. Frame size depends upon the AMC scheme on each TTI. The throughput margin in conventional system is not significant compare to energy consumption which we see in the subsequent result.

The energy metric we consider here is the energy consumption ratio (ECR) [23] such as the energy per transmitted information bit (unit: Joule/bit).

$$ECR = \frac{Energy}{Transmitted\ bit} (Joule/bit)$$

$$[ECR = \frac{Power \times Time}{Transmitted\ bit} = \frac{Watt \times Second}{bits} = Joule/bit]$$
(5.14)

This energy metric provides energy consumption in Joules consumed for transmitted information bit. Reduction of energy consumption which eventually shows energy saving is calculated using (5.14).

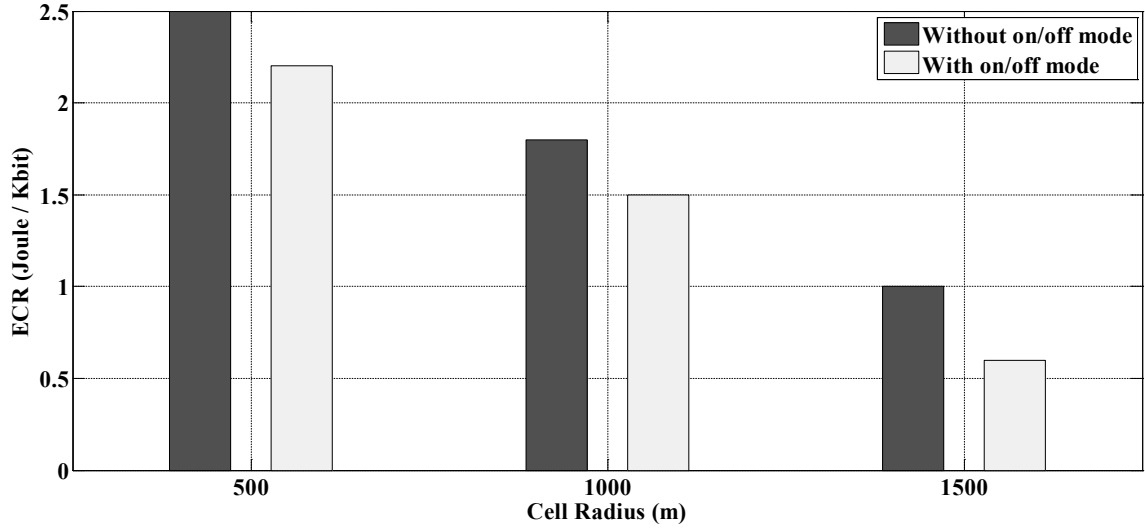


Figure 5.11: ECR vs. Cell radius

Figure 5.11 compares the energy consumption in terms of cell radius for networks employing our algorithm, which clearly shows that our proposed algorithm achieves significant energy savings due to the inactive and active state of traffic; the trend of the energy consumption remains the same even with the cell radius gradually increases.

## 5.4 Conclusions

In this chapter, we proposed a novel algorithm which considers the efficiency of the transmit energy consumption. The performance of the proposed algorithm was evaluated by comparing with the conventional SoA algorithms: the MCI, RR, and PF. The simulation results showed that the EES algorithm applying the proposed minimum transmit energy-based packet scheduling approach to schedule users in MU-MIMO CoMP 3GPP LTE systems showed better

performance in contrast to conventional algorithms as given by Figure 5.3; almost 28% better than MCI, and beyond that in terms of fairness. The system level simulation results suggest that the proposed scheduler for CoMP systems can significantly improve the cell-average and cell edge energy efficiency by up to 16% and 25% respectively, in contrast to MCI. We believe this is a promising scheduling algorithm for IMT-Advanced systems, since it is technology agnostic. Furthermore, we present a simple heuristic traffic threshold based energy efficient transmission system using eNB targeting centralized LTE CoMP systems. The numerical results substantiate the efficiency of our algorithm. We showed that by setting some eNB in sleep mode on the basis of the traffic threshold, we have the potential to save energy.

## Chapter 6

# Advanced HetNet CoMP Architectures for OFDMA

*The Third Generation Partnership Project (3GPP) community has already taken steps towards reducing the energy consumption in future emerging networking technologies (e.g. Long Term Evolution (LTE-A) [110]) by proposing new energy efficient networking topologies, deployment strategies and modulation technologies. In [111], the authors investigated energy efficiency (EE) in heterogeneous network and took into account the effects of cell size on cell energy efficiency by introducing a new concept of area energy efficiency. In [36], the energy efficiency of multi-cell cellular networks with co-channel interference is investigated. MIMO is not considered in both the above mentioned work. The study in [112] has investigated energy efficiency based on SU-MIMO techniques both in slow-fading and fast-fading channels. But it does not provide any suggestions for MU-MIMO scenario. None of the prior research works considers MU-MIMO and coordination between transmission points, let alone HetNet scenarios. In a broader sense, there is a little or no study analyzing the impact of HetNet CoMP using MU-MIMO on the energy efficiency of cellular networks. In the first part, the objective of our research is to design novel wireless architecture utilizing multiple antenna techniques in HetNet CoMP. To the best of our knowledge this is the first attempt which addresses HetNet CoMP using MU-MIMO to investigate energy efficiency. In the second part, EE analysis of different frequency allocations is investigated. Deployment of heterogeneous networks using coordination between the traditional macro cell and low power nodes (LPNs) – such as pico, relay so on– is required to reduce the total energy consumption of cellular radio networks. This study investigates the cell's energy efficiency of a single frequency heterogeneous CoMP networks. Applying the single frequency HetNet CoMP as a baseline network, we further extend our work to different frequency planning network such as fractional frequency reuse (FFR). The simulation results suggest that introducing HetNet CoMP can achieve improved overall cell energy efficiency whereas HetNet CoMP using FFR to increase cell-edge energy efficiency is a trade-off for the operator. In the third part, the EE maximization using convex optimization theory where the primary optimization criterion is the data rate in a downlink multiuser HetNet CoMP OFDMA system is investigated.*

## 6.1 Novel Energy Efficient Design for HetNet CoMP Architecture

Information and communication technology (ICT) is playing an increasingly important role in global greenhouse gas emissions since the amount of energy consumption for ICT has been increasing dramatically [113]. Therefore, pursuing high energy efficiency (EE) is becoming a mainstream concern in future wireless communications design. In today's technology there are effectively three approaches for improving the energy efficiency whilst maintaining system capacity and consuming no additional spectrum. These include:

1. Improving the power channel gain such as reducing the access distance and the number of obstacles between the transmitter and receiver, which can be solved by deploying heterogeneous networks (HetNets) [14].
2. Reduce the interference, specifically reducing the co-channel interference in mobile networks, which can be solved by applying coordinated multi-point (CoMP) transmission and reception techniques [6].
3. Enhanced spectral efficiency promised by multi-user MIMO (MU-MIMO) [82].

One of the reference scenarios are heterogeneous networks (HetNet) [14], network that consists of a mix of macrocells, remote radio head (RRH) and low power nodes (LPNs) such as picocell, femtocell, and relay; where some may be configured with restricted access and some may even lack wired backhaul. CoMP is a coordination technique between transmitters to enhance inter-cell interference (ICI) coordination to improve bit rates and fulfill upcoming communication demands. HetNet combined with CoMP is now a booming research topic, presenting synergies able to enhance future wireless system bit rates.

CoMP was discussed in chapter 4, where we provided a comprehensive baseline performance analysis for the downlink. Downlink CoMP schemes as presented in previous sections, managed to mitigate efficiently ICI at the cell-edges. Furthermore, they can provide enhanced coverage in terms of high data rate and cell-edge throughput. The benefits of CoMP can be further enhanced when Multi-user MIMO (MU-MIMO) [114] is applied. MU-MIMO allows the communication between multi-antenna BS and multiple users by allocating different data streams to different users. In both the coordinated scheduling/beamforming (CS/CB) and joint transmission (JT) mode of operation, if MU-MIMO is used in the downlink instead of Single User-MIMO (SU-MIMO), systems throughput can be further enhanced. This enhancement is more pronounced for higher order MIMO schemes, as the BS's transmit antennas in downlink can serve multiple UEs configured in MU-MIMO transmission mode.

Early research of MIMO techniques mainly focused on single-user MIMO (SU-MIMO), where multiple spatial channels are allocated to a single user and multiple users are served through time-multiplexing. Then MU-MIMO followed, where multiple users are served simultaneously in the same frequency band over user-specific spatial channels [115]. In contrast with SU-MIMO, MU-MIMO substantially improves spectral efficiency and hence is being considered as a strong candidate for future-generation mobile cellular systems. However, it is necessary to design appropriate transmission schemes for MU-MIMO in order to suppress multiuser interference (MUI). The suppression of MUI can be facilitated by precoding schemes at the transmitter or/and decoding schemes at the receiver. In the multiuser downlink system, decoding schemes for mitigating MUI may impose an increased computational burden at

the receiver, which contradicts the objective of energy and cost efficient in hand-held portable terminals. As a design alternative, transmit precoding schemes are capable of shifting the computational burden from the mobile terminal to the eNB [116], that can handle greater computational cost. Specifically, upon utilizing users' CSI, the eNB can design dedicated precoder to sufficiently suppress MUI based on a range of principles, such as zero-forcing (ZF) and minimum mean-square-error (MMSE) [117, 118]. Nonetheless, in addition to the aforementioned MUI, cellular system may suffer from ICI, which cannot be suppressed individually within a single cell. Specifically, in comparison with cell-center users, cell-edge users tend to have lower received signal strength and are therefore more vulnerable to ICI. In this context, CoMP scheme is proposed as a distributed MIMO technology to mitigate MUI as well as ICI through coordination of multiple eNBs [6, 11, 7, 10]. The focus in this part is thus on the downlink HetNet CoMP aspects since uplink CoMP technologies tend to have less standardization impact, as receiver processing at the network side can be performed in an almost transparent way to the user equipment (UE) [6].

### 6.1.1 System Model

We consider a MU-MIMO HetNet CoMP (MHC) system as shown in Figure 6.1. A MHC system composed of several MHC cell-sites. Each MHC cell-site consists of one macro eNB and several low power RRHs based on LTE technology. Our MHC system is composed of  $C$  CoMP-cells, indicated by  $\mathcal{C} = \{1, 2, \dots, c, \dots, C\}$ , where a MHC cell-site comprises one centralized point eNB (indicated by  $E_c$  i.e., the eNB of the MHC  $c$ ) with  $R$  (indicated by  $\mathcal{R} = \{1, 2, \dots, r, \dots, R\}$ ) number of RRHs, serving  $U$  user equipments (UEs) which are uniformly distributed over its coverage area. We should keep in mind that both eNB and RRH are termed as  $T$  number of transmission points, indicated by  $\mathcal{T} = \{1, 2, \dots, t, \dots, T\}$ , i.e.,  $E_c \in \mathcal{T}$  and  $r \in \mathcal{T}$ . Therefore in one MHC cell-site contains transmission signal from both eNB and RRH as well. Furthermore, each transmitter in a MHC cell-site is assumed to have  $N_{TX}$  transmit antennas in order to support  $U$  users with  $N_{RX}$  receive antennas per user.

For the MHC system, interference is classified as intra-MHC and inter-MHC interference. The former is created where multiple users are served simultaneously in the same frequency band over user-specific spatial channel [115], i.e., considered as multi-user interference (MUI). The latter originates from transmission points of other MHC cell-sites and is unknown to the eNBs, but can be estimated; i.e., considered as inter-cell interference (ICI). In both cases, the available information about interference can be used to perform adaptive resource allocation. The CoMP system can be seen as a distributed MU-MIMO system using eNBs and RRHs as a distributed antenna array [82]. In the following we provide SINR calculation for JT, CS/CB and our proposed Novel Energy Efficient Design (NEED) architecture.

We define the channel matrix from transmission point  $t$  within MHC  $c$  to user  $u$  as  $\mathbf{H}_{c,t}^u$ , then a concatenated channel  $\mathbf{H}_{c,:}^u$  can be formed as

$$\mathbf{H}_{c,:}^u = [\mathbf{H}_{c,1}^u, \mathbf{H}_{c,2}^u, \dots, \mathbf{H}_{c,T}^u] \quad (6.1)$$

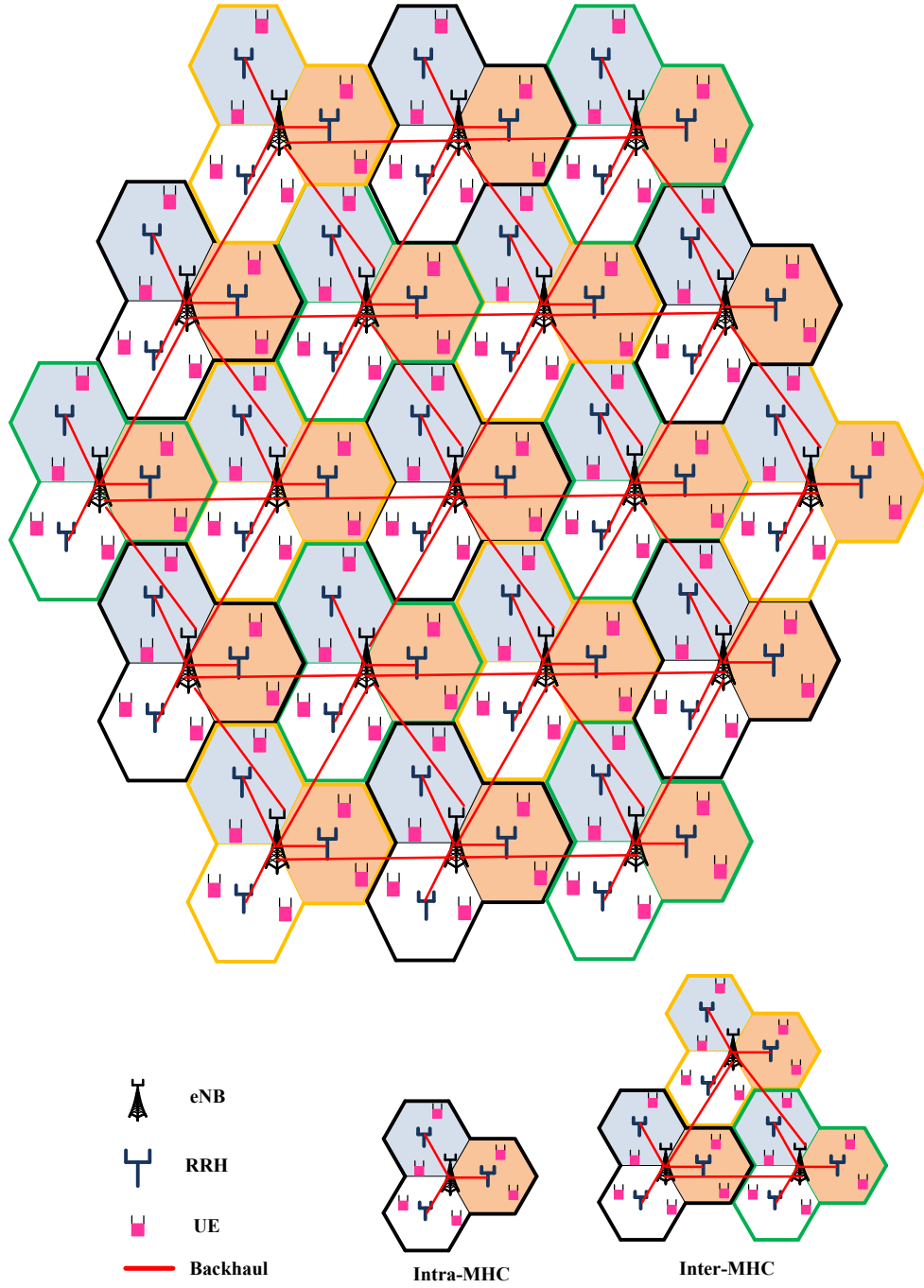


Figure 6.1: MU-MIMO HetNet CoMP (MHC) system model

### 6.1.1.1 SINR calculation for Joint Transmission (JT)

Then the received signal at user can be expressed as

$$y_c^u = \overbrace{\mathbf{H}_{c,:}^u \mathbf{F}_{c,:}^u x_c^u}^{\text{Desired signal}} + \overbrace{\mathbf{H}_{c,:}^u \sum_{l \in \Theta_c, l \neq u} \mathbf{F}_{c,:}^l x_c^l}^{\text{MUI}} + \overbrace{\sum_{i \in \Theta_{c'}, c' \neq c} \mathbf{H}_{c',:}^u \mathbf{F}_{c',:}^i x_{c'}^i}^{\text{ICI}} + n_c^u \quad (6.2)$$

Where  $\mathbf{F}_{c,:}^u$  and  $x_c^u$  are the beamforming (precoding) matrix and the data transmitted from MHC to user  $u$  respectively; and  $\Theta_c$  is the set of transmit precoder associated with MHC  $c$ , and  $\mathbf{n}_c^u$  the receiver noise with AWGN elements, each with variance  $\sigma_n^2$ . When perfect channel state information (CSI) is not available at the eNB, the MUI in equation (6.2) can be reformulated as [116]:

$$\mathbf{H}_{c,:}^u \sum_{l \in \Theta_c, l \neq u} \mathbf{F}_{c,:}^l x_c^l = \sum_{l \in \Theta_c, l \neq u} \left( \sum_{t=1}^T \mathbf{H}_{c,t}^u \mathbf{F}_{c,t}^l \right) x_c^l \quad (6.3)$$

The main channel measurement considered is the Signal-to-Interference-plus-Noise-Ratio (SINR) of the UEs in the system. In order to determine whether a transmission has been successful, the SINR measured for a given path is employed to determine the Packet Error Rate (PER) for the block of data sent on each PRB. The SINR  $\Gamma_c^u$  (JT) perceived by a UE  $u$  of the MHC cell-site  $c$  can be expressed as:

$$\Gamma_c^u (\text{JT}) = \frac{|\mathbf{H}_{c,:}^u \mathbf{F}_{c,:}^u|^2 p_c^u}{\sum_{l \in \Theta_c, l \neq u} \left| \left( \sum_{t=1}^T \mathbf{H}_{c,t}^u \mathbf{F}_{c,t}^l \right) \right|^2 p_c^l + \sum_{i \in \Theta_{c'}, c' \neq c} |\mathbf{H}_{c',:}^u \mathbf{F}_{c',:}^i|^2 p_{c'}^i + \sigma_n^2} \quad (6.4)$$

### 6.1.1.2 SINR calculation for coordinated scheduling/beamforming (CS/CB)

In the CS/CB scheme, the CoMP eNBs within a MCH only share their scheduling information. Therefore, only one transmission point is used to transmit data after coordination. We denote user  $u$ 's transmit precoder applied at the transmission point of MHCs as  $\mathbf{F}_{c,t}^u$ , then the signal received at user  $u$  can be written as equation (6.5), where  $\Phi_c$  is the set of transmit precoder associated with the MCS  $c$ , and  $\Phi = \cup \Phi_c$  is the union set of  $\Phi_c$  [116]. From equation (6.5), it can be observed that MUI for a user only depends on other users within the same cell rather than all other users within the whole MHC cell-site. Then the received signal at user  $u$  can be expressed as

$$y_c^u = \overbrace{\mathbf{H}_{c,t}^u \mathbf{F}_{c,t}^u x_c^u}^{\text{Desired signal}} + \overbrace{\sum_{l \in \Phi_t, l \neq u} \mathbf{H}_{c,t}^u \mathbf{F}_{c,t}^l x_c^l}^{\text{MUI}} + \overbrace{\sum_{\substack{c' \in \Phi, t \neq j \\ 1 \neq u \in c'}} \mathbf{H}_{c',j}^u \mathbf{F}_{c',j}^i x_{c'}^i}^{\text{ICI}} + n_c^u \quad (6.5)$$

Then the SINR  $\Gamma_c^u$  (CS/CB) perceived by a UE  $u$  of the MHC cell-site  $c$  can be expressed as

$$\Gamma_c^u (\text{CS/CB}) = \frac{|\mathbf{H}_{c,t}^u \mathbf{F}_{c,t}^u|^2 p_c^u}{\sum_{l \in \Phi_t, l \neq u} |\mathbf{H}_{c,t}^u \mathbf{F}_{c,t}^l|^2 p_c^l + \sum_{\substack{c' \in \Phi, t \neq j \\ 1 \neq u \in c'}} |\mathbf{H}_{c',j}^u \mathbf{F}_{c',j}^i|^2 p_{c'}^i + \sigma_n^2} \quad (6.6)$$

### 6.1.2 Proposed Novel Energy Efficient Design (NEED) Architecture

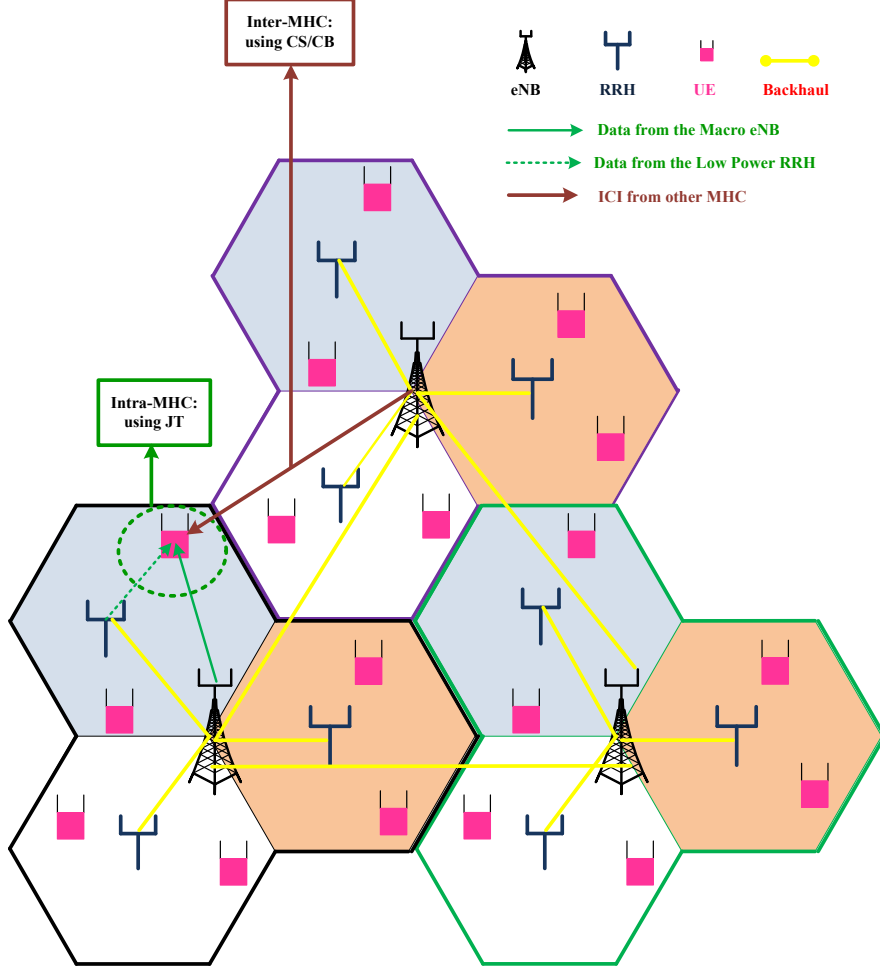


Figure 6.2: Proposed NEED architecture

Although the JT scheme can bring large performance gain to the CoMP system, it also plays host to a range of problems, such as high capacity backhaul requirement for exchanging the CSI and users' data, high computational complexity due to user scheduling and transmit precoding design, and synchronization among all eNBs within the CoMP cluster. By contrast, the CS/CB scheme is capable of lowering the backhaul requirement since there is no need to exchange users' data among eNBs within the CoMP cluster. However, this reduced computational complexity in CS/CB provides much less performance gain in comparison with its JT counterpart.

Therefore a practical architecture is needed to trade-off between system complexity and the system performance (energy efficiency). A method was envisioned for LTE-A [119, 9] which combines both JT and CS/CB for homogeneous SISO scenario. We proposed a novel energy efficient architecture (NEED) architecture which covers HetNet CoMP using MU-MIMO as shown in Figure 6.2. In this implementation, we take advantage of the benefits of both JT and CS/CB, while keeping signaling overhead low and performance is almost near

that of JT. In our proposed method, the JT scheme is used for intra-MHC where cells belong to the same MHC and CS/CB scheme is used for Inter-MHC coordination between eNBs in a distributed or semi-centralized way. In other words CS/CB is used for minimizing the ICI.

#### 6.1.2.1 SINR calculation for NEED

The intra-MHC part constitutes desired signaling and the MUI is calculated by JT, and the inter-MHC part constitutes the ICI which is calculated using CS/CB. The received signal at user  $u$  can be expressed as:

$$y_c^u = \underbrace{\mathbf{H}_{c,:}^u \mathbf{F}_{c,:}^u x_c^u}_{\text{Desired signal}} + \underbrace{\mathbf{H}_{c,:}^u \sum_{l \in \Theta_c, l \neq u} \mathbf{F}_{c,:}^l x_c^l}_{\text{MUI}} + \underbrace{\sum_{\substack{c' \in \Phi, t \neq j \\ i \neq u \in c'}} \mathbf{H}_{c',j}^u \mathbf{F}_{c',j}^i x_{c'}^i}_{\text{ICI}} + n_c^u \quad (6.7)$$

Then the SINR  $\Gamma_c^u(\mathbf{NEED})$  perceived by a UE  $u$  of the MHC cell-site  $c$  can be expressed as

$$\Gamma_c^u(\mathbf{NEED}) = \frac{|\mathbf{H}_{c,:}^u \mathbf{F}_{c,:}^u|^2 p_c^u}{\sum_{l \in \Theta_c, l \neq u} \left| \left( \sum_{t=1}^T \mathbf{H}_{c,t}^u \mathbf{F}_{c,t}^l \right) \right|^2 p_c^l + \sum_{\substack{c' \in \Phi, t \neq j \\ i \neq u \in c'}} |\mathbf{H}_{c',j}^u \mathbf{F}_{c',j}^i|^2 p_{c'}^i + \sigma_n^2} \quad (6.8)$$

#### 6.1.2.2 Interference Mitigation and Coordination

There are two types of interference we can identify in the transmission methods. Those are the MUI and the ICI. Specifically, upon utilizing the users' CSI, the eNB can design a dedicated precoder to sufficiently suppress MUI based on a range of principles, such as zero-forcing (ZF), minimum mean-square-error (MMSE) [115, 117] among others. The MUI is mitigated using zero-forcing (ZF) precoding techniques [115, 120]. Hence the SINR formula in equation (6.8) can be reformulated as

$$\Gamma_c^u(\mathbf{NEED}) = \frac{|\mathbf{H}_{c,:}^u \mathbf{F}_{c,:}^u|^2 p_c^u}{\sum_{\substack{c' \in \Phi, t \neq j \\ i \neq u \in c'}} |\mathbf{H}_{c',j}^u \mathbf{F}_{c',j}^i|^2 p_{c'}^i + \sigma_n^2} \quad (6.9)$$

This MUI cancellation also applies to both JT and CS/CB.

However, in addition to the aforementioned MUI, the cellular system may suffer from ICI, which cannot be suppressed individually within a single cell. Specifically, in comparison with cell-center users, cell-edge users tend to have lower received signal strength and are therefore more vulnerable to ICI. For our scenario, to minimize the ICI we devise a ICI reduction technique using coordination through limited feedback [121, 122]. The proposed algorithm for interference coordination is listed as follows in Algorithm 6.1.

---

**Algorithm 6.1** ICI Coordination Algorithm

---

- 1: Each UE estimates the aggregated channel (macro-cell eNB and RRH) from the serving MU-MIMO HetNet CoMP (MHC).
- 2: Each UE estimates the aggregated channel (macro-cell eNB and RRH) from the interfering MHC.
- 3: Each UE receives the feedback information. The feedback information contains:
  - a) Precoding matrix indicator (PMI) and channel quality indicator(CQI) for the serving cell.
  - b) Reference PMI from the interfering MHCs.
- 4: Information exchange between the MHCs operated by the MHCs.
- 5: Each UE receives the PMI which is used for performance enhancement:
  - a) That means, improvement of SINR while using the recommended set of PMIs at the interfering MHCs.
- 6: Each UE sends back the information, which is fed back to the serving MHC as well as the interfering MHCs.
- 7: Finally, Serving MHC and the interfering MHCs select respective PMI to serve their targeted users.

(Interfering MHCs are evoked to choose the PMI which maximizes the capacity of its own serving UE within the preferable set while no central scheduler is present. On the other hand, the PMI for the serving UE are decided jointly across all the serving MHCs by the central scheduler if a central scheduler is available.)

---

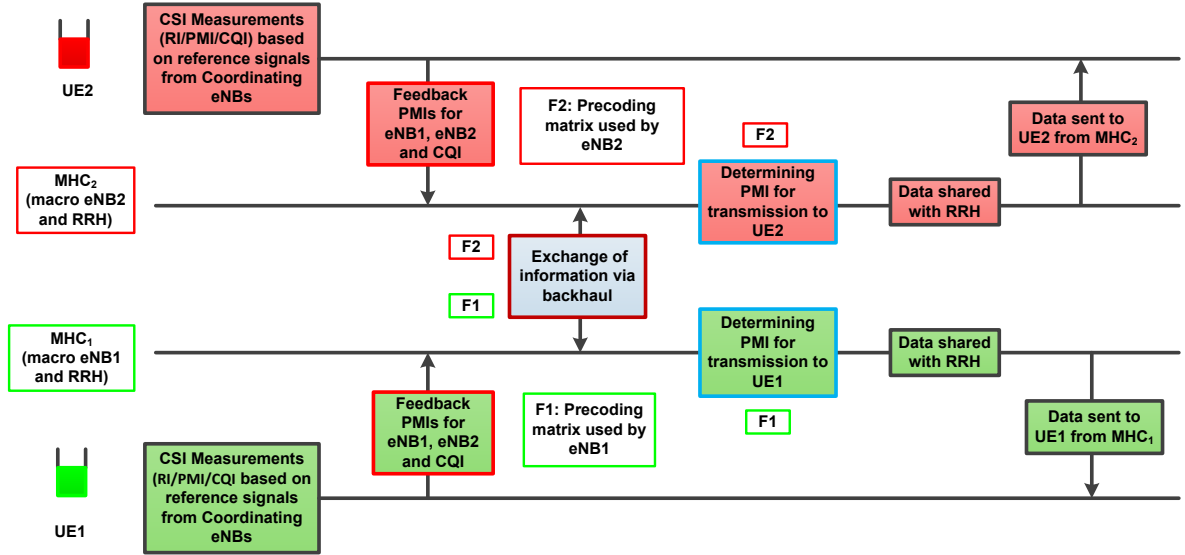


Figure 6.3: ICI coordination for proposed MU-MIMO HetNet-CoMP (MHC) architecture

A sequence chart is given by Figure 6.3 based on using 2 MHCs (MCH<sub>1</sub> and MCH<sub>2</sub>). Each MCH contains their respective macro-eNB and RRH to mitigate ICI impact. Let's say the MCH<sub>1</sub> is the serving MCH and MCH<sub>2</sub> is the interfering MCH which causes ICI to UE<sub>1</sub>. We consider the serving channel from MCH<sub>1</sub> (combined channel from eNB<sub>1</sub> and RRH<sub>MCH<sub>1</sub></sub>) is  $\mathbf{H}_1$  and the interfering channel from MCH<sub>2</sub> (combined channel from eNB<sub>2</sub> and RRH<sub>MCH<sub>2</sub></sub>) is  $\mathbf{H}_2$

for UE<sub>1</sub>. We also denote PMIs as  $\mathbf{F}_1$  and  $\mathbf{F}_2$  for eNB<sub>1</sub> and eNB<sub>2</sub> respectively.  $\mathbf{F}_1$  is calculated using  $\mathbf{H}_1$ , and  $\mathbf{F}_2$  is calculated for minimizing the ICI for UE<sub>1</sub> as  $\mathbf{F}_2$  is the interfering PMI.  $\mathbf{F}_2$  is given by [122]

$$\mathbf{F}_2 = \min \left( (\mathbf{H}_1 \mathbf{F}_1)^H \mathbf{H}_2 \mathbf{F}_2 \right) \quad (6.10)$$

### 6.1.3 Additional performance Metrics

In this analysis we use the performance metrics cell-site capacity, energy efficiency gain, overhead (both signaling and backhaul) percentage and power usage ratio for various CoMP transmissions. Specifically, the description of energy efficiency gain and overhead are given here under.

#### 6.1.3.1 Energy-Efficiency Gain

To demonstrate the EE gain compared to different transmission techniques, the following performance metric is employed, called Relative EE gain (unit: percentage):

$$\begin{aligned} EE_{gain}(\%) &= \frac{EE_C - EE_B}{EE_B} \times 100 \\ EE_{gain}(\%) &= \left( \frac{EE_C}{EE_B} - 1 \right) \times 100 \end{aligned} \quad (6.11)$$

Where  $EE_C$  is the energy efficiency of the compared technique and  $EE_B$  is the energy efficiency of the technique which is used as a benchmark to derive the relative gain.

#### 6.1.3.2 Signaling Overhead

In wireless systems, signaling overhead comprises pilot signaling and/or extra signaling (such as common pilot, dedicated pilot and feedback signaling). The efficiency of the system decreases, while the amount of signaling overhead increases due to the increase of the transmission and reception time for each symbol.

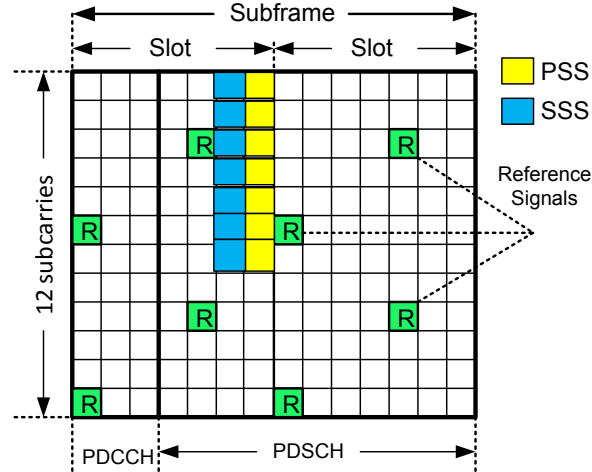


Figure 6.4: LTE-A downlink signaling elements [96]

If the amount of overhead signaling is large, the performance of the transmission and reception for each symbol can be increased, whereas the system performance can be degraded

once the amount of overhead signaling used is larger than a certain threshold. As shown in Figure 6.4, the primary synchronization channel (P-SCH) transporting primary synchronization signal (PSS) and the secondary synchronization channel (S-SCH) transporting secondary synchronization signal (SSS) are placed in symbols of 6 and 7 respectively, occupying 1.08 MHz bandwidth at the center of the transmission band.

The UE can synchronize with the CoMP by monitoring the downlink signal during a 5 ms period for 1.08 MHz bandwidth. The physical broadcast channel (PBCH) is located at the beginning of the first or the second time slot on the first subframe, and also occupies 1.08 MHz bandwidth. This scheme enables the UE to get information about the base station. The user data in the downlink direction is conveyed on the Physical Downlink Shared Channel (PDSCH) (Data), while the Physical Downlink Control Channel (PDCCH) (Control) is used to communicate to the device which resource blocks are allocated to it. Within the 1 ms subframe, only the first 0.5 ms slot contains the PDCCH (1-3 OFDM symbols corresponding to 6.0 - 20.2% physical resources), while the second 0.5 ms slot is purely for PDSCH [96]. In addition, reference signals (RSs) are distributed, which accounts for 4.8% [96] of the available capacity for SISO system, evenly in the time frequency domain for channel estimation. Considering other signaling channels, an approximate 20-40% [96] signaling overhead is generally reasonable.

#### 6.1.4 Simulation Results and Discussion

This section represents the system level simulation (SLS) results and a description of the proposed scenario. Monte Carlo simulation is used where the users are randomly distributed over the geographical area. Full-queue traffic model is used for all the users, which means they always have information ready to be transmitted. The effect of channel delay on the cell throughput will be examined. The key parameters of the simulated system are set according to the LTE Standard [11] which is summarized in Table 4.1.

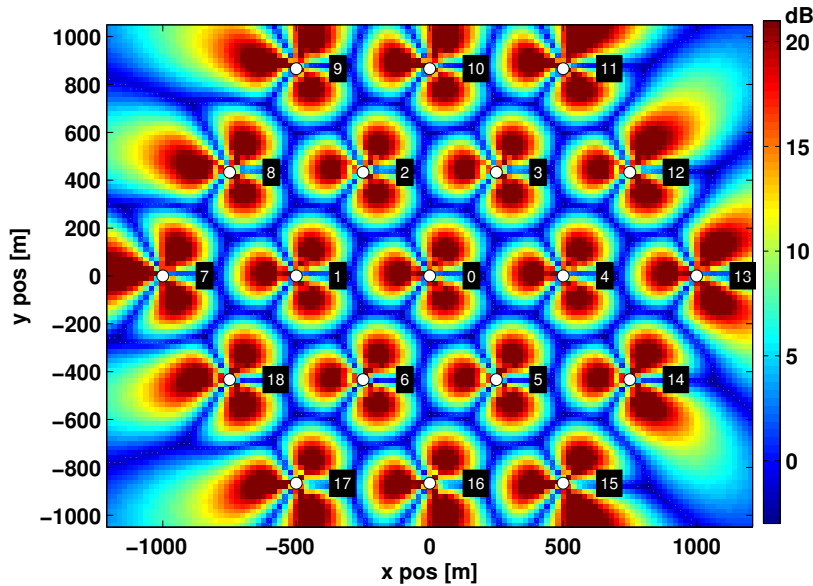


Figure 6.5: Deployment of the MHC system

For SLS purposes, we consider an LTE-A cellular system consisting of 19 MHC cell sites, with six MHC cell-sites in the first tier and twelve MHC cell-sites in the second tier, surrounding the central MHC cell-site. Each CoMP cell-site includes three  $120^\circ$  hexagonal cells, i.e. 57 hexagons in total are simulated. Due to simplicity, all the simulation results are collected from the three hexagons of the central MHC cell-site, with the other 54 hexagons serving as interferers' since the system is fully loaded. A wrap-around model is used to avoid border effects [54]. The deployment of the system is shown by Figure 6.5, where each red-colored block represents an RRH and the each white circle represents an eNB.

Figure 6.6 shows the cumulative distribution function (CDF) concerning the cell-site throughput of different coordinated transmission schemes along with the uncoordinated MU-MIMO transmission (w/o-Cord. means no coordination in Figure 6.6). Cell-site throughput is defined as the ratio of the number of bits transmitted in one cell-site over the time required to transmit them. For a large capacity system the unit can be Kbps, Mbps and so on. From Figure 6.6, we have the following observation:

- ⇒ The JT scheme is capable of outperforming all its counter-parts. Compared with JT, NEED architecture performs slightly worse (4%) than JT. The ICI minimizing technique discussed above employed by the NEED make the performance gap very narrow between JT and NEED.

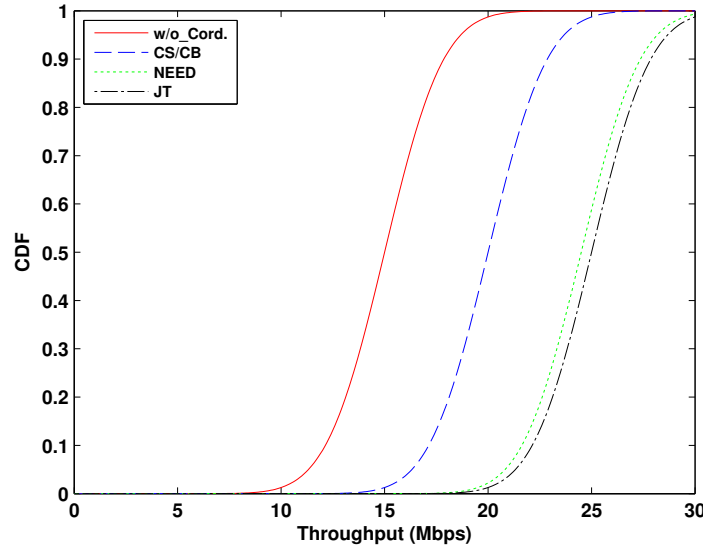


Figure 6.6: Capacity CDF of different CoMP schemes

Figure 6.7 depicts the average and cell edge EE for uncoordinated MU-MIMO and different downlink CoMP transmission schemes. It can be seen that CS/CB, NEED and JT schemes can obtain an EE gain of 25%, 57.3% and 60% respectively with respect to uncoordinated MU-MIMO at cell average. CS/CB, NEED and JT schemes can obtain an EE gain of 22.6%, 31.4% and 33.2% respectively with respect to uncoordinated MU-MIMO at cell edge. From Figure 6.7, we have the following observations:

- JT scheme can achieve the best performance in terms of EE in both cell center and cell edge for intra- and inter-MHC transmissions.

- Cell-edge EE is improved in NEED, compared to its cell average EE in terms of gain over from JT. That means the difference in gain in cell average and cell edge is 2.7% and 1.8%.
- Considering system overhead, CS/CB is a preferred candidate scheme for the sake of improving cell edge EE performance, which is usually a bottleneck problem in realistic green communication scenario.

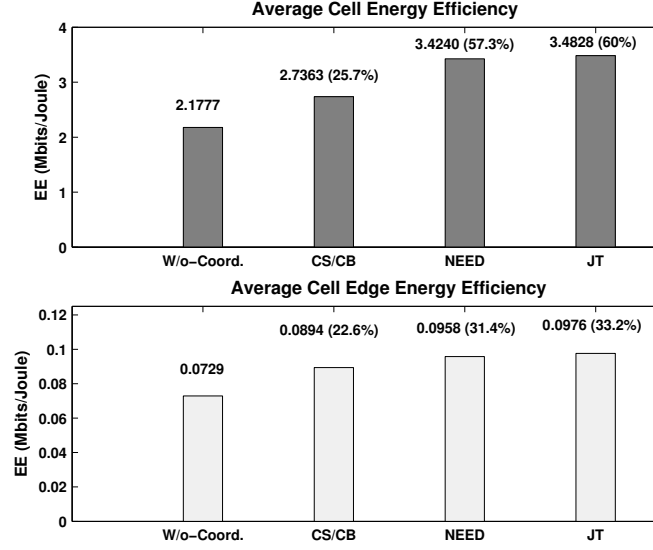


Figure 6.7: Energy Efficiency of different CoMP schemes

Although the JT scheme can bring more performance gain to the MHC system, it also has a range of problems, such as high signaling (radio signaling) overhead and backhaul requirement. Signaling overhead is quantified by the channel frequency response fed back by the UEs [123]. Consider  $\xi(t_s)$  to be the set of all channel frequency response in time slot  $t_s$ . With  $T$  transmitters and  $U$  users there are a total of  $|\xi(t_s)| = (T \cdot N_{TX}) \cdot (U \cdot N_{RX})$  frequency responses. In each time slot a subset  $\beta(t_s) \subseteq \xi(t_s)$  is fed back. The instantaneous feedback load is denoted as  $\lambda(t_s) = |\beta(t_s)|$  in each slot. Eventually we obtain the average number of frequency responses fed back per UE of the system as

$$\Lambda(\%) = \left( \frac{1}{U} \mathbb{E}_{t_s} \{ \lambda(t_s) \} \right) \times 100 \quad (6.12)$$

Figure 6.8 demonstrates the average signaling overhead (in percentage) for different HetNet CoMP techniques as a function of system SINR. It can be clearly seen that the radio signaling overhead increases in the high SINR regime. JT demonstrates the highest signaling overhead among all the HetNet CoMP techniques due to their intra- and inter-MHC JT technique. On the contrary, NEED provides less signaling overhead than JT, but more than CS/CB thanks to intra-MHC JT and inter-MHC CS/CB. The signaling overhead comparison is not that significant to provide a clear distinction among the techniques. To deduce the final decision in favor of the proposed HetNet CoMP technique, a backhaul overhead comparison is required.

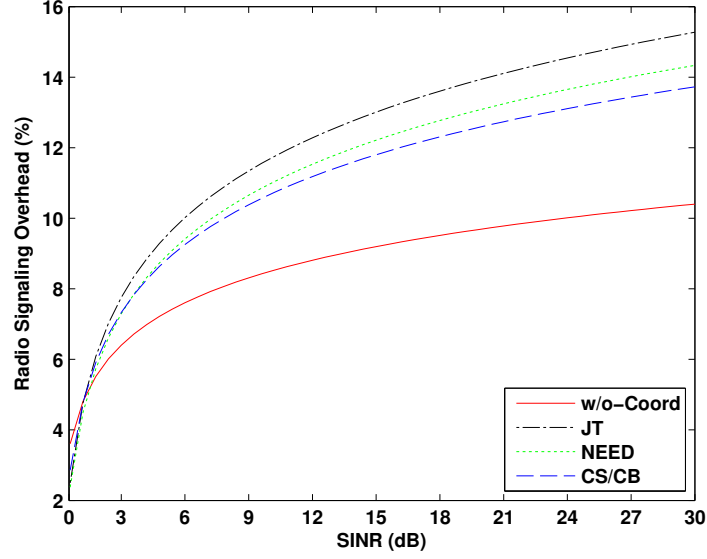


Figure 6.8: Radio signaling overhead comparison of different HetNet CoMP

Backhaul overhead is the result of exchanging the CSI and users' data, and end up with high computational complexity due to user scheduling and transmit precoding design, and synchronization among all eNBs within the same MHC cell-site. In comparison with the JT scheme, each MHC in the NEED scheme only serve its associated users upon designing its transmitter precoder to reduce its ICI to other MHCs. The NEED scheme is capable of lowering the backhaul requirement by removing the need of exchanging users' data among transmission between the MHC cell-sites. The backhaul overhead is the average number of user data streams transmitted per transmitter per time slot. This is determined by the number of zero elements of the precoding / beamforming matrix  $\mathbf{F}_{c,t}^u$ . The number of transmitted streams per transmitter, while coordinating the transmitter for both intra- and inter-MHC case gives an idea of backhaul usage [123]. We consider,  $\zeta(t_s)$  to be the number of zero elements of the beamforming matrix during slot  $t_s$ . The average number of transmitted data streams to calculate backhaul overhead per transmitter is

$$\Sigma(\%) = \left( (T \cdot M) - \frac{1}{T \cdot M} \mathbb{E}_{t_s} \zeta(t_s) \right) \times 100 \quad (6.13)$$

Figure 6.9 demonstrates the backhaul overhead comparison (in percentage) of different transmission techniques against the number of transmitters. As expected JT shows high backhaul overhead compared to other techniques. CS/CB shows less overhead than NEED since it does not need to exchange data signals in intra-MHC and inter-MHC; only scheduling and signaling information needs to be exchanged. In the case of NEED, data exchanging is required in the intra-MHC since can be used with the JT scheme, but not needed in the inter-MHC case (coordinated scheduling information required between MHCs). Therefore NEED provides less overhead than JT, but higher than CS/CB. Uncoordinated MU-MIMO technique has the least overhead due to no signaling information exchange between the MHCs. NEED shows 6% more overhead than CS/CB, whereas JT has 12% more overhead than NEED. Since JT has to exchange data signaling in both the intra- and the inter-MCH, hence the increase in backhaul overhead is quite high compared to NEED where data signaling needs to

be exchange only in the intra-MHC case and not in the inter-MHC. The trend shows that the number of transmitters involved in the coordination process is proportional to the backhaul overhead for every joint transmission technique.

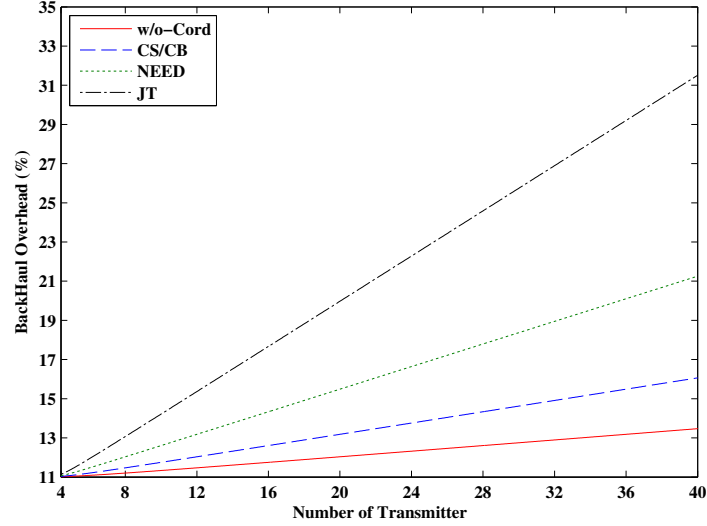


Figure 6.9: Backhaul overhead comparison for different MU-MIMO HetNet CoMP

Figure 6.10 describes the comparison of the power ratio consumption for uncoordinated, CS/CB, NEED and JT techniques under different cell load conditions. It can be concluded that, in contrast to the full reuse case, the proposed strategy has better performance with lower power consumption, except in CS/CB case. This demonstrates the efficiency and necessity of the coordinated power allocation. Note that larger coordination set size, provides higher power efficiency. Moreover, the power consumption increases as the users' number increases.

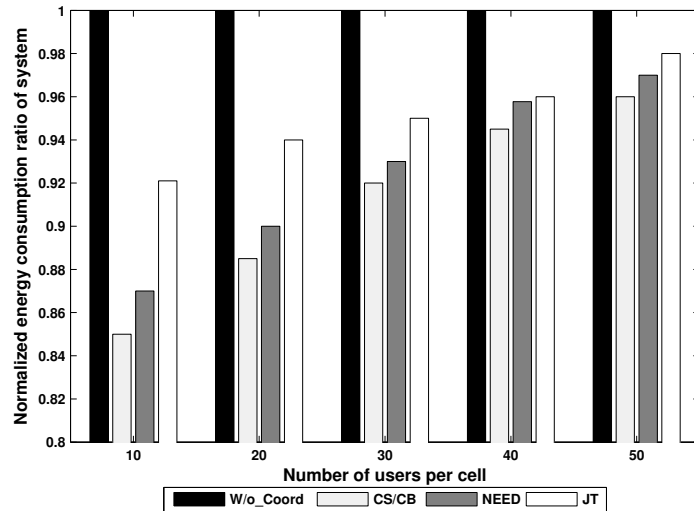


Figure 6.10: Energy consumption ratio of the different techniques.

Based on the above discussion as illustrated by the SLS, it can be concluded that our ar-

chitecture, NEED, provides the best trade-off between performance gain and overhead (both signaling and backhaul) for future energy efficient green communication network. Our architecture does not provide the best performance in every cases, but it does show optimum performance for pragmatic solutions in highly complexed coordinated scenarios. EE in NEED can be a little worse than JT, but considering a realistic implementation JT is too computationally complex for higher backhaul requirement. The power consumption ratio of CS/CB can be less than NEED, but in contrast it shows very poor system performance in terms of EE and throughput.

## 6.2 Frequency Allocation for HetNet CoMP: Energy Efficiency Analysis

In this second part, we plan to extend the work on CoMP by investigating the application of frequency planning approaches, and in particular fractional frequency reuse (FFR) for saving energy. In fact, frequency planning together with capacity planning tries to maximize the information flow over the radio interface and simultaneously to maximize the efficiency of the radio network infrastructure. Frequency planning criteria include the configuration and frequency allocation aspects, such as frequency band splitting between the transmitters and frequency reuse factor implementation. The widely-used inter-cell interference mitigation techniques are frequency reuse and FFR. The former scheme avoids utilizing the same frequencies in the neighboring cells, while the latter scheme allows universal frequency reuse for cell-center users. Conventional frequency reuse scheme yields lower spectrum utilization due to fewer available channels in each cell. To reduce the impact of frequency reuse on the throughput for each BS, the FFR scheme (or called reuse partition) assigns a larger frequency reuse factor for the cell-edge users and a smaller frequency reuse factor for the cell-center users. In 3GPP LTE, Inter-Cell Interference Coordination (ICIC) is considered as a promising technique to deal with the ICI mitigation issue [10]. Among the variety of ICIC strategies, the fractional frequency reuse (FFR) scheme are widely accepted [124]. The FFR scheme is based on the idea of applying a frequency reuse factor of one in cell-center areas, and a higher reuse factor in cell-edge areas. Therefore, the ICI is reduced at the expense of the available frequency resources for each cell.

We consider a CoMP-enabled heterogeneous network and focus on analyzing EE in terms of using the universal frequency reuse as a baseline scenario, and compare this to the (FFR) [125] scheme. Therefore in the first instance, we analyze EE in a HetNet CoMP to determine the optimum Macro transmit power for a given scenario which provides enhanced system EE as well as leading to reduced interference. Secondly we analyze our scenario using the FFR scheme to have an insight in the engineering trade-off between the cell-edge EE and the cell average EE. In [126], the performance of a conventional heterogeneous in terms of EE is first introduced; although, only the pico cell is considered as a low power node (LPN) and no coordination is present. In our system we consider pico and relay as the LPN to enhance the hotspot and coverage holes respectively.

### 6.2.1 System Model and Characteristics

HetNets are networks with multiple nodes with different transmission power. For example, HetNets may comprise of macro-cells, pico-cells, relays and so on. In our scenario we consider

not only conventional HetNets, but design CoMP HetNets from an interference perspective. The scenario considered in this section is based on an outdoor wide area cellular network. We propose a system architecture based on LTE technology [126]. A typical CoMP HetNet system is illustrated by Figure 6.11.

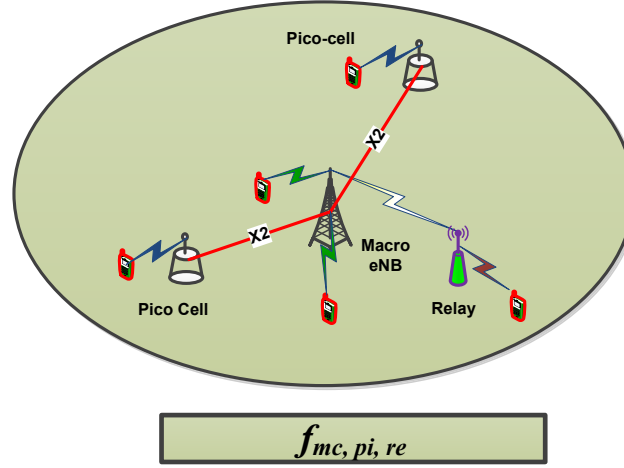


Figure 6.11: CoMP HetNet

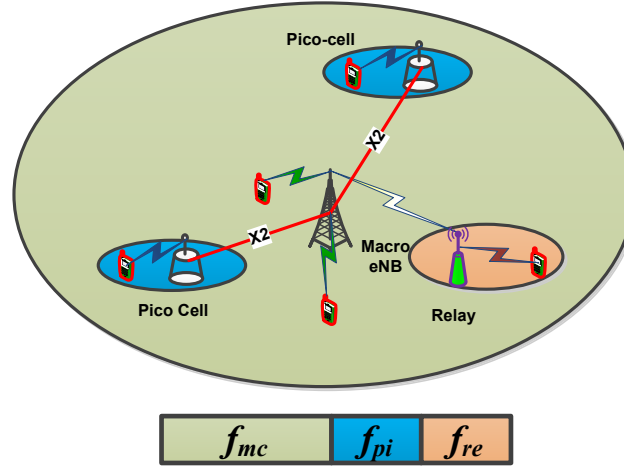


Figure 6.12: CoMP HetNet with FFR

To form a CoMP HetNet network, one macro eNB is deployed alongside pico stations (small base stations (SBSs)), and relay stations (LPN) to provide islands of high speed coverage. All the LPNs are coordinated with the macro cell to enhance ICI coordination. It is considered that those LPNs could provide energy savings by reducing the radiated RF power while ensuring the same quality experience for cell edge user. For the analysis in this section

we define the HetNet deployment scenario using the following algebraic formula:

$$\text{HetNet}(x) = 1_{\text{macro}} + x_{\text{pico}} + 2x_{\text{relay}} \quad (6.14)$$

Where,  $x$  = number of HetNet. For example,  
 HetNet (1) = 1 macro+ 1 pico cell + 2 relay.  
 HetNet (2) = 1 macro+ 2 pico cell+ 4 relay.  
 HetNet (3) = 1 macro+ 3 pico cell + 6 relay.

The CoMP HetNet using FFR is illustrated in Figure 6.12. Each macro, pico and relay is designated a different frequency plan which is demonstrated in the architecture using different colors. Therefore, each LPN receives interference from other LPN which exploits the same plan. We assume that similar frequency LPNs are deployed far from each other, and their transmitted power is much lower than the macro transmission power resulting in negligible interference. It should be kept in mind that the results we achieve from the CoMP HetNet are used as the baseline to compare the EE with the CoMP HetNet using FFR.

## 6.2.2 Simulations and Discussions

We now investigate the EE performance of the CoMP HetNet scenario using as a benchmark with a frequency reuse factor of one, with particular focus on how the number of LPNs affect the cell performance and compare the analysis with the FFR case. All simulations are carried out in the downlink.

### 6.2.2.1 Deployment

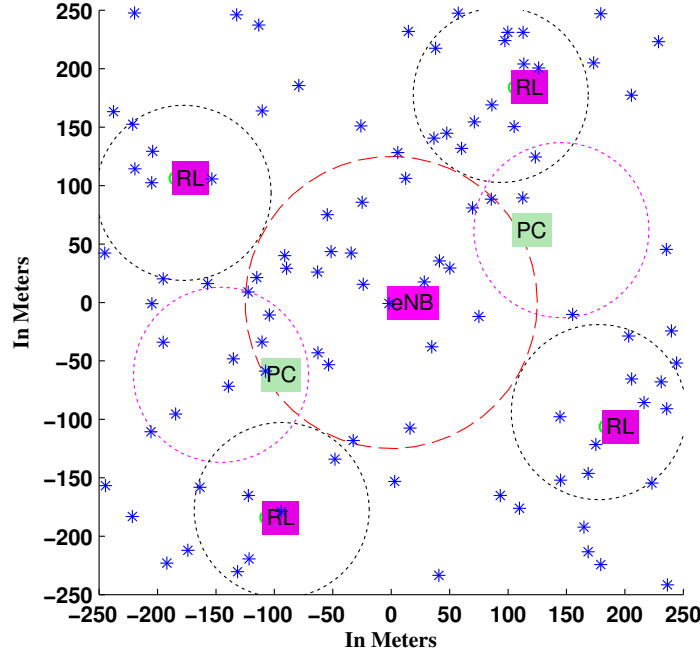


Figure 6.13: Deployment of one reference CoMP HetNet cell

We consider an LTE-Advanced network using an hexagonal deployment with a central reference cell surrounded by six cells in the first tier, and twelve cells in the second tier. To avoid border effects, a wrap-around model is used.

Users are deployed independently with uniform distribution throughout the cell. Monte Carlo simulations are used with Full-queue traffic model for all the users, which means they always have information to transmit. The simulator deployment is given by Figure 6.13, where one macro eNB and several LPNs (Pico and relays) delineate the coverage area. After deploying the CoMP HetNet architecture, one can easily deduce the optimal transmit power for a macro eNB which reduces the interference on its constituent small cells or LPNs, and moreover the optimal HetNet number (i.e. 1 HetNet or 2 HetNet or so on). It is worth mentioning that the optimal HetNet number depends on the cell size, and specifically the cell radius.

Further simulation parameters are described in Table 6.1.

Table 6.1: Simulation parameters

Parameter	Value	
Deployment	Mobile randomly deployed at each cell	
Cellular Layout	Hexagonal grid, 19 cell sites, 3 cell sectors per cell- site	
Inter-HetNet-CoMP distance	500 Meters	
Macro Power	46 dBm (42 dBm gives the optimum for our scenario)	
Pico & Relay power	30 dBm	
Static Circuit Power	Macro	20 dBm
	Pico & Relay	16 dBm
Power amplifier efficiency	Macro	0.38 [70]
	Pico & Relay	0.5
Dynamic circuit power	33.0103 dBm/Mbps[70]	
Carrier Frequency	2.6 GHz	
Bandwidth	10 MHz	
Noise Density	-174 dBm/Hz	
Path-Loss Model	Macro	$PL(\text{dB}) = 40\log_{10}(d) - 11.02$
	Pico & Relay	$PL(\text{dB}) = 22\log_{10}(d) + 34.02$
Log-normal Shadowing	Macro	4 (dB)
	Pico & Relay	6 (dB)
Noise Figure	7 (dB)	
Antenna Gain	Macro: 14dBi, Pico: 5dBi: Relay: 5 dBi	
Number of Pico	1,2,3,4,5,6, (2 gives the optimum result for our scenario)	
Number of Relay	1,2,3,4,5,6, (4 gives the optimum result for our scenario)	
Number of Users	100 per cell	

#### 6.2.2.2 Performance analysis

Figure 6.14 shows the average cell capacity for different number of HetNets. Although more HetNet leads to increased co-channel interference in some overlapped area, on the other side the benefits from frequency reuse are also obtained [126]. As expected, the system capacity improves as the number of HetNet increases. The optimal macro eNB transmission

power which provides maximum capacity is 42 dBm.

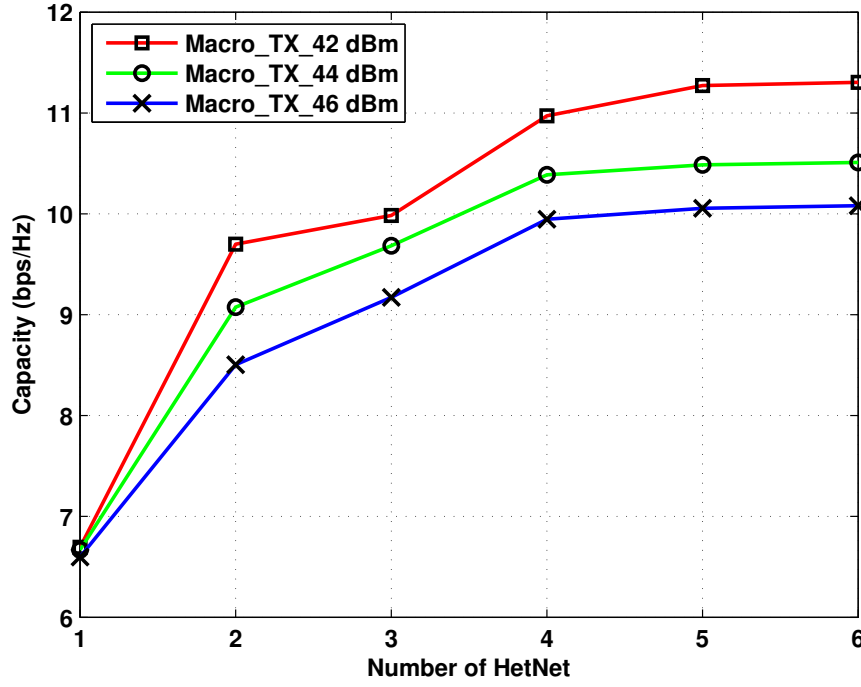


Figure 6.14: Average cell capacity comparison

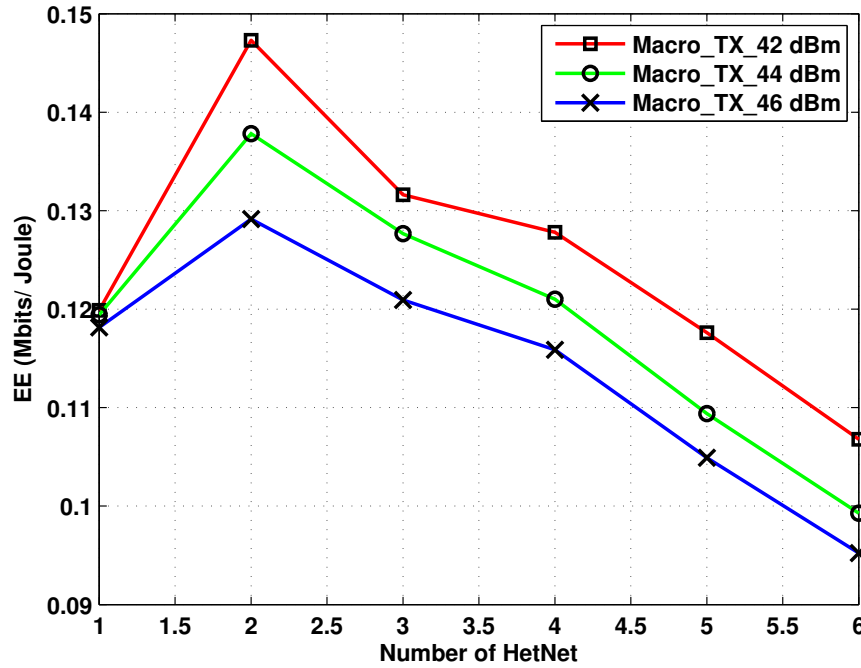


Figure 6.15: Comparison of Energy Efficiency for different HetNet

Figure 6.15 compares the energy efficiency for several HetNet numbers for different macro transmission powers. The heterogeneous network can achieve very high energy efficiency for a reasonable number of HetNets, e.g. 2. There is almost 15%, 20%, and 25% improvement

in EE for HetNet 2 using 46 dBm, 44 dBm and 42 dBm transmit power respectively. This means 2 pico cells and 4 relays together with a macro eNB provide the best performance in terms of the macro transmit power.

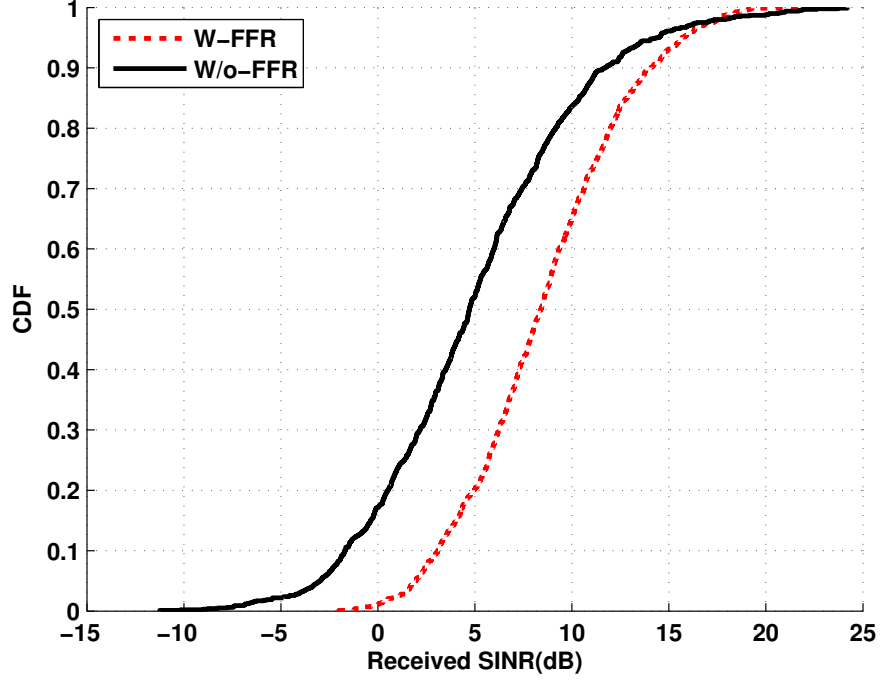


Figure 6.16: CDF of CoMP HetNet between different frequency planning

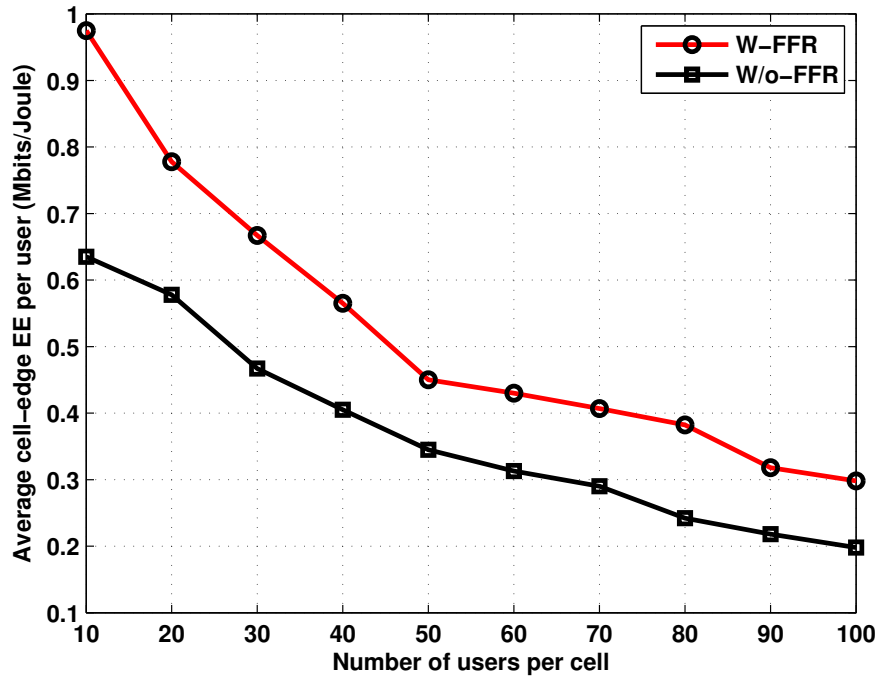


Figure 6.17: Cell-edge EE per user

The results above render a baseline for the CoMP HetNet whilst using frequency reuse

factor of one; a single frequency network. For the purpose of total power saving as well as interference reduction (in frequency reuse one network, the interference between the macro and the LPNs is a crucial issue), we reduce the transmit power of the macro eNB to different levels to observe actual EE and cell capacity performance. In this scenario cell-edge users suffer more which provides the motivation for different frequency planning such as FFR to increase cell-edge EE more, if not overall cell performance.

In Figure 6.16 we represent the CDF of the received SINR for 100 users for different frequency planning. The W-FFR and W/o-FFR represent the system with FFR and without FFR respectively. As expected, W-FFR shows greater improvement than W/o-FFR due to less interference.

Figure 6.17 shows the cell-edge average EE per user for the two different frequency reuse schemes considered in this part this chapter. It can be seen that the average EE per cell-edge users decreases as the number of users increases in the two schemes. This is primarily due to the increase in the probability of physical resource blocks (PRB) overlapping as the number of users increases. In other words, the interference increases when the average number of users per cell grows. Moreover, compared with the W/o-FFR scheme, W-FFR scheme produces a significant improvement in terms of cell-edge average EE owing to the frequency reuse plans designed for cell-edge areas which are served by the LPNs. Compared with the W/o-FFR scheme, the cell-edge average throughput is improved by 50% to 53%, which is achieved mainly owing to the frequency reuse rule designed in the FFR scheme.

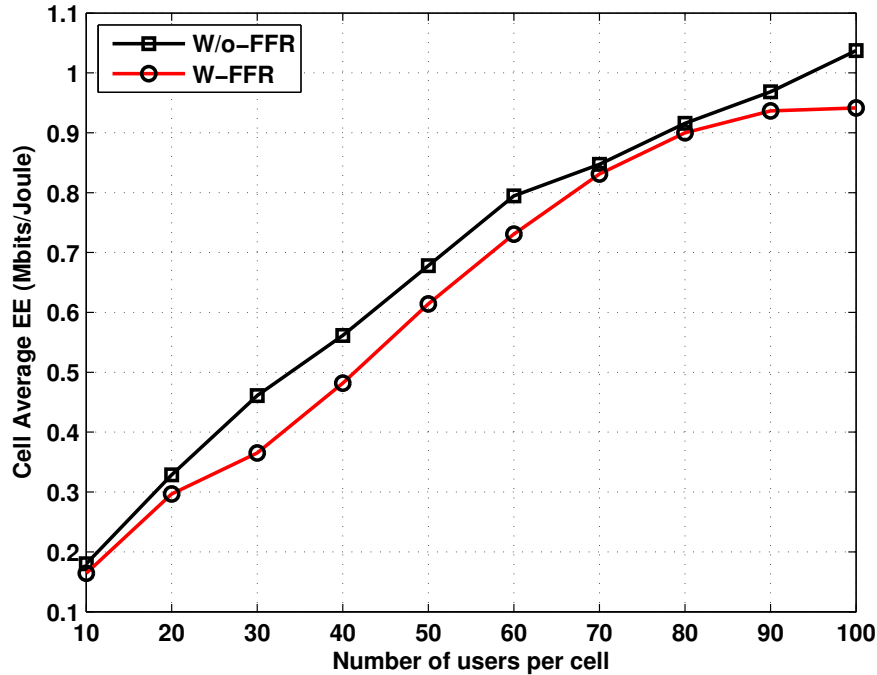


Figure 6.18: Cell average EE vs. Number of user

Figure 6.18 shows the cell-average EE of the two frequencies reuse schemes as a function of the number of users per cell. From the plot, we can observe that the cell-average EE of W/o-FFR scheme outperforms the W-FFR scheme due to the frequency reuse factor one in whole cell. It should be kept in the mind that this result assumes no considering for outer

cell interference. When the number of users is large, the W/o-FFR scheme achieves better results than the W-FFR scheme. Compared with the W-FFR scheme, the average cell EE is improved by 5 to 10% due to single frequency usage. However, the cost for this increased average cell EE in the W/o-FFR scheme is reflected by a degradation in the cell-edge average EE, which can be observed from Figure 6.17.

## 6.3 Optimization of Energy Efficiency considering Backhaul Power

This third part presents an analysis of the power consumption, including the effect of backhaul for two established backhauling technologies, i.e., fiber, and microwave for future HetNet CoMP deployment scenarios. The objective is to make an initial assessment of what is the impact on the total network power for the various technology and architectural options for the backhaul. Then two power models, one for the microwave case and one for the fiber case, will be presented and used in a case study to assess the power performance of each technology. The obtained results will then be leveraged to see how different architectural options for a given backhaul technology affect both the total backhaul and the total mobile network power consumption. In addition, a novel EE optimization algorithm is proposed with a data rate requirement constraint. We account for both radiated power (transmit and circuit) and backhaul power when designing optimal EE systems. The optimization objective is to maximize EE while satisfying SE requirements. This objective function, which is measured as the transmitted bits per unit energy consumption, is particularly suitable for designing green communication systems. Hence, we first formulate the optimization problem where the constraint is modeled as a cubic inequality [88] and then we propose a novel resource allocation algorithm to achieve maximum EE in a given SE which includes backhaul power for HetNet CoMP scenario.

### 6.3.1 HetNet CoMP Backhaul Architecture for Power Consumption Model

This section presents power models for HetNet CoMP including the contribution from the backhaul. A realistic model of the power consumption of the different types of transmitters such as Macro and other SBSs can for example be found in [127] where the model parameters are deduced based on data found in the literature. This section presents a power consumption model for cellular mobile networks including the backhauling part of the network. Different architectures and technologies are available to implement backhauling: we have chosen the solution which seems to be the most readily available and which presents the lowest complexity: a fiber optic network based on point-to-point Ethernet.

Figure 6.19 shows an example of a fiber-optic carrier Ethernet backhauling solution for a heterogeneous mobile network. 3GPP standardized IP/Ethernet interfaces for backhauling beyond mobile data core elements and out towards radio interface controllers of the transmitter [128]. Ethernet switches for backhauling can be flexibly located in the distributed cell sites, or in a centralized aggregation node, or at both locations to have several levels of aggregation. In this study, we have two levels of backhaul – inter-HetNet-CoMP backhaul and intra-HetNet-CoMP backhaul.

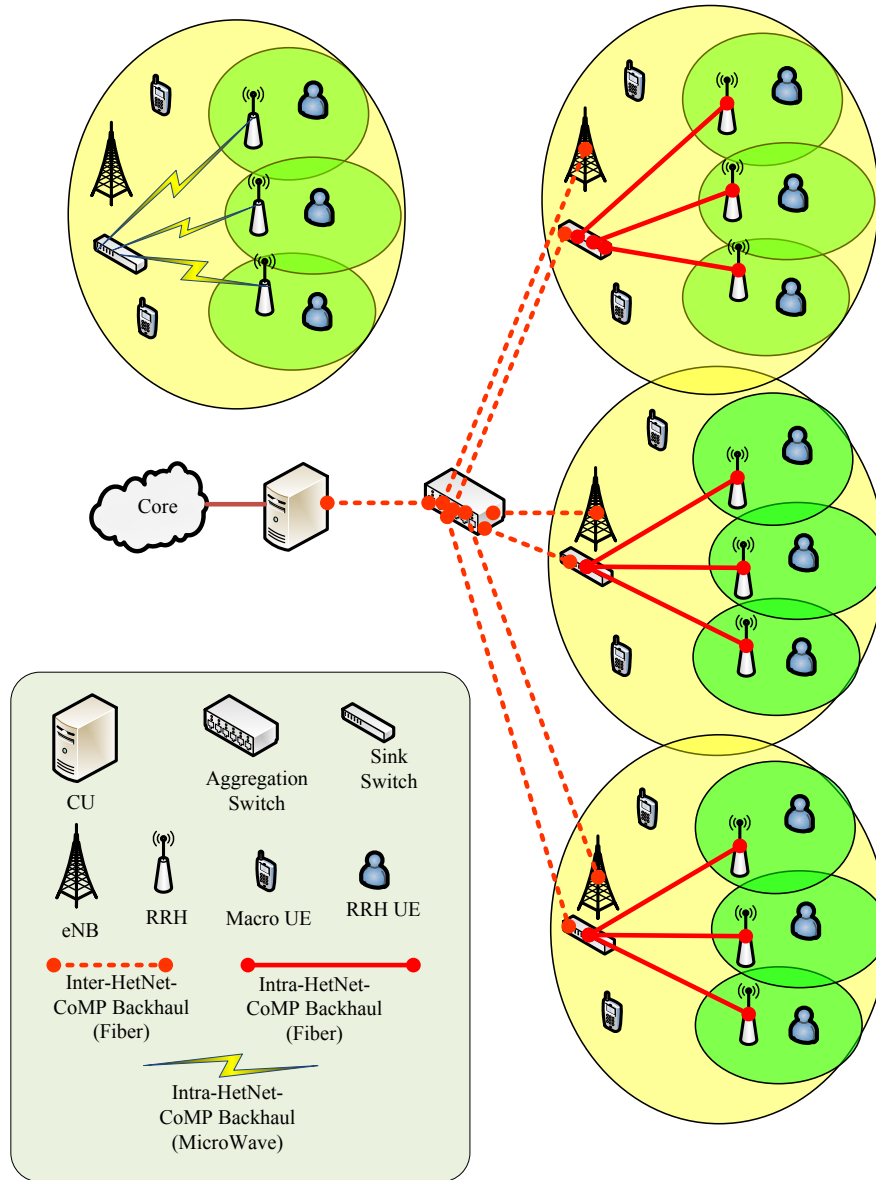


Figure 6.19: System Model with backhaul layout

In the case of inter-HetNet-CoMP backhaul, the traffic from all macro wireless nodes (eNB) are collected at one or more of the aggregation switches, just before the edge service node or the aggregation network. It is assumed that all backhaul links from all the eNBs to the aggregation switch (es) are optical fibers. Each transmitter (eNBs) has an optical small-form factor pluggable (SFP) (used to connect a BS to the aggregation switch) interface connected to an Ethernet switch port at the aggregation site. An alternative solution would be to use copper cable connections for the downlink. Although, using copper cable as a backhauling solution would be acceptable for 3G UMTS networks, but would not provide enough bandwidth to support LTE and LTE Beyond networks which offer 100 Mbps to each user [129].

In the case of intra-HetNet-CoMP backhaul, the traffic from all smaller wireless nodes

(RRH) is collected at one or more sink switches (located at the macrocell eNB for RRH). For this kind of backhaul two types of link are investigated to provide an insight of different backhaul power requirements. Both fiber and Microwave links could be used in this backhaul.

### 6.3.2 Power Consumption Model Including Backhaul

Given the backhauling architecture presented in the previous section, the power consumed to backhaul the traffic from all the base stations to the aggregation network, can be expressed as follows. The average power consumption of a base station  $P_k$  is modeled as a linear function of average radiated power, that is:

$$P_k = \alpha_k \cdot P_{Tx} + \beta_k + \delta \cdot S + \rho_k \quad (6.15)$$

where  $P_{Tx}$  denotes the transmitted or radiated power of each transmitter. The coefficient  $\alpha_k$  accounts for the power consumption that scales with the transmit power due to RF amplifier and feeder losses while  $\beta_k$  models the power consumed independently of the transmit power due to signal processing and site cooling.  $\delta$  is a constant denoting dynamic power consumption per unit data and  $S$  is the data rate. Additionally with respect to the power consumption model presented in [127], on which our model is based, a coefficient  $\rho_k$  is included which represents the power consumption of the SFP used to transmit over the backhauling fiber.

Equation (6.15) defines the power consumed by one base station, but in order to quantify the total power consumption of a heterogeneous mobile network, the power consumed by the backhaul ( $P_{BH}$ ) needs to be added, as shown in the following expression:

$$P_{Total} = \sum_{k=1}^K D_k \cdot P_k + P_{BH} \quad (6.16)$$

where  $K$  is the number of base station types used in the network,  $D_k$  is the total number of base stations of a specific type  $k^{th}$  (e.g., Macro or Small BS), and  $P_k$  is the power consumption of a base station of type  $k$ , which is calculated using equation (6.15).

The backhaul power in the HetNet-CoMP scenario consists two level of backhauling, these are, Inter-backhaul and Intra-backhaul. The expression is given in the following

$$P_{BH} = P_{BH}^{Inter} + P_{BH}^{Intra} \quad (6.17)$$

where  $P_{BH}^{Inter}$  represents the backhaul power consumption of the aggregation node and  $P_{BH}^{Intra}$  represents the power consumption at the sink node (located at the macrocell eNB for RRH only.) In addition, we can deduce that  $P_{BH}^{Inter} = P_{BH}^{Aggregation}$  and  $P_{BH}^{Intra} = P_{BH}^{Sink}$ . Therefore, equation (6.17) can be rewritten as:

$$P_{BH} = P_{BH}^{Aggregation} + P_{BH}^{Sink} \quad (6.18)$$

More elaborately,

$$P_{BH}^{Aggregation} = P_{Switch}^{Aggregation} + P_{Aggregation}(C_{Aggregation}) \quad (6.19)$$

and

$$P_{BH}^{Sink} = P_{Switch}^{Sink} + P_{Sink}(C_{Sink}) \quad (6.20)$$

where  $P_{Switch}^{Aggregation}$  and  $P_{Switch}^{Sink}$  denotes the power consumption of the aggregation switch and sink switch respectively;  $P_{Aggregation}(C_{Aggregation})$  and  $P_{Sink}(C_{Sink})$  denotes the power consumption for transmitting and receiving the backhaul traffic at the aggregation and sink node respectively. The power consumption for transmitting and receiving the backhaul traffic over the fiber/microwave link at the aggregation node switch is given as a function of the total traffic collected from all the corresponding transmitter, and is denoted by  $C_{Aggregation}$ . Similarly,  $C_{Sink}$  stands for the total traffic at the sink node switch. According to [129], several assumptions are taken into consideration expressed in the below:

- a) All switches are of similar characteristics; i.e., for the sake of simplicity both  $P_{Switch}^{Aggregation}$  and  $P_{Switch}^{Sink}$  can be termed as  $P_{Switch}$ ,
- b) Each transmitter in the network, irrespective of its type, utilizes a dedicated downlink interface,
- c) All downlink interfaces demonstrate similar characteristics along with the identical transmission rate.

### 6.3.2.1 Inter-Backhaul Power Consumption Model

The backhaul power consumption model is calculated based on the model presented in [130, 129]. The backhaul power  $P_{BH}^{Inter}$  includes not only the downlink and the uplink power consumption (i.e. from the base station to the aggregation switch(es) and from the switch(es) to the aggregation network, respectively) but also the power consumed at the aggregation switch(es), which is proportional to the total traffic backhauled from the mobile network. The macrocell eNB serves as the sink node for all the RRHs in the intra-backhaul deployments. The aggregation node is responsible for the sink node and the macrocell eNB traffic for backhauling the network traffic to the core network. A detailed expression for  $P_{BH}^{Inter}$  is given by [129]

$$P_{BH}^{Inter} = \left[ \frac{1}{\max_{dl}} \left( \sum_{k=1}^K D_k \right) \right] \cdot P_{Switch} + \left( \sum_{k=1}^K D_k \right) \cdot P_{dl} + N_{ul} \cdot P_{ul} \quad (6.21)$$

where,  $P_{dl}$  is the power consumed by one downlink interface in the aggregation switch used to receive the backhauled traffic.  $N_{ul}$  and  $P_{ul}$  are the total number of uplink interfaces, and the power consumption of one uplink interface, respectively. It is also assumed that all uplink interfaces are identical.  $N_{ul}$  is a function of total aggregate traffic collected at the switch(es) ( $Tot_{Aggregation}$ ) and the maximum transmission rate of an uplink interface ( $U_{\max}$ ). More formally  $N_{ul}$  can be expressed as

$$N_{ul} = \left\lceil \frac{Tot_{Aggregation}}{U_{\max}} \right\rceil \quad (6.22)$$

The constant  $\max_{dl}$  in equation (6.21) represents the maximum number of downlink interfaces available at the aggregation switch and it is used to compute the total number of switches that are needed to collect the backhauled traffic from the mobile network. Finally,  $P_{Switch}$  represents the power consumed by a switch.  $P_{Switch}$  is assumed to have two main contributors [129]. The first one is traffic independent and models the power consumption of the backplane of the switch. The second one depends on the amount of traffic that is traversing the switch

( $C_{Aggregation}$ ). The relative influence of these power quantities is assumed to be regulated by a weighting parameter  $\mu \in [0, 1]$  as shown below:

$$P_{Switch} = \mu \cdot P_{\max} + (1 - \mu) \frac{C_{Aggregation}}{\max_{Aggregation}} \quad (6.23)$$

$P_{\max}$  represents the maximum power consumption of the switch, i.e., when all the downlink interfaces are in use, while  $\max_{Aggregation}$  is the maximum amount of traffic a switch can handle. In other words, the maximum capacity of a switch, i.e.,  $\text{MAX}_{Switch}$ .

### 6.3.2.2 Intra-Backhaul Power Consumption Model

Two types of backhauling technologies can be used for intra-HetNet-CoMP scenario. These are fiber and microwave. In the subsequent sections the power consumption model of these two backhaul technologies are presented. The comparison between these two types of backhaul power consumption model is also given in the numerical results section.

#### 6.3.2.2.1 Backhaul Power Consumption Model for Fiber

In this section the backhaul technology optical fiber used in the intra-HetNet-CoMP configuration is investigated. The macrocell eNB acts as the sink node in the intra-HetNet-CoMP. Each RRH is connected to the macrocell BS, which aggregates the small-cell network traffic with that of the macrocell network and then forwards the collected traffic to the core network. Thus, all the traffic in the Intra-HetNet-CoMP scenario is routed through the macrocell BS. The macrocell eNB backhaul link to the core network is also assumed to be a high-speed low latency optical fiber cable. All the RRH backhaul links are terminated at the sink node located at the macrocell eNB. Each RRH has a dedicated interface at the sink node switch and a SFP interface within its locality, which it is used to transmit over the dedicated fiber optic backhaul. The major difference between inter-backhaul and intra-backhaul power consumption model is the downlink interface which is not needed in the sink node. Hence, the power consumption model intra-backhaul fiber is expressed as

$$P_{BH}^{Intra,FIB} = \left[ \frac{1}{\max_{dl}} \left( \sum_{k=1}^K D_k \right) \right] \cdot P_{Switch} + N_{ul} \cdot P_{ul} \quad (6.24)$$

From (6.24), it is also clear that the power consumption of the sink node is the sum of the power consumption of the sink node switch(es)  $P_{Switch}^{Sink} = \left[ \frac{1}{\max_{dl}} \left( \sum_{k=1}^K D_k \right) \right] \cdot P_{Switch}$  and the power consumption for transmitting and receiving the backhaul traffic  $P_{Sink}(C_{Sink}) = N_{ul} \cdot P_{ul}$ , where in this case  $D_k$  is the total number of RRHs deployed in the network around the edge of the macrocell and  $\max_{dl}$  is the maximum number of downlink interfaces at the sink node switch, which is given by the simulation parameter in the numerical results section.

#### 6.3.2.2.2 Backhaul Power Consumption Model for Microwave

Similar to the fiber intra-backhaul, in the microwave intra-backhaul the macrocell NB has a sink node which receives all the traffic from all the RRHs [130]. The microwave backhaul link could either be operated on licensed or unlicensed spectrum. To ensure that the microwave links do not interfere with one another, careful measures should be taken. The eNB traffic is

aggregated with the RRHs traffic and forwarded to the core network via a high-speed optical fiber inter-backhaul link.

It should be kept in the mind that since no SFP interface is needed for the microwave backhauling technology, then the BS power consumption of the radiated/transmitted power is given in the equation (6.15)

$$P_k = \alpha_k \cdot P_{TX} + \beta_k + \delta \cdot S. \quad (6.25)$$

In the microwave case the intra-backhaul total power consumption of a heterogeneous mobile radio network including the backhaul part can be written as:

$$P_{Bh}^{Intra,MW} = P_{Switch}^{Sink} + P_{Sink}(C_{Sink}) \quad (6.26)$$

, where

$$P_{Switch}^{Sink} = \left\lceil \frac{C_{Sink}}{\max_{Sink}} \right\rceil \cdot P_{Switch} \quad (6.27)$$

and

$$P_{Sink}(C_{Sink}) = \begin{cases} P_{low-c}, & \text{if } C_{Sink} \leq Th_{low-c} \\ P_{high-c}, & \text{otherwise} \end{cases} \quad (6.28)$$

According to equation (6.28) the power consumption for transmitting and receiving the sink backhaul traffic via microwave ( $P_{Sink}$ ) is a step function with respect to the total backhauled capacity ( $C_{Sink}$ ) [130]. Two power regions ( $P_{low-c}$  and  $P_{high-c}$ ) for each base station were defined; one for low capacity traffic conditions and the other for high traffic capacity conditions. The traffic values are given in the numerical results section.

### 6.3.3 Novel Iterative Algorithm for EE Maximization

The total bandwidth  $B$  is equally divided into PRB, each with a bandwidth of  $W = B/M$ . Then, the spectral efficiency,  $SE$ , obtained by Shannon theorem, for user  $u$  on PRB  $m$  is

$$SE_c^{u,m} = \log_2(1 + \Gamma_c^{u,m}) \quad (6.29)$$

Then, the maximum achievable data rate,  $\bar{s}_c^{u,m}$ , for user  $u$  on PRB  $m$  is

$$\bar{s}_c^{u,m} = W \cdot SE_c^{u,m} \quad (6.30)$$

We can also introduce,  $s_c^{u,m}$ , the data rate for user  $u$  on PRB  $m$  at any instant.

Energy efficiency is defined as the ratio of the total system throughput over the energy consumption within a given period at the transmitter side where the unit is bits/Joule [22, 69]. In the subsequent subsection the problem formulation to optimize EE is explained.

#### 6.3.3.1 Problem Formulation in Terms of EE

For a downlink HetNet CoMP OFDMA network, EE,  $\eta_{EE}$  is defined as

$$\eta_{EE} = \frac{\text{Total System Throughput}}{\text{Total Power}} \quad (6.31)$$

Accordingly, the optimization problem can be formulated as shown–

$$\begin{aligned} \max_{\mathbf{s}} \left( = \frac{\sum_{c=1}^C \sum_{u=1}^U \sum_{m=1}^M s_c^{u,m}}{P_{Total}} = \frac{\sum_{c=1}^C \sum_{u=1}^U \sum_{m=1}^M s_c^{u,m}}{\sum_{k=1}^K D_k \cdot P_k + P_{BH}} = \frac{\sum_{c=1}^C \sum_{u=1}^U \sum_{m=1}^M s_c^{u,m}}{\sum_{k=1}^K D_k \cdot (\alpha_k P_{TX} + \beta_k + \delta \cdot S + \rho_k) + P_{BH}} \right), \\ \text{subject to :} \\ 1) \hat{s}_c^{u,m} \leq s_c^{u,m} \leq \bar{s}_c^{u,m} \text{ or } s_c^{u,m} = 0, \\ 2) s_c^{u,m} \geq 0. \end{aligned} \quad (6.32)$$

where  $\hat{s}_c^{u,m}$  denotes the minimum rate requirement of HC for user  $u$  on PRB  $m$  and optimization variable is the rate vector  $\mathbf{s}$

To ensure the convexity of the proposed optimization problem, we redefined our constraint as a cubic inequality [88]. We reformulated our constraint based on non-negativity, as given in the following

$$(s_c^{u,m}) \cdot (s_c^{u,m} - \hat{s}_c^{u,m}) \cdot (\bar{s}_c^{u,m} - s_c^{u,m}) \geq 0 \quad (6.33)$$

From here, we then derive four conditions and find the 1<sup>st</sup> and 3<sup>rd</sup> conditions which satisfy our constraint's non-negativity and convexity. The four conditions are:

$$\begin{aligned} 1) s_c^{u,m} = 0; \quad 2) s_c^{u,m} \in (0, \hat{s}_c^{u,m}); \\ 3) s_c^{u,m} \in [\hat{s}_c^{u,m}, \bar{s}_c^{u,m}]; \quad 4) s_c^{u,m} \in (\bar{s}_c^{u,m}, +\infty) \end{aligned} \quad (6.34)$$

### 6.3.3.2 Optimization

Our problem has a unique optimal solution since its objective function is concave and the solution space defined by the constraints is convex. In other words, this is a convex optimization problem [89].

In this section we develop an algorithm using the gradient method by constructing the Lagrangian function and checking the solution with the Karush–Kuhn–Tucker (KKT)[89] to meet the global optimal solution. Let us formulate the Lagrangian of our problem with Lagrange multiplier  $\lambda$ :

$$L(\mathbf{s}, \lambda) = \eta_{EE} + \sum_{c=1}^C \sum_{u=1}^U \sum_{m=1}^M \lambda_u^m [(s_c^{u,m}) (s_c^{u,m} - \hat{s}_c^{u,m}) (\bar{s}_c^{u,m} - s_c^{u,m})] \quad (6.35)$$

with the corresponding Lagrange dual function

$$g(\lambda) = L(\mathbf{s}, \lambda) \quad (6.36)$$

Hence dual problem is formulated as follows:

$$\min_{\lambda} g(\lambda) ; \lambda \geq 0 \quad (6.37)$$

Since the objective functions of equations (6.35) and (6.37) are differentiable, with respect to the primal variable  $\mathbf{s}$  and dual variable  $\lambda$ , both problems can be solved by the gradient projected method [89] :

$$s_c^{u,m}(t+1) = \left[ s_c^{u,m}(t) + a \cdot \frac{\partial L(\mathbf{s}, \lambda)}{\partial s_c^{u,m}} \right]^+ \quad (6.38a)$$

$$\lambda_c^{u,m}(t+1) = \left[ \lambda_c^{u,m}(t) - b \cdot \frac{\partial L(\mathbf{s}, \lambda)}{\partial \lambda_c^{u,m}} \right]^+ \quad (6.38b)$$

where  $t$  denotes the iteration index and  $a, b$  are positive step sizes [131], and  $[\cdot]^+$  is a projection onto the set of  $\Re^+$ . By setting  $\frac{\partial L(\mathbf{s}, \lambda)}{\partial \mathbf{s}}$  to zero (i.e., the KKT condition), one can obtain a solution.

### 6.3.3.3 Optimal Resource Allocation Algorithm

According to the analysis of the above subsection, we propose the optimal resource allocation algorithm for achieving maximum EE in the downlink CoMP as follows in Algorithm 6.2:

---

**Algorithm 6.2** The novel optimizing rate allocation algorithm to maximize EE

---

1: **Step 1: Initialization**

Set  $s_c^{u,m}(0)$  and  $\lambda_u^{u,m}(0)$  to some non-negative value for all users  $u$  and resource blocks  $m$

2: **Step 2: Optimization**

Applying Gradient method

Update  $s_c^{u,m}(t+1)$  according to equation (6.38a)

Update  $\lambda_c^{u,m}(t+1)$  according to equation (6.38b)

3: **Step 3:**

Iterate until the implementation converges to the optimal point (or the number of iteration is achieved), the algorithm stops, else go back to step 2.

---

## 6.3.4 Numerical Results

### 6.3.4.1 Backhaul Power Consumption Analysis

Table 6.2: Simulation parameters for power consumption model [127, 129, 130]

(a) Parameter for Fiber Intra-backhaul					
BS Type	$P_{TX}$ (dBm)	$\alpha_k$	$\beta_k$	$\rho_k(W)$	$P_{dl}(W)$
eNB	46	21.45	354.44	1	1
RRH	30	5.5	38	1	1

(b) Parameter for Fiber Intra-backhaul					
BS Type	$P_{ul}$ (W)	$\max_{dl}$	$P_{Switch}$ (W)	$\text{MAX}_{Switch}$ (Gbps)	$\mu$
eNB	2	24	300	24	0.9
RRH	2	24	300	24	0.9

(c) Additional parameter for Microwave intra-backhaul					
BS Type	$P_{low-c}$ (W)	$P_{high-c}$ (W)	$Th_{low-c}$ (Mbps)	$P_{Switch}$ (W)	$\text{MAX}_{Switch}$ (Gbps)
eNB	37	92.5	500	53	36
RRH	37	92.5	500	53	36

In this section, the total power consumption of the different backhaul technologies for Intra-backhaul deployments scenarios presented above are compared. Both deployments have the same characteristics in terms of coverage and capacity. In order to compute the power consumption of the backhauling segment (inter and intra backhaul) the values in Table 6.2 are used. The transmission speed for the transmitters and the receivers at the downlink interface is assumed to be 1 Gb/s, while the maximum transmission speed for the uplink interface ( $U_{max}$ ) is 10 Gb/s [129].

In Figure 6.20 the impact of the backhaul on the overall power consumption of the network is shown for the intra-backhaul network deployment schemes. The power is computed in terms of area power consumption and is presented as a function of the area throughput. As can be seen, microwave link consumes more power than fiber links due to fast transmission rate of the optical fiber. The figure shows that a fiber-based backhaul consumes less power over the microwave link. Hence, from a pure energy consumption perspective the fiber-based solution where each base station in the area has a dedicated point-to-point connection with the sink node, is preferable. Obviously, such considerations need to be weighted against other important factors such a deployment costs.

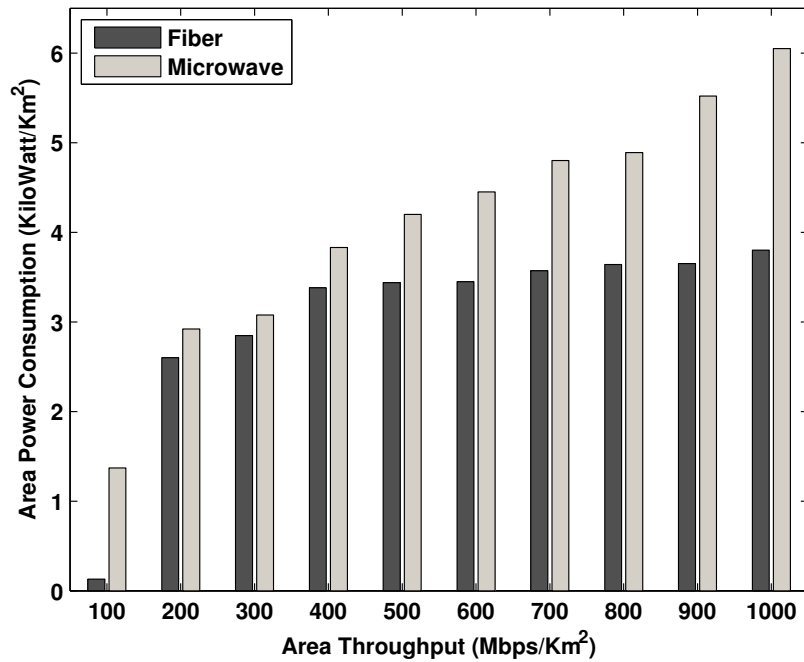


Figure 6.20: Area power consumption for the different types of intra-HetNet-CoMP backhaul.

Figure 6.21 shows the impact of the power consumption of the backhaul segment on the overall network power consumption of HetNet CoMP. The value of the total network power consumption is shown as a function of the area throughput requirements. Both technology options, i.e., fiber and microwave are considered. The figure confirms that the impact of the backhaul power consumption is larger for a heterogeneous network scenario compared to the “exclude backhaul” case. This is true regardless of the technology choice for the backhaul. This means that technology and topology considerations for the backhaul will be increasingly important for optimizing the total network power in a HetNet CoMP scenario.

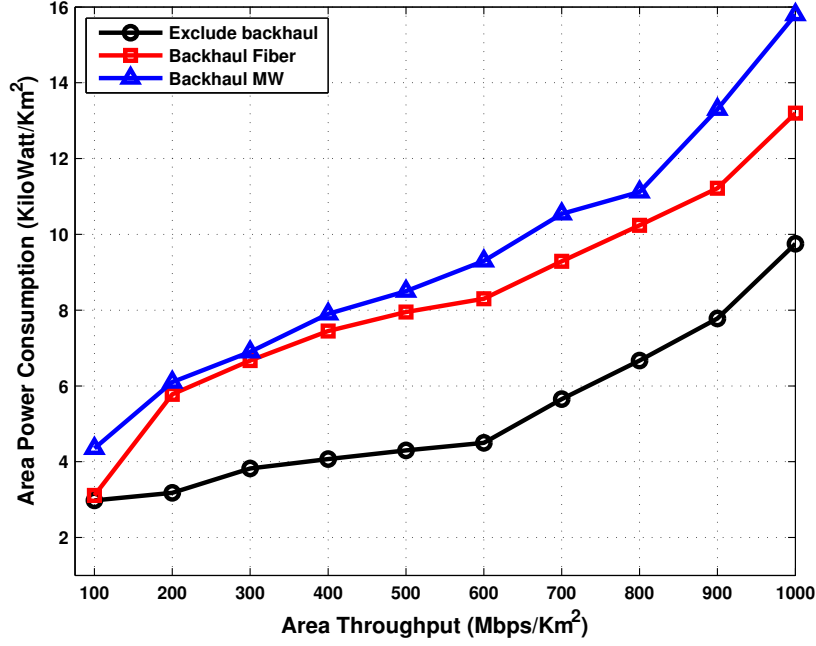


Figure 6.21: Different types of backhaul comparison.

#### 6.3.4.2 Performance Analysis of the Optimization Algorithm

In this section, simulation results are presented to demonstrate the performance of the proposed optimization algorithm. We conduct a numerical experiment to implement the iterative optimization. The optimization model is numerically solved to evaluate the convergence behavior of the proposed algorithm and demonstrate that it is able to achieve the maximum throughput and the corresponding maximum EE as well. We consider an LTE network for our simulation. The key system parameters used in our simulations are given by Table 3.1.

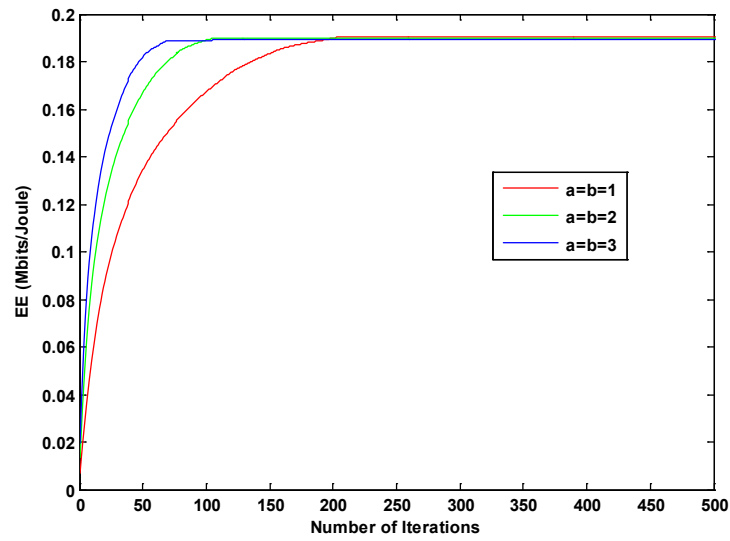


Figure 6.22: Convergence behavior using integer static step size

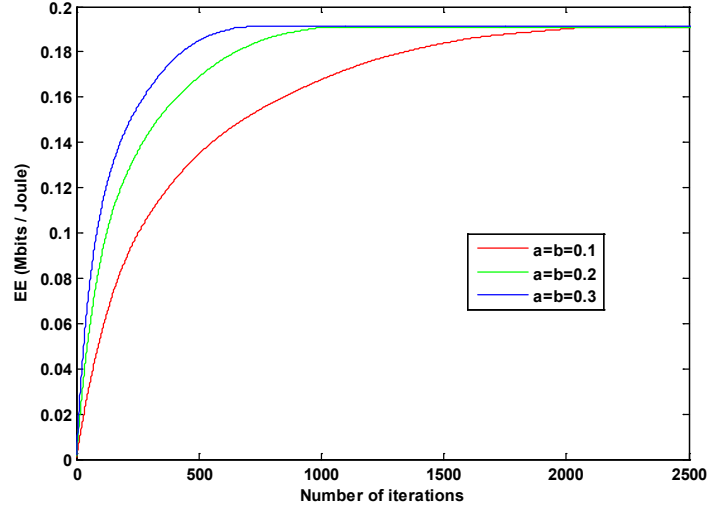


Figure 6.23: Convergence behavior using fractional static step size

Figure 6.22 and 6.23 demonstrate the convergence behavior of the optimization algorithm with a static step size for a range of values. It can be seen that using our algorithm, the EE of the system approaches the optimal value after some iterations. The static step size which contains integer value (with three different step sizes, 3, 2, and 1) can be considered a large step size, and likewise the static step size which contains fractional value (with three different step sizes, 0.3, 0.2, and 0.1) can be considered as small. In both cases, it can be seen that the convergence behavior is smoother but slower when the step size is smaller.

Our algorithm should converge quickly enough in order to have a realistic implementation at the system level. From the above mentioned figure, we observe that our algorithm converges after 100 iterations using integer static step size 2; whereas 1200 iterations are required to converge when fractional step size 0.2 is applied.

Next, we study the impact of dynamic step size on the convergence behavior of EE. Figure 6.24 shows the convergence behavior of EE with two types of static step size (0.2 and 2) and two dynamic decreasing step sizes  $2/(1+0.01*t)$  and  $2/(1+0.02*t)$  [88]. It can be seen that the convergence behavior with a dynamic step size  $2/(1+0.02*t)$  is smoother but converges more slowly than the static step size. The convergence behavior with fractional static step size 0.2 not only demonstrates the slowest convergence but also shows the least smooth property. A major advantage by using the dynamic step size is to allow faster convergence in the initial phase by larger step sizes, and to subsequently use smaller step sizes for fine tuning.

In the end, although a static step size is more convenient in practice and can converge more quickly, a dynamic step size is recommended since a slow-change rate profile is critical for system quality smoothness. Otherwise, a sudden change of access data rate will often result in undesirable quality fluctuation.

Figure 6.25 compares the EE between the proposed energy efficient resource allocation scheme and the rate adaptive power allocation [132] approach. Compared with the rate adaptive power allocation, 6.25 shows that in terms of EE the proposed scheme outperforms. Furthermore, Figure 6.25 shows the optimal envelop of the entire EE-SE region, which offers a global perspective on the EE-SE trade-off. The optimal EE-SE curve shows the existence

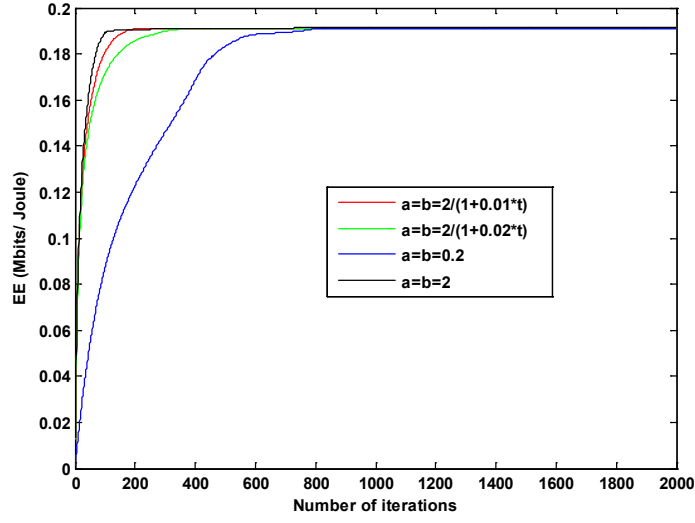


Figure 6.24: Impact of the dynamic step size

of a saturation point, beyond which the EE can no longer be further increased, regardless of how much additional energy is used. Using this result, on one hand, we can design the optimal energy consumption networks based on EE-oriented methods for multiuser CoMP if the system SE is not limited. On the other hand, we can maximize the reduction of energy consumption while satisfying given SE requirement.

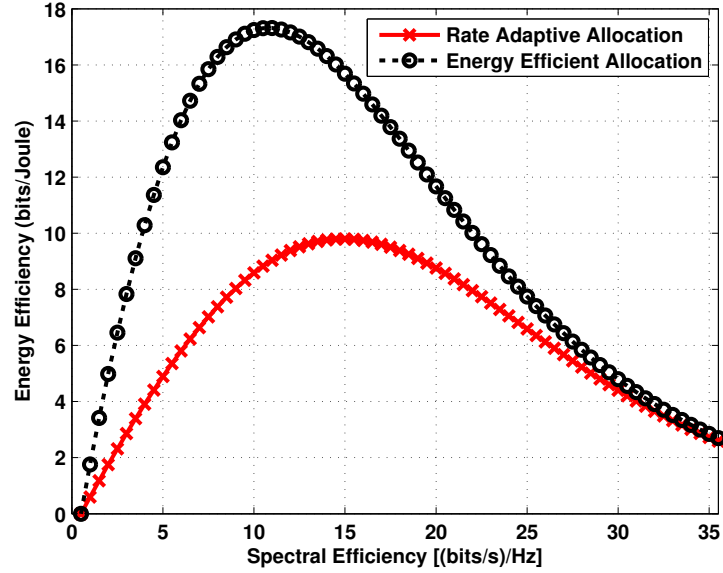


Figure 6.25: Spectral efficiency vs. Energy efficiency.

## 6.4 Conclusions

Usually transmission techniques have been compared from a traditional perspective, using SE as the key performance indicator. However, mobile stakeholders are now increasingly migrating towards energy efficient designs resulting from present and foreseen increase in data traffic. In response to this new research roadmap, 3GPP have introduced CoMP into the latest releases of LTE as a means of increasing not only the throughput for cell edge users, but a means of managing interference and thus a vehicle for controlling energy consumption in the network. In chapter 4, we provided an energy efficiency analysis of CoMP approach in the downlink as a means of establishing an accepted baseline, where EE and SE were measured and the engineering trade-off investigated. In this chapter we extended that work by proposing a novel energy efficient architecture we refer to as “NEED”, which is based on MU-MIMO HetNet CoMP system. The performances of various CoMP techniques are considered as the transmission technique for LTE-A. Our method showed significant advantages over the baseline under practical deployment scenarios, specifically in terms of global system performance and system overhead. It was found that the JT had the potential to deliver greater EE whereas CS/CB generated minimal system overhead. But neither of them could approach a feasible design for real operating conditions, therefore a new approach was required that could deliver a trade-off between these two ends of the spectrum providing the niche for the NEED approach.

Furthermore, we investigated the energy efficiency of HetNet using CoMP that operate in synergy with small cell networks, which is the deployment paradigm for 4G networks and beyond. The future mobile world leans towards a networking environment where LPNs are deployed to provide islands of hotspot coverage for high speed connectivity, even with different frequency plans breaking away from the conventional frequency reuse of one that was reminiscent of the 3G days. Operators see this as a way to create maximum impact for the end-user in order to ensure a sustained market for the introduction of new LTE services and beyond. Therefore it is clear, that an EE analysis for this deployment is required, and beyond that how to best manage these networks for optimizing energy consumption. In this context, we simulate a HetNet environment and develop a comprehensive EE study. Using this as a benchmark, we propose a scenario using different frequency planning approaches such as FFR which mitigates the interference. System-level simulation results demonstrate that average cell energy efficiency and capacity is influenced by the frequency reuse factor. In fact, should operator needs interference free environment they can deploy the HetNet CoMP using FFR. On the other hand if the cell average EE is the prime goal, then the operator can opt for a single frequency scheme, thus a delicate trade-off between these two operating points is required.

In the last part, we studied HetNet CoMP for OFDMA networks with ICI coordination and investigated backhaul power consumption of the system while applying realistic power consumption model. In addition an optimization problem is formulated to maximize EE where the constraint is formulated as a cubic inequality for a given data rate requirement. Both the radiated power and backhaul power are taken into consideration, without which, the SE-EE trade-off analysis for HetNet CoMP would be incomplete.

## Chapter 7

# Concluding Remarks

### 7.1 Summary of the Thesis

This thesis has focused on the resource allocation algorithm design for next generation OFDMA wireless communication systems, namely within the context of CoMP, and HetNet scenarios. Performance results are obtained not only in terms spectral efficiency, but beyond that in terms of energy efficiency that is now increasingly becoming an important design indicator for planning, deploying and optimizing next generation mobile networks. The following provides a summary of the key conclusions that can be taken as design guidelines for building energy efficient networks in OFDMA systems.

In **chapter 3**, we studied the SE-EE trade-off for OFDMA networks. The significance of the circuit power is clearly demonstrated. The results show that the characterization of the EE and SE relationship mainly depends on the static circuit power whereas the dynamic part of the circuit power does not have any significant impact. Moreover, we have investigated the EE-SE relation in a downlink multi-antenna multi-user CoMP system. Simulation and analysis of results show that there is a trade-off between EE and SE, which is very important for designing green communication systems. A novel resource allocation algorithm is proposed to achieve maximum EE where the constraint is formulated as a cubic inequality. We establish an analytical method to optimize energy efficiency of CoMP system with respect to SE constraints. We use this method to analyze the sensitivity of this efficiency to the network parameters. We also provide an upper and a lower bound for the numerical search of our algorithm.

In **chapter 4**, the performances of various classical scheduling algorithms are considered, as a first benchmark for further studies on energy aware algorithms, when using CoMP as the transmission scenario for LTE-Advanced. In CoMP operation, multiple points coordinate with each other in such a way that the transmission signals from/to other points do not incur in serious interference, or can even be exploited for improving received signal performance. The goal of the study was to evaluate the potential performance benefits of CoMP techniques in terms of EE while considering downlink packet scheduling. Gains in terms of the EE index (with respect to the reference Round Robin scheduler) are analyzed for different CoMP techniques. We also provide relative gain in terms of EE with respect to CS/CB to show the feasibility of DPS and JT. DPS can deliver greater EE, whereas JT can provide higher system throughput. CS/CB provides neither optimum energy efficient nor more system throughput, but offers a low, and hence a practical for LTE scheduling. As shown in this chapter, a good

compromise between maximum EE and SE among the considered schedulers is given by the MCI algorithm. It can be an effective trade-off between EE and system throughput as far as the operator point of view is concerned.

In **chapter 5**, we consider the CoMP transmission scenario and investigate an advanced scheduling approach based on the transmit energy consumption. The performance of the proposed algorithm was evaluated by comparing with the conventional SoA algorithms: MCI, RR, and PF. The simulation results showed that the proposed EES algorithm outperformed in the conventional scheduling policies, and moreover showed significant improvement in terms of fairness. The proposed scheduler balances cell-edge energy efficiency as well as cell-average energy-efficiency for multiuser systems. The optimal power allocation scheme is derived for the generalized energy-efficiency proportional fair metric. When the circuit power is non-negligible, the result suggests that transmitting always at a relatively large power seems to be beneficial. We believe this is a promising scheduling algorithm for IMT-Advanced systems that is technology agnostic.

3GPP is currently working towards enhanced LTE performance in Release 12, and initiated a new study item “Enhanced CoMP for LTE” in June 2013. The target is to evaluate the benefits of multi-cell scheduling with non-ideal backhaul, and to define the required interfaces and signaling messages to support multi-cell scheduling and assess the system performance including energy efficiency. The impact of the non-ideal backhaul on packet scheduling in CoMP scenario in terms of energy efficiency is still an open research topic. The earlier CoMP work in 3GPP Releases 10 and 11 considered only ideal backhaul by exchanging packet scheduling information, which is not feasible for most LTE deployments due to OPEX and CAPEX costs. In this chapter, we present a simple heuristic traffic threshold based on energy-efficient transmission system using eNB-made targeting a centralized LTE-CoMP system. The numerical results substantiate the efficiency of our algorithm. We demonstrated that by setting some eNBs in sleep mode on the basis of a defined traffic threshold we consume less energy.

In **chapter 6**, we partition our work into three parts. In the first phase, we extend the homogeneous CoMP architecture to heterogeneous architectures where coordination between macro eNB and low power remote radio heads (RRH) are investigated. To this end, intra-CoMP and inter-CoMP architecture are studied to check the outcome of the coordination. Finally, a Novel Energy-Efficient Design (NEED) was proposed that incorporates the CoMP architecture using MU-MIMO heterogeneous scenarios. Gains in terms of the energy efficiency index are analyzed for different CoMP techniques. We also provided the relative gain considering the energy efficiency and overhead (both for radio signaling and backhaul). The results show that the JT approach can deliver greater EE, whereas CS/CB results in less overhead. But neither of these can be considered practical solutions due to the overhead complexity (in the case of JT) and system performance (in the case of CS/CB). Therefore a trade-off exists between these two. The proposed NEED architecture provides the best trade-off for a realistic implementation from the operator’s perspective.

In the second part of this chapter, we studied the energy efficiency of HetNet using CoMP where low power nodes (LPNs) or small base station (SBSs) coordinates with the macro eNB to find the optimal transmit power for the macro cell which results in less interference, as well as promoting energy efficiency. Using this as a benchmark, we proposed a scenario using different frequency planning strategies such as FFR which mitigate the interference. System-level simulation results demonstrate that average cell energy efficiency is improved by deploying LPNs combined with a reduction in macro transmission power. However, the cell-

edge energy efficiency can be improved further by using FFR, although the average cell energy efficiency is decreased. Therefore an engineering trade-off exists; if the operator requires an interference free environment they can deploy the HetNet CoMP using FFR. On the other hand if the cell average EE is the prime goal then the operator can go for single frequency deployment scheme.

In the third part, we studied HetNet CoMP for OFDMA networks with ICI coordination and investigated backhaul power consumption of the system while applying a realistic power consumption model. In addition, an optimization problem is formulated to maximize EE where the constraint is formulated as a cubic inequality for a given data rate requirement, where not only the radiated power is taken into account, but also the backhaul power, which until now has been omitted in the literature. Simulation and analysis of results show that there is a trade-off between EE and SE. The results presented here are obtained for a specific backhaul solution, and may differ for alternative solutions, but the underlining message is that when assessing the benefits of deployment strategies, the backhaul power consumption cannot be simply ignored. Two backhaul technologies are considered, microwave- and fiber-based. Different topological choices for backhaul were analyzed, and their respective power consumption models were investigated. The presented results confirm that the power consumption of the backhaul segment is an important part of the total network power consumption. For this reason the backhaul needs to be carefully included in any deployment strategy when the primary objective is to minimize the total network power consumption. Furthermore, it was also shown that a complete fiber-based topology for both the inter and intra backhaul is preferable over the microwave-based intra backhaul topology for energy saving.

## 7.2 Future Research Directions

Next generation networks' such as 4G and beyond are required to provide higher capacity, as well as being energy efficient to reduce operational expenditures, and provide media connections at anytime, anyplace, anywhere. This raises different types of technical challenges such as high multi-cell interference levels as well as heavy energy consumption per user. In Chapters 3-6, we have considered several resource allocation approaches for promoting energy efficiency. However, energy efficient system design is a vast research area and many problems are still unsolved. In the following, we propose some ideas for further research in this fast evolving area.

### 7.2.1 Spectral Efficiency and Energy Efficiency Trade-off

Since SE and EE are two important system performance indicators, the trade-off between EE and SE for general OFDMA networks should be exploited to guide system design according to the existing literature. The bounds and achievable SE-EE regions for downlink OFDMA networks are important for the system designer [62]. Meanwhile, proper utility functions should be investigated for locating the optimum operating point on the boundary of SE-EE region [22]. The current state-of-the-art demonstrated that the EE can be achieved through energy-efficient design [62] towards next generation techniques such as MIMO [133], coordinated base station system [134] and relay transmission [135]. However, more effort is needed to characterize the SE-EE trade-off. A better balance between EE and SE is required. With the help of the existing literature [77], the SE-EE trade-off is defined to be a quasi-concave function and the impact of the channel power gain and circuit power is

analyzed. Some of the issues such as imperfect channel state information with average per-user rate requirement have not yet been tackled. Optimization of resources such as power and bandwidth are needed to ensure energy-efficient OFDMA wireless system. Advances in the layering framework in wireless protocol, for example, interdependencies of the different layers such as cross-layer resource optimization, are required to determine the fundamental bounds on achievable energy-efficiency. Correspondingly, research into practical realization and hardware implementations of energy-efficient protocols should be explored. Lastly, the next evolutionary stage of mobile networks is LTE-Advanced, that consider several deployment scenarios also based on OFDMA access such as femto cells and self organizing network (SON), should be researched further to find the SE-EE trade-off for ensuring energy saving and hence reducing the operator's operational expenditure.

### 7.2.2 Interference Modeling and Management in Heterogeneous Networks

Heterogeneous networks have been pivotal towards meeting the challenges on enhancing the spectral and energy efficiency of existing and upcoming wireless standards. In spite of the consorted benefits, going forward with this trend may end up with thronged spectrum bands and increased interference, the latter being nondeterministic due to the random locations and deployment density of small cells. Future work should be focused on illustrating and optimizing the spectral and energy efficiency of HetNets for scenarios based on BS coordination. The modeling and management of cross-tier and co-tier interference is crucial and of paramount importance for successful operation of HetNets. Motivated by the recent initiatives on the deployment and standardization of HetNets, it is significantly interesting to statistically model the cross-tier and co-tier interference in HetNets. In addition, the conventional interference mitigation strategies such as slow, fast and fractional power control and coordinated frequency reuse may also be worth incorporating whilst modeling the statistics of interference in HetNets. Moreover, the interference management and hand-off strategies in HetNets with respect to EE applying hybrid power control are important topics for further study. Since there will be more sources as transmitters and access points with heterogeneous deployment, this will lead to greater interference and increased handoffs. It is expected that further improvements can be achieved through full coordination between all the LPNs by employing some type of power control, since in this work we only assume semi-coordination which means only the coordination between the macro and the LPNs are considered.

### 7.2.3 Signaling Overhead

The trade-off between EE and channel state information (CSI) overhead in coordinated systems also requires more investigation. As indicated in this thesis, for optimal resource allocation CSI is indispensable. On the other hand, acquiring CSI will consume additional energy. Thus, there exists a trade-off between EE and CSI overhead. How to allocate power and other resources to signaling and data symbols to maximize EE is still unknown. Although CSI at the transmitter can assist to improve system capacity; the extra energy consumption due to the overhead of feedback may reduce EE of the system.

### 7.2.4 CoMP with Carrier Aggregation

Energy efficiency is of vital importance for telecommunications equipment in future networks, especially battery-constrained mobile devices. To satisfy the ever increasing demand

for higher throughput and data rates, wireless communication systems need to operate in wider bandwidths. For this reason, in the LTE-Advanced network, the carrier aggregation (CA) technique is employed to optimally utilize their available spectrum resources for increased data rates and promoting at user experience. However, multi-carrier transmission entails increased power consumption at user devices for uplink networks. In future, we could plan to include CA in CoMP scenarios, to further investigate the data rate and energy conservation benefit.

### 7.2.5 D2D Application in CoMP System

Although ad hoc mode has been available in 802.11 for many years, its usage has been very limited compared to infrastructure mode. Nevertheless, there has been an increased interest in device-to-device (D2D) communication recently, as manifested by the WiFi Direct (WiFi-D) specifications and proposals for LTE D2D standardization. The key motivation for this D2D vision is the possibility to introduce new communication patterns where we have local area connectivity, and for offloading traffic from the core network. The current ad hoc mode of communication does not support this seamlessly due to the configuration complexity in unlicensed band. Researchers believe that the interference in the unlicensed spectrum is hard to manage which imposes constraints for QoS provisioning. In future we could plan to include D2D communication in CoMP scenarios to attain EE benefits for proximity based application (i.e. facebook, youtube, twitter etc.). For instance, coordinated paradigm for D2D system model is shown in Figure 7.1. There are two kinds of UEs' in this mode, these are cellular UEs and D2D UEs. Cellular UEs are allocated in the green region (cell center) of each coordinated eNB, whilst D2D UEs are allocated at cell edge in gray region. D2D UE in the gray region received signal from all coordinated eNB to enhance the signal quality. Moreover this scenario will also improve the reliability i.e. there is several channel/radio pipes at the cell edge from D2D to eNB. The probability that all the channels are deteriorated at the same time is quite small.

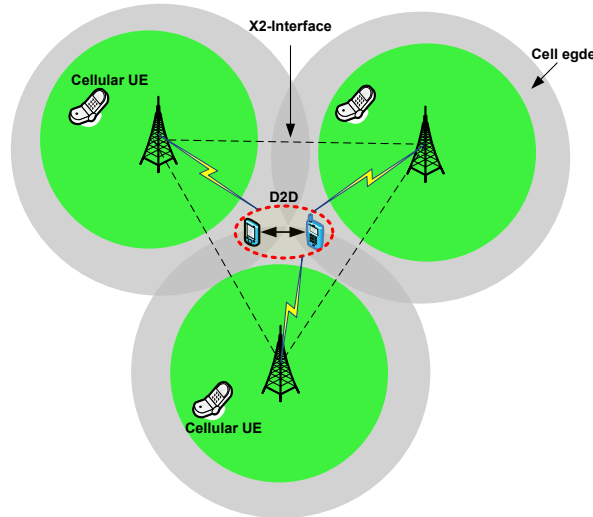


Figure 7.1: Coordinated paradigm for D2D Communication



# References

- [1] V. Chandrasekhar, J. Andrews, and A. Gatherer, “Femtocell networks: a survey,” *IEEE Communications Magazine*, vol. 46, no. 9, pp. 59–67, Sep. 2008. <sup>{1,26}</sup>
- [2] Institute for Information Industry, “Proximity communication,” Institute for Information Industry, Taiwan, Tech. Rep., 2012. <sup>{1}</sup>
- [3] M. S. Alouini and A. J. Goldsmith, “Area spectral efficiency of cellular mobile radio systems,” *IEEE Transactions on Vehicular Technology*, vol. 48, no. 4, pp. 1047–1066, Jul. 1999. <sup>{2}</sup>
- [4] Wing Kwan Ng, “Energy efficient and secure wireless communication systems,” Doctoral Dissertation, THE UNIVERSITY OF BRITISH COLUMBIA, Vancouver, Canada, Jul. 2012, graduate. [Online]. Available: <https://circle.ubc.ca/handle/2429/42810> <sup>{2}</sup>
- [5] Z. Feng, W. Muqing, and L. Huixin, “Coordinated multi-point transmission and reception for LTE-Advanced,” in *5th International Conference on Wireless Communications, Networking and Mobile Computing, 2009. WiCom '09*. IEEE, Sep. 2009, pp. 1–4. <sup>{2,3,55}</sup>
- [6] D. Lee, H. Seo, B. Clerckx, E. Hardouin, D. Mazzarese, S. Nagata, and K. Sayana, “Coordinated multipoint transmission and reception in LTE-advanced: deployment scenarios and operational challenges,” *Communications Magazine, IEEE*, vol. 50, no. 2, pp. 148 –155, Feb. 2012. <sup>{2,3,4,6,51,80,81}</sup>
- [7] M. Sawahashi, Y. Kishiyama, A. Morimoto, D. Nishikawa, and M. Tanno, “Coordinated multipoint transmission/reception techniques for LTE-advanced [coordinated and distributed MIMO],” *IEEE Wireless Communications*, vol. 17, no. 3, pp. 26–34, Jun. 2010. <sup>{2,3,4,5,54,55,81}</sup>
- [8] M. K. Karakayali, G. J. Foschini, and R. A. Valenzuela, “Network coordination for spectrally efficient communications in cellular systems,” *IEEE Wireless Communications*, vol. 13, no. 4, pp. 56–61, Aug. 2006. <sup>{2}</sup>
- [9] Huawei, “R1-083049 consideration for LTE-Advanced,” Huawei Technologies Co. Ltd., Tech. Rep., 2009. <sup>{2,84}</sup>
- [10] 3GPP, “Evolved universal terrestrial radio access (E-UTRA); further advancements for e-utra physical layer aspects (release 9),” TR 36.814,V9.0.0, Tech. Rep., March, 2010. <sup>{3,4,59,70,81,93}</sup>

- [11] —, “Technical specification group radio access network; coordinated multi-point operation for lte physical layer aspects (release 11),” TR 36.819, V11.1.0, Tech. Rep., December, 2011. {3,5,51,59,81,88,132,144}
- [12] I. F. Akyildiz, D. M. Gutierrez-Estevez, and E. C. Reyes, “The evolution to 4G cellular systems: LTE-Advanced,” *Physical Communication*, vol. 3, no. 4, pp. 217–244, 2010. {4,5,14,31}
- [13] L. Qiang, Y. Yang, F. Shu, and W. Gang, “Coordinated beamforming in downlink CoMP transmission system,” in *2010 5th International ICST Conference on Communications and Networking in China (CHINACOM)*. IEEE, Aug. 2010, pp. 1–5. {5}
- [14] A. Damnjanovic, J. Montojo, Y. Wei, T. Ji, T. Luo, M. Vajapeyam, T. Yoo, O. Song, and D. Malladi, “A survey on 3GPP heterogeneous networks,” *IEEE Wireless Communications*, vol. 18, no. 3, pp. 10–21, Jun. 2011. {6,80}
- [15] Sanjay Kumar, “Techniques for efficient spectrum usage for next generation mobile communication networks (an LTE and LTE-A case study),” Doctoral Dissertation, Aalborg University, Aalborg, Denmark, Jun. 2009. {7}
- [16] Mauro De Sanctis, Ernestina Cianca, and Viraj Joshi, “Energy efficient wireless networks towards green communications,” *Wireless Personal Communications*, vol. 59, no. 3, pp. 537–552, Feb. 2011. [Online]. Available: <http://www.springerlink.com.miman.bib.bth.se/content/e764hq2h2h83081t/> {13}
- [17] G. Fettweis and E. Zimmermann, “ICT energy consumption - trends and challenges,” in *Communications*, 2008, no. Wpmc 2008, pp. 2006–2009. {13}
- [18] Stephen McLaughlin, “Green Radio: The Key Issues,” in *Mobile VCE*, 2008. {13}
- [19] Laurent Hrault, “Green wireless communications,” eMobility, Technical Report, 2008. {13}
- [20] CISCO, “CisCo visual netowrking index: global mobile,” Cisco Systems, Inc., Technical Report, 2010. {13}
- [21] O. Sallent, “A perspective on radio resource management in B3G,” in *3rd International Symposium on Wireless Communication Systems, 2006. ISWCS '06*, 2006, pp. 30–34. {14,19}
- [22] Y. Chen, S. Zhang, S. Xu, and G. Y. Li, “Fundamental trade-offs on green wireless networks,” *IEEE Communications Magazine*, vol. 49, no. 6, pp. 30–37, Jun. 2011. {14,15,27,28,29,105,115}
- [23] B. Badic, T. O’Farrell, P. Loskot, and J. He, “Energy efficient radio access architectures for green radio: Large versus small cell size deployment,” in *Vehicular Technology Conference Fall (VTC 2009-Fall), 2009 IEEE 70th*, Sep. 2009, pp. 1–5. {14,77}
- [24] S. Parkvall, A. Furuskar, and E. Dahlman, “Evolution of LTE toward IMT-advanced,” *IEEE Communications Magazine*, vol. 49, no. 2, pp. 84–91, Feb. 2011. {14,52,135}

- [25] M. Bohge, J. Gross, A. Wolisz, and M. Meyer, "Dynamic resource allocation in OFDM systems: an overview of cross-layer optimization principles and techniques," *IEEE Network*, vol. 21, no. 1, pp. 53–59, Feb. 2007. <sup>{14,30}</sup>
- [26] G. Miao, N. Himayat, Y. Li, and A. Swami, "Cross-layer optimization for energy-efficient wireless communications: a survey," *Wirel. Commun. Mob. Comput.*, vol. 9, no. 4, pp. 529–542, 2009, (Geoffrey). <sup>{15,16,27,30,31,41}</sup>
- [27] L. Xiao-hui, H. Ming, Y. Ke-chu, P. Chang-xing, and L. Nai-an, "Radio resource management algorithm based on cross-layer design for OFDM systems," in *Parallel and Distributed Computing, Applications and Technologies, 2006. PDCAT '06. Seventh International Conference on*, 2006, pp. 311–314. <sup>{15}</sup>
- [28] D. Willkomm, S. Machiraju, J. Bolot, and A. Wolisz, "Primary users in cellular networks: A large-scale measurement study," in *3rd IEEE Symposium on New Frontiers in Dynamic Spectrum Access Networks, 2008. DySPAN 2008*, 2008, pp. 1–11. <sup>{16}</sup>
- [29] J. Gong, S. Zhou, Z. Niu, and P. Yang, "Traffic-aware base station sleeping in dense cellular networks," in *2010 18th International Workshop on Quality of Service (IWQoS)*, Jun. 2010, pp. 1–2. <sup>{16,17,74}</sup>
- [30] E. Oh and B. Krishnamachari, "Energy savings through dynamic base station switching in cellular wireless access networks," in *2010 IEEE Global Telecommunications Conference (GLOBECOM 2010)*, 2010, pp. 1–5. <sup>{16,17}</sup>
- [31] Alcatel-Lucent, "Alcatel-lucent demonstrates up to 27 percent power consumption reduction on base stations deployed by china mobile : Software upgrades can offer exceptional power and cost savings for mobile operators worldwide," in *Technical Report*, Feb. 2009. <sup>{17}</sup>
- [32] Opera-Net, "Optimising power efficiency in mobile radio networks," in *OPERA-NET Project*, vol. 42, 2010. [Online]. Available: <http://opera-net.org/Documents/5026v1Opera-Nete-NEM%20Event%20Barcelona%202010Demos%20Presentation290710.pdf> <sup>{17}</sup>
- [33] M. A. Marsan, L. Chiaraviglio, D. Ciullo, and M. Meo, "Optimal energy savings in cellular access networks," in *IEEE International Conference on Communications Workshops, 2009. ICC Workshops 2009*. IEEE, Jun. 2009, pp. 1–5. <sup>{17,73}</sup>
- [34] P. Grant, MCVE Core 5 Programme, "Green radio -the case for more efficient cellular basestations," in *MCVE*, 2010. <sup>{17}</sup>
- [35] T. Chen, H. Zhang, Z. Zhao, and X. Chen, "Towards green wireless access networks," in *2010 5th International ICST Conference on Communications and Networking in China (CHINACOM)*, 2010, pp. 1–6. <sup>{17}</sup>
- [36] Xiaohu Ge, Chengqian Cao, Minh Jo, Min Chen, Jinzhong Hu, and Iztok Humar, "Energy efficiency modelling and analyzing based on multi-cell and multi-antenna cellular networks," *KSII Transactions on Internet and Information Systems*, vol. 4, no. 4, Aug. 2010. [Online]. Available: <http://www.pubzone.org/dblp/journals/itiis/GeCJCHH10> <sup>{17,79}</sup>

- [37] D. Feng, C. Jiang, G. Lim, J. Cimini, L.J., G. Feng, and G. Li, “A survey of energy-efficient wireless communications,” *IEEE Communications Surveys Tutorials*, vol. 15, no. 1, pp. 167–178, 2013. <sup>{17}</sup>
- [38] F. Meshkati, H. V. Poor, S. C. Schwartz, and R. V. Balan, “Energy-efficient resource allocation in wireless networks with quality-of-service constraints,” *Communications, IEEE Transactions on*, vol. 57, no. 11, pp. 3406–3414, Nov. 2009. <sup>{17}</sup>
- [39] P. Kolios, V. Friderikos, and K. Papadaki, “Ultra low energy store-carry and forward relaying within the cell,” in *Vehicular Technology Conference Fall (VTC 2009-Fall), 2009 IEEE 70th*, 2009, pp. 1–5. <sup>{17}</sup>
- [40] —, “Store carry and forward relay aided cellular networks,” in *Proceedings of the seventh ACM international workshop on Vehicular InterNetworking*, ser. VANET ’10. New York, NY, USA: ACM, 2010, p. 7172. [Online]. Available: <http://doi.acm.org/10.1145/1860058.1860071> <sup>{17}</sup>
- [41] Ana I Prez-Neira and Marc Realp Campalans, *Cross-Layer Resource Allocation In Wireless Communications*. ACADEMIC PRESS, 2009. <sup>{18}</sup>
- [42] L. V. d. Perre, J. Craninckx, and A. Dejonghe, “Energy-aware cross-layer radio management,” in *Green Software Defined Radios*, ser. Integrated Circuits and Systems. Springer Netherlands, 2009, pp. 115–133. [Online]. Available: [http://dx.doi.org/10.1007/978-1-4020-8212-2\\_6](http://dx.doi.org/10.1007/978-1-4020-8212-2_6) <sup>{18}</sup>
- [43] ETSI, “Universal mobile telecommunications system (UMTS); selection procedures for the choice of the radio transmission technologies of the UMTS (UMTS 30.03 version 3.2.0),” *TR 101 112 v3.2.0*, Apr. 1998. <sup>{18}</sup>
- [44] W. Guo and T. O’Farrell, “Green cellular network: Deployment solutions, sensitivity and tradeoffs,” in *Wireless Advanced (WiAd), 2011*, 2011, pp. 42–47. <sup>{19}</sup>
- [45] T. Elkourdi and O. Simeone, “Femtocell as a relay: An outage analysis,” *IEEE Transactions on Wireless Communications*, vol. 10, no. 12, pp. 4204–4213, 2011. <sup>{19}</sup>
- [46] C. Han and S. Armour, “Energy efficient radio resource management strategies for green radio,” *IET Communications*, vol. 5, no. 18, pp. 2629–2639, Dec. 2011. <sup>{20}</sup>
- [47] S. Alamouti, “A simple transmit diversity technique for wireless communications,” *Selected Areas in Communications, IEEE Journal on*, vol. 16, no. 8, pp. 1451–1458, Oct. 1998. <sup>{20}</sup>
- [48] A. Pokhariyal, T. Kolding, and P. Mogensen, “Performance of downlink frequency domain packet scheduling for the UTRAN long term evolution,” in *Personal, Indoor and Mobile Radio Communications, 2006 IEEE 17th International Symposium on*, Sep. 2006, pp. 1–5. <sup>{20}</sup>
- [49] M. Shariat, A. Quddus, S. Ghorashi, and R. Tafazolli, “Scheduling as an important cross-layer operation for emerging broadband wireless systems,” *Communications Surveys & Tutorials, IEEE*, vol. 11, no. 2, pp. 74–86, 2009. <sup>{20,21,22}</sup>

- [50] K. Norlund, T. Ottosson, and A. Brunstrom, "Fairness measures for best effort traffic in wireless networks," in *Personal, Indoor and Mobile Radio Communications, 2004. PIMRC 2004. 15th IEEE International Symposium on*, vol. 4, Sep. 2004, pp. 2953 – 2957 Vol.4. {20}
- [51] S. Schwarz, C. Mehlhruer, and M. Rupp, "Low complexity approximate maximum throughput scheduling for LTE," in *Signals, Systems and Computers (ASILOMAR), 2010 Conference Record of the Forty Fourth Asilomar Conference on*, Nov. 2010, pp. 1563 –1569. {21}
- [52] D. Sabella, M. Caretti, and R. Fantini, "Energy efficiency evaluation of state of the art packet scheduling algorithms for LTE," *Wireless Conference 2011 - Sustainable Wireless Technologies (European Wireless), 11th European*, pp. 1 –4, Apr. 2011. {23}
- [53] C. Han, K. C. Beh, M. Nicolaou, S. Armour, and A. Doufexi, "Power efficient dynamic resource scheduling algorithms for LTE," in *Vehicular Technology Conference Fall (VTC 2010-Fall), 2010 IEEE 72nd.* IEEE, Sep. 2010, pp. 1–5. {23}
- [54] Qixing Wang, Dajie Jiang, Guangyi Liu, and Zhigang Yan, "Coordinated multiple points transmission for LTE-Advanced systems," in *5th International Conference on Wireless Communications, Networking and Mobile Computing, 2009. WiCom '09.* IEEE, Sep. 2009, pp. 1–4. {23,57,89,143}
- [55] K. Huq, S. Mumtaz, J. Rodriguez, and R. Aguiar, "Comparison of energy-efficiency in bits per joule on different downlink CoMP techniques," in *2012 IEEE International Conference on Communications (ICC)*, Jun. 2012, pp. 5716 –5720. {23,76}
- [56] EARTH (Energy Aware Radio and neTwork Technologies) FP7 Project, "Deliverable 3.1: Most promising tracks of green network technologies," EU-FP7 Project, Deliverable D3.1 INFISO-ICT-247733 EARTH, Dec. 2010. [Online]. Available: <https://www.ict-earth.eu/publications/deliverables/deliverables.html> {25,26}
- [57] S. Tombaz, M. Usman, and J. Zander, "Energy efficiency improvements through heterogeneous networks in diverse traffic distribution scenarios," in *Communications and Networking in China (CHINACOM), 2011 6th International ICST Conference on*, Aug. 2011, pp. 708 –713. {25}
- [58] A. Khandekar, N. Bhushan, J. Tingfang, and V. Vanghi, "LTE-Advanced: heterogeneous networks," in *Wireless Conference (EW), 2010 European*, 2010, pp. 978–982. {25}
- [59] J. Andrews, "Interference cancellation for cellular systems: a contemporary overview," *IEEE Wireless Communications*, vol. 12, no. 2, pp. 19–29, 2005. {25}
- [60] C. Chiasserini and R. Rao, "Coexistence mechanisms for interference mitigation in the 2.4-GHz ISM band," *IEEE Transactions on Wireless Communications*, vol. 2, no. 5, pp. 964–975, 2003. {25}
- [61] Mounir Ghogho and Ananthram Swami, "Carrier frequency synchronization for OFDM systems," *Interim Report*, Sep. 2003. {26}

- [62] G. Li, Z. Xu, C. Xiong, C. Yang, S. Zhang, Y. Chen, and S. Xu, "Energy-efficient wireless communications: tutorial, survey, and open issues," *Wireless Communications, IEEE*, vol. 18, no. 6, pp. 28–35, 2011. <sup>{26,31,115}</sup>
- [63] Tao Chen, Yang Yang, Honggang Zhang, Haesik Kim, and K. Horneman, "Network energy saving technologies for green wireless access networks," *Wireless Communications, IEEE*, vol. 18, no. 5, pp. 30–38, Oct. 2011. <sup>{27}</sup>
- [64] Farhad Meshkati, H. Vincent Poor, and Stuart C. Schwartz, "Energy-efficient resource allocation in wireless networks," *IEEE Signal Processing Magazine*, vol. 24, no. 3, pp. 58–68, May 2007. <sup>{27}</sup>
- [65] S. Parkvall and D. Astely, "The evolution of LTE towards IMT-Advanced," *Journal of Communications*, vol. 4, no. 3, Apr. 2009. [Online]. Available: <http://ojs.academypublisher.com/index.php/jcm/article/view/0403146154> <sup>{27,59}</sup>
- [66] Claude Elwood Shannon, "A mathematical theory of communication," *The Bell System Technical Journal*, vol. 27, pp. 379–423, 623–656, 1948. <sup>{28,40}</sup>
- [67] D. N. Hatfield, "Measures of spectral efficiency in land mobile radio," in *25th IEEE Vehicular Technology Conference, 1975*, vol. 25. IEEE, Jan. 1975, pp. 23–26. <sup>{28}</sup>
- [68] W. Lee, "Spectrum efficiency in cellular [radio]," *Vehicular Technology, IEEE Transactions on*, vol. 38, no. 2, p. 6975, 1989. <sup>{28}</sup>
- [69] Hyuck M. Kwon and Theodore G. Birdsall, "Channel capacity in bits per joule," *IEEE Journal of Oceanic Engineering*, vol. 11, no. 1, pp. 97–99, Jan. 1986. <sup>{28,52,105,141}</sup>
- [70] C. Xiong, G. Y. Li, S. Zhang, Y. Chen, and S. Xu, "Energy- and spectral-efficiency tradeoff in downlink OFDMA networks," *IEEE Transactions on Wireless Communications*, vol. 10, no. 11, pp. 3874–3886, Nov. 2011. <sup>{30,31,32,33,35,41,44,48,64,96}</sup>
- [71] G. Miao, N. Himayat, Y. Li, and D. Bormann, "Energy efficient design in wireless OFDMA," in *Communications, 2008. ICC '08. IEEE International Conference on*, May 2008, pp. 3307–3312. <sup>{31,41}</sup>
- [72] A. Akbari, R. Hoshyar, and R. Tafazolli, "Energy-efficient resource allocation in wireless OFDMA systems," in *2010 IEEE 21st International Symposium on Personal Indoor and Mobile Radio Communications (PIMRC)*. IEEE, Sep. 2010, pp. 1731–1735. <sup>{32}</sup>
- [73] M. Chiang, S. Low, A. Calderbank, and J. Doyle, "Layering as optimization decomposition: A mathematical theory of network architectures," *Proceedings of the IEEE*, vol. 95, no. 1, pp. 255–312, Jan. 2007. <sup>{35}</sup>
- [74] K. Seong, M. Mohseni, and J. M. Cioffi, "Optimal resource allocation for OFDMA downlink systems," in *2006 IEEE International Symposium on Information Theory*. IEEE, Jul. 2006, pp. 1394–1398. <sup>{35}</sup>
- [75] X. Zhou, G. Y. Li, D. Li, D. Wang, and A. C. Soong, "Probabilistic resource allocation for opportunistic spectrum access," *IEEE Transactions on Wireless Communications*, vol. 9, no. 9, pp. 2870–2879, Sep. 2010. <sup>{35}</sup>

- [76] R. Cheng and S. Verd, "Gaussian multiaccess channels with ISI: capacity region and multiuser water-filling," *Information Theory, IEEE Transactions on*, vol. 39, no. 3, pp. 773–785, 1993. <sup>{35}</sup>
- [77] M. K. Karray, "Spectral and energy efficiencies of OFDMA wireless cellular networks," in *Wireless Days (WD), 2010 IFIP*. IEEE, Oct. 2010, pp. 1–5. <sup>{36,41,115}</sup>
- [78] O. Arnold, F. Richter, G. Fettweis, and O. Blume, "Power consumption modeling of different base station types in heterogeneous cellular networks," in *Future Network and Mobile Summit, 2010*. IEEE, Jun. 2010, pp. 1–8. <sup>{36,73}</sup>
- [79] C. Isheden and G. P. Fettweis, "Energy-efficient multi-carrier link adaptation with sum rate-dependent circuit power," in *2010 IEEE Global Telecommunications Conference (GLOBECOM 2010)*. IEEE, Dec. 2010, pp. 1–6. <sup>{36}</sup>
- [80] G. Miao, N. Himayat, G. Li, A. Koc, and S. Talwar, "Interference-aware energy-efficient power optimization," in *Communications, 2009. ICC '09. IEEE International Conference on*, Jun. 2009, pp. 1–5. <sup>{38}</sup>
- [81] C. He, B. Sheng, P. Zhu, and X. You, "Energy efficiency and spectral efficiency tradeoff in downlink distributed antenna systems," *IEEE Wireless Communications Letters*, vol. 1, no. 3, pp. 153–156, Jun. 2012. <sup>{41,46}</sup>
- [82] L. Liu, R. Chen, S. Geirhofer, K. Sayana, Z. Shi, and Y. Zhou, "Downlink MIMO in LTE-advanced: SU-MIMO vs. MU-MIMO," *Communications Magazine, IEEE*, vol. 50, no. 2, pp. 140–147, Feb. 2012. <sup>{42,80,81}</sup>
- [83] Q. Spencer, A. Swindlehurst, and M. Haardt, "Zero-forcing methods for downlink spatial multiplexing in multiuser MIMO channels," *IEEE Transactions on Signal Processing*, vol. 52, no. 2, pp. 461–471, Feb. 2004. <sup>{42}</sup>
- [84] R. L. Batista, R. B. dos Santos, T. F. Maciel, W. C. Freitas, and F. R. Cavalcanti, "Performance evaluation for resource allocation algorithms in CoMP systems," in *Vehicle Technology Conference Fall (VTC 2010-Fall), 2010 IEEE 72nd*. IEEE, Sep. 2010, pp. 1–5. <sup>{43}</sup>
- [85] Stefania Sesia, Issam Toufik, and Matthew Baker, *LTE - the UMTS long term evolution: from theory to practice ; [Including release 10 for LTE-advanced]*. Chichester: Wiley, 2011. <sup>{43,68,135}</sup>
- [86] C. Y. Wong, R. S. Cheng, K. B. Lataief, and R. D. Murch, "Multiuser OFDM with adaptive subcarrier, bit, and power allocation," *IEEE Journal on Selected Areas in Communications*, vol. 17, no. 10, pp. 1747–1758, Oct. 1999. <sup>{43,66}</sup>
- [87] J. Jang and K.-B. Lee, "Transmit power adaptation for multiuser OFDM systems," *IEEE Journal on Selected Areas in Communications*, vol. 21, no. 2, pp. 171–178, 2003, 01211. <sup>{43}</sup>
- [88] C. Li, H. Xiong, J. Zou, and Z. He, "Joint source and flow optimization for scalable video multirate multicast over hybrid Wired/Wireless coded networks," *IEEE Transactions on Circuits and Systems for Video Technology*, vol. 21, no. 5, pp. 550–564, May 2011. <sup>{44,100,106,110}</sup>

- [89] S. Boyd and L. Vandenberghe, *Convex Optimization*. Cambridge University Press, Mar. 2004. <sup>{45,106}</sup>
- [90] 3GPP, “Spatial channel model for mimo simulations,” TR 25.996, V6.1.0, Tech. Rep., September, 2003. <sup>{47,59,133}</sup>
- [91] R. K. Sundaram, *A First Course in Optimization Theory*. Cambridge University Press, Jun. 1996. <sup>{48}</sup>
- [92] D. Cao, S. Zhou, C. Zhang, and Z. Niu, “Energy saving performance comparison of coordinated multi-point transmission and wireless relaying,” in *2010 IEEE Global Telecommunications Conference (GLOBECOM 2010)*. IEEE, Dec. 2010, pp. 1–5. <sup>{51}</sup>
- [93] P. Kela, J. Puttonen, N. Kolehmainen, T. Ristaniemi, T. Henttonen, and M. Moisio, “Dynamic packet scheduling performance in UTRA long term evolution downlink,” in *Wireless Pervasive Computing, 2008. ISWPC 2008. 3rd International Symposium on*, May 2008, pp. 308–313. <sup>{51}</sup>
- [94] Y. Chen, S. Zhang, and S. Xu, “Characterizing energy efficiency and deployment efficiency relations for green architecture design,” in *Communications Workshops (ICC), 2010 IEEE International Conference on*, May 2010, pp. 1–5. <sup>{52,60,141}</sup>
- [95] Tao Chen, Haesik Kim, and Yang Yang, “Energy efficiency metrics for green wireless communications,” in *2010 International Conference on Wireless Communications and Signal Processing (WCSP)*. IEEE, Oct. 2010, pp. 1–6. <sup>{52,141}</sup>
- [96] R. Wang, J. Thompson, and H. Haas, “A novel time-domain sleep mode design for energy-efficient LTE,” in *Communications, Control and Signal Processing (ISCCSP), 2010 4th International Symposium on*, Mar. 2010, pp. 1–4. <sup>{53,87,88,135}</sup>
- [97] G. Cao, D. Yang, X. Zhu, and X. Zhang, “A joint resource allocation and power control algorithm for heterogeneous network,” in *2012 19th International Conference on Telecommunications (ICT)*, Apr. 2012, pp. 1–5. <sup>{53}</sup>
- [98] S. Mumtaz, L. T. Tu, K. Saidul, and A. Gameiro, “Calibration and evaluation of fixed and mobile relay-based system level simulator,” *J. Comp. Sys., Netw., and Comm.*, vol. 2010, p. 2:12:14, Jan. 2010. [Online]. Available: <http://dx.doi.org/10.1155/2010/149257> <sup>{56,58,138}</sup>
- [99] S. Mumtaz, D. Yang, V. Monteiro, C. Politis, and J. Rodriguez, “Self organized energy efficient position aided relays in LTEA,” *Physical Communication*, vol. 7, no. 0, 2012. [Online]. Available: <http://www.sciencedirect.com/science/article/pii/S1874490712000377> <sup>{56,58,138}</sup>
- [100] Christian Mehlführer, Martin Wrulich, Josep Colom Ikuno, Dagmar Bosanska, and Markus Rupp, “Simulating the long term evolution physical layer,” in *European Signal Processing Conference (EUSIPCO)*, 2009, pp. 1471–1478. <sup>{57,131}</sup>
- [101] 3GPP, “Evolved universal terrestrial radio access (e-utra); physical layer procedures (release 11),” TS 36.213, V11.0.0, Tech. Rep., October 2012. <sup>{57,59,76,135}</sup>

- [102] Christian Mehlführer, Josep Colom Ikuno, Michal imko, Stefan Schwarz, Martin Wrulich, and Markus Rupp, “The vienna LTE simulators - enabling reproducibility in wireless communications research,” *EURASIP Journal on Advances in Signal Processing*, vol. 2011, no. 1, p. 29, Jul. 2011. [Online]. Available: <http://asp.eurasipjournals.com/content/2011/1/29/abstract> {58,131,143}
- [103] R. Batista, Y. Silva, E. Stancanelli, and F. Cavalcanti, “Radio resource allocation strategies for multi-antenna CoMP systems,” in *2012 International Symposium on Wireless Communication Systems (ISWCS)*, Aug. 2012, pp. 840–844. {58}
- [104] X. Zhang, J. Zhang, Y. Huang, and W. Wang, “On the study of fundamental trade-offs between QoE and energy efficiency in wireless networks,” *Transactions on Emerging Telecommunications Technologies*, vol. 24, no. 3, p. 259265, 2013. [Online]. Available: <http://onlinelibrary.wiley.com/doi/10.1002/ett.2640/abstract> {64}
- [105] J. Song, G.-T. Gil, and D.-H. Kim, “Packet-scheduling algorithm by the ratio of transmit power to the transmission bits in 3GPP LTE downlink,” *EURASIP Journal on Wireless Communications and Networking*, vol. 2010, no. 1, p. 251281, Jul. 2010. [Online]. Available: <http://jwcn.eurasipjournals.com/content/2010/1/251281> {65,66}
- [106] Albert W. Marshall, Ingram Olkin, and Barry C. Arnold, *Inequalities: Theory of Majorization and Its Applications*, 2nd ed., ser. Springer Series in Statistics. Springer, 2011, 00021. [Online]. Available: <http://www.springer.com/statistics/statistical+theory+and+methods/book/978-0-387-40087-7> {69}
- [107] H. Shi and H. Sethu, “Greedy fair queueing: a goal-oriented strategy for fair real-time packet scheduling,” in *24th IEEE Real-Time Systems Symposium, 2003. RTSS 2003*, 2003, pp. 345–356. {69,141}
- [108] C. Bontu and E. Illidge, “DRX mechanism for power saving in LTE,” *IEEE Communications Magazine*, vol. 47, no. 6, pp. 48–55, Jun. 2009. {73}
- [109] D. Xenakis, N. Passas, and C. Verikoukis, “A novel handover decision policy for reducing power transmissions in the two-tier LTE network,” in *2012 IEEE International Conference on Communications (ICC)*, 2012, pp. 1352–1356. {75}
- [110] 3GPP, “Technical specification group radio access network; evolved universal terrestrial radio access (e-utra); potential solutions for energy saving for e-utran (release 10),” TR 36.927,V10.0.0, Tech. Rep., September 2011. {79}
- [111] G. Miao, N. Himayat, and G. Y. Li, “Energy-efficient link adaptation in frequency-selective channels,” *IEEE Transactions on Communications*, vol. 58, no. 2, pp. 545–554, Feb. 2010. {79}
- [112] E. V. Belmega and S. Lasaulce, “An information-theoretic look at MIMO energy-efficient communications,” in *Proceedings of the Fourth International ICST Conference on Performance Evaluation Methodologies and Tools*, ser. VALUETOOLS ’09. ICST, Brussels, Belgium, Belgium: ICST (Institute for Computer Sciences, Social-Informatics and Telecommunications Engineering), 2009, p. 58:158:10. [Online]. Available: <http://dx.doi.org/10.4108/ICST.VALUETOOLS2009.7497> {79}

- [113] European Commission, “ICT for Energy Efficiency,” *Ad-Hoc Advisory Group Report*, 24-10-2008. <sup>{80}</sup>
- [114] J. Lee, J.-K. Han, and J. Zhang, “MIMO technologies in 3GPP LTE and LTE-Advanced,” *EURASIP Journal on Wireless Communications and Networking*, vol. 2009, no. 1, p. 302092, Jul. 2009. [Online]. Available: <http://jwcn.eurasipjournals.com/content/2009/1/302092> <sup>{80}</sup>
- [115] D. Gesbert, M. Kountouris, R. W. Heath, C.-B. Chae, and T. Salzer, “Shifting the MIMO paradigm,” *IEEE Signal Processing Magazine*, vol. 24, no. 5, pp. 36–46, Sep. 2007. <sup>{80,81,85}</sup>
- [116] H. Sun, W. Fang, J. Liu, and Y. Meng, “Performance evaluation of CS/CB for coordinated multipoint transmission in LTE-A downlink,” in *2012 IEEE 23rd International Symposium on Personal Indoor and Mobile Radio Communications (PIMRC)*, Sep. 2012, pp. 1061–1065. <sup>{81,83}</sup>
- [117] Y. Jiang, M. Varanasi, and J. Li, “Performance analysis of ZF and MMSE equalizers for MIMO systems: An in-depth study of the high SNR regime,” *IEEE Transactions on Information Theory*, vol. 57, no. 4, pp. 2008–2026, Apr. 2011. <sup>{81,85}</sup>
- [118] M. Vu and A. Paulraj, “MIMO wireless linear precoding,” *IEEE Signal Processing Magazine*, vol. 24, no. 5, pp. 86–105, Sep. 2007. <sup>{81}</sup>
- [119] Hu Wang, “LTE-Advanced development progress,” Huawei Technologies Co. Ltd., TTA IMT-Advanced Workshop, Tech. Rep., Sep. 2009. <sup>{84}</sup>
- [120] H. Zhang and H. Dai, “Cochannel interference mitigation and cooperative processing in downlink multicell multiuser MIMO networks,” *EURASIP Journal on Wireless Communications and Networking*, vol. 2004, no. 2, p. 202654, Dec. 2004. [Online]. Available: <http://jwcn.eurasipjournals.com/content/2004/2/202654> <sup>{85,147}</sup>
- [121] L. Liu, J. C. Zhang, J.-C. Yu, and J. Lee, “Intercell interference coordination through limited feedback,” *International Journal of Digital Multimedia Broadcasting*, vol. 2010, pp. 1–7, 2010. [Online]. Available: <http://www.hindawi.com/journals/ijdmb/2010/134919/> <sup>{85}</sup>
- [122] Ssu-Han Lu and Li-Chun Wang, “Base station cooperation techniques of heterogeneous network in 4G wireless systems,” *Mobile Communications and Cloud Computing Lab, NCTU, Taiwan*, August 2012. <sup>{85,87}</sup>
- [123] A. Papadogiannis, H. Bang, D. Gesbert, and E. Hardouin, “Downlink overhead reduction for multi-cell cooperative processing enabled wireless networks,” in *IEEE 19th International Symposium on Personal, Indoor and Mobile Radio Communications, 2008. PIMRC 2008*, Sep. 2008, pp. 1–5. <sup>{90,91}</sup>
- [124] J. Li, H. Zhang, X. Xu, X. Tao, T. Svensson, C. Botella, and B. Liu, “A novel frequency reuse scheme for coordinated multi-point transmission,” in *Vehicular Technology Conference (VTC 2010-Spring), 2010 IEEE 71st*. IEEE, May 2010, pp. 1–5. <sup>{93}</sup>

- [125] G. Boudreau, J. Panicker, N. Guo, R. Chang, N. Wang, and S. Vrzic, "Interference coordination and cancellation for 4G networks," *Communications Magazine, IEEE*, vol. 47, no. 4, pp. 74–81, Apr. 2009. <sup>{93}</sup>
- [126] W. Wang and G. Shen, "Energy efficiency of heterogeneous cellular network," in *Vehicular Technology Conference Fall (VTC 2010-Fall), 2010 IEEE 72nd*, Sep. 2010, pp. 1–5. <sup>{93,94,96}</sup>
- [127] F. Richter, A. Fehske, and G. Fettweis, "Energy efficiency aspects of base station deployment strategies for cellular networks," in *Vehicular Technology Conference Fall (VTC 2009-Fall), 2009 IEEE 70th*, Sep. 2009, pp. 1–5. <sup>{100,102,107}</sup>
- [128] 3GPP, "SAE architecture revisit and technical review," Transmission System Aspects, Technical Report, 2007. <sup>{100}</sup>
- [129] S. Tombaz, P. Monti, K. Wang, A. Vastberg, M. Forzati, and J. Zander, "Impact of backhauling power consumption on the deployment of heterogeneous mobile networks," in *2011 IEEE Global Telecommunications Conference (GLOBECOM 2011)*, 2011, pp. 1–5. <sup>{101,103,107,108}</sup>
- [130] P. Monti, S. Tombaz, L. Wosinska, and J. Zander, "Mobile backhaul in heterogeneous network deployments: Technology options and power consumption," in *2012 14th International Conference on Transparent Optical Networks (ICTON)*, 2012, pp. 1–7. <sup>{103,104,105,107}</sup>
- [131] W. Yu and R. Lui, "Dual methods for nonconvex spectrum optimization of multicarrier systems," *IEEE Transactions on Communications*, vol. 54, no. 7, pp. 1310–1322, Jul. 2006. <sup>{107}</sup>
- [132] Z. Shen, J. Andrews, and B. Evans, "Optimal power allocation in multiuser OFDM systems," in *IEEE Global Telecommunications Conference, 2003. GLOBECOM '03*, vol. 1, Dec. 2003, pp. 337–341 Vol.1. <sup>{110}</sup>
- [133] S. Cui, A. Goldsmith, and A. Bahai, "Energy-efficiency of MIMO and cooperative MIMO techniques in sensor networks," *Selected Areas in Communications, IEEE Journal on*, vol. 22, no. 6, pp. 1089–1098, Aug. 2004. <sup>{115}</sup>
- [134] O. Onireti, F. Heliot, and M. Imran, "On the energy efficiency-spectral efficiency trade-off in the uplink of CoMP system," *IEEE Transactions on Wireless Communications*, vol. PP, no. 99, pp. 1–6, 2011. <sup>{115}</sup>
- [135] R. Madan, N. Mehta, A. Molisch, and J. Zhang, "Energy-efficient cooperative relaying over fading channels with simple relay selection," *Wireless Communications, IEEE Transactions on*, vol. 7, no. 8, pp. 3013–3025, Aug. 2008. <sup>{115}</sup>
- [136] F. Wang, A. Ghosh, C. Sankaran, P. Fleming, F. Hsieh, and S. Benes, "Mobile WiMAX systems: performance and evolution," *IEEE Communications Magazine*, vol. 46, no. 10, pp. 41–49, 2008. <sup>{136}</sup>
- [137] D. Chase, "Code Combining - A maximum-likelihood decoding approach for combining an arbitrary number of noisy packets," *IEEE Transactions on Communications*, vol. 33, no. 5, pp. 385–393, 1985. <sup>{136}</sup>

- [138] Du Jiu-hui, Li Yong, and Wang Wen-bo, “Investigation on traffic modeling and its applications in wireless communication simulations,” in *IEEE International Symposium on Microwave, Antenna, Propagation and EMC Technologies for Wireless Communications, 2005. MAPE 2005*, vol. 2, 2005, pp. 1472–1475 Vol. 2. <sup>{138}</sup>
- [139] F. A. Cowell, *Measuring Inequality: Techniques for the Social Sciences*. Wiley, 1977. <sup>{141}</sup>
- [140] T. R. Lakshmana, “Dynamic coordinated multipoint transmission schemes,” Master Thesis, Forskningspublikationer frn Chalmers Tekniska Hgskola., Chalmers Publication Library (CPL)., 2010. [Online]. Available: <http://publications.lib.chalmers.se/publication/125971> <sup>{147}</sup>
- [141] T. R. Lakshmana, C. Botella, T. Svensson, X. Xu, J. Li, and X. Chen, “Partial joint processing for frequency selective channels,” in *Vehicular Technology Conference Fall (VTC 2010-Fall), 2010 IEEE 72nd*. IEEE, Sep. 2010, pp. 1–5. <sup>{147}</sup>

## Appendix A

# System Level Simulator for 4G Networks

*This chapter intends to guide the reader with the system level simulation methodology and tool that is used in this thesis. Performance metrics to test the algorithms, and new simulation library modules that were developed are also discussed.*

### A.1 Introduction

Typically, network simulations are divided into two parts: link level and system level simulation (SLS). Although a single simulator approach would be preferred, the complexity of such a simulator (including all aspects from transmitted waveforms to multi-cell network) is far too high with the required simulation resolution. Also, the time granularity of both domains are dramatically different: link level bit transmissions are in the order of milliseconds (ms), while at the system level traffic and mobility models require time intervals in the order of seconds to minutes. Therefore, separating link-level and system-level simulations is a necessity.

In SLS, two different types of simulations can be performed: Combined Snapshot-Dynamic mode or a Fully Dynamic mode. In the fully dynamic mode, mobility and handover are enabled, whilst path loss, fast and slow fading are re-computed at every Transmission Time Interval (TTI). In combined Snapshot Dynamic mode, mobility and handover are not enabled. Mobiles are randomly deployed in every TTI, path loss and slow fading are computed once at the beginning of each TTI. It is worth to mention that we use a combined snapshot-dynamic mode for our simulations.

### A.2 Link to System Interface mapping

The SLS interfaces with the link level simulator (MATLAB-based downlink link level simulator from the Vienna University [102, 100]) through Look up tables (LUTs). Link level simulations are done by assuming single cell and multiple users. In the link level simulator, we deploy different transmission schemes for CoMP i.e. DPS, JT, and CS/CB. These transmission schemes are then simulated using frequency selective channel and with different coding and modulation schemes. The output of the link level simulator is in the form of LUTs, which reflect the function of SNR vs. BLER (block error rate) performance curves. In

practice, we have 3 different LUTs used for [11] three different CoMP transmissions which are then fed to the system level simulation platform. The system level simulator then computes the successfully transmitted packets given the mobility, traffic and channel profiles employed.

### A.3 Deployment Scenario

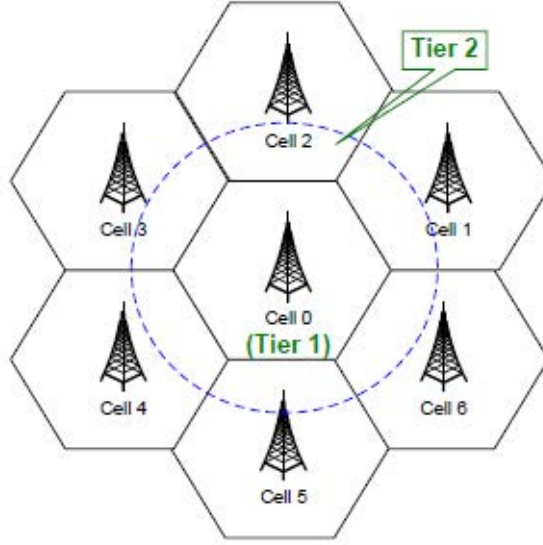


Figure A.1: Omnidirectional-hexagonal Layout

Each base station can be configured with one sector (omni-directional antenna pattern, see Figure A.1) or with three sectors/cells (directional antenna pattern, see Figure A.2). The number of tiers included in the simulation can also be adjusted as well as the frequency reuse pattern.

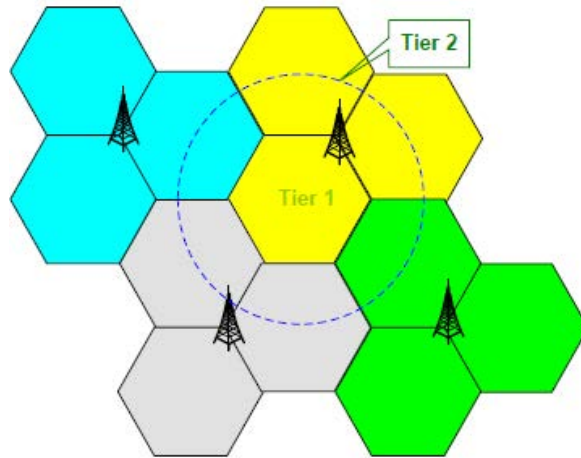


Figure A.2: Sectorized hexagonal Layout

In both modes, mobiles are randomly uniformly distributed over a hexagonal network of base stations. Each base station can be configured with one sector (omni-directional antenna pattern) or with three sectors/cells (directional antenna pattern). All system level simulations conducted in this work were performed assuming an urban environment model. The simulated network constitutes 57 sectors (19 base stations with 3 sectors each), composing a 3 tier hexagonal cellular network layout (see Figure A.3)

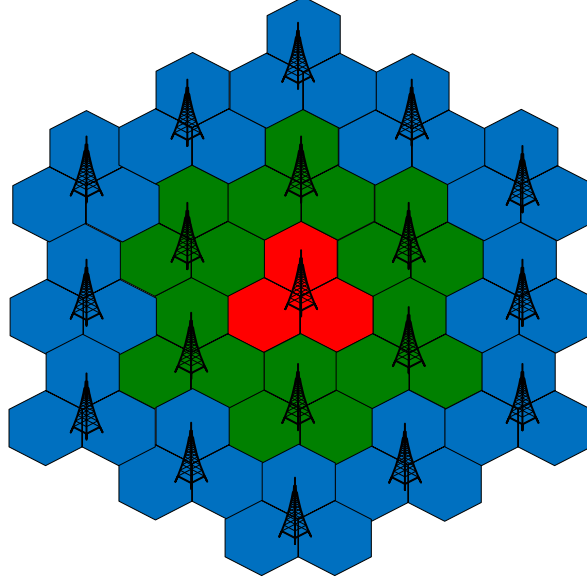


Figure A.3: System model of LTE networks

## A.4 Channel Modeling

There are different methods for modeling the MIMO channel at the system level. These methods are grouped into two different categories:

**Ray-based:** the channel coefficient between each transmit and receive antenna pair is the summation of all rays at each tap of the multi-path filter at each time instant, according to the antenna configuration, gain pattern, angle of arrival (AoA) and angle of departure (AoD) of each ray. The temporal channel variation depends on the traveling speed and direction relative to the AoA/AoD of each ray.

**Correlation based:** The MIMO channel coefficients at each tap are mathematically generated according to independent and identically distributed Gaussian, random variables, the antenna correlation and the temporal correlation, correspond to a particular Doppler spectrum.

**3GPP Spatial Channel Model:** In this model the channel gain between each pair of antennas at both ends of the communication link, results from the superposition of the contributions from each individual path of the tapped delay line model. All simulations are conducted by using 3GPP Spatial Model. More details about this channel model can be found in [90].

The derivation of SINR, given a MIMO channel is performed in two separate parts detailed in [90]: When computing the interference for the SINR calculation, three sources of

interference are considered as shown in Figure A.4.

1. Near strong cells termed as list A, whose interference is modeled by a MIMO channel.
2. Near weak cells termed as list B, whose interference is modeled as wideband (frequency-selective) channel.
3. Far Cells termed as list C, whose interference are modeled as narrowband (flat) channel

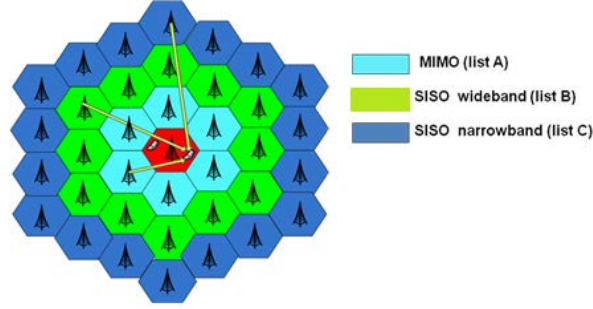


Figure A.4: MIMO Modeling

## A.5 Link Adaptation

The proper transmission mode (modulation and code scheme used-MCS) is defined by the link adaptation method. We have considered 6 MCS schemes (encompassing QPSK, 16 QAM, and 64 QAM modulation schemes) and the Convolutional encoder, according to the profiles envisioned by the 3GPP LTE. For each selected user in each allocated resource, the MCS scheme to be used is chosen according to the following method:

$$i = \max_{i \in MCS_{set}} [(R_i (1 - BLER_i))] \quad (A.1)$$

where  $MCS_{set}$  is the set of modulation and coding schemes,  $R_i$  is the throughput achieved for the MCS scheme and  $BLER_i$  is the predicted BLER for the MCS scheme. Adaptive modulation and coding (AMC) is utilized, and a possible example of the modulation and coding schemes (MCSs) given in LTE is listed in Table A.1, as the bit error rate requirement is set to  $10^{-5}$ . In the case that the perceived SINR at the receiver cannot satisfy the lowest SINR threshold, that is 0 dB, no service can be provided, which is denoted as MCS level 0.

## A.6 Resource allocation

We now briefly describe how resource allocation is handled in LTE, clarifying how it is modeled in the simulator. The scheduler is in charge of generating specific structures called Data Control Indication (DCI) which are then transmitted by the PHY of the eNB to the connected UEs, in order to inform them of the resource allocation on a per subframe basis. By doing this in the downlink direction, the scheduler has to fill some specific fields of the DCI structure with all the information, such as: Modulation and Coding Scheme (glossMCS)

Table A.1: Modulation and coding schemes-20 MHz

MCS level	Modulation	Code rate	Bits per symbol	SINR (dB)	Data Rate (Mbps)
1	QPSK	0.5	1	9.42	8.4
2	QPSK	0.75	1.5	11.8	12.6
3	16QAM	0.5	2	16.6	33.6
4	16QAM	0.75	3	18.9	50.4
5	64QAM	0.5	3	22.6	50.4
6	64QAM	0.75	4.5	24.4	75.6

to be used, MAC Transport Block (TB) size, and the allocation bitmap which identifies which PRBs will contain the data transmitted by the eNB to each user.

For the mapping of resources to physical PRBs, we adopt a localized mapping approach [85]; hence in a given subframe each RB is always allocated to the same user in both slots. The allocation bitmap can be coded in different formats; in this implementation, we considered the Allocation Type 0 defined in [101], according to which the RBs are grouped in Resource Block Groups (RBG) of different size determined as a function of the transmission bandwidth configuration in use.

For certain bandwidth values, not all the PRBs are usable, since the group size is not a common divisor of the group. This is for instance the case when the bandwidth is equal to 25 RBs, which results in a RBG size of 2 RBs, and therefore 1 RB will not be addressable. In the uplink the format of the DCIs is different, since only adjacent RBs can be used because of the SC-FDMA modulation. As a consequence, all RBs can be allocated by the eNB regardless of the bandwidth configuration.

#### A.6.1 LTE-A Frame Architecture

The general frame structure for LTE-FDD [24] is shown in Figure A.5. The time duration of one LTE FDD frame is 10 ms which subdivide into 10 subframes, each 1 ms of duration. In LTE, the Transmission Time Interval (TTI) is equal to 1 subframe. These subframes are further divided into slots of 0.5 ms duration.

So, each subframe contains 2 slots. The slot is the tiniest time-frequency unit for downlink transmission and is called a Physical Resource Block (PRB). Data is allocated to each user in units of PRB. Each PRB spans 12 consecutive sub-carriers at a sub-carrier spacing of 15 kHz, and 7 consecutive symbols over a slot duration of 0.5ms. Thus, a PRB has 84 resource elements ( $12 \text{ sub-carriers} \times 7 \text{ symbols}$ ) corresponding to one slot in the time domain and 180 kHz ( $12 \text{ sub-carriers} \times 15 \text{ kHz spacing}$ ) in the frequency domain. Each user assigns one or more slot according to their traffic demand in time and frequency domain. The size of a PRB is the same for all bandwidths; therefore, the number of available PRBs depends on the transmission bandwidth. In the frequency domain, the number of available PRBs can range from 6 (when transmission bandwidth is 1.4 MHz) to 100 (when transmission bandwidth is 20 MHz). It should be keep in mind that we consider 40% of signaling overhead in each TTI (i.e., first 3 symbols [96]) We adopted a basic LTE FDD frame structure for our dissertation purpose. For the sake of simplicity, we explain the frame of each of the three CoMP techniques on the basis of 1.4 MHz transmission bandwidth which consist of 6 PRBs.

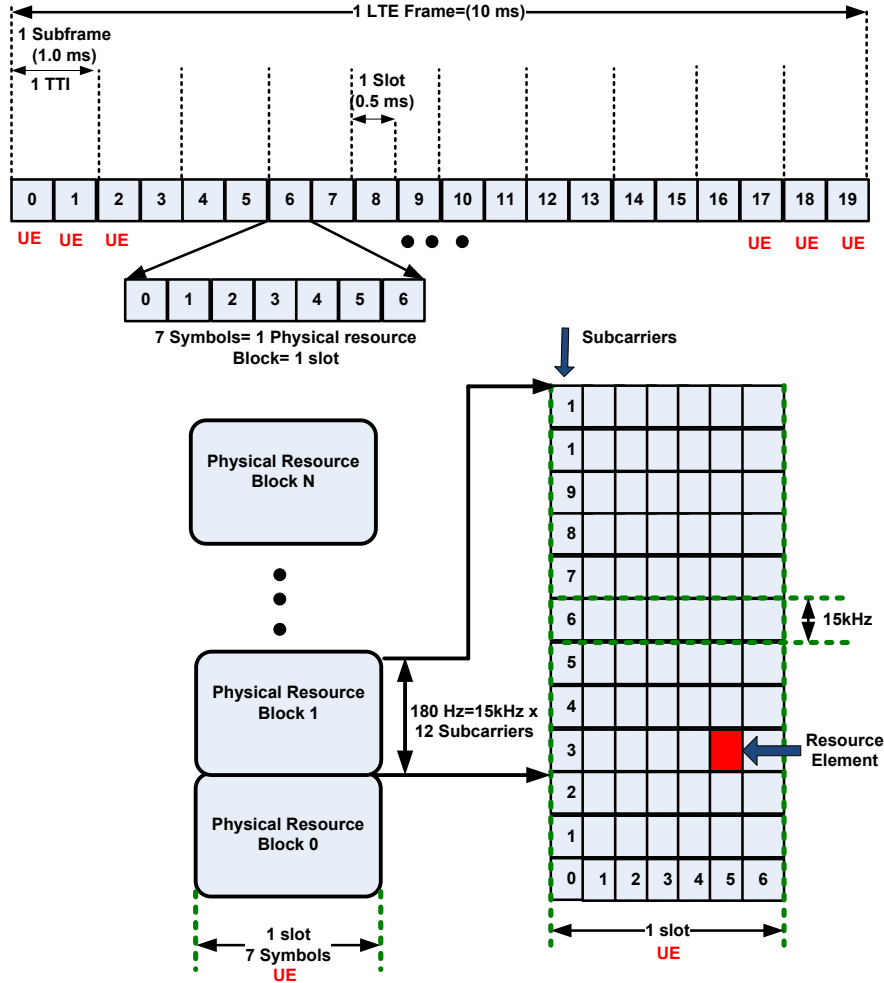


Figure A.5: LTE Frame Architecture with PRB allocation

## A.7 Hybrid Automatic Repeat Request (HARQ)

The number of slots forming the data burst used in the transmission of a given medium access control layer protocol data unit (MPDU) depends on its size and on the selected MCS scheme. HARQ targets error recovery, where soft combining of information associated with new and previous erroneous transmissions is carried out in order to minimize the amount of redundant information and power transmitted over the air interface [136, 137]. According to this mechanism, each MPDU being transmitted for the first time is then mapped into one of the available HARQ processes, for simultaneous transmissions from the same user. Each HARQ process is in charge of the transmission and re-transmissions of a single MPDU until it is successfully received, and is associated to one buffer in the mobile station to store the result of the combination of successive versions of the same MPDU. On the reception of each version, the mobile station combines the current version with previous ones of the same MPDU using Chase Combining [137]. Retransmissions of the same MPDU keep the original MCS scheme used in the first transmission attempt.

Once an HARQ process has been selected for transmission, the scheduler must wait for

an ACK/NACK message from the mobile station before selecting the HARQ process again. HARQ buffers are freed when the radio block is successfully received or when the maximum number of allowed transmission attempts has been achieved. Due to the time required for signaling feedback and processing of the information at both ends of the transmission chain, the minimum time interval between two successive transmissions of a particular HARQ process is equal to two frame periods. In the uplink sub-frame there is an HARQ Acknowledge (HARQ ACK) channel region for the inclusion of one or more ACK channels(s) for HARQ support. This UL-ACK channel is implicitly assigned to each HARQ-enabled DL burst according to its order in the DL-MAP. Thus, the user can quickly transmit ACK or NACK feedback messages for DL HARQ-enabled bursts using this UL ACK channel.

## A.8 Packet Scheduler

Packet schedulers must be designed properly to be reactive to changes in the channel and traffic patterns, in order to respond fast to deviations from the requested QoS of even the most delay sensitive applications. The scheduler is located inside each base station to enable rapid response to traffic requirements and channel conditions. As data packets are associated to service flows with well- defined QoS requirements, the scheduler can correctly determine the packet transmission ordering through the air interface. Packets must be given priority according to the set of QoS metrics which have been negotiated between the network service provider and the end user. At each frame period, the scheduler provides transmission opportunities to eligible mobiles with data to send, starting with the highest ranked user and then proceeding to lower ranked ones in sequence. The CQI reports are obtained from every user on a frame-by-frame basis and the scheduler re-computes the mobiles access priority at every frame period.

## A.9 Traffic Modeling

The application traffic models are categorized into two types of traffic modeling: foreground and background traffic. The foreground traffic model represents a specific user behavior or interaction with a device, whilst the background traffic is not directly related to a user interaction. Traffic models are represented for both user level and IP packet level. The usage of these two levels of model is the following:

### A.9.1 User Level Traffic Model

This type of traffic models the user behavior interaction in an application. It is used with simulations which include detailed application layer, transport layer and IP layer model on top of the physical and MAC layer models. Application performance metrics specific to the application can be evaluated and a scheduling mechanism for the application of QoS in the MAC layer can be evaluated.

### A.9.2 IP packet level traffic model

This type of traffic model is generally obtained from a network traffic measurement and is represented as statistical packet distributions, such as packet size distribution and packet

Table A.2: Traffic parameter used for mixed class traffic in the simulator [138]

Typical Services	VOIP	Video	WWW	FTP
QoS Class	Conversational	Streaming	Interactive	Background
Meaning of session	Call	Video	Web Browsing	File Download
Session rate /(hour)	Exponential (5)	Exponential (2)	Exponential (5)	Exponential (5)
Meaning of packet call	Active Period	Frame	Web page	File
Packet call number	Geometric (24)*	Geometric (50)	Geometric (5)	Constant (1)
Packet call interval (s)	Geometric (3)	Constant (0.1)	Geometric (5)	-
Packet number	Geometric (120)	Constant (8)	Geometric (25)	Lognormal (2e6,4e12) <sup>†</sup>
Packet interval (ms)	Constant (10)	Cut-off Pareto (2.5,1.2)	Geometric (125)	Geometric (30)
Packet size (byte)	Constant (50)	Cut-off Pareto (18,1.2)	Cut-off Pareto (81.5,1.2)	Constant (480)
Bandwidth (kbps)	40	64	32	128

inter-arrival time distribution at the IP layer. This model can be used with a simulation which does not include detailed protocol layers above the MAC layer.

The IP packet level traffic model can be directly applied to the MAC and PHY models. With this type of traffic mode, evaluation of both the application performance and the scheduling mechanism at the MAC layer is not an easy task. This type of traffic model is used generally in system level simulations for the resource allocation. Traffic models employed include:

- **Full Queue (FQ)** traffic model in which it is assumed that there is an infinite amount of data bits waiting in the queue of each active user in the system. This traffic model is particularly interesting in accessing the maximum capacity of the network.
- **Mixed Traffic Model** VoIP and Near Real Time Video with 64 kbps (NRTV64Kbps), which are of type real time (RT) traffic, WWW with 32Kbps, which is of type non-real time (NRT), and File Transfer Protocol with 64 kbps (FTP), which is of type Best Effort (BE).

Traffic models, which are used in SLS purposes, are shown in figure A.6.

## A.10 Energy Module Modeling

The energy computation model metrics have been introduced in the simulator [98, 99] to compare the different schedulers from an energy point of view. Its operation is as follows:

1. In each TTI the number of resource block are simulated according to a given channel bandwidth.
2. Data rate of each resource block is calculated which is a function of the selected MCS scheme, i.e.  $f(R_u^m, MCS_u^m)$  where  $R_u^m \rightarrow$  data rate on each  $m^{th}$  PRB of  $u^{th}$  user.
3. SINR of selected MCS scheme can be found from LUTs for selected transmission.

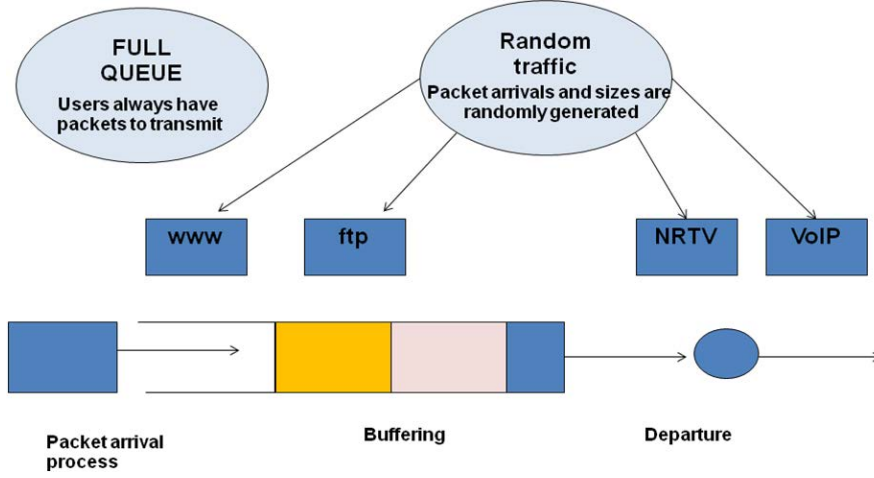


Figure A.6: Traffic Models

4. The achieved data rate according to selected SINR of each resource block is then divided by total transmit power of the eNB. ( i.e. the power allocated to each PRB is  $p^m = P/M$ .)
5. Data rate divided by power of each resource block gives us the EE in bit per joule.
6. An average measurement will be taken over one TTI.

## A.11 Performance metrics

For each TTI, a number of statistics are collected for the computation of metrics used in the performance evaluation of the system level simulation platform. The following parameters are used as inputs for the computation of performance metrics:

- Simulation time per run:  $T_{sim}$
- Number of simulation runs:  $D$
- Total number of cells being simulated:  $N_{cells}$
- Total number of users in cells of interest (cells being simulated):  $N_{users}$

### A.11.1 Average Service Throughput per-Cell

The average service throughput per cell is defined as the sum of the total amount of bits successfully received by all active users in the system, divided by the product of the number of cells simulated and the simulation duration as shown in the following equation.

$$R_{service}^{DL(UL)} = \frac{\sum_{u=1}^{N_k^{usersDL(UL)}} \sum_{i=1}^{p_{u,k}^{DL(UL)}} \sum_{j=1}^{q_{i,u,k}^{DL(UL)}} b_{j,i,u}}{N_{cells} T_{Sim}} \quad (A.2)$$

Where  $N_k^{users, DL(UL)}$  is the number of users transmitting in DL(UL) in the  $k_{th}$  cell,  $p_{u,k}^{DL(UL)}$  is the number of packet calls for user  $u$  in cell  $k$ ,  $q_{i,u,k}^{DL(UL)}$  is the number of packets for the  $i^{th}$  packet call for user  $u$  in cell  $k$  and  $b_{j,i,u}$  is the number of bits received with success in the  $j_{th}$  packet of packet call  $i$  for user  $u$  in cell  $k$ .

### A.11.2 Per-User Average Service Throughput

The average per-user service throughput is defined as the sum of the user service throughput of each user divided by the total number of users in the system, as shown in the following equation.

$$\overline{R_u^{DL(UL)}} = \frac{\sum_{u=1}^{N_{users}} R_u^{DL(UL)}}{N_{users}} \quad (A.3)$$

### A.11.3 Throughput Outage

The throughput outage is defined as the percentage of users with service data rate  $R_u^{DL(UL)}$  less than a pre-defined minimum rate  $R_{min}$ .

### A.11.4 Cell Edge User Throughput

The cell edge user throughput is defined as the 5th percentile point of the CDF of user's average packet call throughput.

### A.11.5 Spectral Efficiency (bps/Hz)

This is the ratio of correctly transmitted bits over the radio resources to the total amount of available bandwidth. The average cell spectral efficiency is defined in the following equation.

$$SE = \frac{R}{BW} \quad (A.4)$$

Where  $R$  is the aggregate cell throughput,  $BW$  is the effective channel bandwidth.

### A.11.6 System Outage

A user is said to be in outage if more than a given percentage of packets experience a delay greater than a certain time. The system is said to be in outage if any individual users are in outage.

### A.11.7 System Capacity

System capacity is defined as the maximum numbers of users that can be serviced without the system exceeding the maximum allowed outage probability.

### A.11.8 Energy Efficiency (EE)

Energy channel capacity is usually defined in bits per joule, as in [69]. We adopt that definition as metric for energy efficiency. For this article, we refer to this as the average EE i.e., the successfully delivered bits over the total power, denoted as  $P_{Total}$ , consumed by the wireless network. It means how many bits per unit power can be transported per second, in other words, the bits per joule. Hence, this definition is useful for measuring whether a wireless system is efficient in terms of consuming energy. The network EE,  $\eta_{EE}$ , is defined [94] as the ratio of the total network throughput per unit bandwidth over the network power consumption within a given period (unit: bits/Joule):

$$\eta_{EE} = \frac{TP_{net}}{P_{Total}} = \frac{TP_{net}}{P_{Tx}} \quad (A.5)$$

where  $TP_{net}$  is the average throughput of the network per unit time (unit: bps or bits/s) and  $P_{Tx}$  is the transmission power of the network (unit: Watt). Therefore, the energy consumption is the multiple of power (Watt) and time (second) whose unit is Joules. Typically, in energy efficient communications, the aim is to maximize the amount of meaningful data transmitted for a given amount of energy. In addition to the transmit power, some power is consumed in the circuitry or dissipated in the form of heat. This kind of power is counted as circuit power, denoted as  $P_{Circuit}$ , which is mostly independent of the transmission state. Then EE can be defined as a

$$\eta_{EE} = \frac{TP_{Net}}{P_{Total}} = \frac{TP_{Net}}{P_{Tx} + P_{Circuit}} \quad (A.6)$$

More elaborately,

$$EE = \frac{\text{Data rate}}{\text{Power}} \left[ \frac{\text{bits/Second}}{\text{Watt}} = \frac{\text{bits}}{\text{Second} \times \text{Watt}} = \text{bits/Joule} \right] \quad (A.7)$$

It should be kept in mind that the above mentioned metric was not directly related to the throughput performance of the system such as GSM and WCDMA since their main service is voice (and here, performance is not measured by the data rate). Nevertheless, in fourth generation (4G) cellular systems like LTE, all services are data. Therefore, this opens the door to measure the performance of the system in terms of throughput by exploring the data rate. Hence bits/Joule is the basic EE metric for fourth generation cellular systems and beyond [95], for any type of service.

### A.11.9 Fairness Index (GINI)

We refer to one fairness index (FI) termed the GINI co-efficient [139]. The generic GINI co-efficient formula is [107].

$$FI_{GINI} = \frac{\sum_{i=1}^n \sum_{j=1}^n |x_i - x_j|}{2n^2 \bar{x}} \quad (A.8)$$

where  $x$  is an observed value,  $n$  is the total number of values observed and  $\bar{x}$  is the mean value.

The value of FI lies between 0 and 1. If the value is 0, complete fairness is achieved, and 1 otherwise. For our simulation, we observed the energy efficiency of different users to measure fairness using the GINI formula.

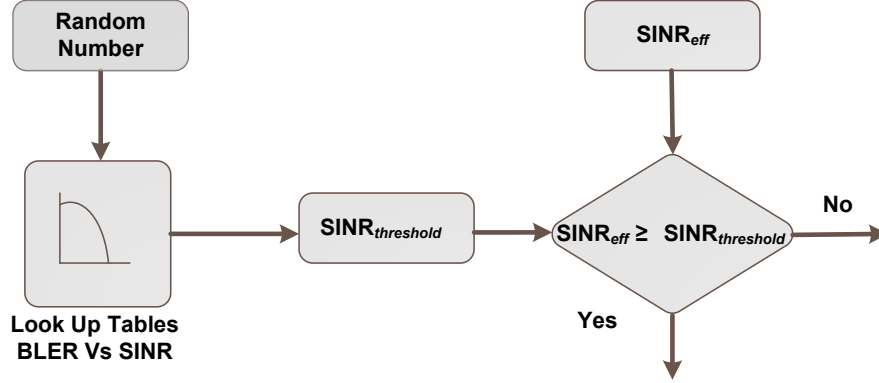


Figure A.7: Packet decoding process

## A.12 System level Simulation Process

As explained in the previous section, two types of cell configurations can be defined for simulations: central-cell and non-central cell approach. In the central-cell approach mobiles are dropped along the coverage of the central base station and statistics are collected only for this cell. Naturally, the central cell approach simulation method can be enabled only in conjunction with the combined snapshot-dynamic mode, as mobility modeling is disabled. The cells in the remaining tiers are assumed as fully loaded, i.e., transmitting with maximum power and contributing to interference only. For each frame interval the following events are generated:

- Packets are generated according to the traffic model.
- The fast fading channel is updated.
- Dynamic resource allocation is executed.
- Packet quality detection is performed.

The BLER resulting from decoding the information transmitted along a single resource unit (RU) is denoted by  $BLER_{RU}(SINR_{RU})$  and is obtained from the link-to-system interface, using as input the Signal to Interference plus Noise Ratio  $SINR_{RU}$ . Then a random variable, uniformly distributed between 0 and 1 is drawn as shown in figure A.7.

If the random value is less than  $BLER_{RU}(SINR_{RU})$ , the block is considered as erroneous and a Negative Acknowledge (NACK) message is sent back to the base station on the associated signalling channel. Otherwise, the block is deemed as error free and an Acknowledge (ACK) message is transmitted. The success or failure in the decoding of the transmitted information block is computed from decoding each individual resource, in spanning the area mapped by the data. Assuming that a total amount of  $N_{res}$  radio resources are used in the transmission and that the decoding is an independent and identically distributed random process, the BLER for the whole radio block is given by equation (A.9) .

$$BLER_{RB} = 1 - [1 - BLER_{RU}(SINR_{RU})]^{N_{res}} \quad (A.9)$$

In each simulation run (snapshot), the following steps are followed, as shown in figure A.8:

1. Mobile stations are dropped independently with uniform distribution throughout the system. Each mobile corresponds to an active user session that runs for the whole duration of the drop.
2. Mobiles are assigned channel models. This can be a channel mix or separate statistical realizations of a single type of channel model.
3. Mobiles are assigned a traffic model.
4. Cell assignment to a mobile station is based on the received power at the mobile station from all potential serving cells. The cell with the best path to the mobile station, taking into account slow fading, path-loss and antenna gains, is chosen as the serving sector.
5. For simulations that do not involve handover performance, evaluation of the location of each mobile station remains unchanged during a drop and the mobiles speed is used only to determine the Doppler effect of fast fading. The mobile station is assumed to remain attached to the same base station for the duration of the drop.
6. Fast fading is computed for each mobile station in each TTI. Slow fading and path loss are assumed as constant during the whole simulation run.
7. Packets are withdrawn from the buffers of the traffic models. Packets are not blocked as the queues are assumed to be infinite. Start times for each traffic type for each user should be randomized.
8. Packets are scheduled with a packet scheduler using the required metric. Packet, decoding errors result in packet retransmissions. In the Dynamic Resource Allocation (DRA) module a Hybrid Automatic Repeat Request (HARQ) process is modeled by explicitly rescheduling a packet as part of the current packet call and after a specified feedback delay period.
9. For a given drop, the simulation is run for a predefined duration, then the process is repeated with the mobile stations being dropped at new random locations.
10. Performance statistics are collected for mobile stations in all cells.

## A.13 Enhanced System Level Simulator

The simulator is further developed to support the features of the proposed scenarios and algorithms in this thesis, which we referred as to the enhanced version of the simulator. For SLS purposes, we consider a LTE-A cellular system consisting of 19 CoMP cell sites, with six CoMP cell sites in the first tier and twelve CoMP cell sites in the second tier, surrounding the central CoMP cell. Each CoMP cell site includes three 120-degree hexagonal sectors, i.e., 57 sectors in total are simulated. All the simulation results are collected from the three central hexagonal sectors in the central CoMP cell site, with the other 54 sectors serving as interferers. A wrap-around model is used to avoid border effects [54].

Figure A.9 demonstrates the logical SLS component which is enhanced for the scope of this dissertation work. The SLS interfaces with the link level simulator [102] through Look up tables (LUTs) as an input to the simulator. Link level simulations are done by assuming

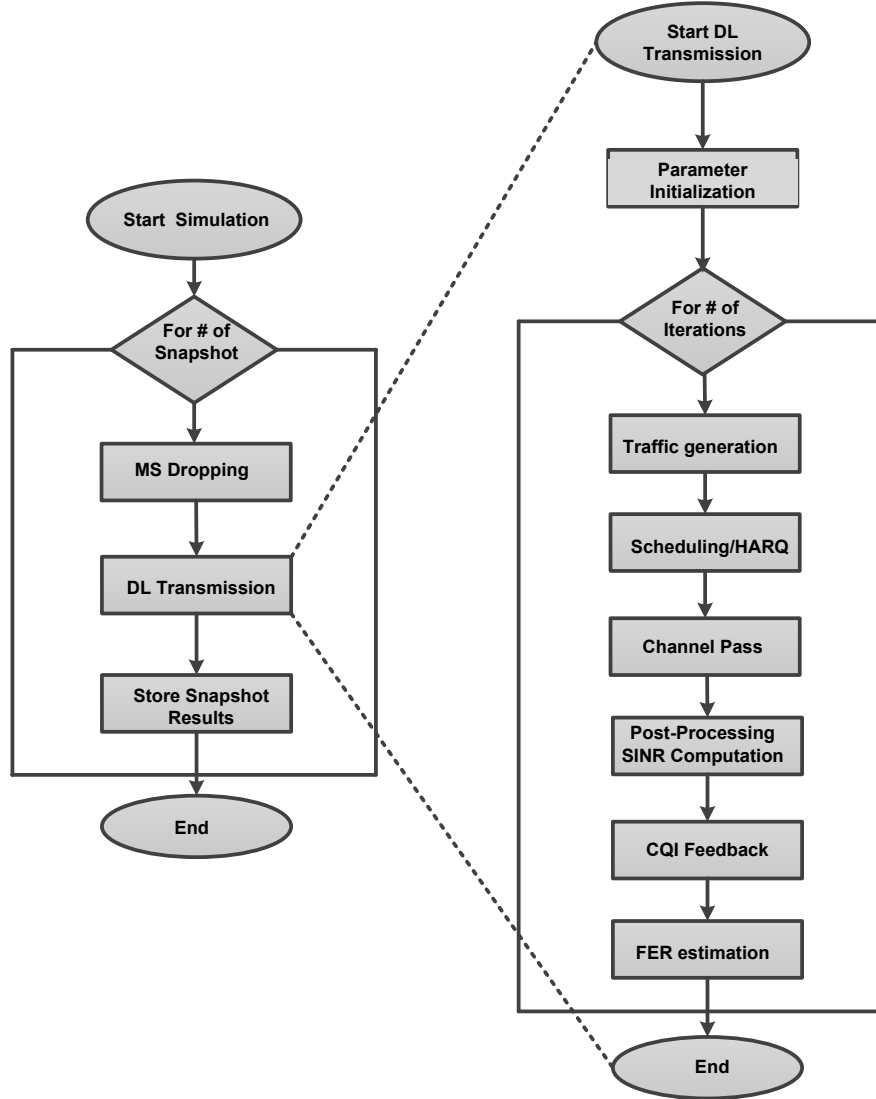


Figure A.8: Simulation Steps

single cell and multiple users. In the link level simulator we deploy different transmission schemes for CoMP i.e. DPS, JT, and CS/CB. These transmission schemes are then simulated using frequency selective channel and different coding and modulation schemes. The output of the link level simulator is in the form of LUTs which reflect the function of SNR vs. BLER (block error rate). In practice, we have 3 different LUTs used for [11] three different CoMP transmissions which are then fed to the system level simulation platform.

The system level simulator then computes the successfully transmitted packets given the mobility, traffic and channel profiles employed. Specifically, the outputs are the parameters that usually characterize packet transmissions: Throughput, BLER, Packet Delay etc. The traffic generation block contains real (i.e., VoIP, WWW) time service traffic models with full queue. The Handover block includes the handover algorithm. The radio resource management block comprises a call admission control algorithm to regulate the operation of the network; a link adaptation algorithm to select the appropriate parameters in function of the current radio

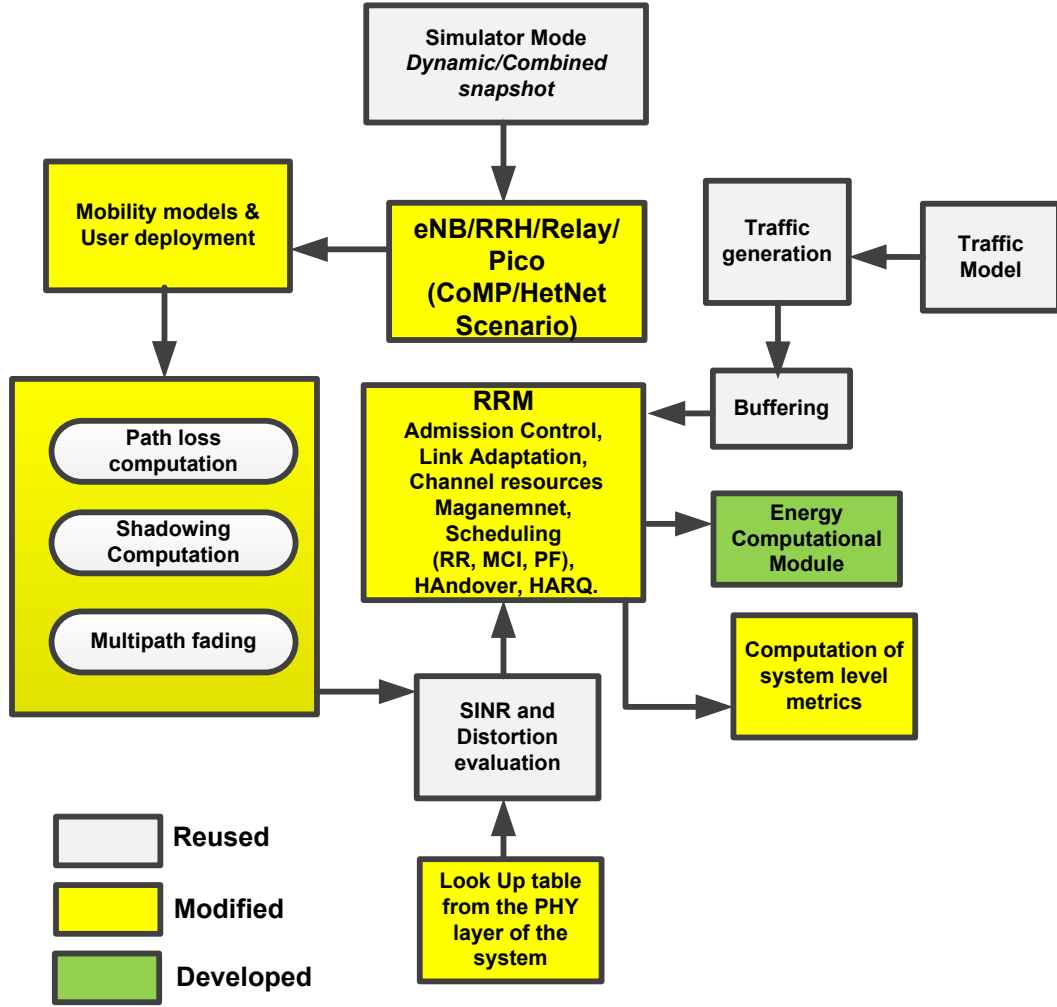


Figure A.9: Logical Simulation Component of CoMP

conditions; and a scheduler that decides how to allocate the appropriate resources based on the service type, amount of data, current load in the cell, etc. The Power control block contains mechanisms to provide similar service quality to all communication links despite the variations in the channel conditions. The interference block determines the average interference power received by central base station, i.e., inter-cell interference.

Finally, the computations of the system level metrics block returns the network results such as Service Throughput (average spectral efficiency), BLER and Packet Delay. The mobility block models the mobile movements in the indoor, urban, and rural environments. Parameters associated with mobility include speed, probability to change speed at position update, probability to change direction, and the de-correlation length. The propagation block models path loss, shadow fading and Multipath fading. Channel models for indoor environments, outdoor urban and rural environments are available. The scheduler mechanism will generate the arrival process of the users, according to a Poisson arrival process.

The objective of Call Admission Control is to regulate the operation of a network in such a way that ensures uninterrupted service provisioning to the already existing connections,

Table A.3: Modulation and Coding schemes-CoMP (20 MHz)

MCS level	Modulation	Code rate	Bits per symbol	SINR (dB)	Data rate (Mbps)	TBS (PDUs)	TBS (bits)
0-3	No Tx	-	-	-1.25	0	0	0
4	QPSK	0.3008	0.6016	-0.94	10.10688	2	384
5	QPSK	0.4385	0.8770	1.09	14.7336	3	576
6	QPSK	0.5879	1.1758	2.97	19.75344	4	768
7	16QAM	0.3691	1.4764	5.31	24.80352	5	960
8	16QAM	0.4785	1.914	6.72	32.1552	6	1152
9	16QAM	0.6016	2.4064	8.75	40.42752	8	1536
10	64QAM	0.4551	2.7306	10.47	45.87408	10	1920
11	64QAM	0.5537	3.3222	12.34	55.81296	12	2304
12	64QAM	0.6504	0.6504	14.37	10.92672	14	2688
13	64QAM	0.7539	4.5234	15.94	75.99312	16	3072
14	64QAM	0.8525	5.1150	17.81	85.932	18	3456
15	64QAM	0.9258	5.5548	20.31	93.32064	20	3840

and at the same time accommodating the new connection request in an optimum manner. The scheduler decides how to allocate the appropriate resources based on the service type, amount of data, load on the common and shared channels, current loading in the cell and the radio performance of each type of transport channel. LA can be considered as a component of Dynamic Channel Allocation (DCA). With the power control mechanism, similar service quality is provided to all communication links despite the variations in the channel conditions, which means larger a proportion of the total available power is consumed for bad channel conditions. Handover is common to all dynamic system level simulators, and required to maintain link quality at the cell boundaries. Simulation Map describes the cellular layout, which includes the cell descriptions, base station locations, and the manner in which it will model mobile movement at the system boundaries. HARQ is employed for non-real time services. DCA algorithm provides extra performance, but it is not a crucial element in the simulator.

## A.14 Conclusions

This chapter presents the design, modeling and implementation of the Link Level and System Level simulators used in this thesis. Traffic and channel models for the SLS were also discussed as well as the cellular layout architecture for SLS. Of particular interest is the definition of the link to system level interface, and how we map physical layer performance to the transmission of packets at the system level; the procedure follows into the derivation of the Signal to Interference plus Noise Ratio (SINR) and the mapping function used to map the vector of SINRs into a single scalar, as input to the look-up tables.

## Appendix B

# Calculation of precoding vector $\mathbf{W}$ and power vector $\mathbf{P}$

The precoding matrix and power matrix are calculated given by the following, using similar approach to [140, 141].

We consider a static  $C$  CoMP cluster with one centralized point CU comprised of three eNBs ( $E = 3$ ) serving  $U$  UEs. The frequency selectivity of the channel is exploited using OFDM. Considering the worst case scenario of an interference limited system and to maintain fairness in this system model, all the users are scheduled in every PRB in the downlink. The coordinated transmission algorithms are applied in the frequency domain on every RB, to remove the interference between users.

Therefore, the discrete-time received signal,  $\mathbf{y} \in \mathbb{C}^{U \times 1}$  at the  $U$  users can be expressed as

$$\mathbf{y} = \mathbf{H}\mathbf{W}\sqrt{\mathbf{P}}\mathbf{x} + \mathbf{n} \quad (\text{B.1})$$

where  $\mathbf{H} \in \mathbb{C}^{U \times E}$  is the channel matrix,  $\mathbf{W} \in \mathbb{C}^{E \times U}$  is the precoding beamforming matrix and  $\mathbf{P} \in \mathbb{R}^{U \times U}$  is the power allocation matrix. The transmitted symbols  $\mathbf{x} \in \mathbb{C}^{U \times 1}$  are normalized to unit power and the receiver noise  $\mathbf{n} \in \mathbb{R}^{U \times 1}$  with AWGN elements, each with variance  $\sigma^2$ . In equation(9), the channel matrix  $\mathbf{H}$  is of the form

$$\mathbf{H} = [\mathbf{h}_1^T \mathbf{h}_2^T \dots \mathbf{h}_U^T]^T \quad (\text{B.2})$$

where  $\mathbf{h}_u \in \mathbb{C}^{1 \times E}$  is the channel from the  $u^{th}$  user to all the eNBs in the cluster. The beamforming matrix  $\mathbf{W}$  is

$$\mathbf{W} = [\mathbf{w}_1 \mathbf{w}_2 \dots \mathbf{w}_U] \quad (\text{B.3})$$

where  $\mathbf{w}_u \in \mathbb{C}^{E \times 1}$  is the beamformer for the  $u^{th}$  user.

Considering the individual  $\mathbf{h}_u$  being available from all the eNBs at the CU, the multiuser interference with a zero-forcing beamforming design, taking the pseudo-inverse of  $\mathbf{H}$ ,

$$\mathbf{W} = \mathbf{H}^H (\mathbf{H}\mathbf{H}^H)^{-1} \quad (\text{B.4})$$

The intra-CoMP interference is completely removed, i.e.,  $\mathbf{H}\mathbf{W} = \mathbf{I}$ , where  $\mathbf{I} \in \mathbb{R}^{U \times U}$  is an identity matrix. At every eNB, the maximum power is restricted to  $P_{\max}$ . Then, the power allocation matrix based on [120] becomes

$$\mathbf{P} = \left\{ \min_{e=1, \dots, E} \left( \frac{P_{\max}}{\|\mathbf{W}^e\|_F^2} \right) \right\} \mathbf{I}_U \quad (\text{B.5})$$

where  $\mathbf{W}^e$  are the rows of the matrix  $\mathbf{W}$  related to the  $e^{th}$  eNB. This power allocation is sub-optimal, since it typically results in only one of the eNBs meeting the maximum transmitted power requirement with equality, and hence, the remaining eNBs transmit below the  $P_{\max}$  value. This model can be generalized to multiple CoMP scenarios. Hence, at the OFDM sub-carrier level, equation B.1 for a particular  $c^{th}$  CoMP becomes,

$$\mathbf{y}_c = \mathbf{H}_c \mathbf{W}_c \sqrt{\mathbf{P}_c} \mathbf{x}_c + \mathbf{n} \quad (\text{B.6})$$

The received downlink signal for the  $u^{th}$  user in the  $c^{th}$  CoMP, considering all the CoMP-clusters is

$$\mathbf{y}_{c,u} = \underbrace{\mathbf{h}_{c,u} \mathbf{w}_{c,u} \sqrt{p_{c,u}} x_{c,u}}_{\text{DesiredSignal}} + \underbrace{\sum_{u' \neq u}^U \mathbf{h}_{c,u} \mathbf{w}_{c,u'} \sqrt{p_{c,u'}} x_{c,u'}}_{\text{Intra-CoMPinterference}} + \underbrace{\sum_{c' \neq c}^C \sum_{u' \neq u}^U \mathbf{h}_{c',u} \mathbf{w}_{c',u'} \sqrt{p_{c',u'}} x_{c',u'}}_{\text{Inter-CoMPinterference}} + n \quad (\text{B.7})$$

where  $\mathbf{h}_{c,u}$ ,  $\mathbf{w}_{c,u}$  and  $\sqrt{p_{c,u}}$  are the channel, the beamformer and the power at which the signal is transmitted to the  $u^{th}$  user in the  $c^{th}$  CoMP cluster, respectively. This forms part of the desired signal. The  $\mathbf{w}_{c,u'}$  and  $\sqrt{p_{c,u'}}$  is the beamformer and the power allocated to the  $u^{th}$  user in the  $c^{th}$  CoMP cluster, respectively. This affects the desired signal within the same cluster due to the transmission to other users other than the  $u^{th}$  user. Hence, this forms the Intra-CoMP interference. The  $c'$  corresponds to the transmission to users in all the clusters. The interference generated in clusters other than the  $c^{th}$  CoMP cluster forms the Inter-CoMP interference. Then the Signal to Interference plus Noise Ratio (SINR) at the  $u^{th}$  user in the  $c^{th}$  cluster is,

$$\gamma_{c,u} = \frac{\|\mathbf{h}_{c,u} \mathbf{w}_{c,u}\|^2 p_{c,u}}{\sum_{u' \neq u}^U \|\mathbf{h}_{c,u} \mathbf{w}_{c,u'}\|^2 p_{c,u'} + \sum_{c' \neq c}^C \sum_{u'}^U \|\mathbf{h}_{c',u} \mathbf{w}_{c',u'}\|^2 p_{c',u'} + \sigma^2} \quad (\text{B.8})$$

For simplicity, in this work, the inter-CoMP interference is assumed to be perfectly removed and the receiver combining weights are not considered. Hence, the generalized SINR in the above equation (B.8) simplifies to

$$\gamma_{c,u} = \frac{\|\mathbf{h}_{c,u} \mathbf{w}_{c,u}\|^2 p_{c,u}}{\sum_{u' \neq u}^U \|\mathbf{h}_{c,u} \mathbf{w}_{c,u'}\|^2 p_{c,u'} + \sigma^2} \quad (\text{B.9})$$

# Index

3GPP, 14, 83  
4G, 1, 2, 8  
  
AMC, 45  
AWGN, 6, 14, 30  
  
backhaul, 105  
BE, 69  
BER, 70  
BLER, 60  
BS, 2, 25, 26, 41  
  
CA, 123  
CCN, 19  
CDF, 63, 74  
CL, 15  
CoMP, 2, 8, 14, 15, 69, 83  
convex, 47, 83  
CQI, 20  
CS/CB, 5, 24, 84  
CSI, 3, 32, 122  
CU, 2, 44  
  
D2D, 123  
DAS, 15  
DCA, 60, 152  
DCI, 140  
DPS, 24  
DRA, 149  
DRX, 78  
  
ECR, 20, 81  
EE, 2, 7, 14, 53, 61  
EES, 69, 73  
eNB, 2, 78  
  
FFR, 27, 83, 98  
FTP, 69  
  
GHG, 2  
GSM, 54  
  
HARQ, 53, 152  
HetNet, 6, 83  
  
ICI, 53, 69  
ICIC, 98  
ICT, 13  
  
JT, 4, 24, 84  
  
LA, 60, 152  
LPN, 83, 122  
LTE, 53  
LTE-A, 2, 83, 149  
LUT, 137, 149  
  
MA, 14, 32  
MAC, 16  
MCI, 7, 20, 69  
MCS, 45, 72  
MHC, 85, 90  
MIMO, 2, 15, 20  
MPDU, 142  
MU-MIMO, 10, 51, 83  
MUD, 18  
MUI, 84  
  
NLOS, 19  
  
OFDM, 29, 32  
OFDMA, 2, 29, 32  
OPEX, 19  
  
P-SCH, 92  
PDCCH, 92  
PDSCH, 92  
PF, 7, 20, 22, 69  
PHY, 16  
picocell, 84  
PRB, 45, 141  
PSS, 92

QoE, 15  
QoS, 15, 16, 18, 69  
  
RA, 14, 32  
relay, 84  
RR, 7, 20, 69  
RRH, 10, 84, 107  
RRM, 6, 13–15, 25, 27  
RT, 69  
  
S-SCH, 92  
SBS, 99  
SE, 2, 14, 29  
SFP, 106, 107  
SINR, 6, 41, 45, 87  
SIR, 17  
SISO, 20, 88  
SLS, 7, 59, 92, 137  
SM, 20  
SoA, 20, 53, 64, 69  
SSS, 92  
SU-MIMO, 84  
  
TTI, 45, 54, 137, 141  
  
UE, 21  
UMTS, 106  
  
WCDMA, 54  
  
ZF, 44, 85